




ADVERTIMENT. L'accés als continguts d'aquesta tesi queda condicionat a l'acceptació de les condicions d'ús establertes per la següent llicència Creative Commons:  http://cat.creativecommons.org/?page_id=184

ADVERTENCIA. El acceso a los contenidos de esta tesis queda condicionado a la aceptación de las condiciones de uso establecidas por la siguiente licencia Creative Commons:  <http://es.creativecommons.org/blog/licencias/>

WARNING. The access to the contents of this doctoral thesis it is limited to the acceptance of the use conditions set by the following Creative Commons license:  <https://creativecommons.org/licenses/?lang=en>



Universitat Autònoma
de Barcelona

Electronic Tongues using Printed Sensor Platforms for Forensic and Security Applications

Dionisia Ortiz Aguayo

Doctoral Thesis

Doctoral Studies in Chemistry

Director: Prof. Manel del Valle Zafra

Departament de Química

Unitat de Química Analítica

Facultat de Ciències

Juny 2022

Memòria presentada per aspirar al Grau de Doctor per la Dionisia Ortiz Aguayo

Dionisia Ortiz Aguayo

Vist i plau,

Dr. Manel del Valle Zafra

Catedràtic de la Universitat Autònoma de Barcelona

Professor de Química Analítica

Bellaterra, 13 de juny del 2022

“Life is short, enjoy the ride”

Three cardinal rules:

One, surround yourself with people whose eyes light up when they see you coming.

Two, slowly is the fastest way to get to where you want to be.

Three, the top of one mountain is the bottom of the next, so keep climbing.

André De Shields

Publications

The research produced during this doctoral thesis has produced the following publications:

1. **Simultaneous Voltammetric Determination of Acetaminophen, Ascorbic Acid and Uric Acid by Use of Integrated Array of Screen-Printed Electrodes and Chemometric Tools.**

Dionisia Ortiz-Aguayo, Marta Bonet-San-Emeterio and Manel del Valle
Sensors, 2019, 3286.

2. **Voltammetric sensing using an array of modified SPCE coupled with machine learning strategies for the improved identification of opioids in presence of cutting agents.**

Dionisia Ortiz-Aguayo, Karolien De Wael and Manel del Valle
Journal of Electroanalytical Chemistry, 902, 115770

3. **Resolution of opiate illicit drugs signals in the presence of some cutting agents with use of a voltammetric sensor array and machine learning strategies.**

Dionisia Ortiz-Aguayo, Xavier Cetó, Karolien De Wael and Manel del Valle
Sensors and Actuators B: Chemical, 357, 131345

4. **Novel Integrated Inkjet Sensor Array for Detecting Simultaneously some Adulterants present in Drug of Abuse Field using Chemometrics.**

Dionisia Ortiz-Aguayo, Xavier Cetó, Gemma Gabriel and Manel del Valle
Sensors and Actuators B: Chemical, submitted

Funding support

This present dissertation has been carried out at the laboratories of *Sensors and Biosensors* group of the Department de Química from Universitat Autònoma de Barcelona. The work involved in the present dissertation are presented in the following projects.

1. Ministerio de Ciencia e innovación (MICINN) for the projects entitled:

- 1.1 “Electronic tongue fingerprinting: aplicaciones en el campo alimentario y de seguridad” (CTQ2013-41577-P).
- 1.2 “Lenguas bioelectrónicas con transducción electroquímica. Explorando nuevas aplicaciones” (CTQ2016-80170-P).
- 1.3 “Lenguas electrónicas con sistemas de reconocimiento mejorados” (PID2019-107102RB-C21).

2. European union Horizon 2020 for the project titled:

- 2.1 Border detection of illicit drugs and precursors by highly accurate electrosensors (Bordersens nº833787).

3. Universitat Autònoma de Barcelona for the predoctoral and mobility fellowships.



Acknowledgements

Después de un largo tiempo en la Universidad; carrera, máster, doctorado... llegó el día de cerrar esta etapa tan larga y costosa con unos agradecimientos a todas aquellas personas que han estado presentes a lo largo del camino.

Primero de todo, quiero darte las gracias a ti, *Manel del Valle*, por no ser solo mi director de tesis, sino esa persona que me ha guiado y ayudado a lo largo de la experiencia. Gracias por abrirme las puertas del laboratorio cuando llamé a tu puerta, y gracias por darme la oportunidad y pelear por esta tesis, que sabemos que no ha sido fácil.

Quiero también dar las gracias a mis compañeros de laboratorio, con los que hemos compartido tanto tiempo. *Andreu, Anna, Marta, Elena, Xavi, Noelia F., Núria y Bàrbara*. Gracias por compartirla conmigo y hacerme pasar buenos momentos. *Munmi, Qing, Ming Yuei*, our international girls, thank you for all! Your talks on grey days made the experience more bearable!

Por otro lado, agradecer a *Gemma Gabriel* la oportunidad de hacer una colaboración juntas. Gracias por ofrecerme tu ayuda, ha sido un placer trabajar contigo.

Seguidamente, quiero agradecer al grupo de investigación A-Sense Lab en la Universidad de Amberes. Sin duda, mi estancia allí ha sido lo mejor del doctorado. Thank you, Prof. *Karolien de Wael*, for giving me the astounding opportunity to work in your team and making me feel like a member of the group during my stay. Thank you *Anca Florea* for lending me a hand when I arrived and helping me in any way you could. I learned a lot working with you. *Liselotte, Sarah, Hannan, Oli, Mats, Nicks, Gert, Frederik, Ehab, Shahid, Jonas, Andrea, Fabio, Ermano*, thanks a lot, you all are wonderful people. Thanks specially to *Rui*, for your attitude, the very useful impedance express classes and your good music in the lab (muito obrigado!!!) and thanks *Stas* for sharing funny moments while working.

Pero, sobre todo, quiero darle las gracias a la persona más especial que he conocido en Bélgica, gracias, *Victoria* por compartir conmigo la experiencia. Recuerdo con mucho cariño todas las aventuras que vivimos (¡que no fueron pocas!). Estoy muy orgullosa de ti y de que estés consiguiendo todo lo que te propusiste. ¡Nos vemos pronto porque life is a gamble!

Bueno, ahora es momento de agradecer a los compañeros que conocí en la carrera, y después de todo, se han acabado convirtiendo en amigos. Gracias, *Dra. Silvia Mena*, por tu optimismo, por ayudarme. Gracias, *Dr. Kevin Morales*, por ser mi compañero de risas y por ayudarme cuando lo he necesitado. Agradecer especialmente a la *Dra. Laia García*. Sin duda, has sido mi apoyo incondicional, siempre hemos vivido alegrías y desgracias juntas y espero que también lo estemos al cerrar esta etapa. ¡Admiro tu paciencia y positivismo!

Y aunque estén los últimos, para mí son los primeros. Quiero agradecer a mi familia todo vuestro amor y cariño. A mi padre *Juan* por enseñarme que con esfuerzo y constancia todo es posible, gracias papa. A mi mayor referente, mi madre, gracias por apoyarme en todo, por tu fortaleza y por dejar que nunca me rindiera, esto no lo hubiera conseguido sin ti. ¡*Te quiero mama, esto va por ti!* A mi hermana *María*, sin ella tampoco lo hubiera conseguido. Gracias, *Merygises* por apoyarme, ayudarme y creer tanto en mí cuando ni yo misma lo hacía. Estoy segura de que el futuro te traerá cosas muy buenas, y por supuesto, ¡que serás una magnífica doctora! Te quiero mucho. Y finalmente, unas palabras para una persona que también ha sufrido esta etapa. Gracias *Manel*, por animarme en los momentos de bajón y alegrarte cuando algo mejoraba.

Por último, gracias, *Madelaine y Alejandro*, por vuestro apoyo y confiar en mí. ¡Prepararos, que ya podemos empezar a organizar el viaje!

¡Gracias a todos!

Dioni

SUMMARY

Summary

The aim of this doctoral thesis is to study new sensor platforms combining electronic tongues principles and chemometric tools. To achieve this goal, the knowledge acquired in the *Sensors and Biosensors group* of the Universitat Autònoma de Barcelona has been applied.

The main objective of this research is focused on the development of electrochemical sensors, using the concept of sensor arrays for applications in different fields of study. The type of sensor employed was printed, either by screen-printing or inkjet printing techniques. The use of these systems provides multicomponent information that needs to be treated with chemometric tools.

The electrochemical measurements were obtained using different electroanalytical techniques based on the fundamentals of Voltammetry, namely Cyclic and Square Wave. The data processing part was treated using Principal Component Analysis and Silhouette Coefficient calculation for qualitative studies. In addition, learning algorithms commonly known as “*Machine Learning Algorithms*” were used for the identification of the mixtures under study. The use of these statistical criteria has served to optimise the composition of the sensor matrix. In contrast, quantitative studies were approached using more complex calculation algorithms such as Partial Least Squares Regression and Artificial Neural Networks as a simulation of the biomimetic systems.

The application of these systems has been focused on two distinct fields of study. One is the quantification of different pharmaceutical compounds (ternary mixtures of acetaminophen, ascorbic acid and uric acid) as a proof of concept to validate the experimental procedure developed. In the second case, the study is focused on the identification and subsequent quantification of different drugs of abuse and their corresponding cutting agents. Specifically, mixtures of opiates such as heroin, morphine and codeine were identified and quantified. Moreover, commonly used concentrations of different cutting agents (paracetamol and caffeine) were added to the mixtures in order to simulate the detection of real samples found in the illicit drug market.

To conclude the study, an application was developed for the quantification of different cutting agents (ternary mixtures of benzocaine, phenacetin, and paracetamol) commonly found in cocaine samples. All these approaches are ultimately aimed at implementing new strategies for the rapid detection of illicit drugs at checkpoints led by the authorities.

Resumen

La presente tesis doctoral tiene como fin el estudio de nuevas plataformas sensoras combinando principios de lengua electrónica y herramientas quimiométricas. Para lograr esta meta se han aplicado los conocimientos adquiridos en el grupo de *Sensores y Biosensores* de la Universidad Autónoma de Barcelona.

El fundamento de esta investigación se centra como objetivo principal en el desarrollo de sensores electroquímicos, empleando el concepto de matrices de sensores para aplicaciones en diferentes campos de estudio. El tipo de sensor utilizado fue impreso, bien mediante la técnica de serigrafía o bien mediante inyección de tinta. El uso de estos sistemas proporciona información multicomponente que requiere ser tratada con herramientas de quimiometría.

Las medidas electroquímicas fueron obtenidas a través de diferentes técnicas electroanalíticas basadas en el fundamento de la voltamperometría, concretamente la cíclica y la de onda cuadrada. La parte matemática y de procesamiento de datos fueron tratados utilizando el análisis de componentes principales y cálculo del coeficiente Silhouette para estudios cualitativos. Además, se utilizaron algoritmos de aprendizaje comúnmente conocidos como “*Machine Learning Algorithms*” para la identificación de las mezclas en estudio. El uso de estos criterios estadísticos ha servido para optimizar la composición de la matriz de sensores. Por otra parte, los estudios cuantitativos se abordaron empleando algoritmos de cálculo más complejos como pueden ser la regresión de mínimos cuadrados parciales y las redes neuronales artificiales como simulación de los sistemas biomiméticos.

Las aplicaciones de estos sistemas se han realizado en dos campos de estudio bien diferenciados. Uno de ellos, es la cuantificación de diferentes compuestos farmacéuticos (mezclas ternarias de acetaminofeno, ácido ascórbico y ácido úrico) como prueba de concepto para validar el procedimiento experimental desarrollado.

En el segundo caso, el estudio está enfocado a la identificación y posterior cuantificación de diferentes drogas de abuso y sus agentes de corte correspondientes. En concreto, se identificaron y cuantificaron mezclas de opiáceos como son la heroína, la morfina y la codeína.

Además, se añadieron a las mezclas concentraciones comúnmente empleadas de diferentes agentes de corte (paracetamol y cafeína) con la finalidad de simular la detección de muestras reales encontradas en el mercado ilícito de la droga. Para concluir el estudio, se desarrolló una aplicación para la cuantificación de diferentes agentes de corte (mezclas ternarias de benzocaína, fenacetina y paracetamol) halladas de forma común en muestras de cocaína. Todas estas aproximaciones tienen como objetivo final la implementación de nuevas estrategias para la rápida detección de drogas ilícitas en puntos de control liderados por las autoridades.

Resum

La present tesi doctoral té com a fi l'estudi de noves plataformes sensores combinant principis de llengua electrònica i eines quimiomètriques. Per assolir aquest objectiu s'han aplicat els coneixements adquirits al grup de *Sensors i Biosensors* de la Universitat Autònoma de Barcelona.

El fonament d'aquesta investigació té com a objectiu principal el desenvolupament de sensors electroquímics, emprant el concepte de matrius de sensors per a aplicacions en diferents camps d'estudi. El tipus de sensor utilitzat va ser imprès, bé mitjançant la tècnica de serigrafia o bé mitjançant injecció de tinta. L'ús d'aquests sistemes proporciona informació multicomponent que cal tractar amb eines de la quimiometria.

Les mesures electroquímiques van ser obtingudes mitjançant diferents tècniques electroanalítiques basades en el fonament de la voltamperometria, concretament la cíclica i la d'ona quadrada. La part matemàtica i de processament de dades van ser tractades utilitzant l'anàlisi de components principals i càlcul del coeficient Silhouette per a estudis qualitius. A més, es van utilitzar algorismes d'aprenentatge coneguts com a "*Machine Learning Algorithms*" per a la identificació de les mescles en estudi. L'ús d'aquests criteris estadístics ha servit per optimitzar la composició de la matriu de sensors. D'altra banda, els estudis quantitatius es van abordar emprant algorismes de càlcul més complexos com ara la regressió de mínims quadrats parcials i les xarxes neuronals artificials com a simulació dels sistemes biomimètics.

Les aplicacions d'aquests sistemes s'han realitzat en dos camps d'estudi ben diferenciats. Un d'ells és la quantificació de diferents compostos farmacèutics (mescles ternàries de acetaminofè, àcid ascòrbic i àcid úric) com a prova de concepte per validar el procediment experimental desenvolupat. En el segon cas, l'estudi està enfocat a la identificació i posterior quantificació de diferents drogues d'abús i els seus agents de tall corresponents. En concret, es van identificar i quantificar mescles d'opiacis com són l'heroïna, la morfina i la codeïna.

A més, es van afegir a les mescles concentracions comunament emprades de diferents agents de tall (paracetamol i cafeïna) amb la finalitat de simular la detecció de mostres reals trobades al mercat il·lícit de la droga. Per concloure l'estudi, es va desenvolupar una aplicació per a la quantificació de diferents agents de tall (mescles ternàries de benzocaïna, fenacetina i paracetamol) trobades de manera comuna en mostres de cocaïna. Totes aquestes aproximacions tenen com a objectiu final la implementació de noves estratègies per a la ràpida detecció de drogues il·lícites en punts de control liderats per les autoritats.

ABBREVIATIONS AND SYMBOLS

Abbreviations and symbols

Name	Abbreviations and symbols
6-monoacetylmorphine	6-MAM
Acetaminophen	PA
Acetonitrile	ACN
Acrylonitrile butadiene styrene	ABS
Additive manufacturing	AM
Ammonium chloride	NH₄Cl
Anodic peak current	I_{pa}
Anodic peak potential	E_{pa}
Area	A
Artificial Neural Networks	ANNs
Ascorbic acid	AA
Auxiliary electrode	AE
Bismuth	Bi
Caffeine	CAF
Carbon nanotubes	CNT
Carbon Paste Electrode	CPE
Cathodic peak current	I_{pc}
Cathodic peak potential	E_{pc}
Causal index	CI
Central Composite Face-centered	CCF
Chemically Modified Electrode	CME
Chemically Sensitized Field Effect Transistor	CHEMFET
Cobalt (II) phthalocyanine	CoPc
Codeine	COD
Concentration	C
Continuous inkjet	CIJ

Name	Abbreviations and symbols
Controlled Substances Act	CSA
Copper (II) oxide	CuO
Counter electrode	CE
Cyclic Voltammetry	CV
Determination Coefficient	R²
Differential Pulse Voltammetry	DPV
Diffusion coefficient	D
Dimethylformamide	DMF
Dimethylsulfoxide	DMSO
Discrete Wavelet Transform	DWT
Disodium phosphate	Na₂HPO₄
Drop-on-demand	DOD
Dropping Carbon Electrode	DCE
Dropping Mercury Electrode	DME
Electronic eye	EE
Electronic nose	EN
Electronic tongue	ET
Energy Dispersive X-Ray Spectroscopy	EDX
Enzyme-Linked Immunosorbent Assay	ELISA
Fast Fourier Transform	FFT
Fourier Transform	FT
Fused Deposition Modeling	FDM
Genetic algorithms	GAs
Glassy Carbon	GC
Glassy Carbon Electrode	GCE
Gold	Au
Graphite screen-printed electrodes	GSPE

Name	Abbreviations and symbols
Graphite-epoxy Composite Electrode	GEC
High-performance Liquid Chromatography	HPLC
Hydrochloric acid	HCl
Hydrogen peroxide	H₂O₂
Inkjet Printing	IJP
Inkjet-printed Electrode	IPE
International Chemometrics Society	ICS
International Union of Pure and Applied Chemistry	IUPAC
Ion-selective sensors	ISEs
Iridium	Ir
K-nearest Neighbour	kNN
Latent Variables	LVs
Mercury	Hg
Methanol	MeOH
Monopotassium phosphate	KH₂PO₄
Multi Partial Least Squares	nPLS
Multi-Walled Carbon Nanotubes	MWCNT
Nanoparticles	Np
Net current	i_{net}
Nonlinear iterative partial least squares	NIPALS
Normalised Root Mean Square Error	NRMSE
Palladium	Pd
Partial Least Squares	PLS
Patter recognition	PARC
Phosphate buffer solution	PBS
Platinum	Pt

Name	Abbreviations and symbols
Poly(3,4-ethylenedioxythiophene) polystyrene sulfonate	PEDOT:PSS
Polyaniline	PANI
Polyethylene naphthalate	PEN
Polyethylene terephthalate	PET
Polylactic acid	PLA
Polypyrrole	PP
Polyvinyl chloride	PVC
Potassium chloride	KCl
Potassium ferricyanide	K₃[Fe(CN)₆]
Potassium ferrocyanide	K₄[Fe(CN)₆]
Potassium hydroxide	KOH
Potassium monophosphate	K₂HPO₄
Potassium nitrate	KNO₃
Potential scan rate	ν
Principal component	PC
Principal Component Analysis	PCA
Principal Component Regression	PCR
Prussian blue	PB
Reference electrode	RE
Relative Standard Deviation	RSD
Root Mean Square Error	RMSE
Scanning Electron Microscopy	SEM
Screen-printed Electrode	SPE
Section	§
Selective Laser Melting	SLM
Silver	Ag
Single-Walled Carbon Nanotubes	SWCNT
Singular Value decomposition	SVD

Name	Abbreviations and symbols
Sodium chloride	NaCl
Sodium hydroxide	NaOH
Square Wave Voltammetry	SWV
Standard Normal Variate	SNV
Stereolithography	SLA
Support Vector Machines	SVM
Tetraalkylammonium	(CH₃)₄NCl
Three-dimensional	3D
Tin (IV) oxide	SnO₂
Universitat Autònoma de Barcelona	UAB
Uric acid	UA
Working electrode	WE

A mis padres, Dionisia y Juan

A mi hermana, María

Table of Contents

I. INTRODUCTION	31
1. Single Sensor vs. Sensor Array	33
2. Chemically Modified Electrodes for Sensing	35
2.1. Sensor Platforms	36
2.1.1. Materials	36
2.1.2. Working Electrode Technologies	38
2.1.3. General Overview of 3D Printed Sensors	48
2.2. Modification Approaches	50
2.2.1. Entrapment through the Formation of a Self-formulated Conductive Ink Via Drop casting	50
3. Analytical Electrochemistry	52
3.1. Key Points to run Electrochemical Measurements	54
3.1.1. Faradaic and Non-Faradaic: The Concept	54
3.1.2. Electrochemical Cells, Solvents, and Supporting Electrolytes	55
3.2. Electrochemical Techniques	56
3.2.1. Voltammetry	56
4. Biomimetic Systems	61
4.1. Electronic Tongue Systems as Analytical Devices	62
4.1.1. Analogy between the Human Taste and Electronic Tongue systems	63
5. Chemometrics	66
5.1. Data Processing	68
5.1.1. Data Compression	70
5.2. Unsupervised Methods	73
5.2.1. Principal Component Analysis	73
5.3. Supervised Methods	76
5.3.1. Machine Learning Algorithms	76
5.3.2. Partial Least Squares Regression	79
5.3.3. Artificial Neural Networks	80
6. Applications	83

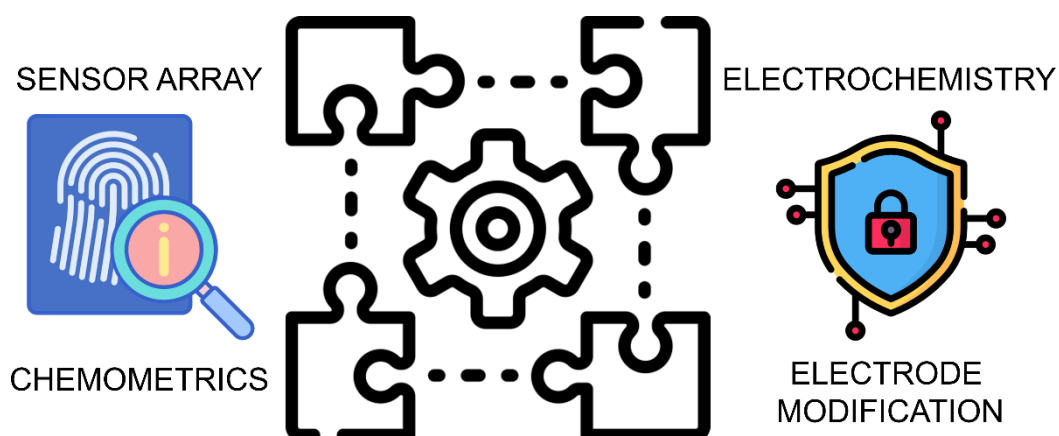
6.1.	Proof of Concept	83
6.1.1.	Acetaminophen, Uric Acid, and Ascorbic Acid	84
6.2.	Illicit Drugs	85
6.2.1.	Opiates and Cutting Agents.....	85
6.2.2.	Cocaine and Cutting Agents.....	87
7.	References	90
II.	OBJECTIVES	101
1.	Objectives.....	103
III.	EXPERIMENTAL.....	107
1.	Materials and Methods	109
2.	Reagents and Samples	111
3.	Instrumentation	112
4.	Sensor Platforms	112
4.1.	Commercial Screen-printed Electrodes.....	113
4.2.	Inkjet Printed Electrodes Fabrication.....	114
5.	Chemical Modification	115
5.1.	Electrode Surface Activation	116
5.2.	Electrochemical Characterization of the Electrode Surface	117
6.	Electrochemical Measurements Performance	118
7.	Experimental Design Selection.....	119
8.	Data Analysis.....	121
9.	Sensor Array Selection.....	121
9.1.	Principal Component Analysis	122
9.2.	Silhouette Calculation	123
10.	Model Assessment.....	125
11.	Model Validation.....	126
11.1.	Qualitative Model	126

11.2. Quantitative Model.....	127
11.2.1. Comparison Graphs Predicted vs. Expected	128
11.2.2. Root Mean Square and Normalised Root Mean Square Errors	128
12. References.....	130
IV. RESULTS AND DISCUSSION	131
ARTICLE 1	135
1. Outline	137
2. Surface Characterization through Scanning Electron Microscopy Studies	138
3. Electrochemical Response	138
4. Modified Screen-printed Electrodes Characterization.....	141
4.1. Calibration Curves.....	141
4.2. Reproducibility and Stability Studies	142
5. Principal Component Analysis	142
6. Partial Least Squares Regression as a Modelling Tool	143
ARTICLE 2	147
1. Outline	149
2. Scanning Electron Microscopy Studies	150
3. Square Wave Voltammetric Response.....	153
4. Principal Component Analysis as a Selection Tool.....	154
5. Optimization through Silhouette Parameter	156
6. Machine Learning Algorithms	160
ARTICLE 3	163
1. Outline	165
2. Sensor Array Characterization.....	166
3. Repeatability and Reproducibility Studies	175

4. Quantitative Analysis of Drug Mixtures using Partial Least Squares Regression.....	177
4.1. Three Drugs' Mixtures.....	180
4.2. Three Drugs and the Two Cutting Agents' Mixtures.....	182
ARTICLE 4	187
1. Outline	189
2. Electrochemical Characterization	190
2.1. Effective Area Calculation	190
3. Evaluation of the Linear Response.....	191
4. Repeatability and Reproducibility Studies	194
5. Surface Electrode Characterization	196
5.1. Morphology Studies	196
5.2. Impedance Measurements.....	198
6. Chemometric Analysis.....	198
6.1. Qualitative Analysis: Principal Component Analysis	199
7. Quantification Analysis	201
8. References	202
V. CONCLUSIONS	205
1. Conclusions.....	207
2. Futures Perspectives.....	210
ANNEX 1: PUBLICATIONS	211

I. INTRODUCTION

This introduction aims to present the main objectives of this dissertation and to string together the theoretical concepts involved in it. This introductory part will help the reader to visualize the puzzle from the assembly pieces that are employed in it: sensor array, electrochemistry, electrode modification and data processing strategies, all this focused on forensic and security applications.



1. Single Sensor vs. Sensor Array

This doctoral thesis will be dealing with sophisticated systems based on the use of sensor arrays. For this reason, before moving through this part, it is important to start with the simple concept of individual sensor.

According to the International Union of Pure and Applied Chemistry (IUPAC), “**a chemical sensor is a device that transforms chemical information, into an analytically useful signal**”. The chemical information can provide from a chemical reaction of the analyte or a physical property of the system investigated¹.

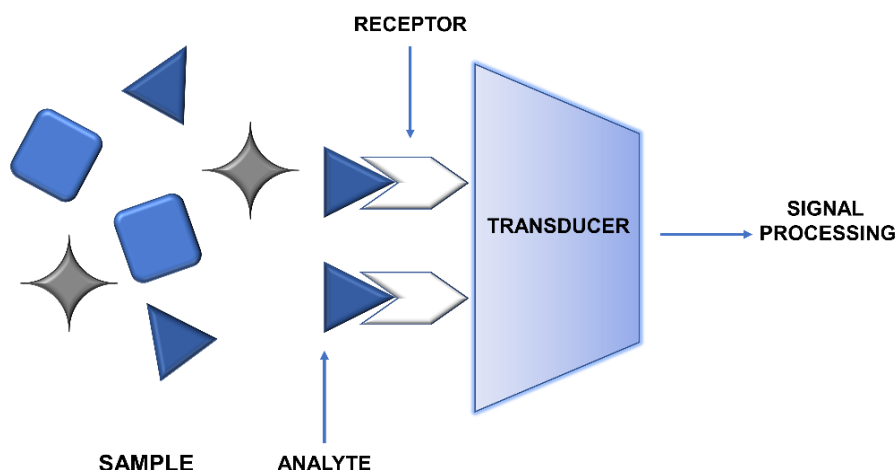


Figure I - 1. Schematic representation of the elements that composed a chemical sensor.

Chemical sensors are composed of two units: a receptor and a transducer (Figure I - 1). In the receptor part of a sensor, the chemical information is transformed into a primary signal which may be measured by the transducer. The receptor part of chemical sensors may be classified as physical, chemical, and biochemical. With physical receptors, no chemical reaction occurs (i.e., absorbance, refractive index, mass change, etc.), meanwhile in the case of chemical one, a chemical reaction with the analyte leads to the analytical signal. Finally, in biochemical receptors, a biochemical process is the source of the analytical signal (immunosensors, microbial potentiometric sensors are some examples). The transducer part is a device capable of transforming the primary signal containing the chemical information about the samples into an analytical signal easily usable (e.g., electronic). The transducer as such does not show any selectivity.

Chemical sensors may be classified based on the nature of the primary signal. According to that, they can be classified in electrical, electrochemical, magnetic, mass sensitive, optical, and thermometric¹. In this work, all the projects were performed using electrochemical transducers, so electrochemical sensors will gain relevance in the present dissertation. The principle of these devices is the conversion of the electrochemical interaction analyte-electrode into an useful signal. Within this group, the following categories may be distinguished as voltammetric sensors, potentiometric sensors, Chemically Sensitized Field-Effect Transistor (CHEMFET), and potentiometric solid electrolyte gas sensors. In the case of this study, all the works are based on voltammetric sensors.

Academically, when an analytical chemist starts his research trying to develop an electrochemical sensor, his purpose is to evolve a powerful device that includes all the specifications of an ideal sensor². However, the path has been evolving to a new perspective breaking the rules of this approach, because it is unmanageable and unnecessary for some applications.

In some instances, samples are complex and present more than one component, which makes difficult the determination. Classical approaches to solving this problem are the application of pre-treatment steps to remove or to mask the interfering species. However, this idea breaks the principle of a sensor, which tries to reduce the maximum number of steps in the analytical procedure. In addition, this strategy presents drawbacks in terms of increasing analysis time, cost of analysis, and the requirement of skilled personnel.

In other context, the problem is that the fingerprint of the molecules under study is practically identical. Therefore, when the signal is monitored, the response is translated into overlapped peaks on display. At this moment, this fact becomes an issue from an analytical point of view, hampering their quantification.

In our research group, the tool commonly employed to overcome such restrictions is the use of sensor arrays. With this recent approach, it is possible to outgrow the disadvantage given by classical strategies. What is more, sensor arrays bring some advantages comprising more chemical information.

Hence, if the analyst can work in controlled conditions, the signal proportioned by each sensor can be treated separately from the other components present in the sample matrix, becoming not necessarily a specific response for each analyte.

Contextualizing, the concept of sensor arrays had its previous development in past reviews by Diamond³ and Stefan *et al.*⁴. Recently, the concept was amplified by Ciosek and Wróblewski⁵. All these previous works demonstrated that sensor arrays are a clear example of integration in electroanalysis providing several advantages. Among others, the possibility to obtain multicomponent data without extra effort and the determination of many analytes in tandem using the same sample pre-processing. This fact can be acquired thanks to the use of multichannel electrochemical instrumentation, making easy storage, visualization, and processing of complex data.

In the deployment of the sensor arrays systems to electroanalysis, the field is capable to classify them in three main categories taking into account the purpose and the type of response (redundant, completely independent, or cross-sensitive)⁶. In this work, the sensor array employed is based on the cross-sensitive response, which is considered the most important for electronic tongue applications. Concretely, this array consists of several non-specific sensors with low selectivity that present a cross-response with slightly different sensitivities towards the analytes under study.

This combination provides the simultaneous determination of the substances present in a complex sample with the use of chemometrics tools to correct the interferences that occurs between them, which makes this approach interesting from an analytical point of view.

Thus, if the main concept is to use a sensor array, different signals must need to get complementary analytical information. To achieve it, different strategies must be implemented.

2. Chemically Modified Electrodes for Sensing

The challenging topic of modifying electrodes for creating new electrochemical devices is one of the continuous goals in the electrochemistry field.

Additionally, the creation of these new surfaces allows researchers to solve problems about overlapping signals when mixtures of compounds are detected simultaneously. In this context, the replacement of simple electrodes with new surface materials with improving stability, sensitivity, and selectivity has become a hot topic nowadays, contributing benefits in terms of improving response over the unmodified electrode avoiding their limitations.

Hence, the projects involved in this thesis are mainly focused on this concept, creating new surfaces for the resolution of mixtures of compounds.

According to the IUPAC Compendium of Chemical Terminology, a Chemically Modified Electrode (CME) is ***“an electrode made of a conducting or semiconducting material that is coated with a selected monomolecular, multimolecular, ionic, or polymeric film of a chemical modifier and that using faradaic (charge-transfer) reactions or interfacial potential different (no net charge transfer) exhibits chemical, electrochemical, and/or optical properties of the film⁷”***.

Several aspects such as mass transfer, thermodynamics, and kinetics of electron transfer must be controlled to consider these devices a powerful tool for some applications. At the end, the most important point is the surface properties of the electrode. Hence, the good behaviour of these electrochemical sensors depends on the electrode materials.

Before explaining extensively the different technologies for chemically modified working electrodes, it is important to consider the different materials commonly used for the fabrication of these devices, as well as the different types of sensor platforms usually available in the market.

2.1. Sensor Platforms

2.1.1. Materials

Generally, the most common materials used in electroanalysis for unmodified electrodes are carbon, gold (Au), mercury (Hg), and platinum (Pt). These materials present several advantages, but at the same time some limitations due to their inherent properties⁸.

Some of them include the fouling effect or application of higher potentials. In the case of mercury, toxic effects can be also included as negative aspects, making at this moment its use as practically residual.

The most conventional material used for electrochemical measurements is carbon. Carbon-based electrodes have an important role in electroanalysis because of their positive properties such as low background current, low price, chemical inertness, and broad potential window⁸, which make them appropriate for several sensing applications.

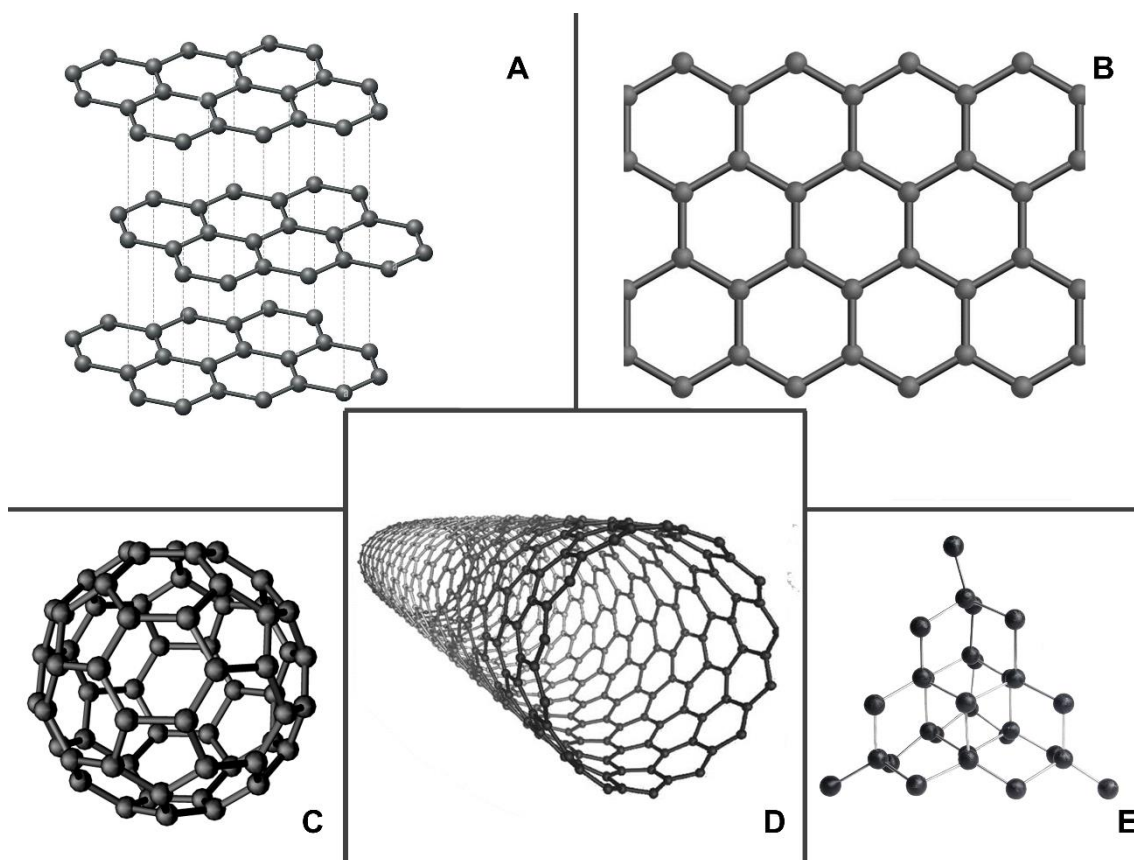


Figure I - 2. Chemical structures of crystalline allotropic forms of carbon: A) graphite, B) graphene, C) fullerene, D) carbon nanotube, and E) diamond.

Furthermore, this non-metallic element is one of the most abundant on Earth and is found uniformly distributed throughout the world. The singularity of this element is its concatenation property, which makes it attractive to form bonds with different or similar atoms. According to this property, it exists in two allotropic forms: amorphous and crystalline. The last commented has an ordered arrangement that includes diamond (sp^3), graphite (sp^2), carbene (sp^1), and fullerenes (distorted sp^2).

Among all, carbene and fullerenes are synthetic, meanwhile diamond and graphite are found in nature. Therefore, within this crystalline classification, it can be included two interesting materials, which play a relevant role for the construction of electrochemical sensors, which are graphene and carbon nanotubes (CNT). In the case of graphene, it is suitable as a carbon material because of its unique physical and chemical properties⁹. Moreover, the benefits of these physical and chemical properties are coupled with electrochemical advantages such as excellent electrochemical activity, low charge-transfer resistance, and wide potential windows, which make it a promising material for the electroanalytical area. In the case of CNT, they have been paid great attention since its discovery in 1991 by Iijima¹⁰. This structure offers several benefits such as anisotropic behaviour, biocompatibility, chemical stability, high surface to volume ratio, and high thermal and electrical conductivity¹¹. The properties discussed above make it an interesting candidate for the development of sensor platforms. Depending on the synthesis conditions, either single or multi-walled carbon nanotubes are formed. Single-Walled Carbon Nanotubes (SWCNT) are single cylinders, meanwhile, Multi-Walled Carbon Nanotubes (MWCNT) are concentric cylinders of graphite sheets¹². All the chemical structures can be represented in Figure I - 2.

As a summary, the versatility of carbon in electrochemistry could be mainly demonstrated, making it interesting for several applications.

2.1.2. Working Electrode Technologies

In this framework, the most common carbon sensor platform used in electrochemistry are Glassy Carbon Electrode (GCE) or Carbon Paste Electrode (CPE). Furthermore, novelty variety emerge considering Screen-printed Electrode (SPE) and Inkjet-printed Electrode (IPE).

In this thesis, all the research was performed by SPE and IPE. Hence, the last two mentioned technologies will be explained in more detail.

2.1.2.1. Glassy Carbon Electrode

GCE is a type of electrode made by carbon prepared by the controlled carbonization of polymeric resins such as polyacrylonitrile or phenol/formaldehyde in an inert atmosphere at high temperature i.e., about 1000 to 3000°C. Its structure is similar to a ribbon wherein the graphitic sheets are cross-linked. This fact makes it harder and more robust in comparison with graphite¹³. This sensational carbon type is commonly used in electroanalytical chemistry because of the broad mechanical and electrical attributes along with its wide working potential window in anodic and cathodic procedures^{14,15}.

The most common procedure to regenerate the electrode surface is a simple mechanical polishing to obtain a shiny mirror-like appearance using an alumina slurry of different particles size followed by sonication in deionized water or cyclohexane. This pre-treatment generates improved electron transfer kinetics, which can be associated with the removal of impurities and exposure of the fresh surface¹⁶. In the literature, there are also several methods for pre-treatment. Some examples are electrochemical, chemical, heat, and laser irradiation¹⁷.

2.1.2.2. Carbon Paste Electrodes

CPEs were reported by Adams in 1958¹⁸. Their discovery is related with Heyrovský polarography and Dropping Mercury Electrode (DME). The key point was to develop a “Dropping Carbon Electrode” (DCE), which simulate the DME performance for anodic oxidation of organic compounds, where the mercury-based electrode could not be used¹⁹.

CPEs consist on carbon powder (graphite) and organic solvents such as mineral oil, nujol, paraffin oil, silicone grease, and bromonaphthalene as binders (pasting liquid)²⁰. The carbon paste electrodes offer a broad range of advantages such as easy renewable surfaces, low cost, and low background current within electroanalysis^{21–23}. Furthermore, CPEs can be prepared to combine a modifier material with graphite powder and binder material, which further acts as modified electrodes for electrochemical measurements.

Nevertheless, this strategy is positive from the point of surface regeneration but presents problems of stability because of continuous leaching of modifier molecules during a large number of electrochemical measurements and also the presence of binder complicates the electrode kinetics, appearing inconvenients in operation stability, long term usage, and storage⁸.

Within this group, it is possible to classify our Graphite-epoxy Composites Electrodes (GECs), based on the same philosophy as CPE.

2.1.2.2.1. Graphite Epoxy Composite Electrodes

GECs are a variety of sensors commonly used in our *Sensors and Biosensors group* at Universitat Autònoma de Barcelona (UAB)²⁴.

These hand-made sensors are constructed filled a mixture of epoxy resin with a hardener and graphite powder in polyvinyl chloride (PVC) tube with a welded copper disk. More details about their construction are shown in Figure I - 3. Furthermore, it is possible to add some modifiers into the paste changing slightly the proportion between the epoxy resin/hardener and graphite.

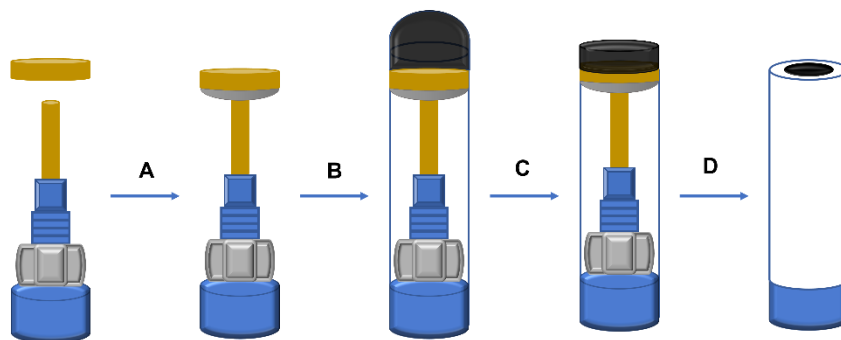


Figure I - 3. Different steps of GEC construction. (1) Weld copper disk, (2) Introduction of the connector in the PVC tube, (3) Fill the cavity with the composite paste, (4) Stage of polishing, and (5) Final device ready to be used.

In our laboratory, a battery of combinations is awarded depending on the final application. The most outstanding is the combination with metal nanoparticles (palladium (Pd)), metal oxides (copper (II) oxide (CuO)), conductive polymers (polyaniline o polypyrrole (PP)) and standard catalysts (prussian blue (PB), or cobalt (II) phthalocyanine (CoPc)), among others. The combination of the epoxy resin with graphite opens up some improvements as good mechanical properties, chemical resistance, low price stability, and adhesive strength^{25,26}.

In addition, it is possible to reuse the device many times with the regeneration of the surface via polishing. This fact makes the devices attractive in economic terms.

2.1.2.3. Printed Sensors

Printed sensors can be classified according to the operation mode of the printing technique employed. As a general classification, printing techniques can be considered as analog and digital printing. The main difference between them is the requirement of an exclusive mask for a contact process (analog), instead of a mask-less non-contact method (digital). More in detail these techniques can be classified as offset printing, gravure printing, flexographic printing, screen printing, and inkjet printing^{27,28}. In the work proposed, two main types of electrodes were explained in detail. One example employing analog printing technology is SPEs and one example of digital printing technique is IPEs.

2.1.2.3.1. Screen-Printed Electrodes

As the vast majority of technologic procedures, traditional techniques such as screen-printing technology has been adapted at the present time to the electroanalytical field with the main purpose of creating new sensors platforms to carry out fast and accurate analysis.

Screen-printing technology fulfils all these requirements offering a massive production because of inexpensive, highly reproducible, and reliable single-use devices from the 1990s until now. This method allows the possibility of improving on-site monitoring. For these reasons, SPEs are currently undergoing widespread growth.

The aforementioned technology consists of layer-by-layer depositions of ink upon a solid substrate, through the use of a screen or mesh, defining the geometry of the sensor. After this printing step, a thermal treatment is done after each ink layer to solidify it. The general fabrication process is outlined in Figure I - 4. During the printing stage of SPEs, the most used pastes are carbon and silver (Ag) inks. The working electrodes are mostly printed using graphite inks, whereas Ag ink is printed as a conductive track. Other materials such as Au and Pt based inks are also used in the construction of SPEs.

It is important to highlight the composition of the various inks used for printing on the electrodes determines the selectivity and sensitivity required for each analysis.

FABRICATION STAGE

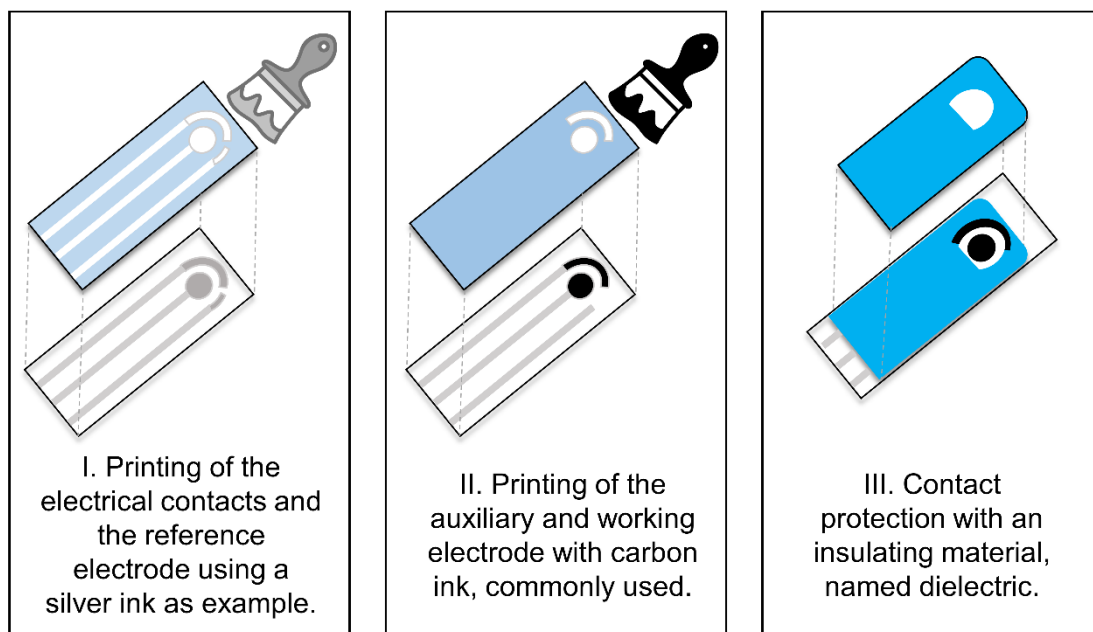


Figure I - 4. Schematic representation of the three important steps in the fabrication process of SPEs. I) Printing of electrical contacts and the reference electrode using silver ink as an example. II) Printing of the auxiliary and working electrode with carbon ink, commonly used, and III) Contact protection with an insulating material named dielectric.

SPEs generally includes a three-electrode configuration (working, counter, and reference electrodes) (Figure I - 5) printed on various types of plastic or ceramic substrates, which is easily modifiable with a great variety of commercial self-made inks.

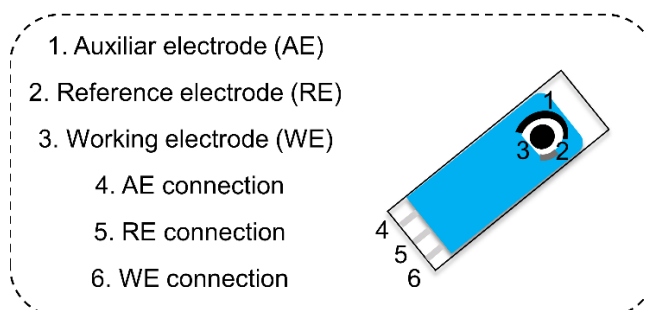


Figure I - 5. Different components of an SPE. 1) auxiliary electrode (AE), 2) reference electrode (RE), 3) working electrode (WE) and their respective connections.

The plastic materials were found to be cheaper, and the carbon ink adheres strongly with the plastic surface compared to the ceramic surface. However, a few years ago it was rediscovered an alternative material for substrate sensor, which is cellulose²⁹.

Paper has been present in the globe of analytical chemistry for centuries, but in recent years, the concept of considering themselves a substrate for sensing devices provoked a huge impact. This simple cellulosic substrate presents an extensive range of benefits, which makes it the former candidate for disposable sensors and integrated sensing platforms. Several examples are good mechanical properties, three-dimensional fibrous structure, biocompatibility and biodegradability, easiness of production and modification, reasonable price, and availability all over the earth³⁰. Kubota *et al.* present in the literature some works using paper-based sensors, showing recently innovative applications^{31,32}. Furthermore, the paper substrate material is gaining relevance in portable Enzyme-linked Immunosorbent Assay (ELISA), proportionating fast results around 40 min, in comparison with traditional methods consuming more time per assay (3 h)³³. In addition, in the microfluidic field, this kind of substrate gives considerable profit in economic terms. The cellulosic substrate is 200 times less expensive than polyethylene terephthalate (PET) and 1000 less expensive than glass^{34,35}. In summary, the rediscovery of such material has implemented some advantages for the sensing world.

Hence, SPEs present some advantages, as well as drawbacks. Positive aspects include easy fabrication, low-cost production, and miniaturization. The principal benefit associated with the miniaturization is the reduction of sample volume required, which is interesting for some experiments wherein this volume is restricted in terms of connecting it to portable instrumentation for *on-site* analysis. Moreover, these devices are capable of providing good flexibility, automation, and acceptable reproducibility. Besides, the surface of SPEs can be easily modified to create a new surface with improved electrochemical aspects. In addition, SPEs have the advantage of being one-shot disposable sensors strips and require no polishing of the electrode surface, as is usually the case for more conventional solid electrodes commented previously³⁶.

However, to be realistic of them, certain kind of limitations also appears. The use of aggressive media or organic solvents can produce some damage to the deposited inks on the substrate, generating problems such as a decrease in the limit of detection and sensitivity³⁷. This negative aspect can be turned upside down, coupling this drawback with the green chemistry concept, trying to substitute aggressive media with sustainable solvents in electrochemical measurements. This idea is a challenge not only for electrochemistry but also for chemistry, which is on the way for developing ionic liquid solvents, for example, replacing the most comment employed organic solvents.

The most common applications for the use of these SPEs³⁸ are the development of biosensors, environmental monitoring assays³⁹, and clinical trials, among others found in the literature.

In the present dissertation, the most common sensor platforms used were based on screen-printed devices. For the first work, an integrated sensor of eight working electrodes was used. The substrate in this case was ceramic. Meanwhile, in the works based on the detection of opioids and their respective cutting agents, single sensors were used employing plastic as a substrate.

2.1.2.4. Inkjet-printed Electrodes

Before getting down to business with this kind of sensor platforms, a brief introduction must be done to understand how this technology is managed. IPEs are built using inkjet printing (IJP). IJP is a digital technique based on a mask-less procedures, which means that is a feasible switch from one design to another without the use of a mask. It is well known that the use of these masks makes it more expensive the stage. Furthermore, it is classified as a non-contact technique, in which materials are deposited onto the substrate in a drop-by-drop way using a micrometric nozzle head.

According to that, the IJP technique can be classified into two main groups: continuous inkjet (CIJ) and drop-on-demand (DOD) (Figure I - 6). CIJ was the first inkjet technology used. It is based on a continuous ink ejection and by acoustic pressure waves, the stream is adapted into volume-regulated droplets (Figure I - 7A).

In DOD techniques, a single drop is ejected by the cartridge nozzle to get the final pattern. Within this group, three types can be classified, which are thermal inkjet, piezoelectric and electrostatic inkjet. The most commonly used techniques are thermal and piezoelectric inkjet. For this reason, slight details are shown about the different operation modes.

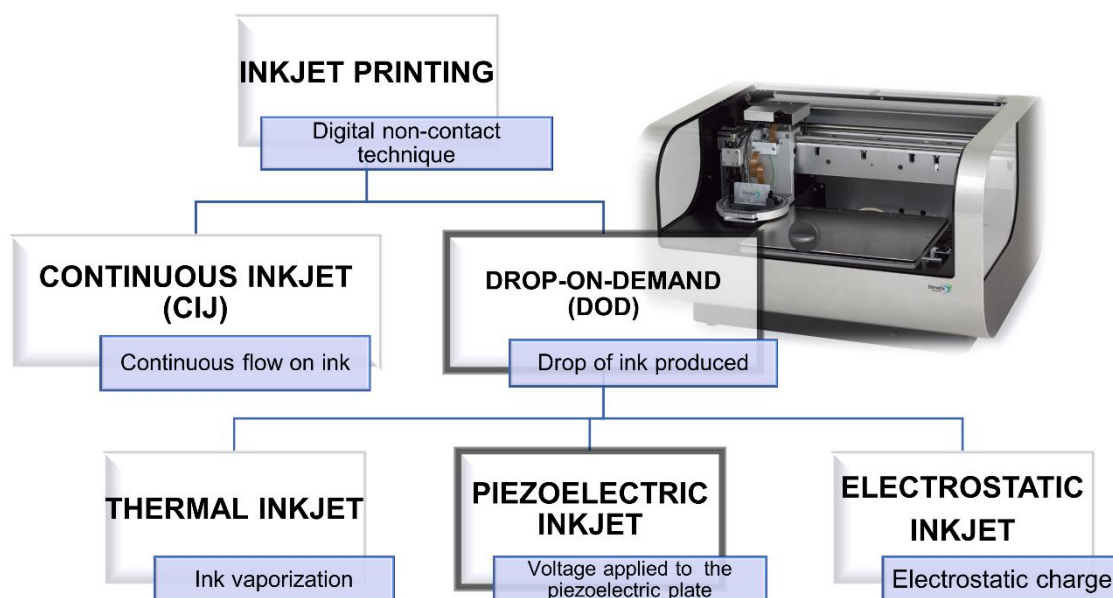


Figure I - 6. Classification of the different strategies of the inkjet printing technique. DOD and piezoelectric inkjet were selected as applied techniques.

Thermal inkjet nozzles are composed of two parts: a resistive heater and an ink reservoir. The operation mode is based on applying a pulse of current inserted on the resistive heater producing vaporization of the ink. After this procedure, a bubble is generated and with a pressure force, the ink (in a droplet form) is propelled. Then, the heater cools down generating a vacuum and the ink reservoir is refilled for a new injection (Figure I - 7 B.1).

It is important to mention that this strategy presents drawbacks, basically in two aspects. Residues are accumulated on the resistive heater causing a short lifespan in nozzles. What is more, specific ink is required to support rapid thermal changes mentioned in the procedure. These negative aspects make this option not feasible in many cases, where inks used are not compatible with this heat treatment.

Opposite to this option exists the piezoelectric systems (Figure I - 7 B.2). In this case, there are commonly used, and the operation mode is quite different.

In this case, a voltage is applied to the piezoelectric plate to cause a deflection, generating an acoustic wave that is propagated inside the chamber and ejects the droplets. This step is quite fast in comparison with the previous commented, which needs a cooling step.

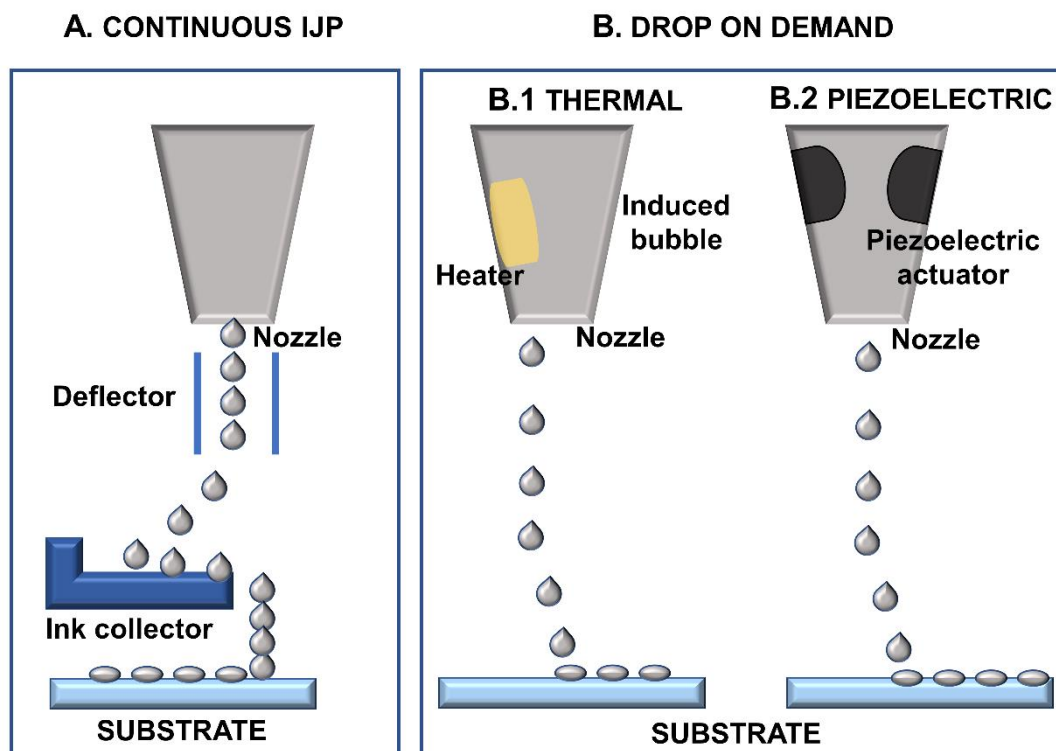


Figure I - 7. Schematic representation of the two of the most common inkjet printing techniques. A) CIJ and B) Drop-on-demand, remarking B.1) thermal and B.2) piezoelectric.

The construction of the IPEs is quite similar to other printing techniques such as microfabrication or screen-printing. The idea is to deposit patterned and stacked layers of conducting and dielectric materials on a substrate. At the end, a drying and a sintering/curing step is required to fix the ink. Schematic representation of all the steps is represented in Figure I - 8.

As the conductive material, focused on the electrochemical sensor field, the most employed are carbon nanomaterials^{40,41} (graphene), conducting polymers ((poly(3,4-ethylenedioxythiophene) polystyrene sulfonate) (PEDOT: PSS))⁴², polyaniline (PANI)⁴³, Au^{44,45} and Ag⁴⁶. The insulator materials (dielectric) used as protection of the conductive tracks are common polymers (poly(amic acid))⁴⁷, or SU-8⁴⁸, among others.

Referring to substrates, the most common is polyethylene naphthalate (PEN)⁴⁵, PET⁴⁹, polyimide (Kapton)⁴⁷, and paper⁵⁰. But it is possible to consider rigid substrates as glass⁴⁸ or silicon⁵¹.

Eventually, to conclude with this section it is important to present advantages and disadvantages and to study whether it is worthwhile or not.

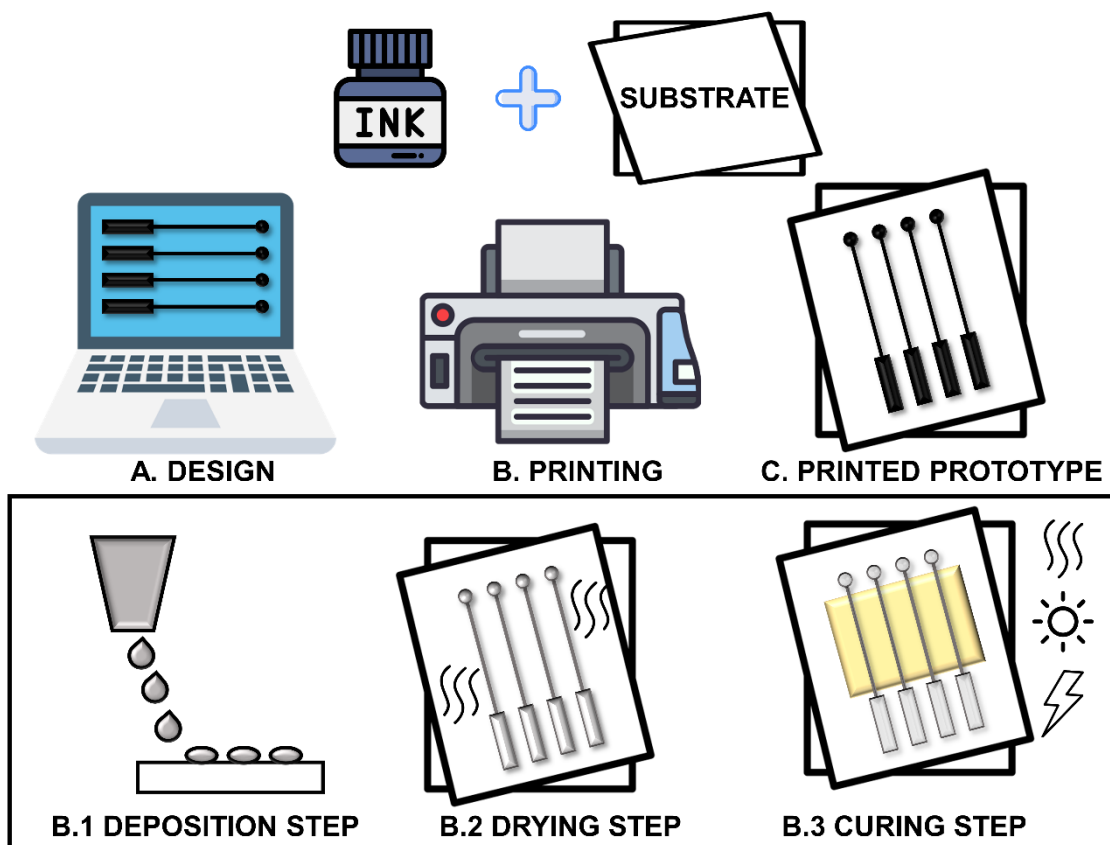


Figure I - 8. Schematic procedure of all the steps of the fabrication of inkjet-printed devices. A) Design, B) Printing, and C) Printed prototype. The steps in detail of the printing process are shown in B.1 deposition, B.2 drying, and B.3 curing step.

On the one hand, the waste of material and ink consumption is minimum and IJP can produce patterned thin films with resolutions around 100-500 nm. As mentioned previously, the technique allows the use of rigid substrates, an aspect not manageable for alternative printing techniques.

On the other hand, to employ this printing technique, it is very important to characterize perfectly all the properties (viscosity, surface tension) of the used ink. In this sense, it presents a difficulty and extensive studies must be done before using them.

Furthermore, the high cost of research equipment is the main factor limiting this technology in the current years and commercial functional inks are expensive, scarce, and have very limited shelf-life. Thus, many researchers are working on the development of self-formulated inks to deal with this problem.

In summary, IJP techniques have a relevant role in several fields of studies, gaining relevance in the environment, biomedical, and food safety applications, as well as research and prototyping goals, specifically in the electrochemical sensor field⁵².

In the present dissertation, IJP techniques will be the focus of the use of an array of five electrodes to detect some cocaine cutting agents simultaneously. To achieve that inkjet sensors platforms were fabricated using DOD technology based on piezoelectric methods.

2.1.3. General Overview of 3D Printed Sensors

As a new trend in sensors platforms, additive manufacturing (AM), well known as three-dimensional (3D) printing has remerged as an alternative in the electrochemical sensors field since 2012⁵³.

Favourable aspects such as low-cost production, variety of geometries, use of a wide range of materials are remarkable^{53,54}. The most common fabrication techniques are classified into three main categories such as Stereolithography (SLA), Fused Deposition Modeling (FDM), and Selective Laser Melting (SLM). As literature showed, the most common technique employed is the first one for its simplicity.

FDM was created by Scott Crum in 1989. The background of the technique is based on the use of thermoplastic materials. Some examples of them are polylactic acid (PLA) and acrylonitrile butadiene styrene (ABS). The main concept is that these materials are heated and extruded from a nozzle to be deposited in layers. The key point is to heat the material until the semi-molten state, then they are deposited as the material solidifies to generate a hardened layer after settling down of the previously made layer (Figure I - 9). These materials are mixed with carbon allotropes to get carbon composite filaments which are used as conductive printable materials.

What is more, the combination also can be done with noble metals (Pt, Au, iridium (Ir), or bismuth (Bi), as examples). In comparison, carbon-based electrodes gain much relevance in the 3D printing field in comparison with noble metals. Although their promising results, their use is expensive, and the variety of materials can restrict some applications.

It is important to consider that using this strategy, it is possible to generate layer thickness in the range of 0.1 to 0.4 mm. Therefore, making a balance of all the factors, FDM represents the most selected 3D printing technology to its simple operation mode. Furthermore, materials and machines are considered affordable in economic terms.

About the fabrication process, three important steps must be deemed, which are the single-step fabrication, the optimization of printing parameters, and depending on the situation, an electrochemical, chemical, or biological pre-treatment to improve the electrochemical behaviour of the sensors⁵⁵. Main applications of this kind of technology can be found in biomedical science⁵⁶, environmental monitoring as well as heavy metal determination⁵⁷.

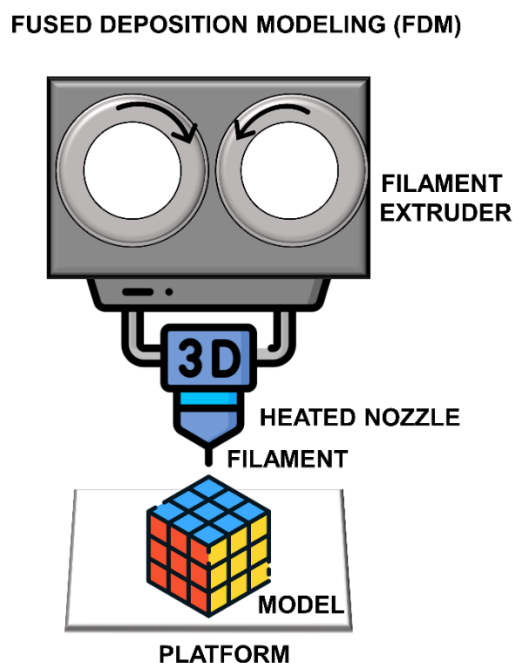


Figure I - 9. Scheme of the operation mode of the most commonly used 3D printing technique (FDM).

2.2. Modification Approaches

Modified electrodes have gained much interest within the area of electroanalysis from past decades, due to the ability to have direct control over the surface structure of the electrode⁵⁸.

Historically, the concept was first introduced by Royce Murray in 1970 from his work in the modification of tin (IV) oxide (SnO_2) electrodes with amine groups. The amine-modified electrode surface has been used for functionalization with various electroactive organic moieties through coupling reactions⁵⁹.

The key point in the modification of the electrode is the electrode/solution interface because all electrochemical reactions occur there. Therefore, the surface structure of the electrode at the interface plays a distinct role in the electrode reaction and it promotes the pathway for the transfer of electrons at the interface which in turn gives the better electrode kinetics⁶⁰.

There are several strategies to modify the electrode surface in the literature⁷. All of these can be broadly grouped into five types namely (i) chemisorption, (ii) covalent bonding, (iii) polymer film coating, (iv) composite, and (v) entrapment through the formation of conductive ink, among others. The last option is more used in this research due to its benefits. The next section will be focused on showing details about its implementation.

2.2.1. **Entrapment through the Formation of a Self-formulated Conductive Ink Via Drop casting**

Since the beginning of the creation of the *Sensors and Biosensors group*, GECs²⁴ are a variety of sensors commonly used for their simplicity and low-cost construction.

These hand-made sensors are constructed filled a mixture of epoxy resin with a hardener and graphite powder in PVC tube with a welded copper disk. More details about their construction are shown in §2.1.2.2.1. Furthermore, it is possible to add some modifiers into the paste changing slightly the proportion between the epoxy resin/hardener and graphite.

Because of this idea, a new concept emerged. In this case, the novelty has incorporated the modifiers (Figure I - 10) in the electrode surface, avoiding introducing it in the bulk paste previously explained. This approximation was applied for the first time by A. Cipri *et al.* in 2014⁶¹. In the mentioned article, the ink-like composite was prepared with MWCNT/Pd, as a modifier, with the proportion proposed in the literature⁶¹. Therefore, a new approach will be assessed by combining different sensors platforms.

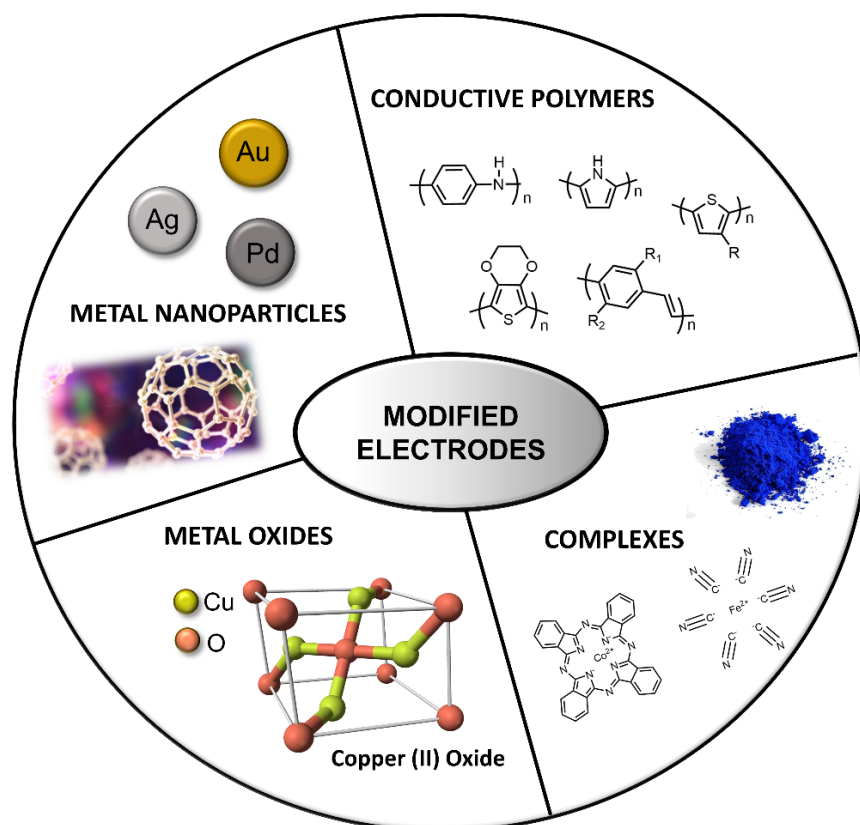


Figure I - 10. A variety of modifiers can be included in the formulation of the ink-like composite ink. Metal nanoparticles, metal oxides, conductive polymers, and complexes as CoPc or PB are some examples.

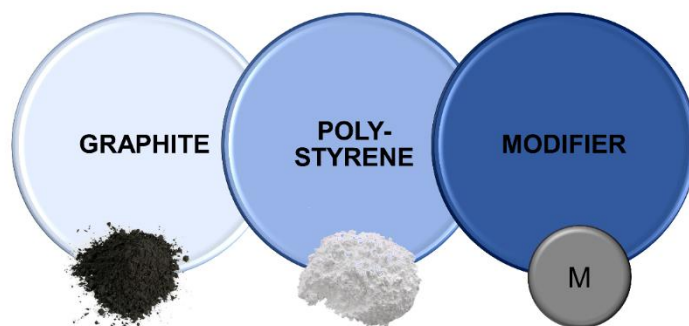


Figure I - 11. Graphical components of the modification ink. All the compounds were dissolved in mesitylene as a binder. The proportions were adapted from⁶¹.

In detail, this strategy is a chemical modification that consist on the formation of a conductive ink-composite. The mentioned nanomaterial is formed by graphite as a conductive material, a polymer, in this case, powdered polystyrene to perform the crosslink, mesitylene as a binder, and the incorporation of the corresponding modifier (Figure I - 11).

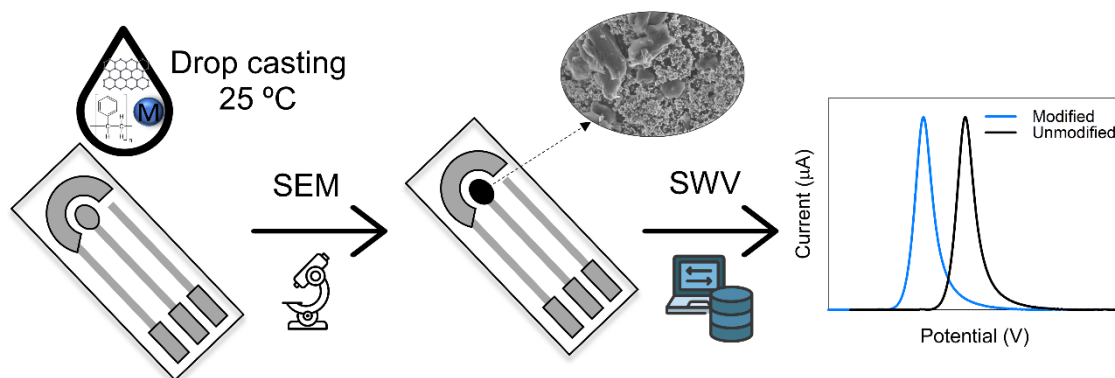


Figure I - 12. Experimental setup of the modification of the electrode surface using a self-formulated ink and drop-casting method.

The mixture was thoroughly mixed and sonicated to obtain a medium-thick solution. The ink-like composite is dropped onto the electrode surface and dried at medium temperature to remove the solvent (Figure I - 12).

When the electrode is completely dried, an activation step with hydrogen peroxide (H_2O_2)^{62,63} is done in some cases. This activation is sometimes needed depending on the sensor platform used and the material of the substrate. After activation, electrodes were rinsed with deionized water and dried in air.

3. Analytical Electrochemistry

Electrochemistry is the branch of chemistry concerned with the interrelation of electrical and chemical effects. This field deals with the study of chemical changes caused by the passage of an electric current and the production of electrical energy by chemical reactions⁶⁴. The field of electrochemistry includes an assortment of different fields (e.g., corrosion electrophoresis), batteries, devices (electroanalytical sensors and electrochromic displays), and fuel cells.

Techniques based on electroanalysis are associated with the interplay between chemistry and electricity, specifically, the measurements of electrical quantities (charge, current, or potential) and their relationship to chemical parameters.

The concept of using electrical measurement to perform analytical studies has found a wide range of applications, being the most remarkable biomedical analysis, environmental monitoring, or industrial quality control.

Electrochemical processes take place at the electrode-solution interface, unlike many chemical measurements, which involve homogeneous bulk solutions. Electroanalytical techniques differ in the type of electrical signal used for the quantification. Therefore, electroanalytical measurements can be classified into two main groups, which are potentiometric and potentiostatic⁶⁵. Either way requires at least two electrodes and an electrolyte, which constitute the electrochemical cell. The nature of electrochemical cells will be explained in more detail in future sections, but in general terms they are classified into electrolytic, which means they consume electricity from an external source or galvanic, which are used to generate electrical energy.

Electroanalytical techniques can be distinguished also depending on if the parameter controlled is the potential or the intensity. The present dissertation will be dealing with controlled-potential methods. These types of techniques are based on the study of charge transfer processes at the electrode-solution interface. Specifically, the application of a potential makes chemical species loss or gain electrons, corresponding to the oxidation and reduction reactions. Consequently, the obtained current shows the rate at which electrons move across the electrode-solution interface. As a conclusion, potentiostatic techniques can measure any electroactive chemical species. Therefore, it is possible to determine the electroactivity for a given compound by knowing the reactivity of its functional group. When chemicals species are non-electroactive, there also are strategies to its determination based on indirect or derivatization procedures.

Furthermore, they present positive aspects such as a huge linear range, high selectivity, and sensitivity toward electroactive species, low-cost instrumentation speciation capability, and portability. Summarizing the use of these strategies proportionate low detection limits and requirement of small sample volumes.

Before explaining the different electroanalytic techniques used in this work, it is convenient to settle in basic concepts based on the electrochemical field.

3.1. Key Points to run Electrochemical Measurements

3.1.1. Faradaic and Non-Faradaic: The Concept

The electrochemical proceedings occurred at electrodes may be classified as faradaic and non-faradaic. The first type, which are named in this way for being events that follow the Faraday law (i.e., the reaction of 1 mol of substance involves a change of $n \times 96487$ C), promotes reactions in which electrons are transferred across the metal-solution interface. This electronic transfer induces oxidation and reduction reactions. In addition, the faradaic current is a direct measure of the rate of the redox reaction. By contrast, the non-faradaic procedures are based on adsorption and desorption as examples. In this case, the structure of the electrode-solution interface is modified by changing potential or solution composition. In this project, the vast majority of the proceedings developed are faradaic.

So, as it was commended previously, the main goal of controlled-potential electroanalytical assays is to get a current response that can be associated with the concentration of the target analyte. This fact can be done by monitoring the transfer of electron(s) during the redox process according to Equation I - 1, where A and B are the redox couple.



This redox reaction happens in a potential zone that is favoured the electron transfer thermodynamics. The potential of the electrode can be used to obtain the concentration of electroactive species according to the Nernst equation (Equation I - 2):

$$E = E^0 = \frac{2.3 RT}{nF} \log \frac{CA(0,t)}{CB(0,t)} \quad \text{Equation I - 2}$$

Where E^0 is the standard potential for the redox reaction, R is the universal gas constant ($8.314 \text{ J}\cdot\text{L}^{-1}\cdot\text{mol}^{-1}$), T is the Kelvin temperature, n is the number of electrons transferred in the redox reaction, F is the Faraday constant (96487 C).

3.1.2. Electrochemical Cells, Solvents, and Supporting Electrolytes

The instrumentation required to perform electrochemical measurements has a relatively low cost and is available commercially. It is formed by a cell (normally a three-electrode system), a potentiostat, and a laptop to monitor the signal (Figure I - 13).

In controlled-potential experiments, the most common performance is formed by three electrodes⁶⁶. Normally, the three electrodes (counter, reference, and working) are submerged between 5-50 mL, seeking to save the amount of solution.

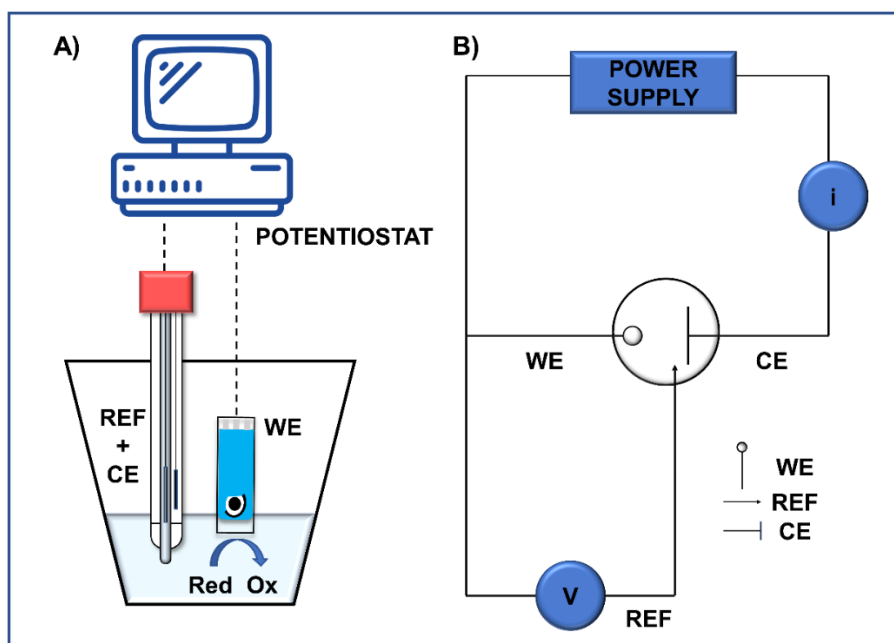


Figure I - 13. A) Experimental setup of an electrochemical cell. B) Scheme of the three-electrode electrochemical cell configuration.

The counter electrode (CE) (or auxiliary electrode) is used to close the current circuit in the electrochemical cell. It is made by inert material (Glassy Carbon (GC), graphite, Pt, Au) and usually does not contribute to the redox phenomenon. The total surface area of the CE must be higher than the area of the WE so that it will not be a limiting factor in the kinetics of the electrochemical procedure under investigation because the current is flowing between the WE and the CE.

The RE has a stable and well-known electrode potential. It is commonly used as a point of reference in the electrochemical cell for potential control and measurement. Its high stability is usually reached by employing a redox system with constant (buffered or saturated) concentrations of each participant of the redox reaction.

The WE is the electrode in which the reaction of interest takes place. Classical working electrodes are made of inert materials such as GC, Au, Ag, Pt. Variety of shapes and sizes can be found depending on the final application.

Electrochemical measurements are performed in a medium of a solvent containing a supporting electrolyte. The key point is that the solvent does not react with the analyte and should not undergo electrochemical reactions over a wide potential range. All of these requirements promote MilliQ water such a proper candidate, being the most commonly used in electrochemistry. The use of non-aqueous solvents (dimethylformamide (DMF), dimethylsulfoxide (DMSO), acetonitrile (ACN), or methanol (MeOH) has also been described. However, it is true that to protect the world everything is evolving towards green chemistry, avoiding the use of aggressive and toxic media⁶⁷.

The role of supporting electrolytes is also crucial in the electrochemical measurements because they decrease the resistance of the solution, erasing electromigration effects and maintaining a constant ionic strength. The most used are potassium chloride (KCl) or potassium nitrate (KNO₃), ammonium chloride (NH₄Cl), sodium hydroxide (NaOH), or hydrochloric acid (HCl) when water is employed as a solvent, tetraalkylammonium ((CH₃)₄NCl) salts are often employed in organic media. The use of buffer systems (such as acetate, phosphate, or citrate) remains important when pH control is essential.

3.2. Electrochemical Techniques

3.2.1. Voltammetry

Voltammetry is classified within the group of electroanalytical methods where information about the analyte is provided by measuring a current as a function of an applied potential under conditions that promote polarization of a working electrode.

Historically, voltammetry's field was developed from polarography, discovered by Czech chemist Jaroslav Heyrovský in the early 1920s. He was awarded the Nobel Prize in Chemistry in 1959 for his achievement. Polarography is different in comparison with other voltammetry types referring that the working microelectrode employed as the DME.

Voltammetry was used by many inorganic chemists, physicists, and biologists to study oxidation and reduction processes in different media, electronic transfer mechanisms on chemically modified electrode surfaces, and adsorption processes. Some years ago, voltammetry, concretely classic polarography, was a relevant tool used by chemists to determine inorganic ions and chemical species in aqueous solutions.

However, in the late 1950s and early 1960s, these applications were largely replaced by other spectroscopic methods, and voltammetry became less important in analysis, excluding applications such as the determination of molecular oxygen in solution. In the mid-1960s, certain important modifications were developed in classical voltammetry techniques, which significantly enhanced the sensitivity and selectivity of the methods and instrumentation. The result of this progress became a revival of interest in voltammetry techniques. Particularly, they were applied to detect species of pharmaceutical interest.

Furthermore, voltammetry coupled with some chromatographic methods such as High-performance Liquid Chromatography (HPLC) has become a very useful tool for the analysis of a mixture of different analytes.

Nowadays, current voltammetry persists to be a powerful technique used in many areas such as biochemistry, chemistry, the environmental sciences for studying oxidation, reduction and adsorption processes, materials science, and engineering.

The response of the set of voltammetry techniques depends on the application of the employed excitation signal. This excitation signal (which is a variable potential) is applied and it causes a current intensity response with a characteristic form. The standard voltammetric excitation signal is the linear scan, where the voltage applied to the cell increases linearly as a function of time.

The range of a complete scan may be as small as a few hundred millivolts or as large as 2-3 V.

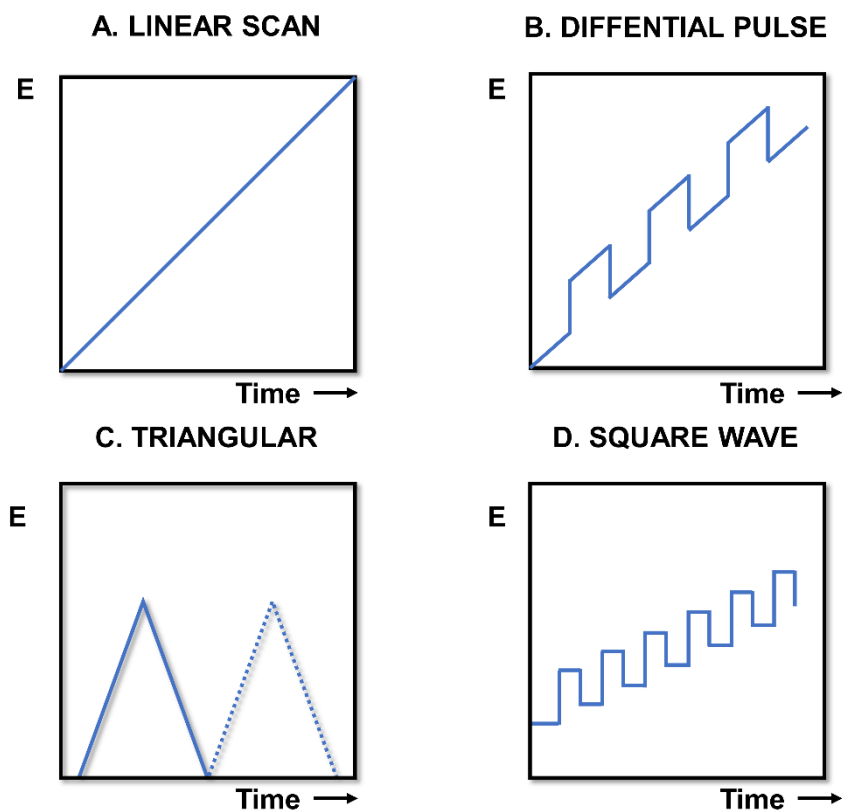


Figure I - 14. Voltage versus time excitations signals used in voltammetry. (A) Linear scan, (B) Differential pulse, (C) Triangular, and (D) Square wave.

Referring to the current in the cell, it is recorded as a function of time, and thus as a function of the applied voltage. Another type of excitation is a pulse. As it can be observed in Figure I - 14, two types can be observed, which correspond to differential pulse (Figure I - 14B) and square wave (Figure I - 14D). Lastly, another possibility is the triangular waveform shown in Figure I - 14C when the potential is cycled between two values. Firstly, there is an increasing linearly to a maximum and then decreasing linearly with the same slope to its original value.

In the present thesis, the most common electrochemical techniques employed were based on a triangular (Cyclic Voltammetry (CV)) and square wave excitation signal (Square Wave Voltammetry (SWV)). Both will be commented in detail in the following sections.

3.2.1.1. Cyclic Voltammetry

CV is classified within the electroanalytical techniques, specifically, controlled potential techniques. It is the most suitable technique employed for acquiring qualitative information about the electrochemical redox process. It offers a rapid visualization of redox potentials of the electroactive species and a convenient evaluation of the effect of the solvent in the redox reaction. In addition, this technique is also powerful to provide information about the kinetics of heterogeneous electrons transfer reactions and thermodynamics of redox processes.

Theoretically, the technique is based on scanning linearly the potential of a stationary working electrode (without stirring) using a triangular potential waveform, as an excitation signal. Single or multiple cycles can be applied depending on the final application. The potentiostat measures the current resulting from the applied potential during the potential sweep. The obtained current-potential diagram is called *cyclic voltammogram* (Figure I - 15B).

Therefore, the important parameter in a cyclic voltammogram is the cathodic peak potential (E_{pc}), the anodic peak potential (E_{pa}), the cathodic peak current (i_{pc}), and the anodic peak current (i_{pa}). In the case of the study, which is a reversible electron reaction system, anodic and cathodic peak currents are approximately equal in absolute value but opposite in sign. For this kind of system, the difference in peak potential, ΔE_p , is expected to be:

$$\Delta E_p = |E_{pa} - E_{pc}| = \frac{0.0592}{n} \quad \text{Equation I - 3}$$

Where n is the number of electrons involved in the half-reaction, in this case, $n=1$. The peak current for a reversible couple (at 25^o) is described by the Randles-Sevcik equation⁶⁴:

$$i_p = (2.69 \times 10^5) n^{\frac{3}{2}} A C D^{\frac{1}{2}} \nu^{\frac{1}{2}} \quad \text{Equation I - 4}$$

Where n is the number of electrons, A is the electrode area (in cm²), C the concentration (in mol/cm³), D the diffusion coefficient (in cm²/s), and ν the potential scan rate in V/s.

Accordingly, the current is directly proportional to concentration and increases with the square root of the scan rate. Hence, CV also allows the termination of diffusion coefficients if the rest of the parameters are known.

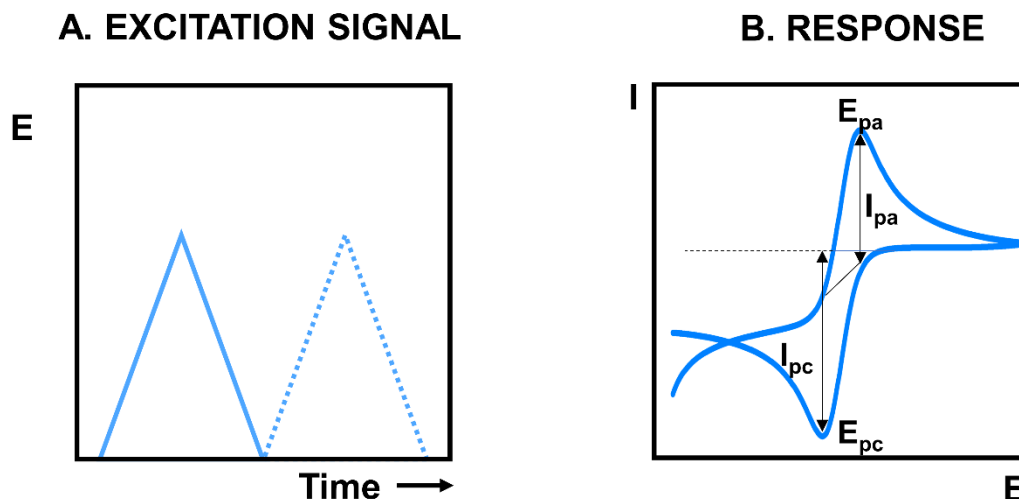


Figure I - 15. A) Excitation signal of CV. B) Voltammogram obtained using CV technique.

It can be occurred also that some of the systems studied are irreversible or quasi-reversible. In this case, the problem is afforded differently by following the equations found in the literature⁶⁴.

In conclusion, CV is highly useful in specific situations because it is possible to obtain more information about the completed voltammogram. However, there are other scenarios where the use of more sensitive techniques such as SWV is necessary.

3.2.1.2. Square Wave Voltammetry

By the 1960-decade, linear sweep voltammetry and similar voltammetry techniques become less relevant in the analytical chemistry field. This fact can be explained because these techniques have some disadvantages such as slow response and poor detection limits. These limitations were solved by the development of pulse methods. The most employed are square wave SWV and Differential Pulse Voltammetry (DPV). Since SWV was more used in this thesis, it will be focused on its theoretical background.

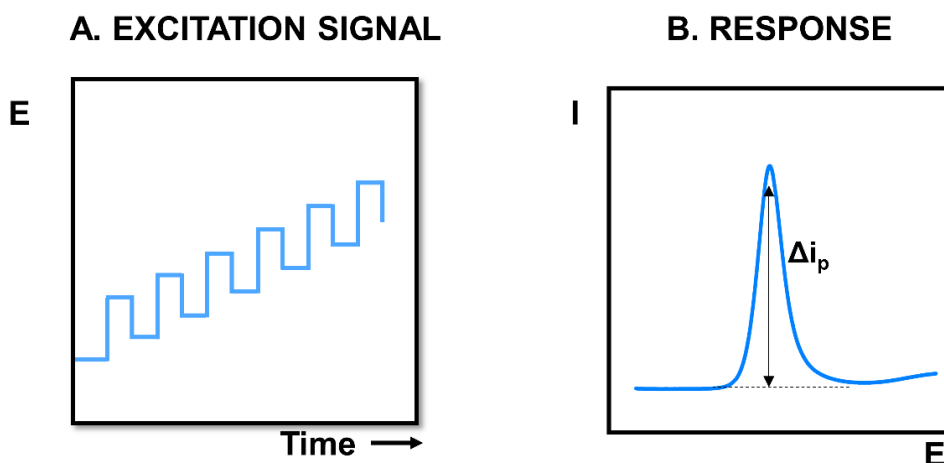


Figure I - 16. A) Excitation signal of SWV. B) Square wave voltammogram using SWV as technique.

The excitation signal is based on a symmetrical square wave pulse of amplitude superimposed on staircase waveform of step height ΔE (Figure I - 16A). The forward pulse of the square wave matches with the staircase step. The net current, i_{net} , is obtained by taking the difference between the forward and reverse currents ($i_{for} - i_{rev}$) and is centred on the redox potential. The peak height is directly proportional to the concentration of the electroactive species. The sensitivity of SWV is about two to three times higher than DPV showing detection limits for SWV are reported to be 10^{-7} to 10^{-8} M. What is more, it presents the rejection of background currents and excellent sensitivity. In addition, measurements are running very fast in comparison with other methods, which makes them interesting.

Some applications are the study of electrode kinetics about preceding, following, or catalytic homogeneous chemical reactions, determination of some species at trace levels, and its use with electrochemical detection in HPLC.

4. Biomimetic Systems

Nowadays there has been a change in analytical chemistry referring to the strategy on handling information in the measurements process. As commented previously, the first approximation was based on getting information on quantitative analysis of specific compounds using specific sensors to measure single parameters (§1). Currently, the aim was slightly modified incorporating sensor arrays with low selectivity to resolve mixtures of compounds.

Thanks to the rich information given by these sensor array systems, the novelty in the analytical chemistry field is to draw a parallel from the natural world leading to the famous biomimetic systems. Simplifying, these systems are born from the fusion of sensors combination and mathematical treatment. These challenging systems are focused on mimicking different senses of mammals, a principle that together with a complex stage of information processed in the brain, allows the quantification or qualification of a great number of substances.

In this way, these types of systems have a different approach in comparison with classical methods. In this case, low selective and/or cross-responsive sensors are required to obtain complementary and rich analytical information. After, this multi-dimensional information needs to be processed with data treatment strategies. This step requires the implementation of chemometrics science. The combination of both concepts has been declared one of the ways of progress in developing new sensing schemes.

Therefore, two parts can be differentiated in this kind of system. At first instance, the matrix of sensors, which tries to simulate different senses and perceptions, and not least the chemometric tools, which allows the processing of the collected data obtaining a response as the brain would.

In the current state of art, the main biomimetic systems developed are based on three mammal senses: sight, smell, and taste⁶⁸. Using the same principle, are named electronic eye (EE), electronic nose (EN), and electronic tongue (ET).

All the experimentations done in this dissertation will be focused on the last mode, for this reason, the next step is the centre of attention to the details using these electronic tongues systems type.

4.1. Electronic Tongue Systems as Analytical Devices

As previously commented, the strategy relies on approaching the human tongue and the electronic tongue system. To achieve it, it is important to know how human taste works.

4.1.1. Analogy between the Human Taste and Electronic Tongue systems

Mammals are believed to have five taste modalities that are bitter, salty, sour, sweet, and umami. Several studies in humans have reported that different zones of the tongue show different gustatory preferences, and numerous physiological studies in animals have shown that taste receptor cells can respond in a selective way to different tastants⁶⁹.

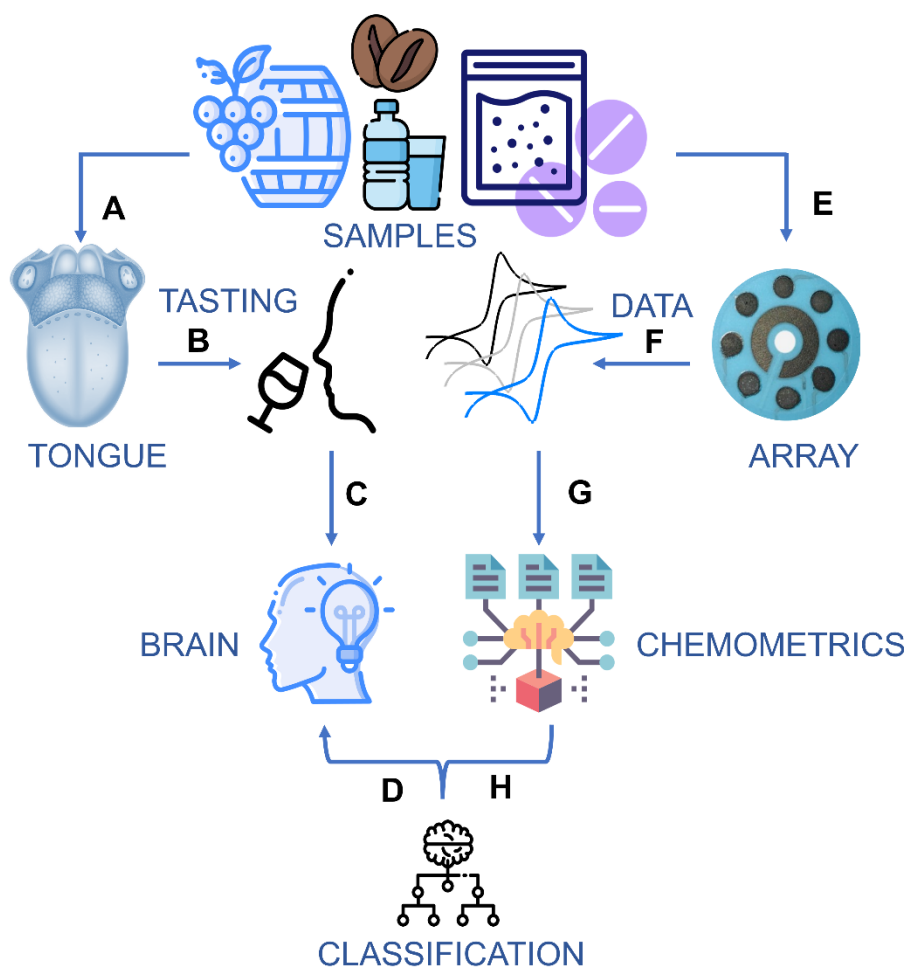


Figure I - 17. The analogy between the human taste (left) and the electronic tongue approach (right).

In brief, the concept of ET is based on imitate the biological system. As it can be observed in Figure I - 17, taste buds in the tongue (A) when keep in contact with foodstuffs (B) send an electrical stimulus to the brain (C), which can group them into specific patterns to classify tastes (D). In parallel, a sensor array modified (E) in contact with liquids (F) creates a fingerprint of the analytes thanks to different electroanalytical responses. Multi-component information can be treated using chemometrics (G) to finally identify a taste or sample (H).

4.1.1.1. History, Types, and Applications

According to IUPAC, an electronic tongue is defined as **“a multisensor system, which consists of several low-selective sensors and uses advanced mathematical procedures for signal processing based on pattern recognition (PARC) and/or multivariate data analysis [artificial neural networks (ANNs), principal component analysis (PCA), etc.]”**⁷⁰. The use of this system applied to analysis in liquids provide multidimensional analytical information after the proper chemometric treatment, which can extract the maximum chemical information from convoluted data.

The beginning of the ET was proposed in the late 1990s⁷¹ by a collaboration of two sensor groups in Europe, Prof. Vlasov group in Saint Petersburg University and D'Amico group in Tor Vergata University in Rome to describe an array of sensors using ion-selective sensors (ISEs)^{72,73}. In 1989, Toko *et al.* presented the first electronic tongue, that later was made commercially available. The mentioned array was called “taste sensor” and it was formed by potentiometric electrodes modified with lipid polymeric membranes^{74,75}. These works were supplemented by Prof. Winqvist in Linköping from Sweden, who developed a system capable of classifying solutions using different metallic electrodes and voltammetry technique⁷⁶.

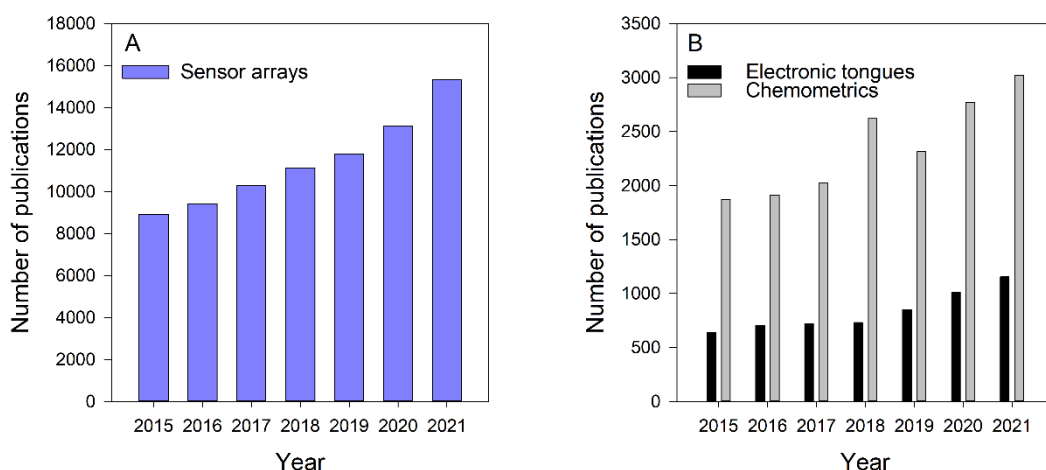


Figure I - 18. Publications from 2015 to 2021. A) sensor array. B) ET (in grey) and Chemometrics (black), as keywords.

As Figure I - 18 depicts, the concept of sensor arrays and ET have been growing in popularity, creating a considerable impact in the world of electroanalytical chemistry. The results collected in the *Web of Science database* show the growth of sensor arrays systems, showing 15328 publications in 2021. This result is followed by the impact of electronic tongues providing 1153 publications in the last year (2021). In black, it is possible to see the slower growth merging chemometrics, as a keyword. In all cases, it has been demonstrated this research is considered a hot topic nowadays.

According to this technology, different sensors can be used to form the sensor array. In general, they can be classified as electrochemical (potentiometric, amperometric, voltammetric, impedimetric, conductometric) through gravimetric to optical (absorbance, luminescence, reflectance)^{5,77}. In the present dissertation, all the projects were performed using voltammetric sensors. For this reason, special attention will be paid to electronic tongues employing voltammetric sensors.

For many years, the *Sensors and Biosensors group* is a pioneer in the development and implementation of these chemical systems. Initial works were reported using potentiometric sensor⁷⁸, but the vast majority were voltammetric applied to quantification of mixtures of oxidizing analytes or beverages^{79,80}.

Focusing on the voltammetric case, the signal is intrinsically linear, which means that the different concentration of oxidable/reducible compounds under study is proportional in a certain ratio to the current signal. Therefore, at the end, a currents vector is created per each sensor selected in the sensor array.

$$i_x(V) = i_o + x_1 \cdot C_1 + x_2 \cdot C_2 + x_3 \cdot C_{13} + \dots, \quad \text{Equation I - 5}$$

In this equation, i_x (V) is the vector of currents of electrode x and the concentrations of the different compounds present in a sample are indicated by C1, C2, C3, etc.

More in detail, if each sensor contributes to a long vector, a sensor array can be done the system more complex, creating a huge amount of data with high dimensionality. This fact makes more difficult the data treatment of the raw data, which means that the analytical chemist must deal with an unforeseen difficulty.

To put into context, voltammograms obtained may be normally formed by many current intensities. What is more, the system is working with a three-way matrix formed by *samples x current x sensors*, so it is impossible to process the data with ordinary data treatments. To overcome this problem, there are different pathways to afford it. One option is the use of strategies to reduce the data, which can be PCA or Partial Least Squares (PLS), examples. Approaches based on the *unfolding* of the data, which means, combining the sensor singles into one single vector or some examples based on compressions like PCA, feature extraction, Wavelet, or Fourier transforms, among others⁸¹. Eventually, there are the multiway treatment strategies (PARAFAC or Multi Partial Least Squares (nPLS))⁶, which can treat the three-way data matrix directly. It is important to mention that they are rarely used in ET systems, probably because of their high complexity.

Therefore, the raw data generated by this kind of analytical system must be treated with mathematical tools to simplify the information given by the analysis of the samples.

There are many applications involved in the ET systems such as beverages, food industry (quality, origin, process monitoring or adulteration/contamination), biomedical (in vitro analysis), pharmaceuticals⁸² and security field. In the present work, the most field entailed is forensic, through the identification and quantification of some drugs of abuse in the presence of their most common cutting agents.

5. Chemometrics

In previous sections of this thesis, the advantage of using voltammetric array systems for the extraction of chemical information from mixtures of compounds has been presented. However, the use of these methods provides us with certain difficulties that we, as analytical chemists, must overcome.

This problem refers to the fact of obtaining high complexity and dimensionality of the generated data, which means that traditional methods cannot deal with the huge amount of raw data obtained (*sensor x intensities x samples*).

To afford this difficulty, there is a need to resort to chemometrics to be able to select relevant information from huge data amount.

Therefore, before getting into the subject, three questions should be clear: what is chemometrics, what are its beginning, and in which spheres of research can it be useful.

Chemometrics is, according to the actual definition of the International Chemometrics Society (ICS), ***“the chemical discipline that uses mathematics, statistics, and formal logic to design or select optimum experimental and measurement procedures, to provide maximum relevant chemical information by analyzing chemical data and to obtain knowledge about chemical systems statistical and mathematical methods were first applied in psychology, biology, and agriculture at the beginning of the last century”***.

This discipline was born at the end of the 1960s and in the 1970s it became an independent working field. The name “chemometrics” was first coined by Svante Wold in the early 1970s⁸³. His collaboration with Bruce R. Kowalski, the outcome in the foundation of the ICS in 1974. In 1984 the first German working group was founded followed by other chemometrics working groups in many countries. Therefore, its fast implementation led to the publication of two journals: Chemometrics and Intelligent Laboratory Systems (1986)⁸⁴ and the Journal of Chemometrics (1987)^{85,86}. Furthermore, networks teaching chemometrics and first monographs were published also in the 1980s, showing the impact of this discipline in many aspects.

There are a lot of working fields⁸³ for today’s chemometrics, but in this work, chemometrics strategies are mainly focused on calibration and multivariate data analysis to distinguish simultaneously mixtures of compounds. To summarize, chemometrics can be considered interdisciplinary to a great extent.

Therefore, two pathways can be classified according to the final application (qualitative or quantitative). Before explaining the main differences between them, it is important to emphasize the three important steps to afford chemometrics analysis, which are weighting, signal compression, and modelling. Steps before modelling are not mandatory. However, their use shows significant benefits in the performance of the model.

5.1. Data Processing

As previously mentioned, the complexity of the data makes hard the construction of the model. So, there are several data processing treatments⁸⁷ that can be applied to the raw data before the multivariate analysis for improving their performance.

One alternative is the use of the *unfolding*, which means to convert voltammograms into a two-dimension matrix, as shown in Figure I - 19. In other words, this strategy combines the sensors' signals into one single vector. After this *unfolding* step, the corresponding chemometric multivariate method (linear or not) can be applied. Some works report that the combination of this pre-step with the compression proportionate improvements in terms of modelling⁸⁸.

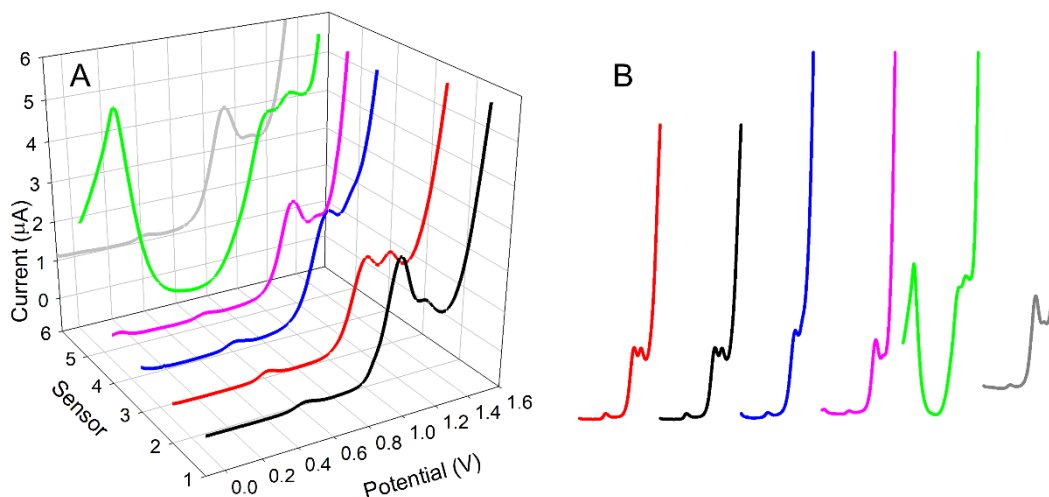


Figure I - 19. A) Initially 3D matrix with the three dimensions (*current x sensors x samples*). B) Conversion to the 2D using the *unfolding*.

Some strategies can also be used to verify the consistency of the raw data and observe the previous contribution of each sensor. Auto-scaling, centering, normalization, and standardization can be some examples commonly used.

Once this previous step was checked, the next step is based on reducing the signal's complexity, maintaining the useful information⁸⁸. This process can be named data compression.

According to the literature, there is a variety of compression methods as windowed slicing integral method⁸⁹, PCA, Legendre's polynomials⁹⁰, kernel functions⁹¹, Discrete Wavelet Transform (DWT)⁹² or Fast Fourier Transform (FFT)⁹³ and feature selection (Genetic Algorithms (GAs)) and Causal Index (CI)⁹⁴, among others. The application of these tools before the modelling is built provides some advantages such as avoiding redundancy in input data, saving time in terms of calculation (training step), and noise reduction. All these factors contribute to the obtention of simpler models with less risk of over-fitting.

Once the raw data is collected and pre-processed it is needed to perform the last step of the procedure, which includes the building of the model. Depending on the final application (qualitative or quantitative) different operations may be done.

Therefore, the next step in this way will be to present the different PARC methods, focusing on the most used in the present dissertation. Current approaches to PARC methods include the use of machine learning because of the increase availability of big data and the increasing availability of processing power. These methods can be classified into two main

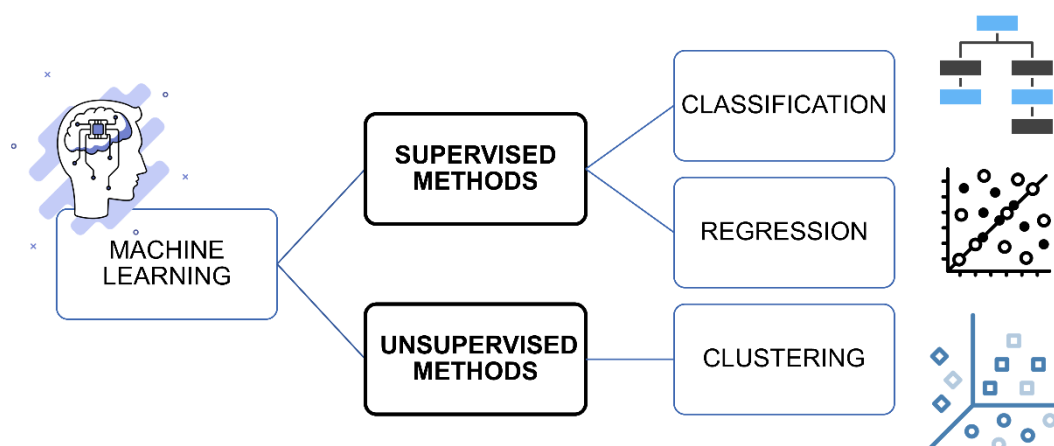


Figure I - 20. Machine learning types. Supervised methods incorporated classification and regression applications; meanwhile, unsupervised methods are focused mainly on clustering.

Among the different methods available nowadays, PCA, k-nearest Neighbour (kNN), PLS, and ANNs are the most well-known for ET applications. Specifically, PCA is most used in qualitative applications to obtain better visualization, meanwhile, PLS and ANNs are more attractive for quantitative applications.

Machine learning algorithms such as kNN, Random Forest, and Naive Bayes, among others, are commonly used as classification methods, emphasizing Support Vector Machines (SVM), which is an enhanced alternative to some of the more classical approaches.

5.1.1. Data Compression

As previously commented before the last step, which corresponds to modelling, data compression pre-processing is recommended to reduce the dimensionality of the raw data obtained. Applying this tool is possible to avoid the overfitting of the models and to reduce the modelling time. Although there are methods which their use is not so critical (PLS), there are reports in the literature claiming that its application improves the performance of the created models⁹⁶. There are several ways to manage the data compression step: in this sense, DWT and GAs will be explained in more detail.

5.1.1.1. Discrete Wavelength Transform

In the late 1980s, WT appeared as a signal processing technique, which is derived from Fourier transform (FT). The main difference between them is the type of function where the signal is projected. In the case of FT, the signal is projecting in a sinusoidal function, whereas WT is a wavelet function. This last option gains an advantage in this regard to FT because it captures not only the frequency but also the location (temporal) of the information.

More in detail, the operation mode of WT is based on decomposing a signal into a set of basic functions. These functions are obtained from translations and dilations of a single function named the mother wavelet function⁹². There are several wavelets, but the most common use is the *Daubechies*. This process is done through Mallat's pyramid algorithm, which acts on a discrete signal of length M by decomposing it into orthogonal subspaces of length ca. $M/2$ in each step^{92,97} (Figure I - 21).

Thus, by increasing the degree of decomposition to a level X (which means repeating the decomposition process x times), the degree of compression can be increased.

However, this increase in the degree of compression is at the expense of the degree of reconstruction since the fidelity of signal reproduction degrades at each step. Finally, the transformation can be reversed, and the degree of reconstruction can be evaluated in this way, allowing the choice of the optimum number of coefficients to be used.

As in the case of FT, WT also has the advantage that it can be used to remove the noise present in the signals. In addition, WT can be implemented as a data compression method if we use only the most relevant coefficients obtained in the signal decomposition. Therefore, it is a very efficient tool in these situations because it accomplishes, in a single step, data compression, feature extraction, and noise reduction.

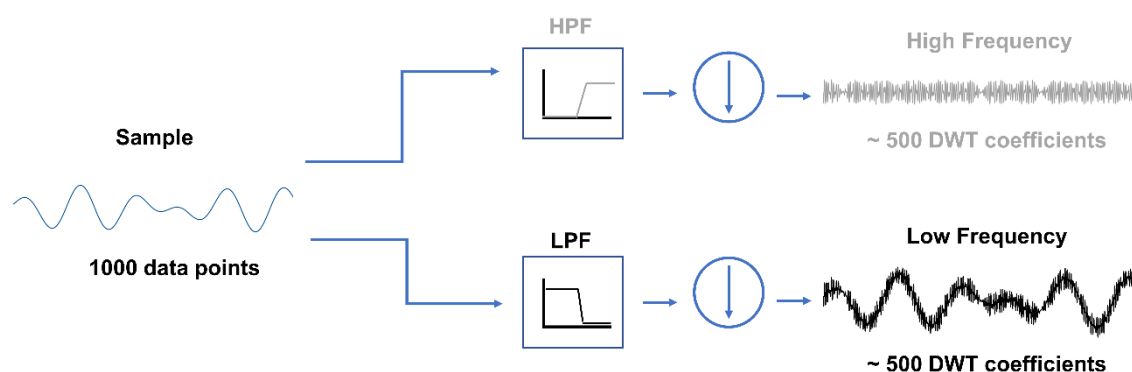


Figure I - 21. DWT operation mode based on Mallat's pyramid algorithm.

5.1.1.2. Genetic Algorithms

John Henry Holland was the father of GAs in the early 1970s. It is considered an advanced feature selection method simulating Darwin's theory of evolution and the concept of natural selection⁹⁸. To understand briefly how GAs is managed, five basic steps⁹⁹ can be considered more in detail which are:

- i. Coding of variables: referring to the coding, each variable (gene) is binary coded into a vector (chromosome).
- ii. Initiation of population: in this step to generate many individuals, each one defined by a number of chromosomes, the original one is perturbed.
- iii. Evaluation of the response: the aim herein is to get a numeric value that describes the quality of the model. In this case, this process is done through the generation of a model contributed by each of the chromosomes.

- iv. Reproduction: this step is based on a creation of a new population of chromosomes. They are creating making combination of the original chromosomes.
- v. Mutation: this mutation step must be added to avoid genes that would never be generated from the original chromosomes.

Therefore, one question can be, when is the evolution process completed? It can be considered completed when a termination criterion is defined. In this case, steps (iii) to (iv) are then repeated until reaching this point. This point can be established by a maximum number of generations, otherwise when improvement on the modelling decreases below a limit. To clarify the process, which is difficult to imagine, the operation mode of GAs is represented in Figure I - 22.

In a summary, GAs is considered sophisticated data feature selection method, very useful in the variable selection and optimization in calibration and modelling steps.

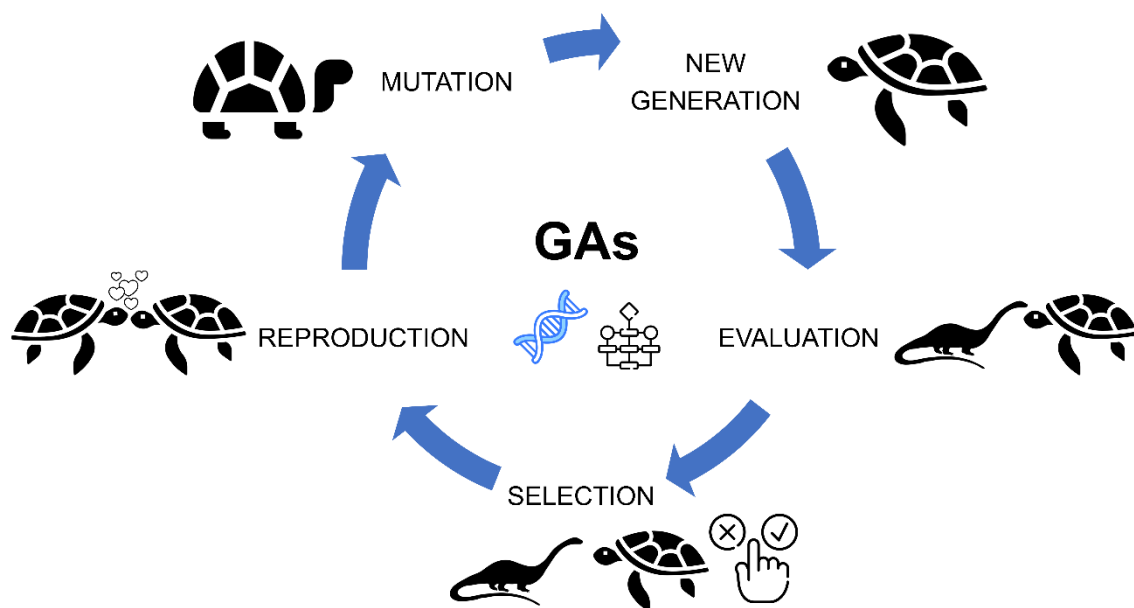


Figure I - 22. Schematic representation of how GAs works.

5.2. Unsupervised Methods

5.2.1. Principal Component Analysis

As defined in the literature, PCA is described as a linear unsupervised pattern recognition method able to reduce the dimensionality of multivariate data. In this sense, it helps to visualize the different categories by remarking differences and similarities between sample clusters⁷⁷.

The purpose is to reduce the number of variables to new latent variables (orthogonal) called principal components (PCs) (Figure I - 23). To get the first axis those with maximum variance variation, a change of axis directions is required. In addition, this new visualization helps to simplify the elucidation of the variability contained in the information. In many situations, the complication is to understand these PCs depending on the sample composition.

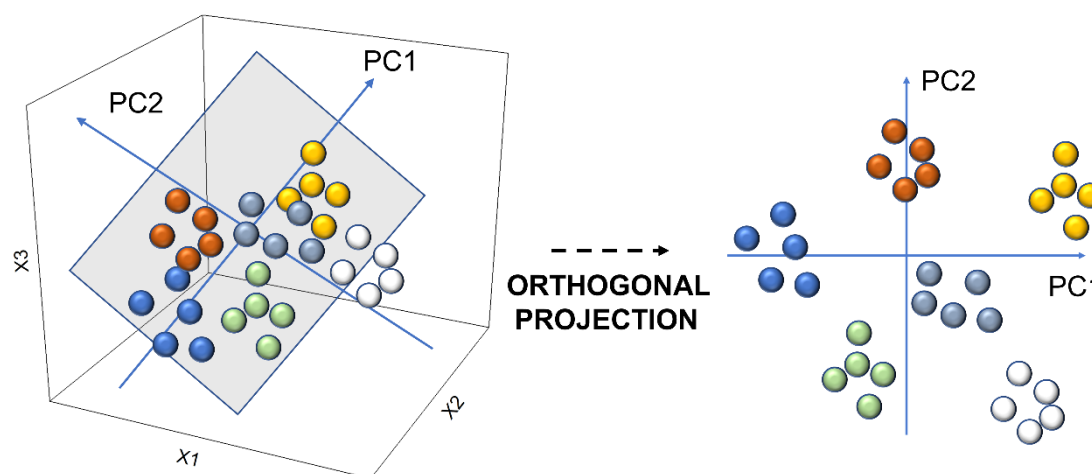


Figure I - 23. Simulation of the orthogonal projection done by PCA. On the left, data sets are represented in three variables. On the right, the representation of the two most important PCs shows the formation of six clusters.

Thus, at this point it could be interesting to analyse just a bit the math behind this pattern recognition method. As discussed above, PCA consists of a transformation of the original variables to a new orthogonal coordinate system, the principal components, which are described by Equation I - 6 and where X is the matrix of the original data, of dimension $(s \times v)$.

$$X = TP' + E$$

Equation I - 6

Each of the s rows corresponds to an object (the samples), and each of the v columns contains one of the variables. In this thesis, it will be the voltammograms. T is the matrix of the scores, of dimension $(s \times a)$, where a is the number of PCs needed to contain the desired information. The scores contain the information of the samples. P is the matrix of the loadings, of dimension $(v \times a)$, containing the information about the variables of the original matrix. E is the residuals matrix, which contains the information from the original data that has not been explained by the principal components chosen in the models. All the parameters used in the PCA are clearly defined in Figure I - 24.

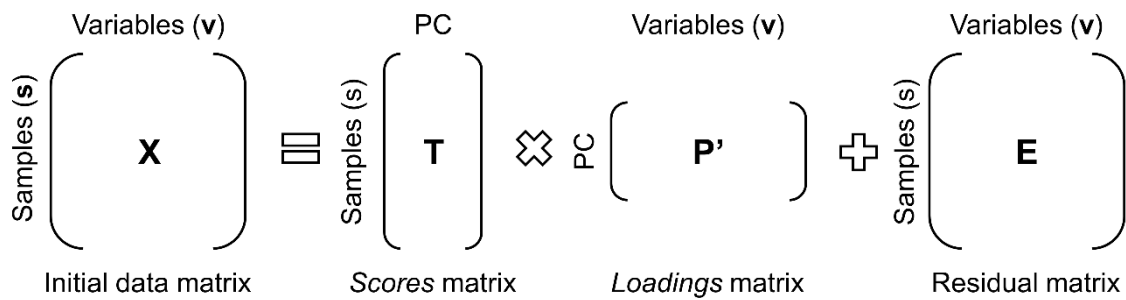


Figure I - 24. Schematic representation of the different matrices involved in the transformation process done by PCA.

There are several algorithms able to calculate T and P matrices. The most commonly used are singular value decomposition (SVD) or nonlinear iterative partial least squares (NIPALS).

In conclusion, PCA is considered an excellent visualization tool. What is more, it can be also classified within the group of data compression methods, referring to the data reduction, showing its feasibility as a feature extraction tool.

In the present dissertation, PCA is always the first option to visualize the different clustering and perform a previous optimization of the best selection for the future sensor array used

5.2.1.1. Clustering Metrics: Silhouette Parameter

As was commented in previous sections, PCA is an excellent alternative as a visualization tool for analyzing sample clusters. However, in all the cases, this visualization can be a bit subjective in mathematical terms, which means that sometimes it is difficult to analyse which transformation is better in comparison with another if we only make evidence of the clinical eye.

To overcome this problem, for the first time in our group a strategy was developed to afford the clustering metrics topic.

In the literature, it can be found several methods to assess clustering process, i.e., how compact a cluster is and how well separated are different cluster. Some examples are the F-factor¹⁰⁰, the silhouette parameter, and the sum of squared errors¹⁰¹. Due to its simplicity, in the present work, silhouette (*s*) was selected as a clustering degree metric. The calculations performed in getting the parameter will be shown in detail in the experimental section. In brief, this parameter calculation is a measure of how easy to distinguish between clusters associated with the different samples under study. This strategy coupled with PCA allows the interpretation and validation of consistency within clusters of data, providing a numerical criterion of how well each sample matches its cluster. In this case, if the value of *s* is close to +1, indicates that the sample is well matched to its cluster, verifying that the clustering configuration is suitable. In the opposite case, the reasoning is opposite.

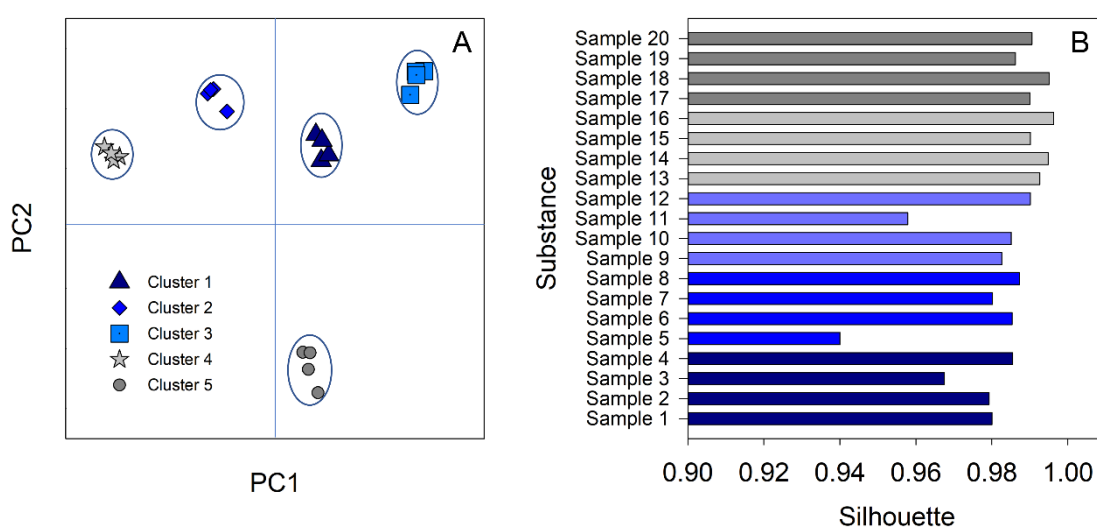


Figure I - 25. A) Scores plot of PCA showing 5 clusters as an example. B) Silhouette plot.

In this context, in our case study, the combination of these two strategies allowed us having a quantitative metric for the proper selection of the working electrodes used in the array. This step was very useful because the redundant information of sensors that were not useful to improve the clustering were then removed.

Therefore, benefits in terms of computer calculations such as saving time are observed thanks to this pre-selection step. Figure I - 25 shows a typical silhouette diagram obtained in a classification approach of a number of samples.

5.3. Supervised Methods

5.3.1. Machine Learning Algorithms

There are several supervised machine learning algorithms used in chemometrics nowadays. Random Forest, Naïve Bayes, and SVM are some examples^{102,103}.

- Random Forest: predict using an ensemble of decision trees.
- Naïve Bayes: a fast and simple probabilistic classifier based on Bayes' theorem with the assumption of feature independence.
- SVM: this algorithm maps inputs to a higher dimensional feature to facilitate differentiation.

In the present work, the machine learning algorithm preferred in developing applications was kNN. For this reason, it will be explained more in detail.

5.3.1.1. K-nearest Neighbour

The kNN algorithm is a machine learning algorithm that belongs to the simple and easy-to-apply supervised learning algorithms that can be used to afford regression and classification problems¹⁰⁴, focusing on the second cases as more commonly used.

Using this algorithm, it is possible to keep all the data and classify a new data point (sample) based on the similarity¹⁰³.

What is more, it is considered as a lazy learner and non-parametric algorithm. It is not parametric because it does not make any supposition on subjacent data. A lazy character is referred to because its learning from the training set is not immediate.

To understand how this algorithm works, a schematic representation is shown in Figure I - 26, followed by a simple case as an example.

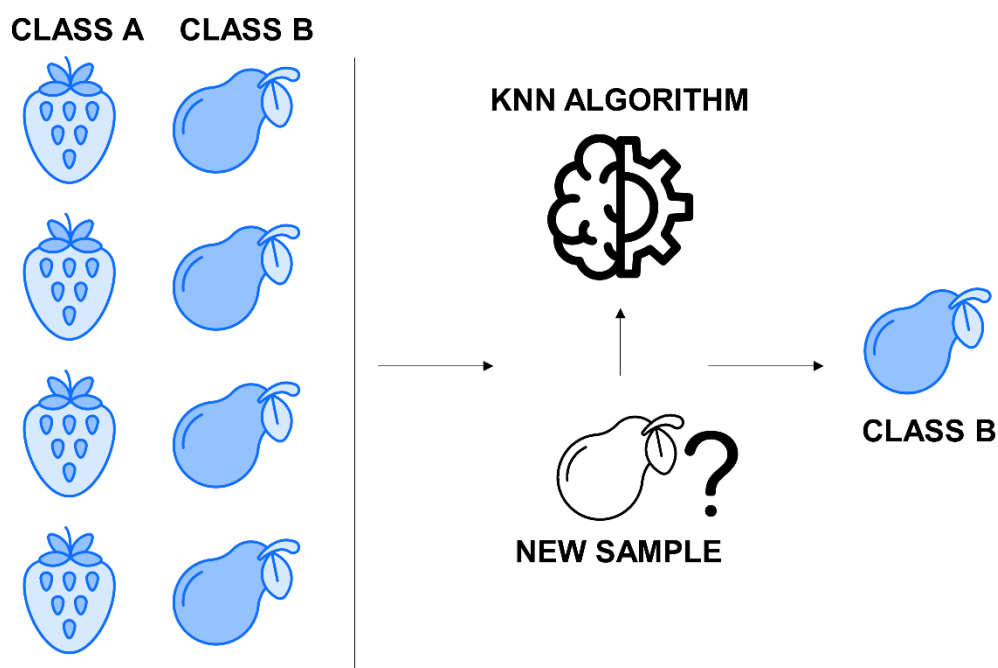


Figure I - 26. Schematic representation of how the kNN algorithm works.

In this example, two categories A and B are first presented defining two clusters, and next, a new data point (x_1) enters into the system and needs to be classified (Figure I - 27). To achieve it, kNN is applied to classify the new sample in some of the two categories previously defined. Therefore, following the below diagram six steps can be remarked.

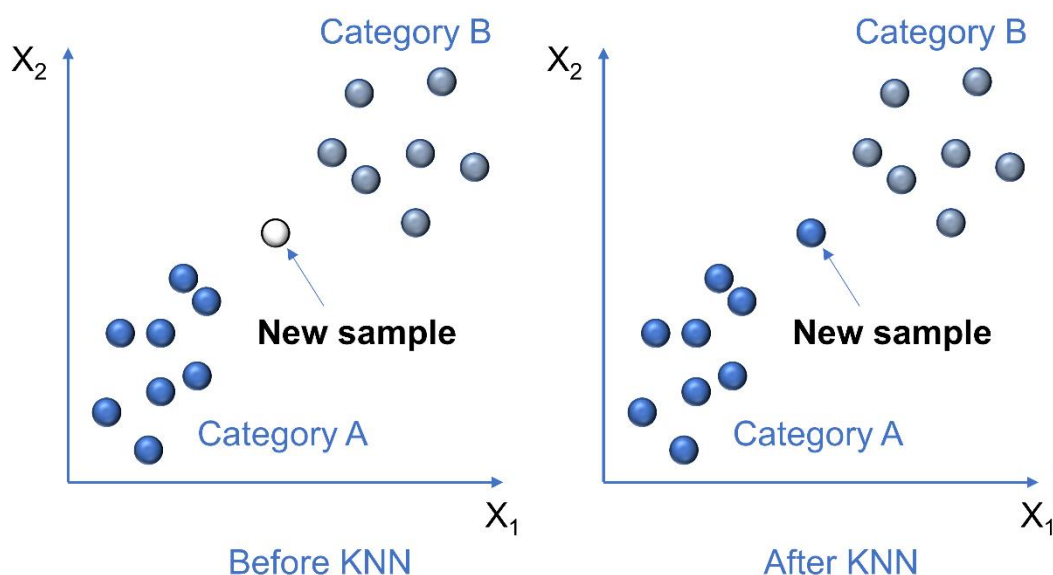


Figure I - 27. Comparison of results obtained before and after than applied kNN algorithm.

1. Selection of the number of k of the neighbours: this k value is normally between 3-5, but sometimes this selection is a key point during the process and there is no systematic way to determine the most appropriate value of this parameter. However, it is known that very low values can be noisy and introduction of outliers in the final model. In this case, it is possible to considerate k=5 as an example.
2. Calculation of the Euclidean distance (Figure I - 28A). It is defined as the distance between two points, and it can be calculated as follow:

$$A_1 \text{ and } B_2 = \sqrt{(X_2 - X_1)^2 + (Y_2 - Y_1)^2} \quad \text{Equation I - 7}$$

3. Define a pertinence to a class, taking the k nearest neighbours in consideration of the calculated Euclidean distance.
4. Count the number of the data points in each class, among these k neighbours.
5. Assign the new data points (samples) to that category for which the number of the neighbour is maximum (Figure I - 28B). In this example, the three nearest neighbours are from category A, meanwhile, two are selected from category B.
6. The model is ready. In conclusion, the model verifies that the new sample belongs to category A.

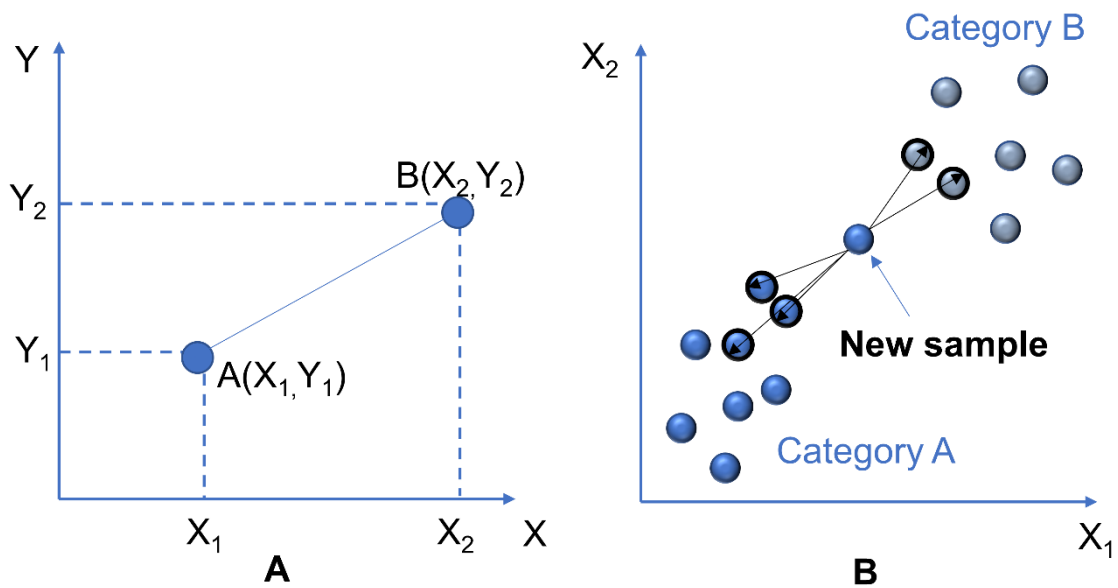


Figure I - 28. A) Calculation of the Euclidean distance. B) Classification of the new sample in the proper category after calculating k=5 distances.

As summarizing of this section, it is demonstrating the feasibility of the kNN model showing its simplicity of application and presenting its robustness in front of noisy training data. As negative aspects can be remarking the determination of k parameter, which can be complex in some cases. When the amount of data is huge, it can attribute high cost in computation since the multiple calculation of all the distances might be necessary.

5.3.2. Partial Least Squares Regression

Quantitative analytical determinations based on instrumental analysis require the use of calibration methods. When samples involve one analyte or several analytes if their responses do not interfere with each other, classical methods can be applied to deal with the calibration. In this case, typical methods are external calibration, internal standard (minimization of signal drifts), or standard addition to deal with matrix effects. In the commented situations, it is used univariate calibration methodologies. However, the way to afford the problem changes when there are interactions between species and/or overlapping signals that must be considered. In this sense, the application of these univariate methodologies becomes difficult, and the use of multivariate strategies is necessary. At this point, chemometrics plays an important role in terms of data treatment.

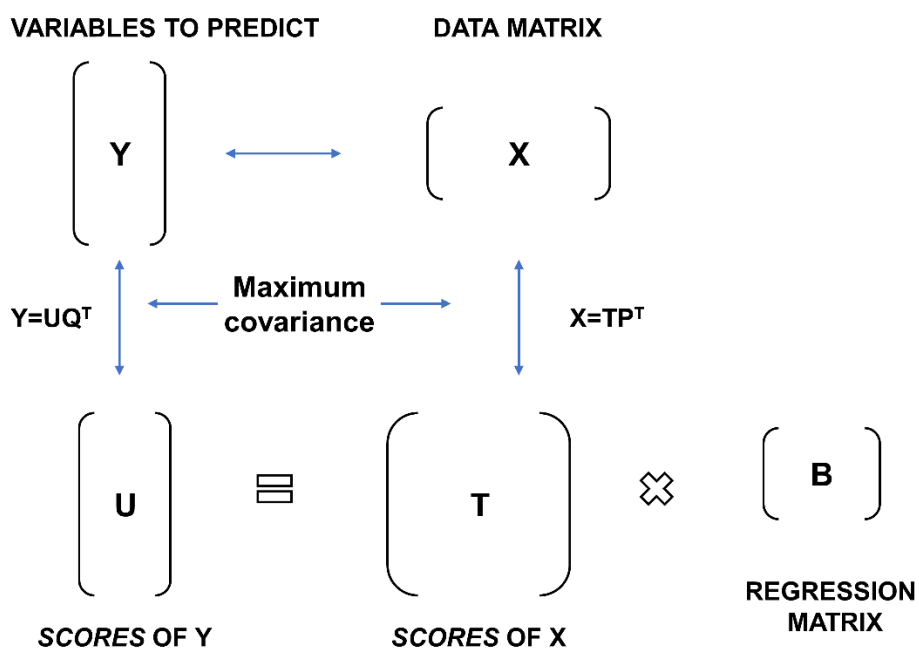


Figure I - 29. Schematic representation of PLS.

In the present dissertation, the most common method applied to calibration was multivariate since most of the signals in these works were overlapping. In this case, PLS is selected as a multi-calibration method in some of the works reported.

PLS is a linear method in which linear combinations of the original variables are used to reduce the number of variables¹⁰⁵, Figure I - 29. Unlike PCA and principal component regression (PCR), where only the data matrix (**X**) is decomposed into *scores* and *loadings*, in this case, both the data matrix (**X**) and the matrix of the parameters to be predicted (**Y**) are decomposed and the new variables, called latent variables (LVs) are calculated to maximize the covariance between **X** and **Y**. This decomposition of the two matrices implies that the PLS assumes that the error is not focused on the **X** matrix but is equally present in the **Y** matrix. Depending on the number of variables to predict, we distinguish between PLS1 (1 variable) and PLS2 (several variables)⁸⁸.

To finish with this PLS section is important also commenting on a more sophisticated variant which is nPLS. This method is used when the departure data has more than one dimension¹⁰². The advantages it provides are based on the avoidance of using some pre-treatments⁸⁸. In the case of reduction of the dimensionality, the *unfolding* in the data is not needed, as an example. As main difference characteristic of PLS is that the loadings matrix is 2D. Therefore, it is considered a promising method for some applications. However, the model building, and interpretation indeed presents some complexity, and that is why it is not widely applied.

5.3.3. Artificial Neural Networks

In the past decades, ANNs have gained an important role in different knowledge areas because of their use as adaptive tools for processing data in many applications. ANNs attract attention because in opposite to classical statistical techniques they are powerful in nonlinear systems' modelling⁸⁷.

The *Sensors and Biosensors group* is a pioneer in the development and application of these modelling tools with electroanalytical techniques, showing its applicability and feasibility in many reported works^{106–109}.

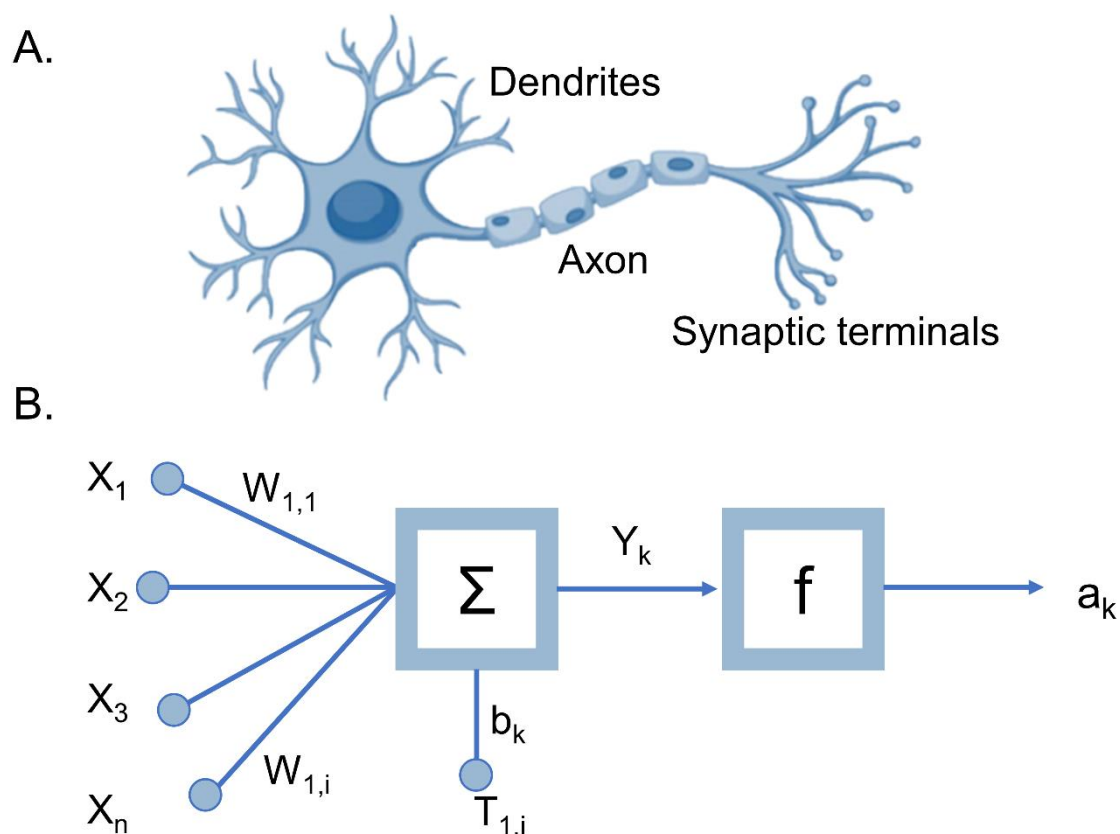


Figure I - 30. The analogy between A) neuron and B) perceptron in an artificial neural network system.

ANNs are defined as parallel information processing tools inspired in the animal nervous systems, whose maximum expression is the human brain. The basic unit of an ANN is what is called *perceptron*¹¹⁰, which approximates a neuron in the nervous system. The analogy between both concepts is shown in Figure I - 30. In short, ANNs are based on the combination of different neurons, which receive a series of inputs through their interconnections, and finally, the output is emitted. This output is determined by three different operations: propagation, activation, and transfer.

ANNs are involved in the artificial intelligence world, which makes them attractive but at the same time, their mathematical interpretation is not evident. Therefore, a simple interpretation of the mathematical is attempted to allow the reader to dive a little deeper into these concepts.

In math terms, the perceptron is the unit that has many input connections defined as X_n and a single output (a_k). Each input can be attributed by a weight (w_i) and, in some cases, a bias (b)¹¹¹.

The next question at this point is: when the perceptron is activated? The answer is related to the sum of the weighted inputs (Σ). If a certain threshold is reached, the perceptron is activated generating an output signal, meanwhile, this value has not reached the perceptron remains not activated. Equation I - 8 defines well the issue:

$$y_k = \sum_{i=1}^n w_i x_i + b \quad \text{Equation I - 8}$$

In a summary, the learning process consists of adjusting the values of the weights applied to each signal and the bias. What is more, the threshold value must be exceeded to transfer the information and the appropriate transfer function for it to produce the desired stimulus. These parameters are adjusted to minimize an error function, which compares the values obtained in the output with the values expected by a series of known patterns.

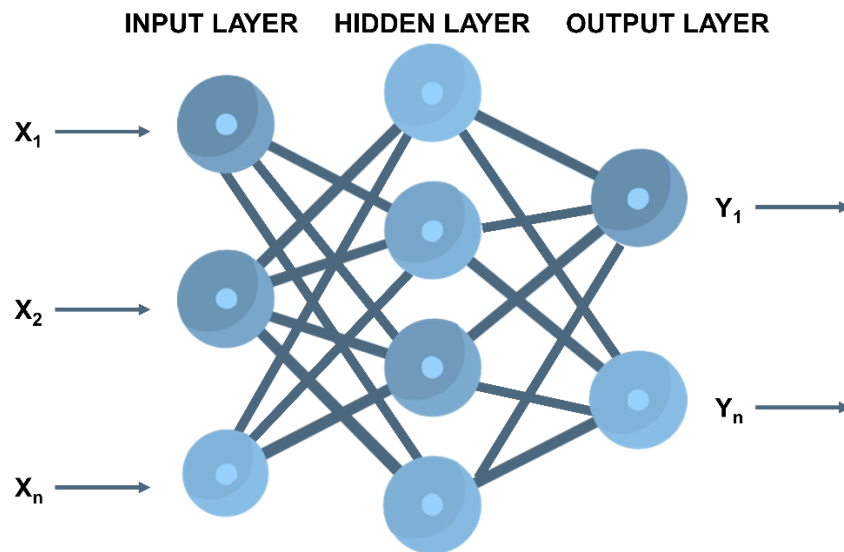


Figure I - 31. Multi-layered ANNs representation shows the three important layers: input, hidden, and output.

At this point, this will be the simplest situation considering only the actuation of one perceptron. To be more realistic, biological mechanisms are based on multi-layered structure as in the case of the brain. For this reason, parallelism based on the previous idea is performed using a multi-layered of ANNs. Therefore, three important layers composed by the multilayer model in the following are commented. One of them is the input layer, which is the first of the layers and the one in charge of introducing the information inside the network.

It contains as many neurons as inputs and receives the set of inputs (x_i). The next one is the hidden layer, which tries to process the information, and finally, the output layer which has the role to receive the signals processed in the previous layers and provides useful information. Referring to the learning process the same concepts are applied than in the case of a single perceptron.

An important remark must be done to the transfer functions, which allows the possibility to offer outputs signals not limited only to the binary response. The most used in the ANNs field are *tansig*, *logsig*, *purelin*, *satlin*, and *satlins*⁸⁷. A fact that it is important to highlight is that working with this type of chemometric tools is not trivial, which means that to find the best configuration it is needed to evaluate centenars of them.

In conclusion, ANNs are suitable chemometric tools to perform the modelling. As commented in the beginning, they are very useful when cases of nonlinear situations are presented. In this thesis, it could be interesting for the last work presented based on detection of some cutting agents, where analytes did not present a linear behaviour.

6. Applications

Thanks to the advantages provided by these machine learning systems mentioned in previous sections, many applications have been developed in the world today. However, this work is focused on very prominent applications based on forensic and security fields.

6.1. Proof of Concept

When a Ph.D. student begins his carrier in the research world it is important to know that he/she is using the proper tools and the measurement system is working under controlled conditions. This issue is not always trivial in all cases. Therefore, before starting with this research, it was verified the materials employed to modify the electrodes' surface and the different sensing platforms. To achieve it, it is important to select a mixture of references, in which the behaviour of the analytes was observed previously, and it is well known.

In our group, this mixture is based on three compounds, two of them, very famous in the pharmaceutical field which are acetaminophen (PA), uric acid (UA), and ascorbic acid (AA) (Figure I - 32). Thus, it would be interesting to present the analytical problem involved in the following section.

6.1.1. Acetaminophen, Uric Acid, and Ascorbic Acid

As it was commented previously, these three compounds have an important role in the life of humans, for this reason, their analytical interest is presented nowadays.

As it is well known, PA, most common as paracetamol is used in society as an analgesic and antipyretic drug used against muscle aches, headache, fever, menstrual cramps, and arthritis, among others¹¹². Abusive consumption of this drug provokes toxic metabolites, developing problems based on nephrotoxicity and hepatotoxicity¹¹³. In the case of AA, also known as vitamin C it is commonly employed as an antioxidant and as a good component to control a good dietary intake¹¹⁴. Its excessive dose in the body can cause also some problems based on trouble sleeping, flushing of the skin, or gastrointestinal discomfort¹¹⁵, in some cases. Finally, the determination of UA in the body is essential because abnormal levels of this substance proportionate may be the cause of diseases such as gout and hyperuricemia¹¹⁶. What is more, pneumonia and leukemia are also related to the increase in urate levels.

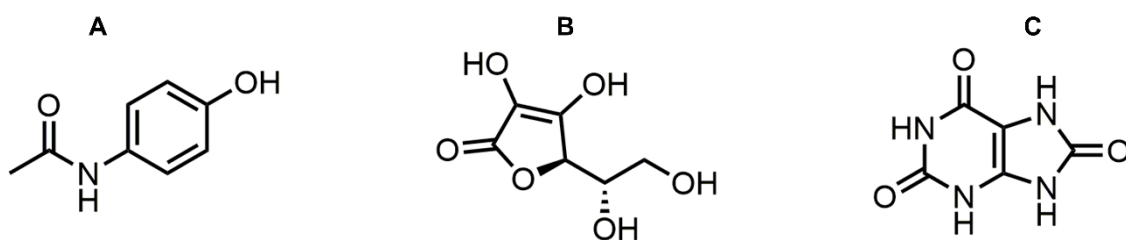


Figure I - 32. Chemical structures of (A) acetaminophen, (B) ascorbic acid, and (C) uric acid.

For all these reasons, the analytical determination of the compounds is necessary in relation to the mentioned illnesses. In the literature, it is possible to find many analytical methods capable of determining them in an individual or simultaneous way. Capillary zone electrophoresis^{117,118}, chromatography^{119,120}, spectrophotometry^{121,122} and spectrofluorometry^{123,124} are some of the analytical techniques use for this purpose.

Normally, the main problem is that these methods need complex procedures and are high cost. To deal with that problem, our proposal is the application of electrochemical sensors¹²⁵. Many works were reported in our group addressing the problem with different strategies^{100,126,127}.

Specifically, in this work, we proceeded to the simultaneous detection of these three compounds with CME using a self-formulated conductive ink. A multisensor platform and chemometric tools were used to afford the analytical problem. At the end, this work was used as proof of concept to validate the way of modifying and the sensor platform used.

6.2. Illicit Drugs

6.2.1. Opiates and Cutting Agents

The following applications are based on the forensic and security field. Over the last years, society has been dealing with a problem of the trafficking of illicit drugs. This issue is damaging economy, health of people and creating an increase of criminality in the population¹²⁸. The benefits are going to illicit drug markets, which are growing increasingly. Therefore, authorities try to disarticulate them as soon as possible to safeguard the public.

To deal with this problem, the most common methods employed are colour and mass-spectrometric tests. These methods can be improved due to their low accuracy and in the case of spectroscopic, the high cost and low portability may be a handicap in their applications. For this reason, the implementation of new drug test systems is urgent.

In this sense, this dissertation is framed in the *Bordersens* project¹²⁹ which has the main aim of the development of a portable device able to perform *on-site* analysis to test different precursors, drugs, and cutting agents improving accuracy and reducing problems caused by classical methods. The project is ambitious; thus, these works are helping to reach the final objective.

The Controlled Substances Act (CSA) classifies the drugs into five groups which are anabolic steroids, stimulants, hallucinogens, narcotics, and depressants¹³⁰. Our interest is focused on the narcotic group also called opioids.

This category is responsible for 63% of deaths by overdose in the USA in 2015 and 70% in 2018¹³¹. So, it is evident that consumption is creating an economic and health impact.

More in detail, within this opioids group, exists an especial class which named opiates. They are coming naturally from poppy species (*Papaver somniferum*)¹³², Figure I - 33, and the most famous are codeine, heroin, and morphine (Figure I - 34). These drugs can be adulterated with different cutting agents to modify the effects produced by them, or to maximize profits the gangs make trafficking with them. In this case, two of these substances were studied which corresponds to paracetamol and caffeine. In the case of caffeine, it facilitates the smoking of heroin because allows to vaporize it at a lower temperature. Otherwise, paracetamol encourages heroin's analgesic effect. For this reason, can be present in illicit samples composition.



Figure I - 33. *Papaver somniferum* from poppy species.

Again, classical methods are capable of distinguishing opiates individually and also simultaneously^{133–137}. However, most of the techniques are not adapted to *on-site* drug monitoring, are time-consuming, and have high costs despite their power. To afford the limitation, electrochemical sensors were also selected. The advantages in terms of simple usage, high portability, the rapid response among others permit the selection of this method before classical approaches.

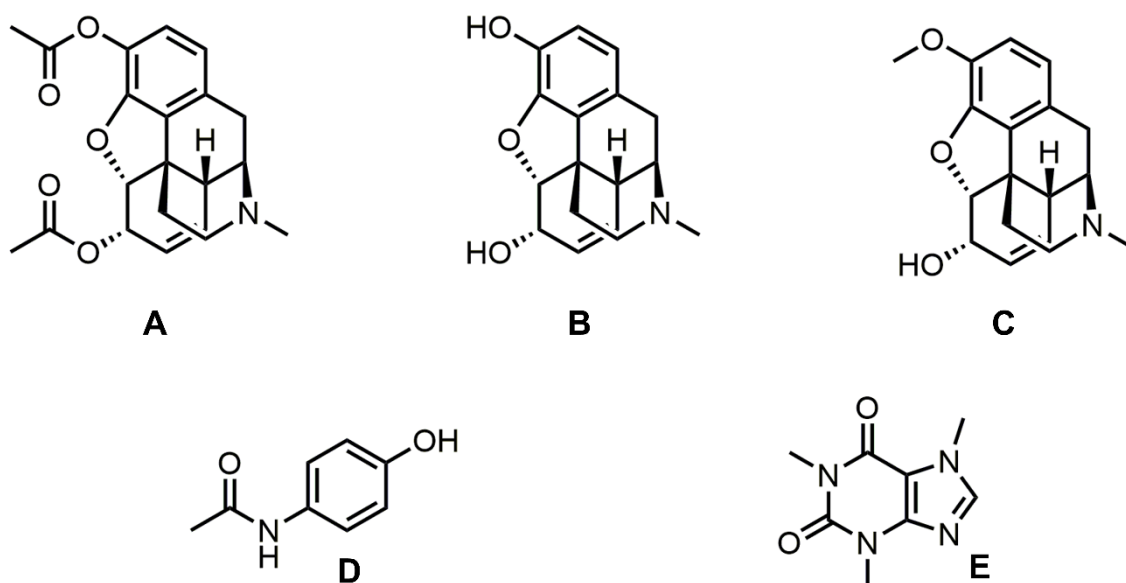


Figure I - 34. Chemical structure of (A) heroin, (B) morphine, (C) codeine, (D) paracetamol, and (E) caffeine.

In brief, the works involved with determination of drugs of abuse can be divided into two parts. The first one was based on performing an accurate optimization of the best sensor array for the desired application. To achieve this proposal, the use of chemometrics, particularly, machine learning algorithms were applied. Once this step was completed the next goal was quantitative. For that, the system was analysed with the three opiates under study and then, it was complemented with the two most common cutting agents. In this case, individual sensors were used as members of the array, and the optimized modification performed in previous works was applied.

6.2.2. Cocaine and Cutting Agents

Previous sections are based on opiates, but the stimulants group is also known for the same problem. The most famous is cocaine, which comes from the leaves of the coca plant (*Erythroxylum coca*), Figure I - 35, in South America. If statistics are shown, cocaine is defined as the second most consumed illicit drug in the European Union, reaching values of 9.1 billion Euros¹³⁸ coming from the European cocaine market. Most countries involved in the European Union are Belgium, the Netherlands, and Spain¹³⁹. Again, statistical numbers showed that in 2018 these countries were responsible for a total of 78% of the cocaine seizures¹³⁹.



Figure I - 35. *Erythroxylum coca* plant.

As in the previous case, cocaine is mixed with other compounds to modify its effects. In this case, prescription drugs such as acetylsalicylic acid, ibuprofen, paracetamol, and phenacetin are very common due to their low cost. In the past years, it was used as a drug to combat the pain but currently, it is forbidden in many countries. Finally, the group of local anaesthetics (procaine, lidocaine, tetracaine, and benzocaine) is also used in adulterating cocaine seizures samples, remarking benzocaine¹⁴⁰ as the most encountered cutting agent.

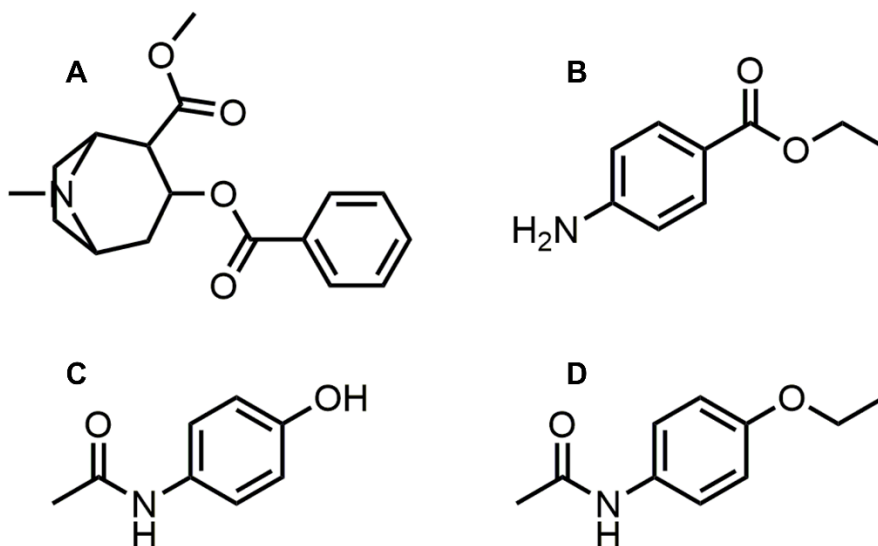


Figure I - 36. Chemical structure of (A) cocaine, (B) benzocaine, (C) paracetamol, and (D) phenacetin.

Again, the motivation is to improve analytical systems by the implementation of fast and reliable methods.

Therefore, in this case, the proposal was based on the simultaneous determination of three relevant cuttings agents (benzocaine, paracetamol, and phenacetin) present in cocaine seizure samples (Figure I - 36). The methodology was based on the previous works with the main innovation in the manufacturing technology employed. In this case, the sensor platform used was developed by inkjet printing, which is considered a relatively recent printing technique that tries to compete with screen printing or 3D printing⁵² nowadays.

7. References

- (1) Hulanicki, A.; Glab, S.; Ingman, F. Chemical Sensors: Definitions and Classification. *Pure Appl. Chem.* **1991**, 63 (9), 1247–1250. <https://doi.org/10.1351/pac199163091247>.
- (2) Senesac, L.; Thundat, T. G. Nanosensors for Trace Explosive Detection. *Mater. Today* **2008**, 11 (3), 28–36. [https://doi.org/10.1016/S1369-7021\(08\)70017-8](https://doi.org/10.1016/S1369-7021(08)70017-8).
- (3) Diamond, D. Progress in Sensor Array Research. *Electroanalysis* **1993**, 5 (9–10), 795–802. <https://doi.org/10.1002/elan.1140050913>.
- (4) Stefan, R. I.; van Staden, J. F.; Aboul-Enein, H. Y. Estimation of Uncertainties for the Application of Electrochemical Sensors in Clinical Analysis. *Accredit. Qual. Assur.* **2003**, 8 (2), 86–89. <https://doi.org/10.1007/s00769-002-0560-1>.
- (5) Ciosek, P.; Wróblewski, W. Sensor Arrays for Liquid Sensing – Electronic Tongue Systems. *Analyst* **2007**, 132 (10), 963. <https://doi.org/10.1039/b705107g>.
- (6) del Valle, M. Electronic Tongues Employing Electrochemical Sensors. *Electroanalysis* **2010**, 22 (14), 1539–1555. <https://doi.org/10.1002/elan.201000013>.
- (7) Durst, R. A. Chemically Modified Electrodes: Recommended Terminology and Definitions (IUPAC Recommendations 1997). *Pure Appl. Chem.* **1997**, 69 (6), 1317–1324. <https://doi.org/10.1351/pac199769061317>.
- (8) Adarakatti, P. S.; Baranova, E. A.; Dennany, L.; Kempahanumakkagari, S. K.; Mohamed, M. A.; Woo, T. K.; Monyoncho, E. A.; Randviir, E. *Electrochemistry Volume 15*; 2019; Vol. 15.
- (9) Novoselov, K. S. Electric Field Effect in Atomically Thin Carbon Films. *Science* (80-.). **2004**, 306 (5696), 666–669. <https://doi.org/10.1126/science.1102896>.
- (10) Iijima, S. Helical Microtubules of Graphitic Carbon. *Nature* **1991**, 354 (6348), 56–58. <https://doi.org/10.1038/354056a0>.
- (11) Goyal, R. N.; Chatterjee, S.; Rana, A. R. S. The Effect of Modifying an Edge-Plane Pyrolytic Graphite Electrode with Single-Wall Carbon Nanotubes on Its Use for Sensing Diclofenac. *Carbon N. Y.* **2010**, 48 (14), 4136–4144. <https://doi.org/10.1016/j.carbon.2010.07.024>.
- (12) Varadan, V. K.; Pillai, A. S.; Mukherji, D.; Dwivedi, M.; Chen, L. Carbon Nanomaterials. In *Nanoscience and Nanotechnology in Engineering*; World Scientific, 2010; pp 107–152. https://doi.org/10.1142/9789814277938_0004.
- (13) Bokros, J. C. Carbon Biomedical Devices. *Carbon N. Y.* **1977**, 15 (6), 353–371. [https://doi.org/10.1016/0008-6223\(77\)90324-4](https://doi.org/10.1016/0008-6223(77)90324-4).
- (14) Engstrom, R. C. Electrochemical Pretreatment of Glassy Carbon Electrodes. *Anal. Chem.* **1982**, 54 (13), 2310–2314. <https://doi.org/10.1021/ac00250a038>.
- (15) Fagan, D. T.; Hu, I. F.; Kuwana, T. Vacuum Heat-Treatment for Activation of Glassy Carbon Electrodes. *Anal. Chem.* **1985**, 57 (14), 2759–2763. <https://doi.org/10.1021/ac00291a006>.
- (16) Chen, P.; Fryling, M. A.; McCreery, R. L. Electron Transfer Kinetics at Modified Carbon Electrode Surfaces: The Role of Specific Surface Sites. *Anal. Chem.* **1995**, 67 (18), 3115–3122. <https://doi.org/10.1021/ac00114a004>.
- (17) Van der Linden, W. E.; Dieker, J. W. Glassy Carbon as Electrode Material in Electro- Analytical Chemistry. *Anal. Chim. Acta* **1980**, 119 (1), 1–24.

- [https://doi.org/10.1016/S0003-2670\(00\)00025-8](https://doi.org/10.1016/S0003-2670(00)00025-8).
- (18) Adams, R. N. Carbon Paste Electrodes. *Anal. Chem.* **1958**, 30 (9), 1576–1576. <https://doi.org/10.1021/ac60141a600>.
- (19) Švancara, I.; Vytrás, K.; Kalcher, K.; Walcarius, A.; Wang, J. Carbon Paste Electrodes in Facts, Numbers, and Notes: A Review on the Occasion of the 50-Years Jubilee of Carbon Paste in Electrochemistry and Electroanalysis. *Electroanalysis* **2009**, 21 (1), 7–28. <https://doi.org/10.1002/elan.200804340>.
- (20) Wang, J. *Analytical Electrochemistry*, 3ed Editio.; John Wiley & Sons: Hoboken, New Jersey, 2006.
- (21) Olson, C.; Adams, R. N. Carbon Paste Electrodes Application to Anodic Voltammetry. *Anal. Chim. Acta* **1960**, 22 (C), 582–589. [https://doi.org/10.1016/S0003-2670\(00\)88341-5](https://doi.org/10.1016/S0003-2670(00)88341-5).
- (22) Urbaniczky, C.; Lundström, K. Voltammetric Studies on Carbon Paste Electrodes. *J. Electroanal. Chem. Interfacial Electrochem.* **1984**, 176 (1–2), 169–182. [https://doi.org/10.1016/S0022-0728\(84\)80315-0](https://doi.org/10.1016/S0022-0728(84)80315-0).
- (23) Rice, M. E.; Galus, Z.; Adams, R. N. Graphite Paste Electrodes. *J. Electroanal. Chem. Interfacial Electrochem.* **1983**, 143 (1–2), 89–102. [https://doi.org/10.1016/S0022-0728\(83\)80256-3](https://doi.org/10.1016/S0022-0728(83)80256-3).
- (24) Céspedes, F.; Martínez-Fàbregas, E.; Alegret, S. New Materials for Electrochemical Sensing I. Rigid Conducting Composites. *TrAC - Trends Anal. Chem.* **1996**, 15 (7), 296–304. [https://doi.org/10.1016/0165-9936\(96\)00042-8](https://doi.org/10.1016/0165-9936(96)00042-8).
- (25) Kausar, A.; Anwar, Z.; Muhammad, B. Recent Developments in Epoxy/Graphite, Epoxy/Graphene, and Epoxy/Graphene Nanoplatelet Composites: A Comparative Review. *Polym. Plast. Technol. Eng.* **2016**, 55 (11), 1192–1210. <https://doi.org/10.1080/03602559.2016.1163589>.
- (26) Yao, S.-S.; Jiang, D.; Zhang, Q.-Z.; Wang, X.-X. Preparation and Properties of Graphite/Epoxy Resin Conductive Composites. *IOP Conf. Ser. Mater. Sci. Eng.* **2020**, 740 (1), 012064. <https://doi.org/10.1088/1757-899X/740/1/012064>.
- (27) Kipphan, H. *Handbook of Print Media: Technologies and Production Methods*; Media, S. S. & B., Ed.; 2001.
- (28) de la Fuente Vornbrock, A.; Sung, D.; Kang, H.; Kitsomboonloha, R.; Subramanian, V. Fully Gravure and Ink-Jet Printed High Speed PBTTT Organic Thin Film Transistors. *Org. Electron.* **2010**, 11 (12), 2037–2044. <https://doi.org/10.1016/j.orgel.2010.09.003>.
- (29) Ummartyotin, S.; Manuspiya, H. A Critical Review on Cellulose: From Fundamental to an Approach on Sensor Technology. *Renew. Sustain. Energy Rev.* **2015**, 41, 402–412. <https://doi.org/10.1016/j.rser.2014.08.050>.
- (30) Nery, E. W.; Kubota, L. T. Sensing Approaches on Paper-Based Devices: A Review. *Anal. Bioanal. Chem.* **2013**, 405 (24), 7573–7595. <https://doi.org/10.1007/s00216-013-6911-4>.
- (31) Carvalhal, R. F.; Simão Kfour, M.; de Oliveira Piazzetta, M. H.; Gobbi, A. L.; Kubota, L. T. Electrochemical Detection in a Paper-Based Separation Device. *Anal. Chem.* **2010**, 82 (3), 1162–1165. <https://doi.org/10.1021/ac902647r>.
- (32) Shrivastava, K.; Monisha; Kant, T.; Karbhal, I.; Kurrey, R.; Sahu, B.; Sinha, D.; Patra, G. K.; Deb, M. K.; Pervez, S. Smartphone Coupled with Paper-Based Chemical Sensor for on-Site Determination of Iron(III) in Environmental and Biological Samples. *Anal. Bioanal. Chem.* **2020**, 412 (7), 1573–1583. <https://doi.org/10.1007/s00216-019-02385-x>.

- (33) Liu, X. Y.; Cheng, C. M.; Martinez, A. W.; Mirica, K. A.; Li, X. J.; Phillips, S. T.; Mascarenas, M.; Whitesides, G. M. A Portable Microfluidic Paper-Based Device for ELISA. In *2011 IEEE 24th International Conference on Micro Electro Mechanical Systems*; IEEE, 2011; pp 75–78. <https://doi.org/10.1109/MEMSYS.2011.5734365>.
- (34) Tseng, S.-C.; Yu, C.-C.; Wan, D.; Chen, H.-L.; Wang, L. A.; Wu, M.-C.; Su, W.-F.; Han, H.-C.; Chen, L.-C. Eco-Friendly Plasmonic Sensors: Using the Photothermal Effect to Prepare Metal Nanoparticle-Containing Test Papers for Highly Sensitive Colorimetric Detection. *Anal. Chem.* **2012**, *84* (11), 5140–5145. <https://doi.org/10.1021/ac300397h>.
- (35) Barr, M. C.; Rowe, J. A.; Lunt, R. R.; Xu, J.; Wang, A.; Boyce, C. M.; Im, S. G.; Bulović, V.; Gleason, K. K. Direct Monolithic Integration of Organic Photovoltaic Circuits on Unmodified Paper. *Adv. Mater.* **2011**, *23* (31), 3500–3505. <https://doi.org/10.1002/adma.201101263>.
- (36) Ruas de Souza, A. P.; Foster, C. W.; Kolliopoulos, A. V.; Bertotti, M.; Banks, C. E. Screen-Printed Back-to-Back Electroanalytical Sensors: Heavy Metal Ion Sensing. *Analyst* **2015**, *140* (12), 4130–4136. <https://doi.org/10.1039/C5AN00381D>.
- (37) Taleat, Z.; Khoshroo, A.; Mazloum-Ardakani, M. Screen-Printed Electrodes for Biosensing: A Review (2008–2013). *Microchim. Acta* **2014**, *181* (9–10), 865–891. <https://doi.org/10.1007/s00604-014-1181-1>.
- (38) Renedo, O. D.; Alonso-Lomillo, M. A.; Martínez, M. J. A. Recent Developments in the Field of Screen-Printed Electrodes and Their Related Applications. *Talanta* **2007**, *73* (2), 202–219. <https://doi.org/10.1016/j.talanta.2007.03.050>.
- (39) Li, M.; Li, Y.-T.; Li, D.-W.; Long, Y.-T. Recent Developments and Applications of Screen-Printed Electrodes in Environmental Assays—A Review. *Anal. Chim. Acta* **2012**, *734*, 31–44. <https://doi.org/10.1016/j.aca.2012.05.018>.
- (40) da Costa, T. H.; Song, E.; Tortorich, R. P.; Choi, J.-W. A Paper-Based Electrochemical Sensor Using Inkjet-Printed Carbon Nanotube Electrodes. *ECSS J. Solid State Sci. Technol.* **2015**, *4* (10), S3044–S3047. <https://doi.org/10.1149/2.0121510jss>.
- (41) Lesch, A.; Cortés-Salazar, F.; Amstutz, V.; Tacchini, P.; Girault, H. H. Inkjet Printed Nanohydrogel Coated Carbon Nanotubes Electrodes For Matrix Independent Sensing. *Anal. Chem.* **2015**, *87* (2), 1026–1033. <https://doi.org/10.1021/ac503748g>.
- (42) Ihalainen, P.; Määttä, A.; Pesonen, M.; Sjöberg, P.; Sarfraz, J.; Österbacka, R.; Peltonen, J. Paper-Supported Nanostructured Ultrathin Gold Film Electrodes – Characterization and Functionalization. *Appl. Surf. Sci.* **2015**, *329*, 321–329. <https://doi.org/10.1016/j.apsusc.2014.12.156>.
- (43) Bardpho, C.; Rattanarat, P.; Siangproh, W.; Chailapakul, O. Ultra-High Performance Liquid Chromatographic Determination of Antioxidants in Teas Using Inkjet-Printed Graphene–Polyaniline Electrode. *Talanta* **2016**, *148*, 673–679. <https://doi.org/10.1016/j.talanta.2015.05.020>.
- (44) Sjöberg, P.; Määttä, A.; Vanamo, U.; Novell, M.; Ihalainen, P.; Andrade, F. J.; Bobacka, J.; Peltonen, J. Paper-Based Potentiometric Ion Sensors Constructed on Ink-Jet Printed Gold Electrodes. *Sensors Actuators B Chem.* **2016**, *224*, 325–332. <https://doi.org/10.1016/j.snb.2015.10.051>.
- (45) Adly, N. Y.; Bachmann, B.; Krause, K. J.; Offenhäusser, A.; Wolfrum, B.; Yakushenko, A. Three-Dimensional Inkjet-Printed Redox Cycling Sensor. *RSC*

- Adv.* **2017**, 7 (9), 5473–5479. <https://doi.org/10.1039/C6RA27170G>.
- (46) Jović, M.; Cortés-Salazar, F.; Lesch, A.; Amstutz, V.; Bi, H.; Girault, H. H. Electrochemical Detection of Free Chlorine at Inkjet Printed Silver Electrodes. *J. Electroanal. Chem.* **2015**, 756, 171–178. <https://doi.org/10.1016/j.jelechem.2015.08.024>.
- (47) Xu, Z.; Dong, Q.; Otieno, B.; Liu, Y.; Williams, I.; Cai, D.; Li, Y.; Lei, Y.; Li, B. Real-Time in Situ Sensing of Multiple Water Quality Related Parameters Using Micro-Electrode Array (MEA) Fabricated by Inkjet-Printing Technology (IPT). *Sensors Actuators B Chem.* **2016**, 237, 1108–1119. <https://doi.org/10.1016/j.snb.2016.09.040>.
- (48) Qin, Y.; Alam, A. U.; Howlader, M. M. R.; Hu, N.-X.; Deen, M. J. Inkjet Printing of a Highly Loaded Palladium Ink for Integrated, Low-Cost PH Sensors. *Adv. Funct. Mater.* **2016**, 26 (27), 4923–4933. <https://doi.org/10.1002/adfm.201600657>.
- (49) Jović, M.; Zhu, Y.; Lesch, A.; Bondarenko, A.; Cortés-Salazar, F.; Gummy, F.; Girault, H. H. Inkjet-Printed Microtiter Plates for Portable Electrochemical Immunoassays. *J. Electroanal. Chem.* **2017**, 786, 69–76. <https://doi.org/10.1016/j.jelechem.2016.12.051>.
- (50) Hu, C.; Bai, X.; Wang, Y.; Jin, W.; Zhang, X.; Hu, S. Inkjet Printing of Nanoporous Gold Electrode Arrays on Cellulose Membranes for High-Sensitive Paper-Like Electrochemical Oxygen Sensors Using Ionic Liquid Electrolytes. *Anal. Chem.* **2012**, 84 (8), 3745–3750. <https://doi.org/10.1021/ac3003243>.
- (51) Le, D. D.; Nguyen, T. N. N.; Doan, D. C. T.; Dang, T. M. D.; Dang, M. C. Fabrication of Interdigitated Electrodes by Inkjet Printing Technology for Application in Ammonia Sensing. *Adv. Nat. Sci. Nanosci. Nanotechnol.* **2016**, 7 (2), 025002. <https://doi.org/10.1088/2043-6262/7/2/025002>.
- (52) Moya, A.; Gabriel, G.; Villa, R.; Javier del Campo, F. Inkjet-Printed Electrochemical Sensors. *Curr. Opin. Electrochem.* **2017**, 3 (1), 29–39. <https://doi.org/10.1016/j.coelec.2017.05.003>.
- (53) Symes, M. D.; Kitson, P. J.; Yan, J.; Richmond, C. J.; Cooper, G. J. T.; Bowman, R. W.; Vilbrandt, T.; Cronin, L. Integrated 3D-Printed Reactionware for Chemical Synthesis and Analysis. *Nat. Chem.* **2012**, 4 (5), 349–354. <https://doi.org/10.1038/nchem.1313>.
- (54) Ambrosi, A.; Pumera, M. 3D-Printing Technologies for Electrochemical Applications. *Chem. Soc. Rev.* **2016**, 45 (10), 2740–2755. <https://doi.org/10.1039/c5cs00714c>.
- (55) Abdalla, A.; Patel, B. A. 3D Printed Electrochemical Sensors. *Annu. Rev. Anal. Chem.* **2021**, 14 (1), 47–63. <https://doi.org/10.1146/annurev-anchem-091120-093659>.
- (56) Han, T.; Kundu, S.; Nag, A.; Xu, Y. 3D Printed Sensors for Biomedical Applications: A Review. *Sensors* **2019**, 19 (7), 1706. <https://doi.org/10.3390/s19071706>.
- (57) Khosravani, M. R.; Reinicke, T. 3D-Printed Sensors: Current Progress and Future Challenges. *Sensors Actuators, A Phys.* **2020**, 305, 111916. <https://doi.org/10.1016/j.sna.2020.111916>.
- (58) Edwards, G. A.; Bergren, A. J.; Porter, M. D. Chemically Modified Electrodes. In *Handbook of Electrochemistry*; Elsevier, 2007; Vol. 11, pp 295–327. <https://doi.org/10.1016/B978-044451958-0.50021-5>.
- (59) Murray, R. W. Chemically Modified Electrodes. *Acc. Chem. Res.* **1980**, 13 (5),

- 135–141. <https://doi.org/10.1021/ar50149a002>.
- (60) Wang, J. Modified Electrodes for Electrochemical Sensors. *Electroanalysis* **1991**, 3 (4–5), 255–259. <https://doi.org/10.1002/elan.1140030404>.
- (61) Cipri, A.; del Valle, M. Pd Nanoparticles/Multiwalled Carbon Nanotubes Electrode System for Voltammetric Sensing of Tyrosine. *J. Nanosci. Nanotechnol.* **2014**, 14 (9), 6692–6698. <https://doi.org/10.1166/jnn.2014.9370>.
- (62) Daniels, J. S.; Pourmand, N. Label-Free Impedance Biosensors: Opportunities and Challenges. *Electroanalysis* **2007**, 19 (12), 1239–1257. <https://doi.org/10.1002/elan.200603855>.
- (63) González-Sánchez, M. I.; Gómez-Monedero, B.; Agrisuelas, J.; Iniesta, J.; Valero, E. Highly Activated Screen-Printed Carbon Electrodes by Electrochemical Treatment with Hydrogen Peroxide. *Electrochem. commun.* **2018**, 91 (February), 36–40. <https://doi.org/10.1016/j.elecom.2018.05.002>.
- (64) Bard J, Allen; Faulkner, L. R. *Electrochemical Methods: Fundamental and Applications*, 2nd ed.; Inc, J. W. & S., Ed.; 2001.
- (65) Skoog, Douglas A.; Holler F, J.; R. Crouch, S. *Principles of Instrumental Analysis*, 7th ed.; Cengage Learning, Ed.; 2017.
- (66) Unwin, R. P.; Stratmann, M.; Bard, J. A. Instrumentation and Electroanalytical Chemistry; Volume 3. *Encyclopedia of Electrochemistry*; 2003.
- (67) Sajid, M.; Płotka-Wasyłka, J. Green Analytical Chemistry Metrics: A Review. *Talanta* **2022**, 238, 123046. <https://doi.org/10.1016/j.talanta.2021.123046>.
- (68) Valle, M. del. Bioinspired Sensor Systems. *Sensors* **2011**, 11 (11), 10180–10186. <https://doi.org/10.3390/s111110180>.
- (69) Latha, R. S.; Lakshmi, P. K. Electronic Tongue: An Analytical Gustatory Tool. *J. Adv. Pharm. Technol. Res.* **2012**, 3 (1), 3–8. <https://doi.org/10.4103/2231-4040.93556>.
- (70) Vlasov, Y.; Legin, A.; Rudnitskaya, A.; Di Natale, C.; D'Amico, A. Nonspecific Sensor Arrays (“electronic Tongue”) for Chemical Analysis of Liquids (IUPAC Technical Report). *Pure Appl. Chem.* **2005**, 77 (11), 1965–1983. <https://doi.org/10.1351/pac200577111965>.
- (71) Otto, M.; Thomas, J. D. R. Model Studies on Multiple Channel Analysis of Free Magnesium, Calcium, Sodium, and Potassium at Physiological Concentration Levels with Ion-Selective Electrodes. *Anal. Chem.* **1985**, 57 (13), 2647–2651. <https://doi.org/10.1021/ac00290a049>.
- (72) Legin, A.; Rudnitskaya, A.; Vlasov, Y.; Di Natale, C.; Davide, F.; D'Amico, A. Tasting of Beverages Using an Electronic Tongue. *Sensors Actuators B Chem.* **1997**, 44 (1–3), 291–296. [https://doi.org/10.1016/S0925-4005\(97\)00167-6](https://doi.org/10.1016/S0925-4005(97)00167-6).
- (73) Vlasov, Y.; Legin, A. Non-Selective Chemical Sensors in Analytical Chemistry: From “Electronic Nose” to “Electronic Tongue.” *Fresenius. J. Anal. Chem.* **1998**, 361 (3), 255–260. <https://doi.org/10.1007/s002160050875>.
- (74) Hayashi, K.; Yamanaka, M.; Toko, K.; Yamafuji, K. Multichannel Taste Sensor Using Lipid Membranes. *Sensors Actuators B Chem.* **1990**, 2 (3), 205–213. [https://doi.org/10.1016/0925-4005\(90\)85006-K](https://doi.org/10.1016/0925-4005(90)85006-K).
- (75) Tahara, Y.; Toko, K. Electronic Tongues – A Review. **2013**, 13 (8), 3001–3011.
- (76) Winquist, F.; Wide, P.; Lundström, I. An Electronic Tongue Based on Voltammetry. *Anal. Chim. Acta* **1997**, 357 (1–2), 21–31. [https://doi.org/10.1016/S0003-2670\(97\)00498-4](https://doi.org/10.1016/S0003-2670(97)00498-4).

-
- (77) del Valle, M. Sensor Arrays and Electronic Tongue Systems. *Int. J. Electrochem.* **2012**, *2012*, 1–11. <https://doi.org/10.1155/2012/986025>.
- (78) Gallardo, J.; Alegret, S.; Del Valle, M. Application of a Potentiometric Electronic Tongue as a Classification Tool in Food Analysis. *Talanta* **2005**, *66* (5), 1303–1309. <https://doi.org/10.1016/j.talanta.2005.01.049>.
- (79) Cetó, X.; Gutiérrez-Capitán, M.; Calvo, D.; del Valle, M. Beer Classification by Means of a Potentiometric Electronic Tongue. *Food Chem.* **2013**, *141* (3), 2533–2540. <https://doi.org/10.1016/j.foodchem.2013.05.091>.
- (80) Cetó, X.; Apetrei, C.; del Valle, M.; Rodríguez-Méndez, M. L. Evaluation of Red Wines Antioxidant Capacity by Means of a Voltammetric E-Tongue with an Optimized Sensor Array. *Electrochim. Acta* **2014**, *120*, 180–186. <https://doi.org/10.1016/j.electacta.2013.12.079>.
- (81) Bro, R. PARAFAC. Tutorial and Applications. *Chemom. Intell. Lab. Syst.* **1997**, *38* (2), 149–171. [https://doi.org/10.1016/S0169-7439\(97\)00032-4](https://doi.org/10.1016/S0169-7439(97)00032-4).
- (82) Podraźka, M.; Bączyńska, E.; Kundys, M.; Jeleń, P.; Witkowska Nery, E. Electronic Tongue—A Tool for All Tastes? *Biosensors* **2017**, *8* (1), 3. <https://doi.org/10.3390/bios8010003>.
- (83) Einax, J. W. Chemometrics in Analytical Chemistry. *Anal. Bioanal. Chem.* **2004**, *380* (3), 368–369. <https://doi.org/10.1007/s00216-004-2792-x>.
- (84) Wold, S. Chemometrics; What Do We Mean with It, and What Do We Want from It? *Chemom. Intell. Lab. Syst.* **1995**, *30* (1), 109–115. [https://doi.org/10.1016/0169-7439\(95\)00042-9](https://doi.org/10.1016/0169-7439(95)00042-9).
- (85) Esbensen, K.; Geladi, P. The Start and Early History of Chemometrics: Selected Interviews. Part 2. *J. Chemom.* **1990**, *4* (6), 389–412. <https://doi.org/10.1002/cem.1180040604>.
- (86) Shepherd, P. T. Retrospective. *J. Chemom.* **1987**, *1* (1), 3–6. <https://doi.org/10.1002/cem.1180010103>.
- (87) Díaz-Cruz, J. M.; Esteban, M.; Ariño, C. *Chemometrics in Electroanalysis*; Scholz, F., Ed.; Springer, 2019.
- (88) Cetó, X.; Céspedes, F.; del Valle, M. Comparison of Methods for the Processing of Voltammetric Electronic Tongues Data. *Microchim. Acta* **2013**, *180* (5–6), 319–330. <https://doi.org/10.1007/s00604-012-0938-7>.
- (89) Cetó, X.; Céspedes, F.; del Valle, M. Assessment of Individual Polyphenol Content in Beer by Means of a Voltammetric BioElectronic Tongue. *Electroanalysis* **2013**, *25* (1), 68–76. <https://doi.org/10.1002/elan.201200299>.
- (90) Simons, J.; Bos, M.; van der Linden, W. E. Data Processing for Amperometric Signals. *Analyst* **1995**, *120* (4), 1009. <https://doi.org/10.1039/an9952001009>.
- (91) Gutierrez-Osuna, R.; Nagle, H. T. A Method for Evaluating Data-Preprocessing Techniques for Odour Classification with an Array of Gas Sensors. *IEEE Trans. Syst. Man Cybern. Part B* **1999**, *29* (5), 626–632. <https://doi.org/10.1109/3477.790446>.
- (92) Moreno-Barón, L.; Cartas, R.; Merkoçi, A.; Alegret, S.; del Valle, M.; Leija, L.; Hernandez, P. R.; Muñoz, R. Application of the Wavelet Transform Coupled with Artificial Neural Networks for Quantification Purposes in a Voltammetric Electronic Tongue. *Sensors Actuators B Chem.* **2006**, *113* (1), 487–499. <https://doi.org/10.1016/j.snb.2005.03.063>.
- (93) Cetó, X.; Céspedes, F.; del Valle, M. BioElectronic Tongue for the Quantification
-

- p of Total Polyphenol Content in Wine.
- Talanta*
- 2012**
- , 99, 544–551.
- <https://doi.org/10.1016/j.talanta.2012.06.031>
- .
- (94) Boger, Z. Selection of Quasi-Optimal Inputs in Chemometrics Modeling by Artificial Neural Network Analysis. *Anal. Chim. Acta* **2003**, 490 (1–2), 31–40. [https://doi.org/10.1016/S0003-2670\(03\)00349-0](https://doi.org/10.1016/S0003-2670(03)00349-0).
- (95) Naes, T.; Isaksson, T.; Fearn, T.; Davies, T. *A User-Friendly Guide to Multivariate Calibration and Classification*; NIR publications, Ed.; 2004.
- (96) Palacios-Santander, J. M.; Cubillana-Aguilera, L. M.; Cocchi, M.; Ulrici, A.; Naranjo-Rodríguez, I.; Seeber, R.; Hidalgo-Hidalgo de Cisneros, J. L. Multicomponent Analysis in the Wavelet Domain of Highly Overlapped Electrochemical Signals: Resolution of Quaternary Mixtures of Chlorophenols Using a Peg-Modified Sonogel–Carbon Electrode. *Chemom. Intell. Lab. Syst.* **2008**, 91 (2), 110–120. <https://doi.org/10.1016/j.chemolab.2007.10.004>.
- (97) Mallat, S. G. A Theory for Multiresolution Signal Decomposition: The Wavelet Representation. *Fundam. Pap. Wavelet Theory* **2009**, 1 (7), 494–513. <https://doi.org/10.1515/9781400827268.494>.
- (98) Leardi, R. Genetic Algorithms in Chemometrics and Chemistry: A Review. *J. Chemom.* **2001**, 15 (7), 559–569. <https://doi.org/10.1002/cem.651>.
- (99) Niazi, A.; Leardi, R. Genetic Algorithms in Chemometrics. *J. Chemom.* **2012**, 26 (6), 345–351. <https://doi.org/10.1002/cem.2426>.
- (100) Sarma, M.; Romero, N.; Cetó, X.; Valle, M. Del. Optimization of Sensors to Be Used in a Voltammetric Electronic Tongue Based on Clustering Metrics. *Sensors* **2020**, 20 (17), 4798. <https://doi.org/10.3390/s20174798>.
- (101) Thinsungnoen, T.; Kaoungku, N.; Durongdumronchai, P.; Kerdprasop, K.; Kerdprasop, N. The Clustering Validity with Silhouette and Sum of Squared Errors. In *The Proceedings of the 2nd International Conference on Industrial Application Engineering 2015*; The Institute of Industrial Applications Engineers, 2015; pp 44–51. <https://doi.org/10.12792/iciae2015.012>.
- (102) Berrueta, L. A.; Alonso-Salces, R. M.; Héberger, K. Supervised Pattern Recognition in Food Analysis. *J. Chromatogr. A* **2007**, 1158 (1–2), 196–214. <https://doi.org/10.1016/j.chroma.2007.05.024>.
- (103) Osisanwo F.Y., Akinsola J.E.T., Awodele O., Hinmikaiye J. O., Olakanmi O., A. J. Supervised Machine Learning Algorithms: Classification and Comparison. *Int. J. Comput. Trends Technol.* **2017**, 48 (3), 128–138. <https://doi.org/10.14445/22312803/IJCTT-V48P126>.
- (104) R.G Brereton. *Applied Chemometrics for Scientists*; John Wiley & Sons, Ed.; Chichester, 2007.
- (105) Abdi, H. Partial Least Squares Regression and Projection on Latent Structure Regression (PLS Regression). *WIREs Comput. Stat.* **2010**, 2 (1), 97–106. <https://doi.org/10.1002/wics.51>.
- (106) Serrano, N.; González-Calabuig, A.; del Valle, M. Crown Ether-Modified Electrodes for the Simultaneous Stripping Voltammetric Determination of Cd(II), Pb(II) and Cu(II). *Talanta* **2015**, 138, 130–137. <https://doi.org/10.1016/j.talanta.2015.01.044>.
- (107) Cetó, X.; O'Mahony, A. M.; Wang, J.; Del Valle, M. Simultaneous Identification and Quantification of Nitro-Containing Explosives by Advanced Chemometric Data Treatment of Cyclic Voltammetry at Screen-Printed Electrodes. *Talanta* **2013**, 107, 270–276. <https://doi.org/10.1016/j.talanta.2012.12.042>.

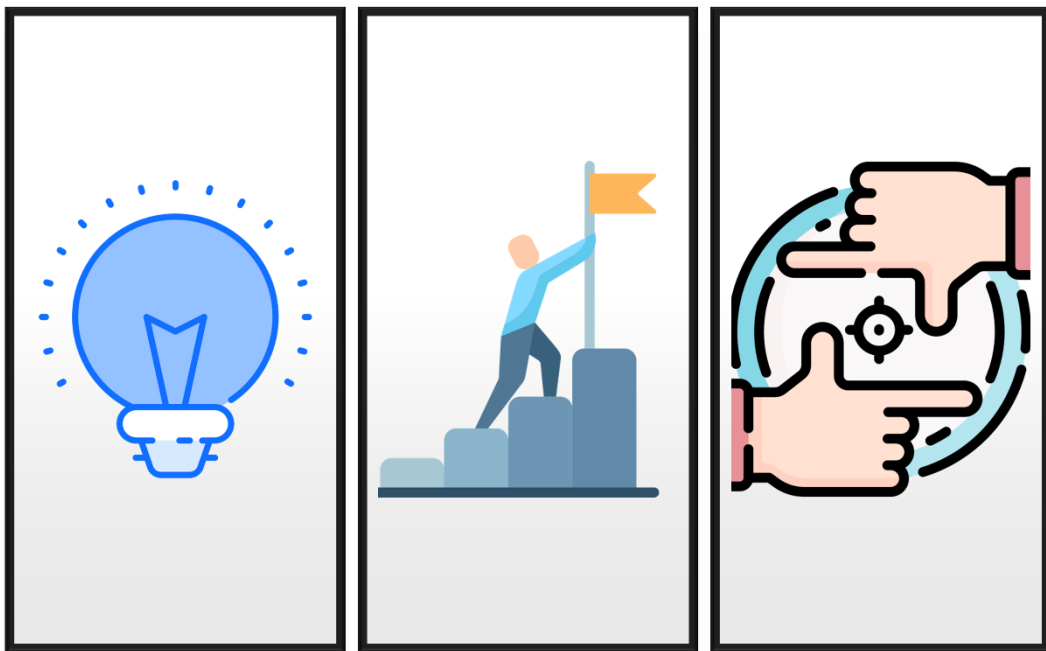
-
- (108) González-Calabuig, A.; del Valle, M. Voltammetric Electronic Tongue to Identify Brett Character in Wines. On-Site Quantification of Its Ethylphenol Metabolites. *Talanta* **2018**, *179* (July 2017), 70–74. <https://doi.org/10.1016/j.talanta.2017.10.041>.
- (109) De Sá, A. C.; Cipri, A.; González-Calabuig, A.; Stradiotto, N. R.; Del Valle, M. Resolution of Galactose, Glucose, Xylose and Mannose in Sugarcane Bagasse Employing a Voltammetric Electronic Tongue Formed by Metals Oxy-Hydroxide/MWCNT Modified Electrodes. *Sensors Actuators, B Chem.* **2016**, *222*, 645–653. <https://doi.org/10.1016/j.snb.2015.08.088>.
- (110) Rosenblatt, F. The Perceptron: A Probabilistic Model for Information Storage and Organization in the Brain. *Psychol. Rev.* **1958**, *65* (6), 386–408. <https://doi.org/10.1037/h0042519>.
- (111) Oliveri, P.; Chiara Casolino, M.; Forina, M. Chemometric Brains for Artificial Tongues. In *Advances in Food and Nutrition Research*; Elsevier Masson SAS, 2010; Vol. 61, pp 57–117. <https://doi.org/10.1016/B978-0-12-374468-5.00002-7>.
- (112) Sanghavi, B. J.; Srivastava, A. K. Simultaneous Voltammetric Determination of Acetaminophen, Aspirin and Caffeine Using an in Situ Surfactant-Modified Multiwalled Carbon Nanotube Paste Electrode. *Electrochim. Acta* **2010**, *55* (28), 8638–8648. <https://doi.org/10.1016/j.electacta.2010.07.093>.
- (113) Madrakian, T.; Haghshenas, E.; Afkhami, A. Simultaneous Determination of Tyrosine, Acetaminophen and Ascorbic Acid Using Gold Nanoparticles/Multiwalled Carbon Nanotube/Glassy Carbon Electrode by Differential Pulse Voltammetric Method. *Sensors Actuators B Chem.* **2014**, *193*, 451–460. <https://doi.org/10.1016/j.snb.2013.11.117>.
- (114) Hu, G.; Ma, Y.; Guo, Y.; Shao, S. Electrocatalytic Oxidation and Simultaneous Determination of Uric Acid and Ascorbic Acid on the Gold Nanoparticles-Modified Glassy Carbon Electrode. *Electrochim. Acta* **2008**, *53* (22), 6610–6615. <https://doi.org/10.1016/j.electacta.2008.04.054>.
- (115) Beard, E. L. The American Society of Health System Pharmacists. *JONA's Healthc. Law, Ethics, Regul.* **2001**, *3* (3), 78–79. <https://doi.org/10.1097/00128488-200109000-00003>.
- (116) Miland, E.; Ordieres, M. A.; Blanco, P. T.; Smyth, M.; Fagain, C. Poly(-Aminophenol)-Modified Bionzyme Carbon Paste Electrode for the Detection of Uric Acid. *Talanta* **1996**, *43* (5), 785–796. [https://doi.org/10.1016/0039-9140\(95\)01825-5](https://doi.org/10.1016/0039-9140(95)01825-5).
- (117) Capella-Peiró, M.-E.; Bose, D.; Rubert, M. F.; Esteve-Romero, J. Optimization of a Capillary Zone Electrophoresis Method by Using a Central Composite Factorial Design for the Determination of Codeine and Paracetamol in Pharmaceuticals. *J. Chromatogr. B* **2006**, *839* (1–2), 95–101. <https://doi.org/10.1016/j.jchromb.2006.04.023>.
- (118) Sun, X.; Niu, Y.; Bi, S.; Zhang, S. Determination of Ascorbic Acid in Individual Rat Hepatocyte Cells Based on Capillary Electrophoresis with Electrochemiluminescence Detection. *Electrophoresis* **2008**, NA-NA. <https://doi.org/10.1002/elps.200700792>.
- (119) Akay, C.; Gümüşel, B.; Degim, T.; Tartılmıs, S.; Cevheroglu, S. Simultaneous Determination of Acetaminophen, Acetylsalicylic Acid in Tablet Form Using HPLC. *Drug Metabol. Drug Interact.* **1999**, *15* (2–3). <https://doi.org/10.1515/DMDI.1999.15.2-3.197>.
- (120) Thomis, R.; Roets, E.; Hoogmartens, J. Analysis of Tablets Containing
-

- Aspirin, Acetaminophen, and Ascorbic Acid by High-Performance Liquid Chromatography. *J. Pharm. Sci.* **1984**, 73 (12), 1830–1833. <https://doi.org/10.1002/jps.2600731246>.
- (121) Sirajuddin; Khaskheli, A. R.; Shah, A.; Bhanger, M. I.; Niaz, A.; Mahesar, S. Simpler Spectrophotometric Assay of Paracetamol in Tablets and Urine Samples. *Spectrochim. Acta Part A Mol. Biomol. Spectrosc.* **2007**, 68 (3), 747–751. <https://doi.org/10.1016/j.saa.2006.12.055>.
- (122) Ortega Barrales, P.; Fernández de Córdova, M. .; Molina Díaz, A. Indirect Determination of Ascorbic Acid by Solid-Phase Spectrophotometry. *Anal. Chim. Acta* **1998**, 360 (1–3), 143–152. [https://doi.org/10.1016/S0003-2670\(97\)00688-0](https://doi.org/10.1016/S0003-2670(97)00688-0).
- (123) Dejaegher, B. Validation of a Fluorimetric Assay for 4-Aminophenol in Paracetamol Formulations. *Talanta* **2008**, 75 (1), 258–265. <https://doi.org/10.1016/j.talanta.2007.11.029>.
- (124) Llorent-Martínez, E. J.; Šatínský, D.; Solich, P.; Ortega-Barrales, P.; Molina-Díaz, A. Fluorimetric SIA Optosensing in Pharmaceutical Analysis: Determination of Paracetamol. *J. Pharm. Biomed. Anal.* **2007**, 45 (2), 318–321. <https://doi.org/10.1016/j.jpba.2007.05.004>.
- (125) Svorc, L. Determination of Caffeine: A Comprehensive Review on Electrochemical Methods. *Int. J. Electrochem. Sci.* **2013**, 8, 5755–5773.
- (126) Gutes, A.; Calvo, D.; Céspedes, F.; del Valle, M. Automatic Sequential Injection Analysis Electronic Tongue with Integrated Reference Electrode for the Determination of Ascorbic Acid, Uric Acid and Paracetamol. *Microchim. Acta* **2007**, 157 (1–2), 1–6. <https://doi.org/10.1007/s00604-006-0660-4>.
- (127) Wang, M.; Cetó, X.; del Valle, M. A Novel Electronic Tongue Using Electropolymerized Molecularly Imprinted Polymers for the Simultaneous Determination of Active Pharmaceutical Ingredients. *Biosens. Bioelectron.* **2022**, 198, 113807. <https://doi.org/10.1016/j.bios.2021.113807>.
- (128) Florea, A.; de Jong, M.; De Wael, K. Electrochemical Strategies for the Detection of Forensic Drugs. *Curr. Opin. Electrochem.* **2018**, 11, 34–40. <https://doi.org/10.1016/j.coelec.2018.06.014>.
- (129) Bordersens: Border Detection of Illicit Drugs and Precursors by Highly Accurate Electrosensors, 2021. <https://bordersens.eu/> (accessed Jul 30, 2021).
- (130) United Nations Office on Drugs and Crime. Drugs of Abuse 2017 Edition: A DEA Resource Guide. *Forensic Toxicol.* **2017**, 37 (2), 2352–2362.
- (131) O'Donnell, J. K.; Gladden, R. M.; Seth, P. Trends in Deaths Involving Heroin and Synthetic Opioids Excluding Methadone, and Law Enforcement Drug Product Reports, by Census Region — United States, 2006–2015. *MMWR. Morb. Mortal. Wkly. Rep.* **2017**, 66 (34), 897–903. <https://doi.org/10.15585/mmwr.mm6634a2>.
- (132) Garrido, J. M. P. J.; Delerue-Matos, C.; Borges, F.; Macedo, T. R. A.; Oliveira-Brett, A. M. Electrochemical Analysis of Opiates - An Overview. *Anal. Lett.* **2004**, 37 (5), 831–844. <https://doi.org/10.1081/AL-120030282>.
- (133) Salem, M. Y.; Ross, S. A.; Murphy, T. P.; ElSohly, M. A. GC-MS Determination of Heroin Metabolites in Meconium: Evaluation of Four Solid-Phase Cartridges. *J. Anal. Toxicol.* **2001**, 25 (2), 93–98. <https://doi.org/10.1093/jat/25.2.93>.
- (134) Zhang, Z.; Yan, B.; Liu, K.; Liao, Y.; Liu, H. CE-MS Analysis of Heroin and Its Basic Impurities Using a Charged Polymer-Protected Gold Nanoparticle-Coated Capillary. *Electrophoresis* **2009**, 30 (2), 379–387. <https://doi.org/10.1002/elps.200800069>.

-
- (135) Zhuang, Y.; Cai, X.; Yu, J.; Ju, H. Flow Injection Chemiluminescence Analysis for Highly Sensitive Determination of Noscapine. *J. Photochem. Photobiol. A Chem.* **2004**, *162* (2–3), 457–462. [https://doi.org/10.1016/S1010-6030\(03\)00391-5](https://doi.org/10.1016/S1010-6030(03)00391-5).
- (136) Moros, J.; Galipienso, N.; Vilches, R.; Garrigues, S.; De La Guardia, M. Nondestructive Direct Determination of Heroin in Seized Illicit Street Drugs by Diffuse Reflectance Near-Infrared Spectroscopy. *Anal. Chem.* **2008**, *80* (19), 7257–7265. <https://doi.org/10.1021/ac800781c>.
- (137) Sakai, G.; Ogata, K.; Uda, T.; Miura, N.; Yamazoe, N. A Surface Plasmon Resonance-Based Immunosensor for Highly Sensitive Detection of Morphine. *Sensors Actuators, B Chem.* **1998**, *49* (1–2), 5–12. [https://doi.org/10.1016/S0925-4005\(98\)00107-5](https://doi.org/10.1016/S0925-4005(98)00107-5).
- (138) European Monitoring Centre for Drugs and Drug Addiction and Europol. *EU Drug Markets Report 2019*; 2019. <https://doi.org/10.2810/561192>.
- (139) European Monitoring Centre for Drugs and Drug Addiction. *European Drug Report 2020: Trends and Developments*; Luxembourg, 2020. <https://doi.org/10.2810/420678>.
- (140) Khair-ul-Bariyah, S.; Arshad, M.; Ali, M.; Din, M. I.; Sharif, A.; Ahmed, E. Benzocaine: Review on a Drug with Unfold Potential. *Mini-Reviews Med. Chem.* **2020**, *20* (1), 3–11. <https://doi.org/10.2174/1389557519666190913145423>.

II. OBJECTIVES

In this chapter, the main goals of this dissertation will be described in detail.



1. Objectives

In the present doctoral thesis, the main general goal is to develop electronic tongues using divers sensor platforms for applications in the forensic and security fields. To achieve this general purpose, several specific objectives were raised hereunder.

1. To design, evaluate, and characterize of the different printed sensor platforms.

1.1 To use an eight-sensor integrated array of screen-printed electrodes supplied by DropSens. In this case, working and auxiliary electrodes were based on carbon and pseudo reference was silver. Ceramic material is used as substrate.

1.2 To use ItalSens graphite screen-printed electrodes containing a graphite working electrode, a carbon counter electrode and a (pseudo)silver reference electrode. Polyester material is used as substrate.

1.3 To use a five-sensor inkjet printed platform array supplied by the Instituto de Microelectrónica de Barcelona (IMB-CNM, CSIC), specifically with the *Centro de Investigación Biomédica en Red, Biomateriales y Nanomedicina* (CIBER-BBN). Working and (pseudo)reference electrodes were based on silver; meanwhile auxiliary electrode is fabricated with carbon ink. Polyethylene terephthalate is used as substrate.

In all the works, electrochemical and morphology characterization were done using electrochemical techniques such as CV and SWV. To study the morphology, SEM studies were also performed.

2. To optimize the polystyrene self-formulated inks to modify voltammetric sensors by the employment of several modifiers belonging to different groups regarding its chemical composition.

2.1 To use some standard catalysts employed in electroanalysis, as are cobalt (II) phthalocyanine and prussian blue.

- 2.2** To use some metal oxides such as copper (II) oxide.
- 2.3** To use some carbon material such as carbon nanotubes and graphite.
- 2.4** To use some metal nanoparticles such as palladium.
- 2.5** To use some conductive polymers such as polypyrrole.

The ink-like composite was coated on the surface via drop-casting. In most of the cases, this deposition was carried out following an activation step to prepare the sensor for the measurements.

- 3.** To validate the technology employed using a mixture of compounds as proof of concept (ascorbic acid, uric acid, and acetaminophen) with the use of an integrated array of eight electrodes provided by DropSens, an electronic tongue was performed considering the previous mixture of previous studies by the protocol followed in our laboratory.
- 4.** To develop a strategy to identify opioids in presence of cutting agents.
 - 4.1** To achieve this objective, Principal Component Analysis was used as a visualization tool. To perform a more complex study, clustering metrics were achieved using the Silhouette parameter. With this experiment, an optimization of the sensor array was achieved to lead to the final application with non-redundant information.
 - 4.2** Machine learning algorithms (k-nearest Neighbour, Random Forest, Naive Bayes and Support Vector Machines) were applied to verify the feasibility of the identification model.
- 5.** To evolve a strategy for opioids (heroin, morphine, and codeine) quantification in presence of cutting agents (caffeine and paracetamol).
 - 5.1** To perform two sets of experiments: firstly, the generation of a model with the three opioids, and subsequently the addition of the cutting agents in order to ensure that the identification is accomplished.

- 5.2** To deal with this objective the multicomponent data must be processed with chemometric tools. Specifically, in the case of the study, Genetic Algorithms were used to feature selection coupled with Partial Least Squares Regression as modelling tool.
- 6.** To implement a strategy to quantify some cuttings agents (benzocaine, phenacetin, and paracetamol) present in some drugs of abuse using Inkjet Printing as emergent technology. Referring to chemometrics in this case, a Discrete Wavelength Transform for data compression was followed by the classical Artificial Neural Networks as modelling tool commonly used in the research group.

III. EXPERIMENTAL

All the materials, instrumentation, and procedures listed in this chapter are related to the works presented in the following list.



1. Materials and Methods

This section will pay attention to describing the materials and methods employed to run the experiments in the following works. In detail, reagents and samples, instrumentation, sensor platforms, chemical modification, electrochemical, characterization, experimental design, and sensor array selection and model validation were specified in this chapter.

- **ARTICLE 1**

Simultaneous Voltammetric Determination of Acetaminophen, Ascorbic Acid and Uric Acid by Use of Integrated Array of Screen-Printed Electrodes and Chemometric Tools.

Dionisia Ortiz-Aguayo, Marta Bonet-San-Emeterio and Manel del Valle
Sensors, 2019, 3286.

- **ARTICLE 2**

Voltammetric sensing using an array of modified SPCE coupled with machine learning strategies for the improved identification of opioids in presence of cutting agents.

Dionisia Ortiz-Aguayo, Karolien De Wael and Manel del Valle
Journal of Electroanalytical Chemistry, 902, 115770

- **ARTICLE 3**

Resolution of opiate illicit drugs signals in the presence of some cutting agents with use of a voltammetric sensor array and machine learning strategies.

Dionisia Ortiz-Aguayo, Xavier Cetó, Karolien De Wael and Manel del Valle
Sensors and Actuators B: Chemical, 357, 131345

- **ARTICLE 4**

Novel Integrated Inkjet Sensor Array for Detecting Simultaneously some Adulterants present in Drug of Abuse Field using Chemometrics.

Dionisia Ortiz-Aguayo, Xavier Cetó, Gemma Gabriel and Manel del Valle

Sensors and Actuators B: Chemical, submitted

2. Reagents and Samples

Potassium ferricyanide ($K_3[Fe(CN)_6]$), potassium ferrocyanide $K_4[Fe(CN)_6]$, sodium chloride (NaCl), potassium chloride (KCl), disodium phosphate (Na_2HPO_4) were obtained from Merck (Darmstadt, Germany). Monopotassium phosphate (KH_2PO_4) was obtained from Sigma Aldrich (St. Louis, MO, USA).

Cobalt (II) phthalocyanine (CoPc), Copper (II) oxide (CuO) nanopowder (<50 nm), Polypyrrole doped (PP) and Palladium, powder submicron 99.9+% (Pd), which were used as modifiers, were purchased from Sigma-Aldrich (St. Louis, MO, USA). Prussian blue (PB) was from Acros Organics (Geel, Belgium). The preparation of the ink composite was done using mesitylene and polystyrene, obtained from Sigma-Aldrich (St. Louis, MO, USA). Graphite powder (particle size <50 μm) was received from BDH (BDH Laboratory Supplies, Poole, UK).

Acetaminophen (PA), ascorbic acid (AA), uric acid (UA), and hydrogen peroxide (H_2O_2) solutions were purchased from Sigma-Aldrich (St. Louis, MO, USA). Codeine (COD), caffeine (CAF), and heroin were provided by the National Institute of Criminalistics and Criminology (NICC) of Belgium. Morphine hydrochloride, potassium monophosphate (K_2HPO_4) and potassium hydroxide (KOH) were purchased from Sigma-Aldrich (Overijse, Belgium). Benzocaine and phenacetin were purchased from Sigma-Aldrich (St. Louis, MO, USA).

Samples were prepared in buffers listed in Table III - 1. All aqueous solutions were prepared using Milli-Q water (Millipore, Billerica, MA, USA). The reagents were of analytical grade and used without supplementary purification. Fresh stock solutions were prepared the same day of the measurements, to avoid/reduce the day variability.

Table III - 1. Names and chemical compositions of the different phosphate buffer solution (PBS) solutions employed.

Buffer name	pH	Chemical composition
PBS1	7.0	50 mM (K_2HPO_4/KH_2PO_4), 0.1 M KCl
PBS2	7.0	20 mM (K_2HPO_4), 0.1 M KCl

3. Instrumentation

Cyclic Voltammetry (CV) measurements were performed at room temperature (25°C), using a portable Multi Potentiostat/Galvanostat μ Stat 8000 from DropSens controlled through its Dropview Multichannel 5.5 software package and Autolab PGStat 20 (Metrohm Autolab B.V, Utrecht, The Netherlands). GPES software was used for the acquisition of the data.

Square Wave Voltammetry (SWV) measurements were performed using a Multi-channel Potentiostat/Galvanostat/Impedance Analyzer (MultiPalmSens4, The Netherlands) controlled by Multitrace software.

AC impedance measurements were performed with an Autolab PGStat 20 (Metrohm Autolab B.V, Utrecht, The Netherlands). FRA software was used for the acquisition of the data and the control of the experiments. Finally, Z-view (Scribner Associates Incorporated, Carolina, USA) software was used for data processing. A three-electrode cell was used to perform the impedance: a platinum-ring auxiliary electrode (Crison 4.75, Barcelona, Spain), an Ag/AgCl reference electrode, and a printed electrode as the working electrode.

The morphological characterization of the modified screen-printed electrode was performed by a scanning electron microscope with field emission gun (FEG-SEM) of Zeiss, model MERLIN SM0087 and an Energy Dispersive X-Ray spectroscopy (EDX). Imaging was performed based on secondary (back-scattered) electrons. Furthermore, other instruments were used such as Eppendorf Thermomixer C to control temperature incubations, pH-meter GLP22 (Crison 52-67 1, Barcelona, Spain), Vortex shaker MS3 basic (IKA, Staufen, Germany), and rotary stirrer Trayster basic (IKA, Staufen, Germany) to shake the solutions.

4. Sensor Platforms

This section will be described the different sensor platforms employed to perform the different experimentation done in this thesis.

4.1. Commercial Screen-printed Electrodes

The commercial screen-printed electrodes were provided by DropSens (Oviedo, Spain). The electrochemical cell consisted of: 8 working electrodes (carbon, 2.95 mm diameter), ceramic substrate: 50 x 27 x 1 mm (Length x Width x Height), auxiliary electrode (carbon), and (pseudo) reference electrode (Ag)¹, see Figure III - 1.

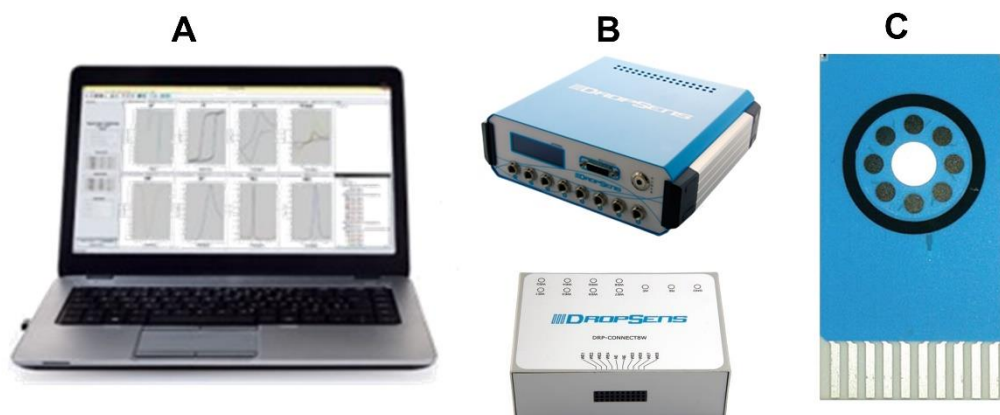


Figure III - 1. Screen printed technology supplied by DropSens. (A) Computer to process the data, (B) Multi Potentiostat/Galvanostat μ Stat 8000 and connector and (C) Array of 8 working electrodes.

ItalSens graphite screen-printed electrodes (GSPE) containing a graphite working electrode (3 mm diameter), a carbon counter electrode, and a (pseudo)silver reference electrode were supplied by PalmSens (The Netherlands, Holland), see Figure III - 2.

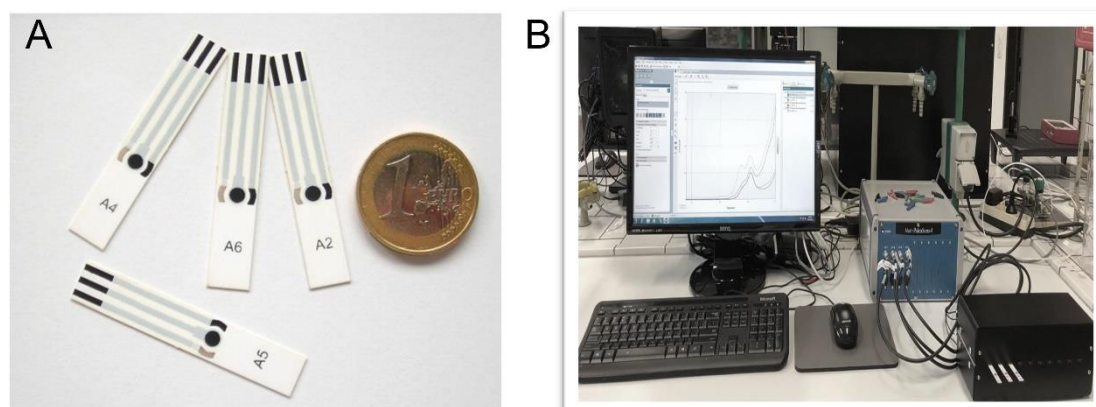


Figure III - 2. Screen-printed technology supplied by PalmSens. (A) ItalSens working electrodes and (B) Multi-channel Potentiostat/Galvanostat/Impedance Analyzer (MultiPalmSens4, The Netherlands).

4.2. Inkjet Printed Electrodes Fabrication

The fabrication of Inkjet Printed Electrodes (IPEs) (Figure III - 3) was done in collaboration with the Instituto de Microelectrónica de Barcelona (IMB-CNM, CSIC), specifically with the *Centro de Investigación Biomédica en Red, Biomateriales y Nanomedicina* (CIBER-BBN)². In detail, silver microelectrodes were prepared by using a drop-on-demand inkjet printer (DMP-2831 Dimatix Fujifilm, Santa Clara, USA) and a disposable cartridge containing 16 individually addressable nozzles with nominal droplet volumes of 10 pL. The electrodes were printed over a flexible and transparent PET substrate using commercially available Ag and SU-8 inks. Optimization of the IJP process was done as previously reported^{3,4}. The first step was the IJP of the Ag of the WE of 1 mm diameter (geometric surface area of 0.785 mm²), tracks and pads with a DS 20 µm and dried at 80°C for 15 min. Then, it was thermally sintered in an oven at 150°C for 30 min. Afterward, to define the microelectrode area and to insulate the tracks for the connections another cartridge with SU-8 ink was used to print this dielectric material with DS of 15 µm, and finally cured using a UV lamp for 30 s.

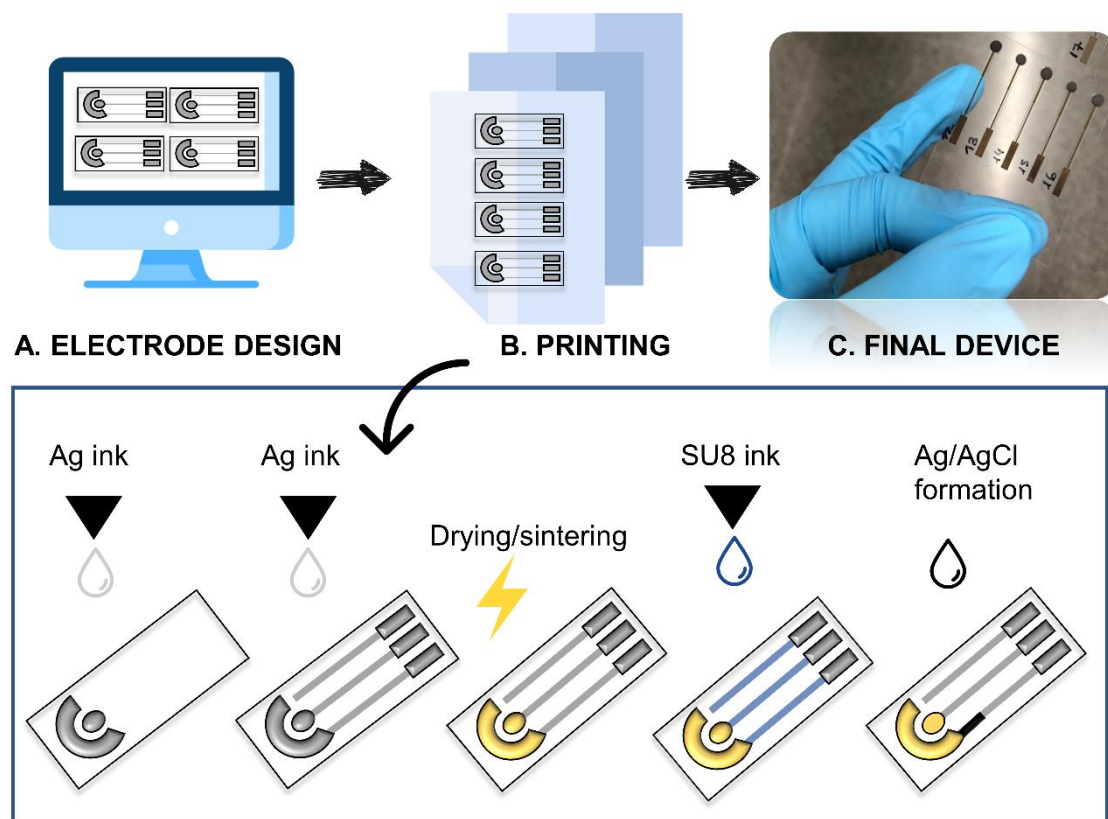


Figure III - 3. Fabrication process of IPEs: from electrode design to final device.

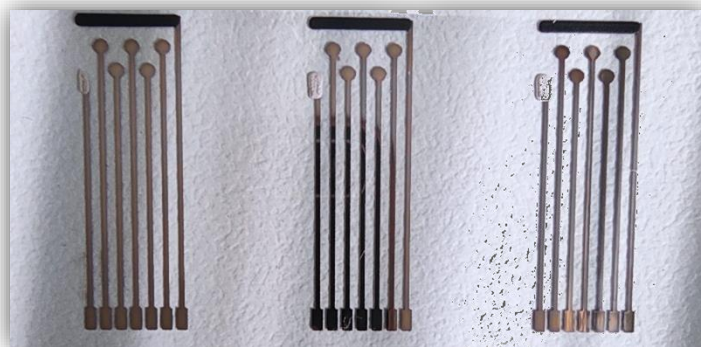


Figure III - 4. Multi-sensor platform device printed by IJP techniques. In this case, the WE is composed by a silver ink, CE is based on graphite ink and RE is based on Ag/AgCl.

5. Chemical Modification

The chemical modification consists of the formation of a conductive ink-composite in order to obtain differentiated electrochemical response. The mentioned nanomaterial is formed by graphite (58%) as a conductive material, powdered polystyrene (32%) to perform the agglutination, mesitylene as a solvent, and the incorporation of the corresponding modifier (10%). The mixture was thoroughly mixed for 2 h using a magnetic stirrer. After that, 2 min of sonication was performed to obtain a medium-thick solution. The ink-like composite was dropped onto the electro surface. For DropSens SPEs 5 μL was used, meanwhile, Italsens SPEs and IPEs 1 μL was enough to cover the surface. In terms of temperature, some small differences are also remarked. SPEs were dried at 40°C instead of IPEs, room temperature is needed. In both cases, 1 h was required to remove the solvent.



Figure III - 5. Drop casting method followed by soft heating and microscopy studies for the IPEs case.

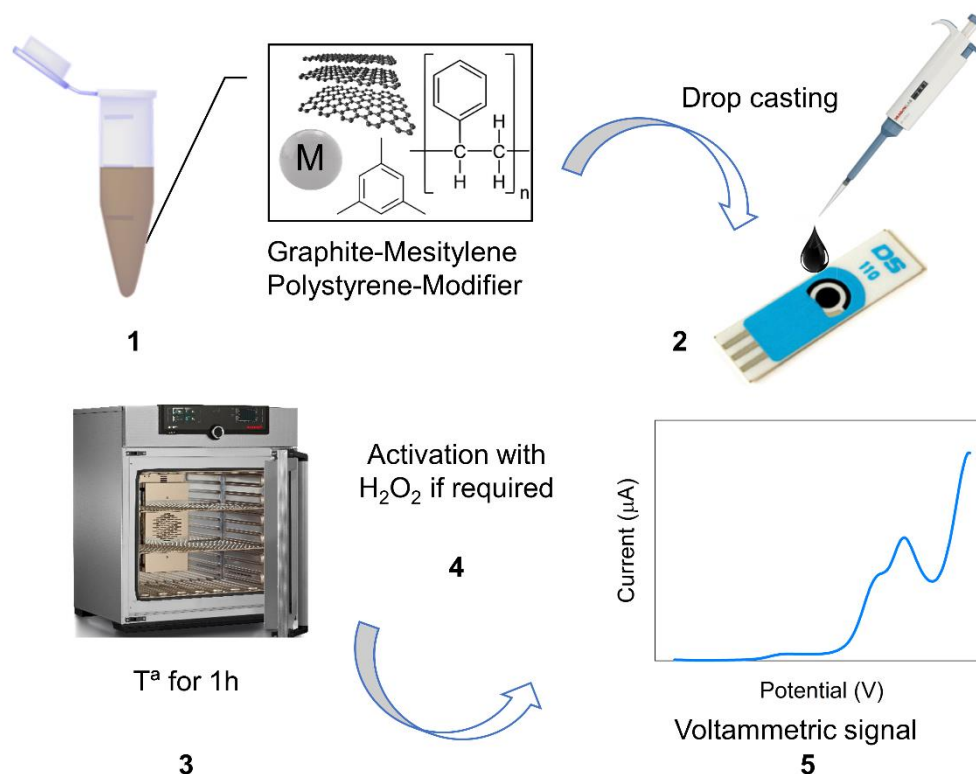


Figure III - 6. Experimental procedure of electrode surface modification for SPCEs. 1. Preparation of the suspension, 2. Deposition of μL on the surface, 3. Heat at T^a for 1 h, 4. Activation with H_2O_2 if required and 5. Record the electrochemical signal.

5.1. Electrode Surface Activation

Once the sensor was prepared, the next step is an activation to enhance sensing performances of modified ink^{5,6}. Figure III - 7 displays the typical gain achieved after activation. Electrochemical activation⁶ consisted of 10 repetitive voltammetric cycles at $50 \text{ mV}\cdot\text{s}^{-1}$ between 1.5 and -1.5 V using 10 mM H_2O_2 in phosphate buffer (pH 7). After activation, electrodes were rinsed with deionized water and dried in air. It is important to make clear that this activation was applied only for DropSens SPEs. In the rest of the cases, activation of the electrodes was done softer, measuring a stock solution with the desired analytes during repeated electrochemical measurements.

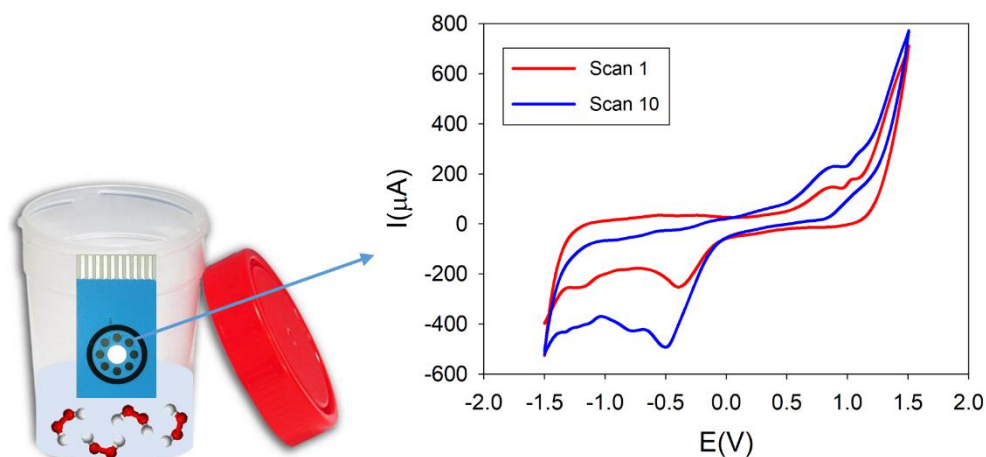


Figure III - 7. Activation using H_2O_2 . Electrochemical activation consists of 10 repetitive voltammetric cycles at $50 \text{ mV}\cdot\text{s}^{-1}$ between 1.5 and -1.5 V using 10 mM H_2O_2 in phosphate buffer (pH 7). After activation, electrodes were rinsed with deionized water and dried in air.

5.2. Electrochemical Characterization of the Electrode Surface

After performing the surface modification of the WE, an electrochemical characterization was done to determine the active area. The effective surface area of bare and modified electrodes was evaluated according to the Randles–Sevcik equation (Equation III - 1)⁷.

$$I_p = 0.446 \cdot n \cdot F \cdot c \cdot A \cdot \sqrt{\nu} \cdot \left(\frac{nDF}{RT} \right)^{\frac{1}{2}} \quad \text{Equation III - 1}$$

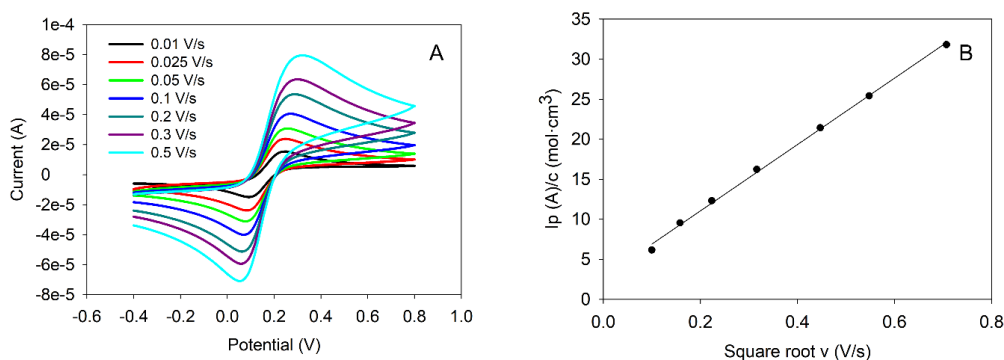


Figure III - 8. A) Cyclic voltammetry of 5 mM $\text{K}_3\text{Fe}(\text{CN})_6/\text{K}_4\text{Fe}(\text{CN})_6$ redox couple in 0.1 M KCl varying scan rate from 0.01 V/s to 0.5 V/s using Graphite/SPCE-Ink. The range potential was from -0.4 V to 0.4 V with a step potential of 0.005 V. (B) Regression line of $\nu^{1/2}$ ($\text{V}\cdot\text{s}^{-1}$) vs. $I_p \cdot c^{-1}$ ($\text{A}\cdot\text{cm}^3 \text{mol}^{-1}$).

In this equation, n is the number of transferred electrons for the redox reaction (in this case 1), F is the Faraday's constant ($96485 \text{ C}\cdot\text{mol}^{-1}$) and C the concentration of an electroactive substance ($\text{mol}\cdot\text{cm}^{-3}$).

A is the effective area in cm^2 , v the scan rate ($\text{V}\cdot\text{s}^{-1}$), R the gas constant ($8.314 \text{ J}\cdot\text{mol}^{-1}\cdot\text{K}^{-1}$), T the temperature in K and D is the diffusion coefficient for ferrocyanide ($\text{cm}^2\cdot\text{s}^{-1}$). For that CV experiments using 20 mM KH_2PO_4 and 100 mM KCl containing 5 mM $[\text{Fe}(\text{CN})_6]^{3-}/[\text{Fe}(\text{CN})_6]^{4-}$ solution in the potential range of -0.4 to 0.8 V were performed. Applying 5 different scan rates (0.01, 0.025, 0.05, 0.1, 0.2, 0.3, and $0.5 \text{ V}\cdot\text{s}^{-1}$) it could be calculated the active area of WE from the slope of the regression line of $v^{1/2}$ ($\text{V}\cdot\text{s}^{-1}$) vs. $I_p\cdot\text{c}^{-1}$ ($\text{A}\cdot\text{cm}^3\cdot\text{mol}^{-1}$).

6. Electrochemical Measurements Performance

The electrochemical measurements in this thesis were performed using voltammetry techniques, concretely, CV and SWV. All the background corresponding to these techniques and the electrochemical cells employed for the different works are described in § 3.2 of introduction.

The selection of the technique used depends on the final application. In the case of pharmaceutical compounds, it is more important to have the information corresponding to the oxidation and reductions signals, instead of working with more sensitivity. On the contrary, in the case of drugs of abuse, it is more relevant to work with a sensitive technique, capable of determining low detection limits. For this reason, the most suitable technique used in the first case is CV, meanwhile, SWV is more suitable for opioids and cutting agents electrochemical determination.

Therefore, in the case of pharmaceuticals determination, the potential was cycled between -1.5 and 1.5 V with a step potential of 9 mV and a scan rate of $50 \text{ mV}\cdot\text{s}^{-1}$. For the determination of the opiate substances, the potential range was -0.2 V to 1.5 V using a step potential of 5 mV, an amplitude corresponding to 25 mV, and a frequency of 10 Hz. The last work, focusing on cutting agents from cocaine, SWV measurements were performed using a potential range from -0.1 V to 1.3 V, step potential of 5 mV, the amplitude of 25 mV, and frequency of 10 Hz.

In all the cases, the solutions prepared for all the experimental work were dissolved in *PBS1* and *PBS2* containing 0.1 M KCl as support electrolyte. Typical voltammograms obtained are represented in Figure III - 9.

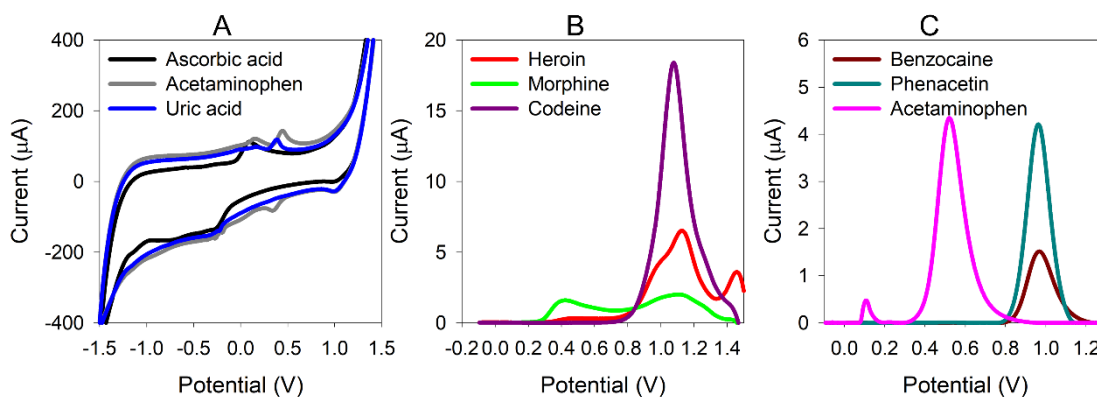


Figure III - 9. A) Cyclic voltammogram from the mixture of ascorbic acid, acetaminophen, and uric acid. B) Square wave voltammogram from the mixture heroin, morphine, and codeine and C) Square wave voltammogram from the mixture benzocaine, phenacetin, and paracetamol. All the results were measured using CoPc modified electrode.

7. Experimental Design Selection

One of the most disadvantages of the electronic tongues systems is the high number of samples required to construct the quantitative model and its validation. This fact can be explained because to build a robust model with good predictive capabilities, it will need to consider all the possible interactions between the analytes under study and the array of sensors employed. For this reason, the selection of the experimental design concerns a huge impact before preparing the samples.

Hence, the first step to be considered to design an experiment is the definition of the experimental domain, which means the concentration range for each different analyte. It can be remarked that the different concentration ranges can be equal or different for the different studied compounds. Then, the type of design can be chosen, which will define the number of samples required by the construction of the model and the spatial distribution.

Once the experimental domain and the number of samples are defined (*train subset*), it is needed the construction of a set of samples to evaluate the prediction capability of the model (*test subset*). The samples employed to validate the model are distributed along with the experimental domain. As a general rule, 2/3 of the samples are used to train the model and 1/3 to validate it.

In this thesis, it is used a modified factorial design, commonly used in the *Sensors and Biosensors group*⁸.

This model is a tilted factorial design, which consists of a factorial design with a 45° rotation in each axis⁹. With this approach, it is possible to avoid the repetition of numeric values. To afford more complex cases, a Central Composite Face-centered (CCF) experimental design was used (Figure III - 10) Both were used commonly to construct the training subset. In all the cases, the samples belonging to the test model were prepared randomly, as mentioned before.

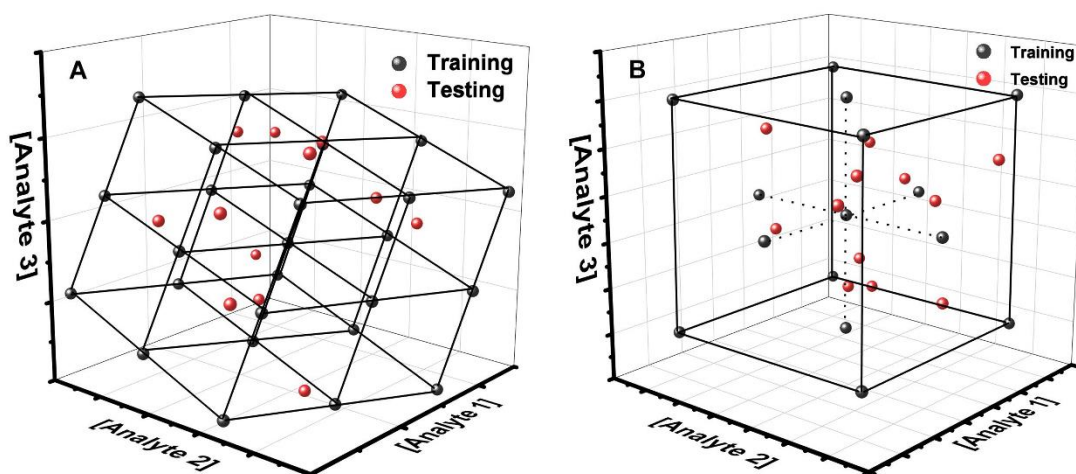


Figure III - 10. (A) Tilted factorial design (3^3) with a 45° rotation in each axis. The black dots correspond to the train and the red to the test samples. (B) CCF, in black the train and blue the test samples.

Specifically, **article 1** was done using a tilted factorial experimental design (3^3) (27 samples) for the training subset and to validate the model, 12 samples were distributed randomly along the experimental domain, in this case from 0 to 500 μM . **Article 4** was done with the same criteria, only narrowing the concentration range from 0 to 200 μM .

In the drug of abuse case, **article 3**, two different sets of samples were prepared. Firstly, one for the ternary mixtures of heroin, codeine, and morphine. In this case, samples for the training subset (27 samples) were prepared based on the tilted design commented previously and 15 extra samples forming the test subset. The determined range was from 0 to 750 μM . Secondly, in the complex case, adding the cutting agents were prepared to employ a CCF with 3 levels of concentrations (27 samples) and 17 extra samples for the test subset maintaining the same range of concentrations.

In all the cases, the samples were measured in random order to prevent periodic trends and alternating different cleanings stages to have control of the surface.

With SPEs, experiments were running with the same sensing units, meanwhile, in the case of IPEs, every 10 measurements electrodes were changed due to fouling effects detected.

8. Data Analysis

Calculation of the peak heights and areas for stock solutions was done using MultiTrace software (PalmSens, Houten, The Netherlands). Graphics were plotted using SigmaPlot (Systat Software Inc., San Jose, CA, USA). Chemometric analysis was done in Matlab R2018b (Mathworks, Natick, MA, USA), making use of its Statistics and Machine Learning Toolbox, by specific routines written by the authors. The web page Clustvis¹⁰ (Figure III - 11) was the tool used for online PCA calculation in some cases. Orange open-source programming language¹¹ (University of Ljubljana, Slovenia) was used to perform some Silhouette calculations and to generate the identification models for which kNN, Random Forest, Naive Bayes, and SVM algorithms were employed and compared.

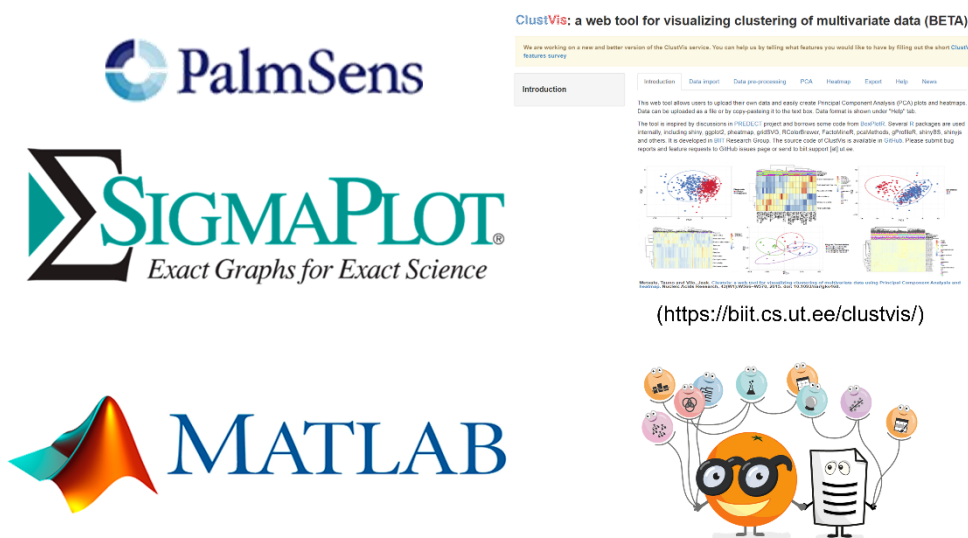


Figure III - 11. Softwares employed to perform the data analysis.

9. Sensor Array Selection

For more than a decade, our group is specialized in having many modifications adapted to electrochemical sensors.

Some examples are metallic nanoparticles, metal oxides, conductive polymers and standard catalysts, among others. In most cases, it is difficult to choose which of these modifications is the most suitable to apply to our final application. Therefore, it is necessary to resort to different tools that provide us with this information. According to established procedures, PCA is our first option followed by Silhouette calculation.

9.1. Principal Component Analysis

Briefly, PCA is a suitable linear visualization method of multivariate data, that allows the reduction of the dimensionality of a multivariate problem and facilitates the visualization of the groupings of the multivariate profiles by remarking similarities and differences between them, forming sample clusters. PCA is very useful to identify these clusters, but it is normally hard to interpret and validate the grouping. For this reason, the Silhouette calculation¹² was introduced as a measure of clustering, i.e., how easy is to distinguish between the clusters associated with the different compounds. Therefore, the first strategy is to make a first interpretation with PCA and then use the Silhouette index as a metric to perform a more detailed optimization to select the most suitable working electrodes.

Normally, there are two common representations of PCA, which are showed in Figure III - 12. In the right, the representation included the *scores* plot of different sensors employed, in the example, four, and is a procedure that helps in visualizing the contributions of each individual sensor. Furthermore, it is possible to distinguish between compounds if subgroups between a given electrode are found. In the left, the *unfolding* is processed, and the *scores* plot in this case, is represented through five clusters, corresponding to the different studied compounds. Although both representations are interesting, the most widely used is the second one, where the information given for each sensor is grouped into a single vector for each selected compound and is equivalent to the final procedure employed in an identification application. The intrinsic second representation in the standard PCA treatment, the *loadings* plot, is not so useful in this case, as it provides individual potentials from individuals electrodes, and interpreting their meaning is not straightforward.

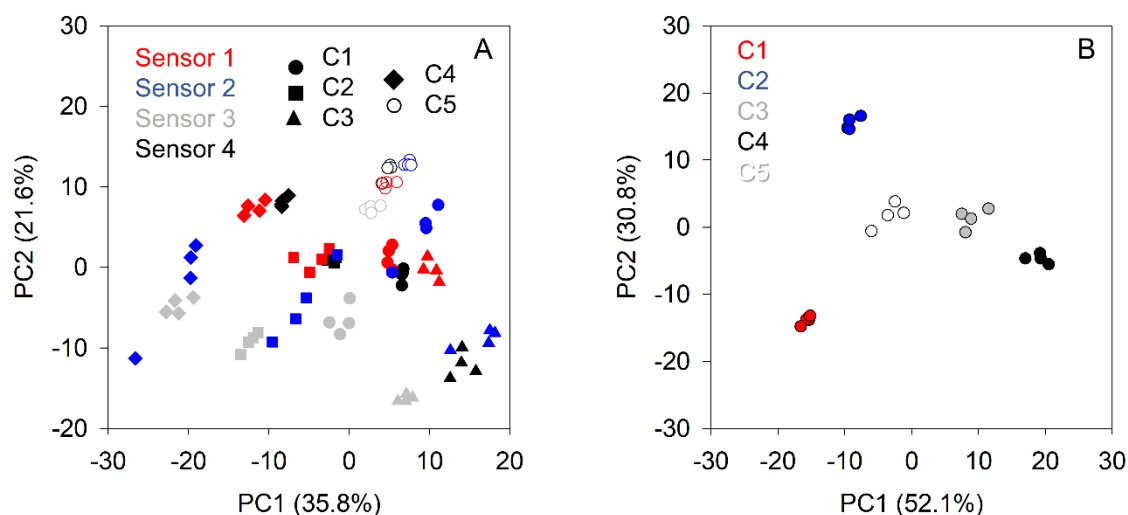


Figure III - 12. A) Scores plot representing the different sensors (Sensor 1-Sensor 4) and compounds studied (C1-C5). B) Scores plot representing the different compounds (C1-C5) formed by the array selected from the unfolded information.

9.2. Silhouette Calculation

This strategy refers to a method of interpretation and validation of consistency within clusters of data, providing a numerical figure of how well each object matches its cluster (Figure III - 13).

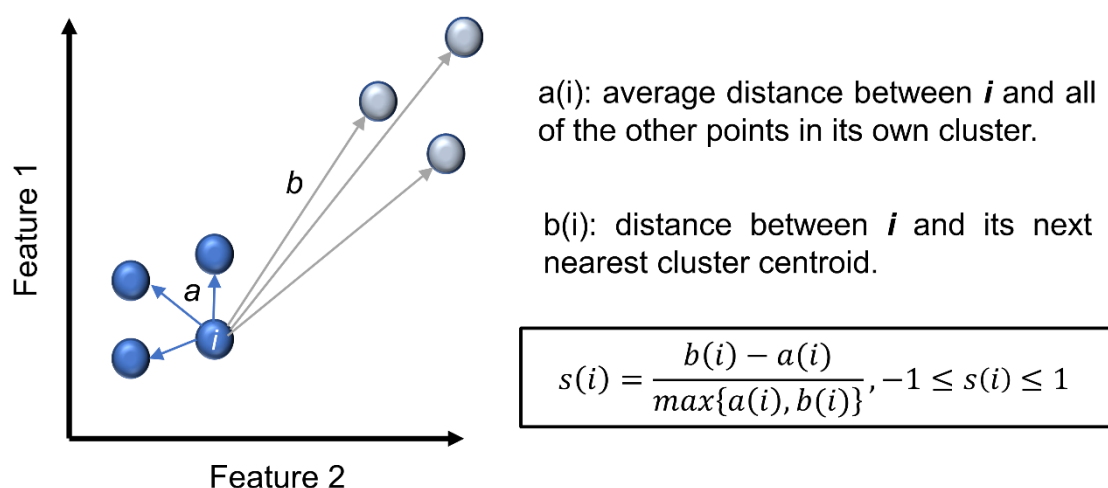


Figure III - 13. Schematic representation of the Silhouette calculation.

The Silhouette is based on the calculation of two parameters: a and b . For each sample, i , $a(i)$ is the average distance between i and all other samples within the same cluster.

In the case of $b(i)$ is the smallest average distance of i to all samples in any other cluster, of which i is not a member. Silhouette parameter is calculated following Equation III - 2.

$$s(i) = \frac{b(i) - a(i)}{\max\{a(i), b(i)\}}$$

Equation III - 2

Which can be also written as Equation III - 3:

$$s(i) = \begin{cases} 1 - \frac{a(i)}{b(i)}, & \text{if } a(i) < b(i) \\ 0, & \text{if } a(i) = b(i) \\ \frac{b(i)}{a(i)} - 1; & \text{if } a(i) > b(i) \end{cases}$$

Equation III - 3

The Silhouette value is a measure of how similar an object is to its own cluster (cohesion) compared to other clusters (separation). The Silhouette ranges from - 1 to +1, where a high value (close to +1) indicates that the object is well matched to its own cluster. If most samples have a high Silhouette value, then the clustering configuration is appropriate. If many points have a low or negative value, then the clustering configuration may have too many or too few clusters. The average of the Silhouette parameter for the whole set of samples can then be employed as an index to evaluate the overall clustering ability of the selected sensor configuration, as it will provided how well clusterized is a given PCA representation.

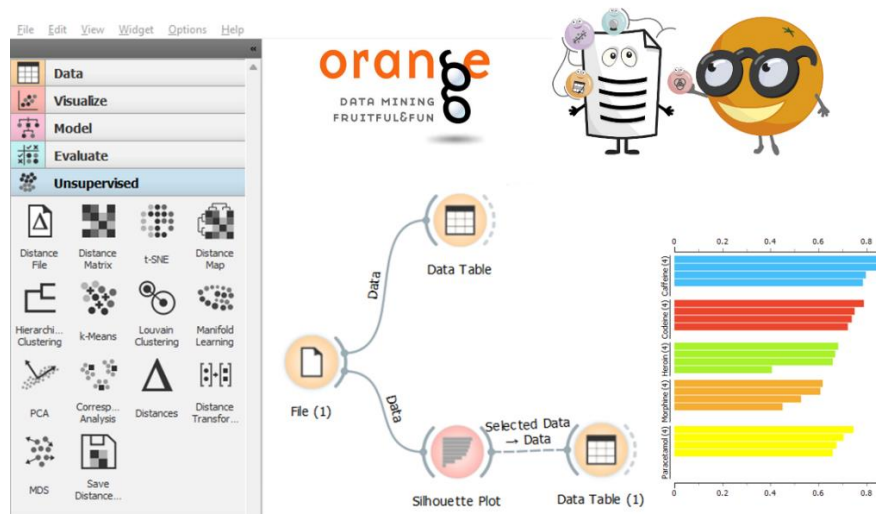


Figure III - 14. Orange Script (<https://orangedatamining.com/>).

10. Model Assessment

The procedure of model assessment will be divided into three stages: data pre-processing, model building and model validation. As discussed in previous sections, the aim of the first stage is to reduce the high dimensionality of data set. Even though it is not a mandatory step, it has been performed to obtain improved results. One common data pre-processing highly used in this doctoral thesis is the *unfolding*. Figure III - 15 represents the transformation from a 3D to a 2D matrix.

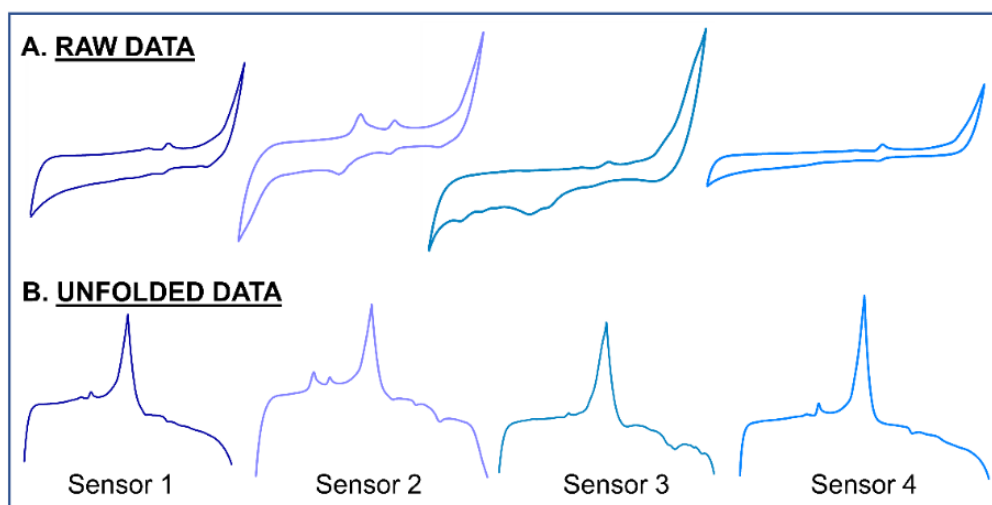


Figure III - 15. *Unfolding* procedure from raw data employing a four-array sensor.

The next step is the construction of the model, using as input the electrode responses or the coefficients obtained in the pre-processing stage.

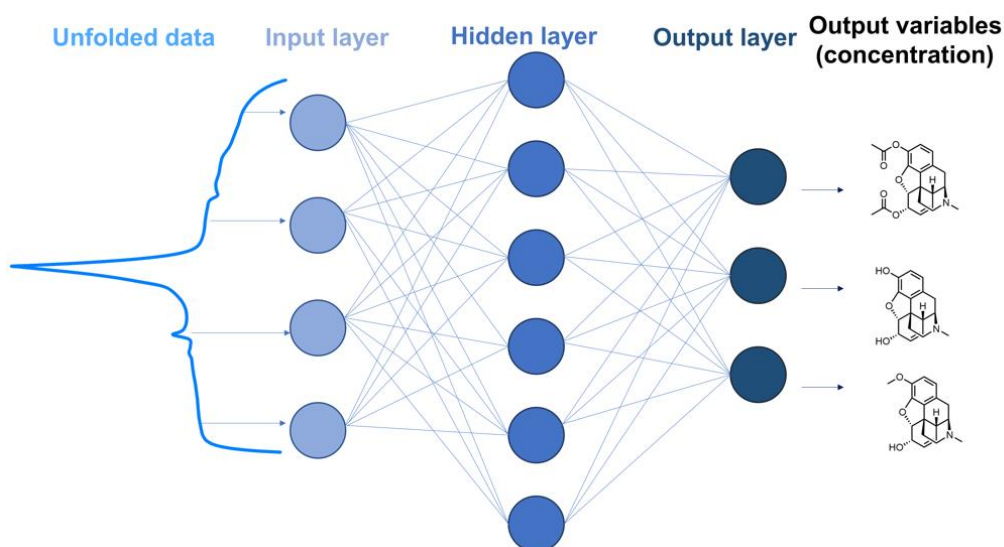


Figure III - 16. Operation mode of ANNs using the unfolded data.

To clarify this term, Figure III - 16 shows an example where the *unfolded* voltammogram is introduced into the neural network to obtain finally the concentrations as output variables of the different compounds under study. At the end, the predictive capability of the model is evaluated by carrying out the validation stage. This step will be explained in more detail in the next section.

11. Model Validation

One important step in the multivariate data analysis is the model validation. It is just as important to build the model as it is to validate it and to evaluate its capability of prediction. In general terms, the aim of the validation is to make a comparison between the expected real values and the predicted ones for an independent subset of samples.

Therefore, to achieve the model validation it is needed to divide the samples in two subsets. One is the training subset, which is used to construct the model and then the testing subset, which is used to validate it and verify the predictive capability of the model. There are many types of validations methods: cross validation, external validation, k-fold, leave and out and repeated random sub- sampling validation, among others.

Depending on the final application (qualitative or quantitative), some parameters are calculated to demonstrate the feasibility of the model.

11.1. Qualitative Model

Within this group, the main evaluation is done by the matrix confusion. Parameters such as classification accuracy, precision, sensitivity, and specificity are calculated. To explain in detail how all these calculations are done, previously, it is needed to understand how a confusion matrix works.

Table III – 2. Confusion matrix example of a binary system.

		<i>Predicted</i>	
		Positive	Negative
<i>Expected</i>	Positive	True Positive (TP)	False Negative (FN)
	Negative	False Positive (FP)	True Negative (TN)

- **Accuracy:** accuracy is defined as the ratio of the total value of correctly classified samples, whether positive or negative, to the total number of samples. This parameter is calculated with Equation III - 4.

$$Accuracy = \frac{TN + TP}{TN + TP + FN + FP} \quad \text{Equation III - 4}$$

- **Precision:** precision is defined as the ratio of true positive outcomes to the positive outcomes designated by the model. It is calculated through Equation III - 5.

$$Precision = \frac{TP}{TP + FP} \quad \text{Equation III - 5}$$

- **Sensitivity:** this property refers to the ability of the model to recognise that a sample is truly positive (and not classify it as negative, generating false positives). Sensitivity would be the rate of true positives and is expressed as a ratio or percentage and is calculated according to Equation III - 6.

$$Sensitivity = \frac{TP}{TP + FN} \quad \text{Equation III - 6}$$

- **Specificity:** specificity is defined as the ability of the model to recognise that a sample is negative (and not as positive, generating false positives). Specificity would be the rate of true negatives. Like sensitivity, it is expressed as a ratio or percentage and is calculated according to the Equation III - 7.

$$Specificity = \frac{TN}{TN + FP} \quad \text{Equation III - 7}$$

11.2. Quantitative Model

To assess whether a model is good or not, it is necessary to analyse the goodness of fit. There are two methods for this. The first is based on the construction of the comparison graphs between the response predicted by the model and the expected concentration for each of the analytes, while the second is based on the calculation of the Root Mean Square Error (RMSE) and some variant such as the Normalised Root Mean Square Error (NRMSE).

11.2.1. Comparison Graphs Predicted vs. Expected

As mentioned above, a plot of predicted vs. expected concentrations is constructed and a linear fit of the two data sets is performed by calculating the slope, the intercept, and the correlation coefficient. These three parameters are catalogued as evaluators of the predictive ability of the system by comparison with the ideal values (1, 0, 1), respectively. Figure III - 17 is an example of the typical graphs obtained.

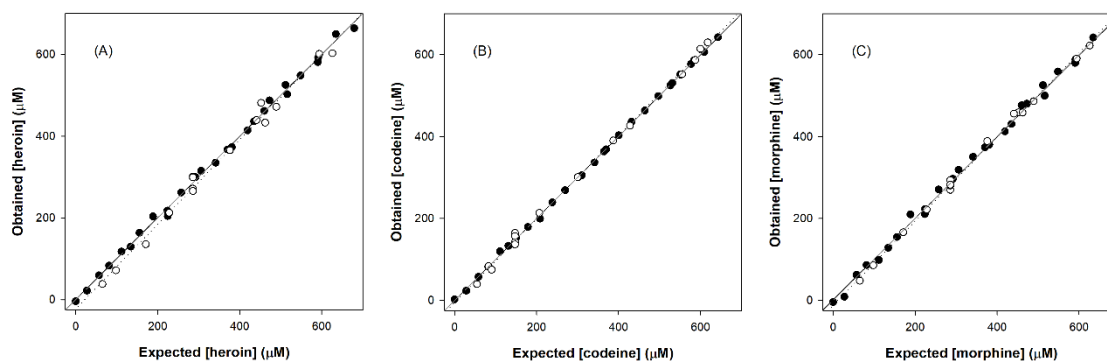


Figure III - 17. Modelling ability of the optimized GA-PLS model for the three compounds case. Comparison graphs of obtained vs. expected concentrations for (A) heroin, (B) morphine and (C) codeine, for both (\bullet , solid line) and test subsets (\circ , dotted line). The dashed line corresponds to the ideal comparison line ($y = x$).

It is important to consider that these calculations are applied in both the training subset, obtaining good results, and in the testing subset, showing worse results but providing an indicative about the model confidence.

11.2.2. Root Mean Square and Normalised Root Mean Square Errors

The RMSE is a measure of how close the fitted line is to the points of the original values (Equation III - 8). For each point, the error between the value extracted from the fit and the true value is calculated, i.e., the distance from the true point (c_{ij}) to the corresponding fitted value (\hat{c}_i), considered with respect to the ordinate axis. The sum of these values is squared, to avoid negative values offsetting positive values, divided by the number of points (n) minus 1 and square-rooted to the corresponding units. In case of recalculating the total RMSE of the model, the total number of analytes to be determined (k) must be also considered, since for each of the analytes we will have n points.

$$RMSE = \sqrt{\frac{\sum_{ij}(c_{ij} - \hat{c}_{ij})^2}{k \cdot n - 1}}$$

Equation III - 8

In summary, the smaller the RMSE value, the closer the fitted line is to the data, and therefore the better fit and predictive ability of the model is obtained.

Similarly, the NRMSE is used as an alternative to the above calculation. In this case the RMSE is normalised by dividing by the range of concentrations of each analyte (Equation III - 9) thus obtaining a new indicator between 0 and 1 which provides a measure of the error for each analyte (j=1) or the overall error for the set of analytes (j>1).

$$NRMSE = \frac{1}{j} \sum \frac{RMSE_i}{c_{i,max} - c_{i,min}}$$

Equation III - 9

12. References

- (1) Dropsens. 8WScreen-Printed Carbon Electrode. http://www.dropsens.com/pdfs_productos/%0Anew_brochures/8w110.pdf (accessed Jul 25, 2019).
- (2) Instituto de Microelectrónica de Barcelona (IMB-CNM-CSIC). Centro Nacional de Microelectrónica <http://www.cnm.es/> (accessed Mar 14, 2022).
- (3) Moya, A.; Sowade, E.; del Campo, F. J.; Mitra, K. Y.; Ramon, E.; Villa, R.; Baumann, R. R.; Gabriel, G. All-Inkjet-Printed Dissolved Oxygen Sensors on Flexible Plastic Substrates. *Org. Electron.* **2016**, *39*, 168–176. <https://doi.org/10.1016/j.orgel.2016.10.002>.
- (4) Moya, A.; Ortega-Ribera, M.; Guimerà, X.; Sowade, E.; Zea, M.; Illa, X.; Ramon, E.; Villa, R.; Gracia-Sancho, J.; Gabriel, G. Online Oxygen Monitoring Using Integrated Inkjet-Printed Sensors in a Liver-on-a-Chip System. *Lab Chip* **2018**, *18* (14), 2023–2035. <https://doi.org/10.1039/C8LC00456K>.
- (5) Daniels, J. S.; Pourmand, N. Label-Free Impedance Biosensors: Opportunities and Challenges. *Electroanalysis* **2007**, *19* (12), 1239–1257. <https://doi.org/10.1002/elan.200603855>.
- (6) González-Sánchez, M. I.; Gómez-Monedero, B.; Agrisuelas, J.; Iniesta, J.; Valero, E. Highly Activated Screen-Printed Carbon Electrodes by Electrochemical Treatment with Hydrogen Peroxide. *Electrochem. commun.* **2018**, *91* (February), 36–40. <https://doi.org/10.1016/j.elecom.2018.05.002>.
- (7) Bard J, Allen; Faulkner, L. R. *Electrochemical Methods: Fundamental and Applications*, 2nd ed.; Inc, J. W. & S., Ed.; 2001.
- (8) Mimendia Sancho, A. Desenvolupament i Aplicació de Llengües Electròniques per Anàlisi Ambiental, Universitat Autònoma de Barcelona, 2011.
- (9) Cetó, X.; Céspedes, F.; Pividori, M. I.; Gutiérrez, J. M.; Del Valle, M. Resolution of Phenolic Antioxidant Mixtures Employing a Voltammetric Bio-Electronic Tongue. *Analyst* **2012**, *137* (2), 349–356. <https://doi.org/10.1039/c1an15456g>.
- (10) Metsalu, T.; Vilo, J. ClustVis: A Web Tool for Visualizing Clustering of Multivariate Data Using Principal Component Analysis and Heatmap. *Nucleic Acids Res.* **2015**, *43* (W1), W566–W570. <https://doi.org/10.1093/nar/gkv468>.
- (11) Naik, A.; Samant, L. Correlation Review of Classification Algorithm Using Data Mining Tool: WEKA, Rapidminer, Tanagra, Orange and Knime. *Procedia Comput. Sci.* **2016**, *85*, 662–668. <https://doi.org/10.1016/j.procs.2016.05.251>.
- (12) Thinsungnoen, T.; Kaoungku, N.; Durongdumronchai, P.; Kerdprasop, K.; Kerdprasop, N. The Clustering Validity with Silhouette and Sum of Squared Errors. In *The Proceedings of the 2nd International Conference on Industrial Application Engineering 2015*; The Institute of Industrial Applications Engineers, 2015; pp 44–51. <https://doi.org/10.12792/iciae2015.012>.

IV. RESULTS AND DISCUSSION

In the present chapter, it will be explained the different articles published based on the main fields of this doctoral thesis: the pharmaceutical field as a proof of concept and the forensic and security field.



Contextualization

The motivation of this work has been firstly the development of new sensor platforms based on screen-printed and inkjet techniques, and then the use of modifiers to change the electrode surface behaving as better sensing materials in comparison to the unmodified electrode. This fusion has been possible by combining an array of sensors and applying ET principles. In this direction, the resolution of mixtures of compounds in two discernible fields (pharmaceutical and forensic and security) was achieved.

The first publication was applied to the pharmaceutical field. This work was focused on using a multi-sensor array platform (supplied by DropSens) to detect simultaneously three common pharmaceutical compounds like ascorbic acid, uric acid, and acetaminophen. The mentioned substances present overlapping signals in the electrochemical measurements, thus affecting their simultaneous detection. Because of this difficulty, the search for new strategies to distinguish the oxidation peaks is required. Our proposal was the surface modification, which allows their quantification by applying electronic tongue principles and chemometric tools. The chemical modification employed in this case was the deposition of a self-formulated graphite ink incorporating the desired modifier.

The second and third publications are the result of my stay at the University of Antwerp (UA), specifically in the A-Sense group. A-Sense Lab is mainly focused on the performance of (electro)chemical analysis in a wide area of applications. Therefore, one of their applications implies the determination of some illicit drugs in the presence of some cutting agents using their corresponding electrochemical fingerprint. As a result, the work done was divided into a qualitative stage, where the main objective was the most suitable selection of the sensors for the determination of some derivatives opiates compounds in the presence of caffeine and paracetamol as cutting agents. Then, this previous work was followed by a third publication thinking in a quantitative application. For that, the optimized sensor array developed in the second publication was employed for the simultaneous determination of heroin, morphine, and codeine in the presence of paracetamol and caffeine. In this situation, ItalSens screen-printed electrodes were used as a sensor platform and the modification of the electrode surface was done applying the background developed in **article 1**.

Last work was based on the simultaneous detection of cocaine's cuttings agents (benzocaine, phenacetin and paracetamol) considering as emergent manufacturing technology as IJP is.

To summarise, this chapter of the manuscript will be organized into article sections, each one explaining the results obtained in each work.

ARTICLE 1

Simultaneous Voltammetric Determination of Acetaminophen, Ascorbic Acid, and Uric Acid by Use of Integrated Array of Screen-Printed Electrodes and Chemometric Tools

Dionisia Ortiz-Aguayo, Marta Bonet-San-Emeterio and Manel del Valle

Sensors, 2019, 19(15), 3286

1. Outline

This work was used as a proof of concept to validate the material and methods employed during the present doctoral thesis. The aim was to resolve a mixture of acetaminophen, ascorbic and uric acid using the CV technique and ET principles (Figure IV - 1). The sensor platform used was screen printed formed by eight working electrodes and the modifiers employed, in this case, were, CoPc, CuO, graphite, and PB, which were integrated through an in-house self-formulated graphite polystyrene ink. Samples were prepared using a titled (3^3) factorial design ranging from 0 to 500 μM . PLS was used as a chemometric tool to construct the model and the validation was done using an external subset of samples with concentrations defined randomly along the working experimental domain. The goodness of fit was obtained demonstrating the feasibility of the modified sensor platform for the simultaneous determination of the mixture under study.

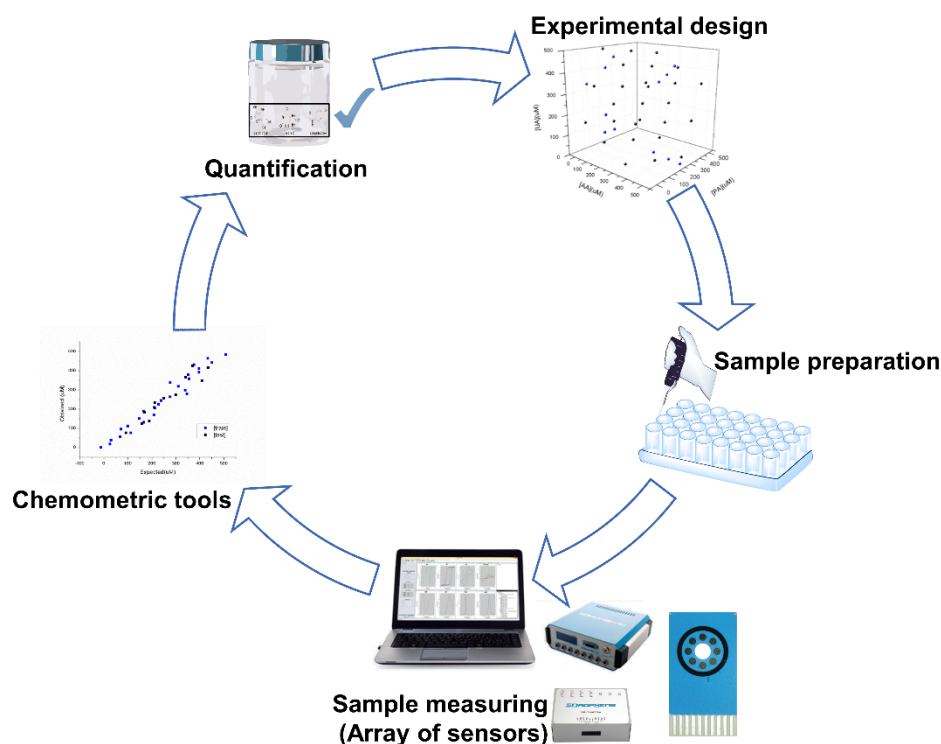


Figure IV - 1. Schematic representation of the experimental setup done by the simultaneous determination of the mixture under study formed by PA, AA, and UA. Experimental design, sample preparation, sample measuring, chemometric processing, and quantification are all the steps involved in the experimental procedure.

2. Surface Characterization through Scanning Electron Microscopy Studies

Scanning Electron Microscopy (SEM) studies were achieved to analyse the morphology of the modified surface. With these studies, the motivation was to observe if the modifiers selected were distributed in the inner layers or the external surface. As can be observed in Figure IV - 2, the modifier's particles were homogeneously distributed between the graphite flakes.

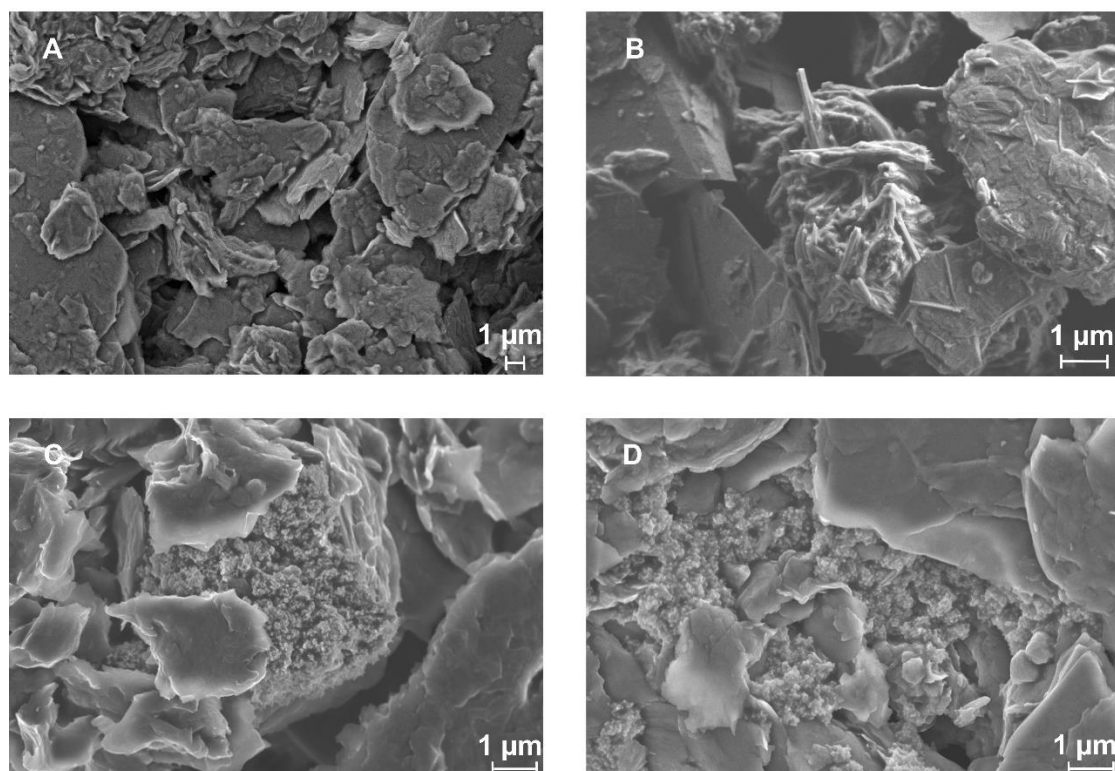


Figure IV - 2. SEM studies. A) graphite/SPCE-Ink, B) CoPc/SPCE-Ink, C) CuO/SPCE-Ink and D) PB/SPCE-Ink.

3. Electrochemical Response

In the *Sensor and Biosensors group*, a set of different modifiers were optimized over the years to select the best one with the most attractive properties from an electrochemical point of view. Within this group, metal nanoparticles, standard catalysts, conductive polymers, and metal oxides among others, are different examples. In this work, the starting modifiers were six to construct the sensor array: graphite, CoPc, CuO, PB, PP, and Pd.

Therefore, these modifications were coated on the surface to evaluate their behaviour in front of each substance individually.

As a standard operation mode to work, the first step of the experimental setup is to collect the data and perform a preliminary PCA using the unfolded data to evaluate sensors complementarity. Results can be observed in Figure IV - 3. As a powerful visualization tool, in the scores plot it would be expected that redundant electrodes will appear superimposed, meanwhile different electrodes appear separated. As a general overview, each modified electrode showed different electrochemical performance in different regions. This conclusion is considered as a key factor when ET principles are applied.

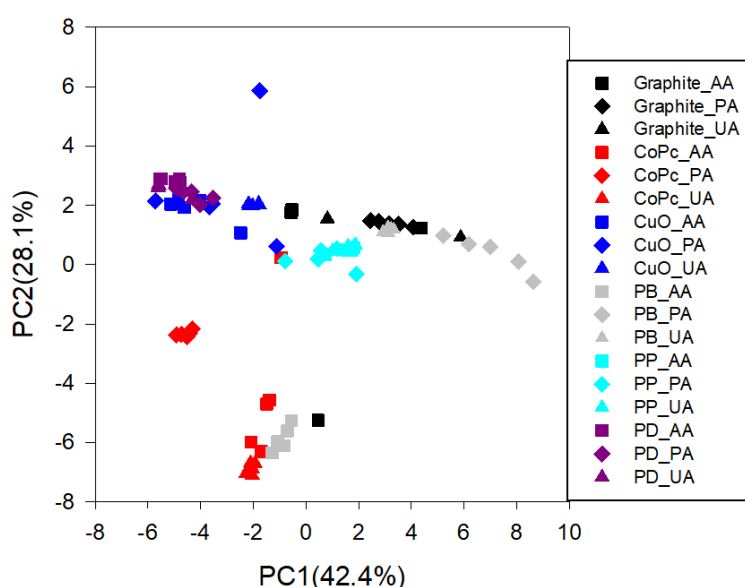


Figure IV - 3. Score plot of the two components obtained after PCA analysis. Five replicates for each sensor were done determining the three compounds of interest: acetaminophen, ascorbic acid, and uric acid.

Another feature to comment is the role of PP and Pd in the sensor array. As it can be observed in Figure IV - 3, these two modifiers do not provide a clear distinction between the three analytes under study. This reasoning could be used to remove them from the array and reduce the number of sensors to four. The rest of the candidates present differentiable responses in front of the substances, contributing to the variability of response of the system.

Additionally, in all the cases, the obtained signals were far away from zero, giving valuable information to the system.

Therefore, once this pre-selection step of the candidates is done, the second step is based on the evaluation of the cyclic voltammograms obtained. Currently, two scans were measured selecting the second one to make the representation of the voltammetric response. As it can be observed in Figure IV - 4, slightly different signals were analysed for the different analytes studied. This is a crucial requirement to carry out an electronic tongue.

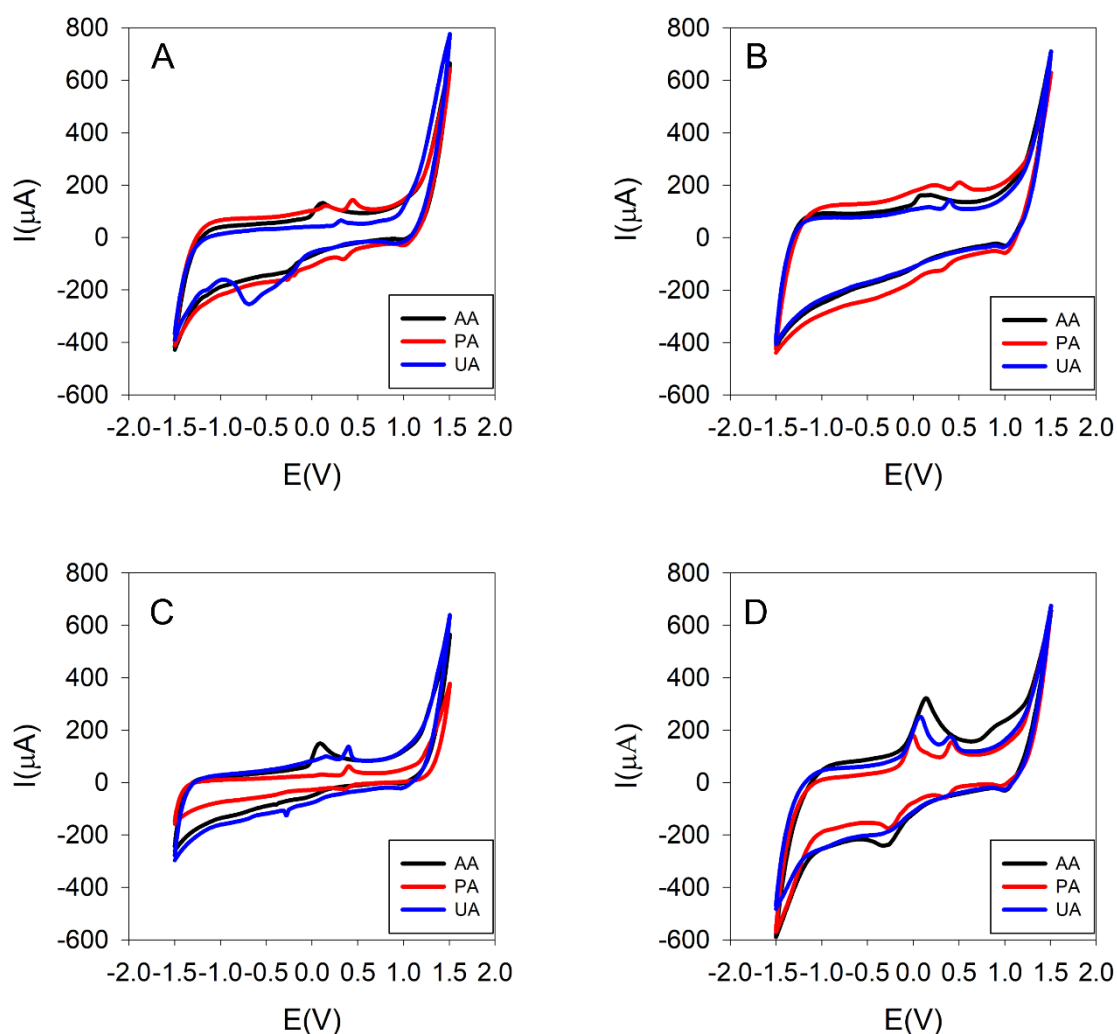


Figure IV - 4. Voltammetric response for PA, AA, and UA using the four finally selected inks. (A) Cobalt (II) phthalocyanine/SPCE-Ink; (B) Prussian blue/SPCE-Ink; (C) Graphite/SPCE-Ink; (D) Copper oxide (II)/SPCE-Ink. The range of potential was from -1.5 to 1.5 V. The scan rate was $50 \text{ mV} \cdot \text{s}^{-1}$ and step rate of 9 mV . A $300 \mu\text{mol} \cdot \text{L}^{-1}$ individual solution was employed for the four modified screen-printed electrodes.

4. Modified Screen-printed Electrodes Characterization

After the modification step, a characterization of the modified screen-printed electrodes is needed to evaluate the goodness of the drop deposition onto the surface. To achieve it, some experiments were carried out such as calibration curves, reproducibility, and stability studies.

4.1. Calibration Curves

Calibration curves were performed using the CV technique representing the peak height which corresponds to the maximum of the oxidation signal. The behaviour of each sensor for each analyte was evaluated separately. The determination of the linear ranges and the maximum concentration detectable by each sensor for each compound are valuable analytical information before the execution of the ET. As it can be shown in Figure IV - 5, the three compounds presented linear range from 0 to 500 μM . Analytical parameters were represented in Table IV - 1.

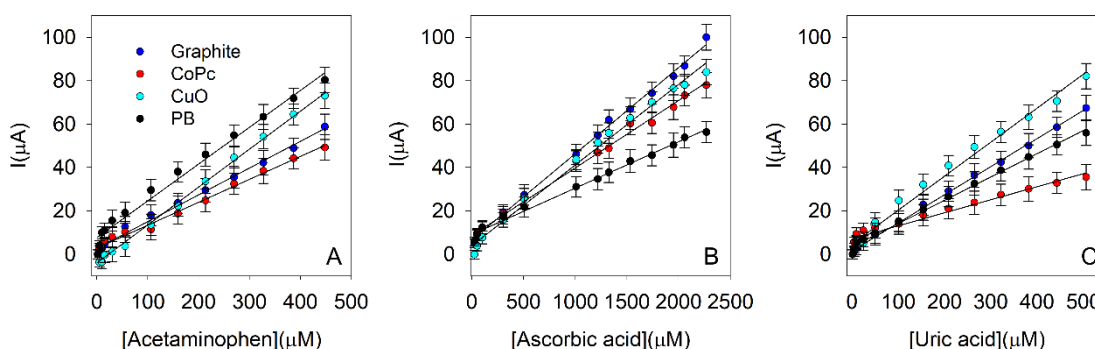


Figure IV - 5. Calibration curves for three replicates ($n=3$) to determine the concentration working range for the three compounds under study for the four modified screen-printed electrodes. A) acetaminophen, B) ascorbic acid and C) uric acid.

Table IV - 1. Calibration data (y vs. x) for the separate determination of acetaminophen, ascorbic acid, and uric acid employing the integrated sensor array chosen.

Compounds	Acetaminophen	Ascorbic Acid	Uric Acid
Graphite	$y = 0.1234x + 2.6656$ $R^2 = 0.993$	$y = 0.0398x + 6.5307$ $R^2 = 0.997$	$y = 0.1298x + 4.6275$ $R^2 = 0.999$
CoPc	$y = 0.1057x + 2.7753$ $R^2 = 0.991$	$y = 0.0311x + 8.5678$ $R^2 = 0.993$	$y = 0.0534x + 9.3828$ $R^2 = 0.996$
CuO	$y = 0.1749x - 4.0453$ $R^2 = 0.997$	$y = 0.0372x + 3.8868$ $R^2 = 0.992$	$y = 0.1569x + 15.231$ $R^2 = 0.988$
PB	$y = 0.1696x + 7.5897$ $R^2 = 0.984$	$y = 0.0214x + 9.0457$ $R^2 = 0.992$	$y = 0.1074x + 7.6534$ $R^2 = 0.995$

4.2. Reproducibility and Stability Studies

When experiments about ETs are carried out, sensors are subjected to a large number of measurements. For that, reproducibility and stability studies need to be done to verify the number of measurements allowed and the electrode performance.

In this case, experiments were done using a stock solution of acetaminophen 165 μ M measured thirty times. A blank, in PBS solution, was introduced between each measurement to evaluate if the system was presenting some fouling effect.

In all the situations, the four modified sensors showed stable responses with Relative Standard Deviation (RSD) of 8.2%, 5.5%, 6.3%, and 3.9% for CoPc, PB, CuO, and graphite, respectively. When trends in the blanks were observed, no fouling effect was either detected in the measurements.

As the electrodes are prepared by drop casting, it is important to check the reproducibility of the construction of electrodes as well. To achieve it, four sensors were modified by triplicate and measured consecutively with an acetaminophen stock solution. Afterward, results were calculated and summarized in Table IV - 2, showing outstanding results for PB with an RSD of 0.8%.

Table IV - 2. Reproducibility of construction of each sensor with the results of the RSD (n=3).

Sensor	RSD (%)
Graphite/SPCE-Ink	2.9
Cobalt (II) phthalocyanine/SPCE-Ink	7.5
Copper oxide (II)/SPCE-Ink	1.3
Prussian blue/SPCE-Ink	0.8

5. Principal Component Analysis

Once the morphology and electrochemical characterization were done, further experiments were based on evaluating the power of discrimination of the working sensors. PCA calculation was used to deal with this aim. Different data can be collected to perform this calculation. In this case, the sensitivity of the calibration curves done previously was selected.

Results of the score plot are observed in Figure IV - 6, in which three differentiated clusters corresponding to the three compounds under study can be observed. In the case of acetaminophen and uric acid more dispersion is presented, for this reason, the ellipses stretched. In the case of ascorbic acid, better clustering is observed.

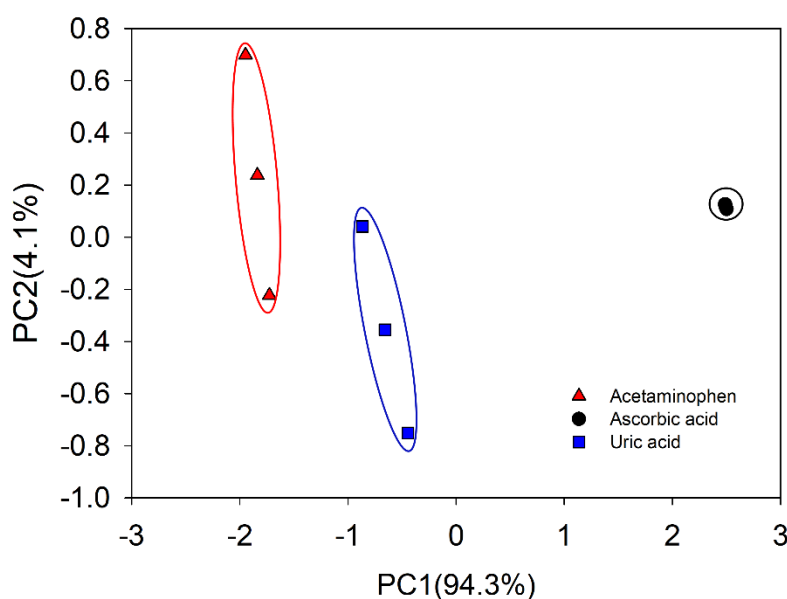


Figure IV - 6. Score plot of the two components obtained after PCA analysis. PCA shows three clusters across the PC1 (94.3%). These clusters correspond to the studied compounds for n=3 replicates. These results were obtained using the sensor array chosen.

6. Partial Least Squares Regression as a Modelling Tool

The final step of this study is the construction of a model to be able to detect each compound individually. Because the data collected present high complexity, the need for pre-treatments steps facilitates the removal of noise interpreting data more homogeneous. Standard Normal Variate (SNV) was selected as a pre-treatment tool. It is based on a reduction of the scatter effect using easy mathematical treatment. In this case, the subtraction of the measurement mean to the measure divided the data by its standard deviation¹. With this operation, it is possible to get a normalized baseline for all the samples. Referring to the construction of the model, PLS was used as a power to perform multivariate calibration analysis. In the case of the study, the variant was PLS1, in which one model with single output was used for each compound.

RESULTS AND DISCUSSION

LVs² were also optimized to avoid the overfitting of the model getting the lowest error. In the case of PA, eight LVs were selected, whereas seven LVs were chosen for AA and UA.

In Figure IV - 7, the comparison between the obtained vs. expected results for the training subset is represented by dark dots for each analyte. In the same representation, the testing subset, in white dots, was projected, enabling the feasibility of the model.

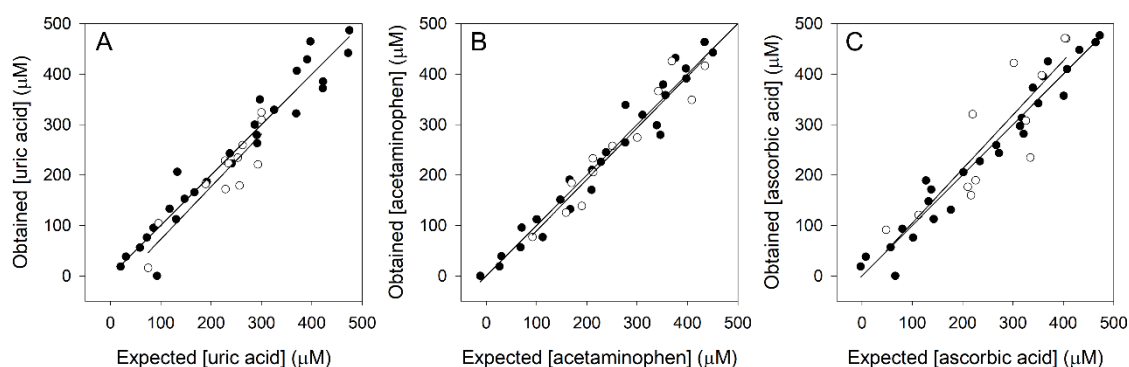


Figure IV - 7. Obtained vs expected concentrations results plots for the training set (black dots) and the testing set (white dots) for A) acetaminophen, B) ascorbic acid and C) uric acid.

All the parameters related to the regression line are shown in Table IV - 3. As it can be observed the y-intercept and the slope of the training and testing regressions include zero and one, respectively for all the analytes studied. If the correlation coefficients are examined, in all the cases, they are close to one. Therefore, it can be concluded that the approach is working properly giving promising results.

Table IV - 3. Results of the fitted regression curves for comparison graphs of obtained vs. expected concentrations, for the training and testing subsets of samples and the three considered compounds (intervals calculated at the 95% confidence level).

Set	Analyte	R ²	Slope	Intercept (μM)	NRMSE
Training subset (n = 27)	Acetaminophen	0.962	1.00 ± 0.09	0 ± 25	0.90
	Ascorbic acid	0.955	1.00 ± 0.09	0 ± 25	0.97
	Uric acid	0.940	1.00 ± 0.11	0 ± 31	1.12
Testing subset (n = 12)	Acetaminophen	0.915	1.02 ± 0.22	-13 ± 28	0.7
	Ascorbic acid	0.762	1.07 ± 0.42	-3 ± 54	1.41
	Uric acid	0.829	1.04 ± 0.33	-32 ± 36	0.85

NRMSE parameter was also calculated as a test of the fitting degree of the models. In practice, acetaminophen and uric acid presented the lowest NRMSE for the test subset, verifying the good predictive capabilities of the models. Concerning the correlation coefficients, the training subset presents better results, as expected.

At this point, it could be interesting comparing the obtained results in front of the results obtained in the group in the previous work³. Previous works reported the simultaneous determination of the three compounds using the same modifiers but different technology such as bulk modification using GECs electrodes⁴. These results can be observed in Table IV - 4.

Table IV - 4. Results of the fitted regression curves for comparison graphs of obtained vs. expected concentrations, for the training and testing subsets of samples and the three considered compounds (intervals calculated at the 95% confidence level) for antecedent work in the laboratory³.

Set	Analyte	R ²	Slope	Intercept (μM)
Training subset (n = 33)	Acetaminophen	0.968	0.942 ± 0.031	32 ± 21
	Ascorbic acid	0.947	0.933 ± 0.040	36 ± 25
	Uric acid	0.923	0.873 ± 0.046	58 ± 25
Testing subset (n = 15)	Acetaminophen	0.848	0.895 ± 0.105	82 ± 71
	Ascorbic acid	0.908	0.919 ± 0.081	65 ± 41
	Uric acid	0.753	0.871 ± 0.138	-8 ± 86

As the main conclusion, if both results are compared, it can affirm that the proposed methodology improved slightly the results in terms of slope and intercept for the comparison regressions lines.

Therefore, the proposed work reports the powerful coupling between the combination of the screen-printed integrated array and the use of chemometrics to construct the model for the quantification of AA, PA, and UA simultaneously.

ARTICLE 2

Voltammetric sensing using an array of modified SPCE coupled with machine learning strategies for the improved Identification of opioids in presence of cutting agents

Dionisia Ortiz-Aguayo, Karolien De Wael and Manel del Valle

Journal of Electroanalytical Chemistry, 902, 115770.

1. Outline

This research depicts an intelligent sensor strategy, which combines the use of a modified screen-printed sensor array to extract the fingerprint of each compound on each sensor and the coupling with advanced data processing for its identification and subsequent classification. The analytes studied in this project were some opiates such as heroin, morphine, and codeine. Paracetamol and caffeine were used as common cutting agents present in these illicit samples. SWV was required as a voltammetry technique to elucidate the voltammogram.

The work applied the use of the modification through a self-formulated graphite polystyrene ink. The sensor array was optimized by a systematic evaluation procedure combining PCA as a visualization tool and Silhouette calculation as a measurement of clustering metrics. The fusion of these two strategies allows an accurate optimization of the sensor array used to study a mixture of opiates. Finally, kNN was applied as a pattern recognition model to carry out automatic identification of the compounds analysed.

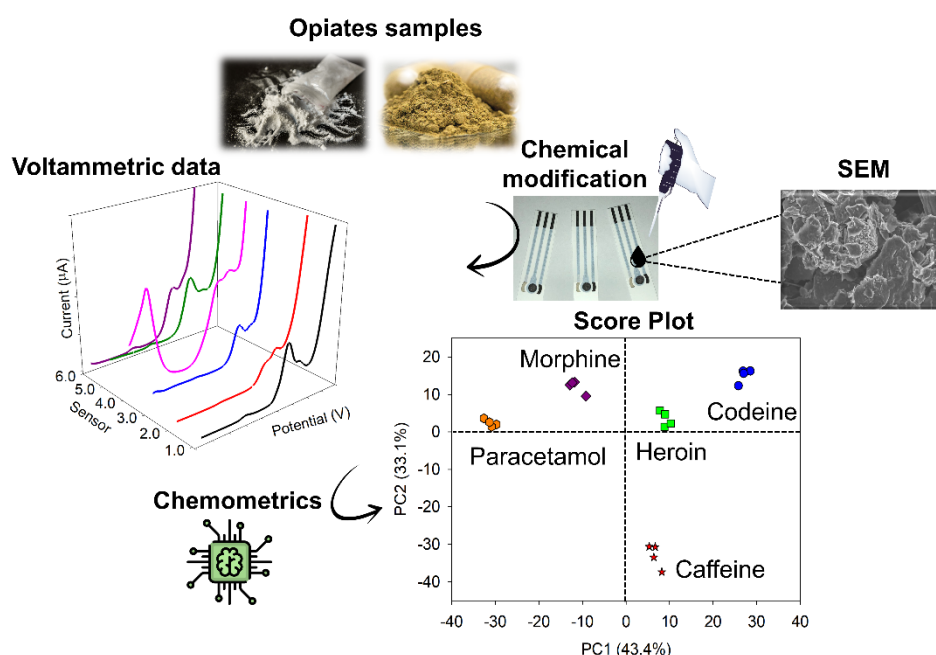


Figure IV - 8. Steps involved in the experimental process: from the acquisition of the samples until its identification using chemometrics.

2. Scanning Electron Microscopy Studies

The first step in this research was the characterization of the sensor platforms employed. This goal was achieved using electrochemical techniques and SEM characterization.

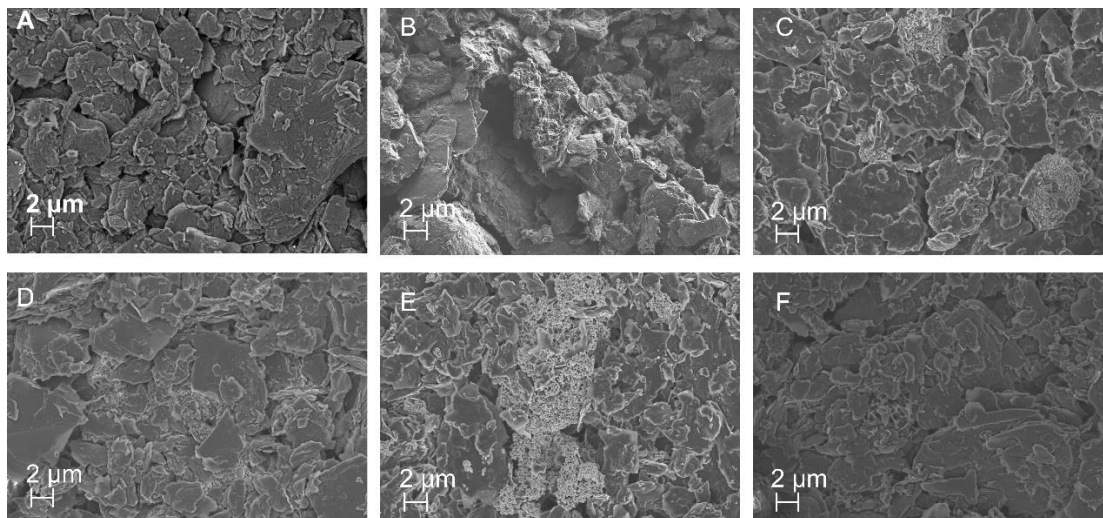


Figure IV - 9. SEM images of the polystyrene inks over the Italsens SPCE electrodes. A) graphite/SPCE-Ink, B) CoPc/SPCE-Ink, C) CuO/SPCE-Ink, D) PB/SPCE-Ink and F) PP/SPCE-Ink.

The first motivation was to study the distribution of the modifiers into the ink. For that, microscopy studies were achieved to observe if they were distributed on the external or internal layers. Figure IV - 9 represents its morphology structure showing a fairly homogeneous distribution. To complement the studies EDX was also done (Figure IV - 10), which verify the presence of the employed metals. Spectra of PP and unmodified electrodes are not represented due to their absence of metallic signals.

Thereafter, the calculation of the active area before and after modifying is an interesting parameter to analyse to observe the improvement given by the modification selected. To make these calculations, the Randles–Sevcik equation⁵ (Equation IV - 1) was used. All the parameters and constants employed are collected in Table IV - 5.

$$I_p = 0.446 \cdot n \cdot F \cdot c \cdot A \cdot \sqrt{v} \cdot \left(\frac{nDF}{RT} \right)^{\frac{1}{2}} \quad \text{Equation IV - 1}$$

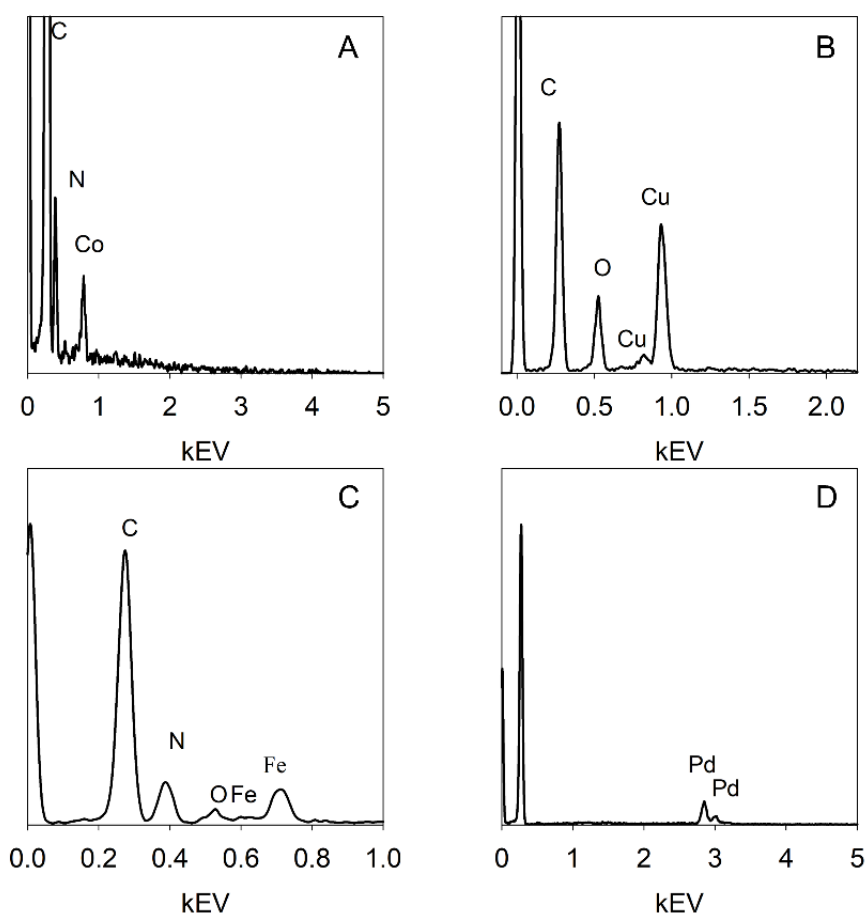


Figure IV - 10. EDX studies. A) CoPc/SPCE-Ink, (B) CuO/SPCE-Ink, C) PB/SPCE-Ink and D) PD/SPCE-Ink.

CV experiments were using 0.02 M KH_2PO_4 and 0.1 M KCl containing 5 mM $[\text{Fe}(\text{CN})_6]^{3-}/[\text{Fe}(\text{CN})_6]^{4-}$ solution. Potential range was defined from -0.4 to 0.8 V. Five scan rates (0.01, 0.025, 0.05, 0.1, 0.2, 0.3 and 0.5 $\text{V}\cdot\text{s}^{-1}$) were used.

Table IV - 5. Parameters employed in the Randles–Sevcik equation.

Symbol	Parameter	Value
n	Number of transferred electrons	1
F	Faraday's constant	$96485 \text{ C}\cdot\text{mol}^{-1}$
c	The concentration of electroactive substances	$\text{Mol}\cdot\text{cm}^{-3}$
A	Effective area	Cm^2
v	Scan rate	$\text{V}\cdot\text{s}^{-1}$
R	Gas constant	$8.314 \text{ J}\cdot\text{mol}^{-1}\cdot\text{K}^{-1}$
T	Temperature	298.15 K
D	The diffusion coefficient for ferrocyanide	$6.32\cdot 10^{-6} \text{ cm}^2\cdot\text{s}^{-1}$

RESULTS AND DISCUSSION

Once the voltammetric data is collected, the calculation of the active area can be done representing the slope of the calibration curve of $v^{1/2}$ ($V \cdot s^{-1}$) in front of $I_p \cdot c^{-1}$ ($A \cdot cm^3 \cdot mol^{-1}$). Typical CV graphs and the corresponding calibration curves obtained are represented in Figure IV - 11.

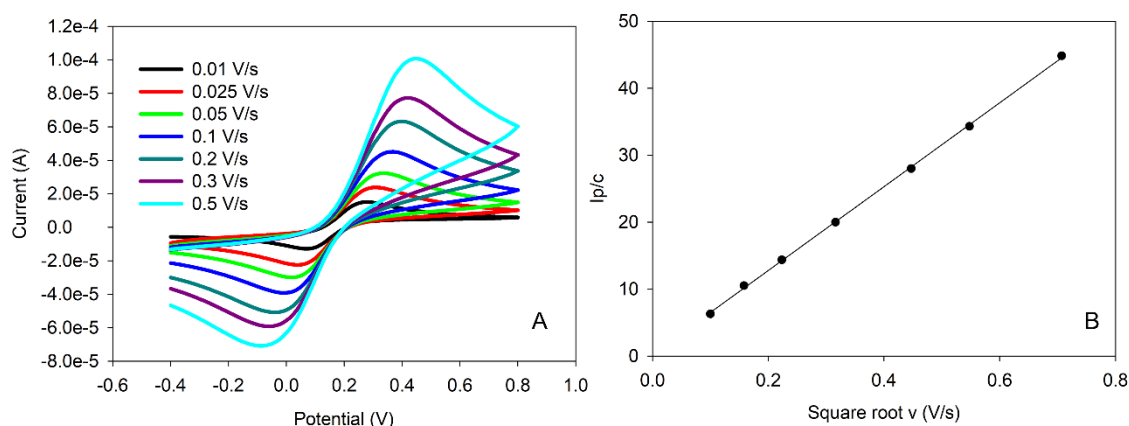


Figure IV - 11. A) CV obtained using 5 mM $K_3Fe(CN)_6/K_4Fe(CN)_6$ changing scan rate from 0.01 to 0.5 V/s using CoPc/SPCE-Ink as an example. B) Calibration curve (I_p/c ($mol \cdot cm^{-3}$) vs $v^{1/2}$ ($V \cdot s^{-1}$)).

Calculations of the active areas and comparisons with the geometric are shown in Table IV - 6.

Table IV - 6. Comparison between the active area and the geometric ones for the six modified electrodes used.

Modified sensor	Active Area (mm^2)	Geometric Area (mm^2)
Bare	11.7	7.1 ($\varnothing=3$ mm)
Graphite/SPCE-Ink	8.2	
CuO/SPCE-Ink	8.5	
PB/SPCE-Ink	8.1	
CoPc/SPCE-Ink	9.3	
Pd/SPCE-Ink	9.4	
PP/SPCE-Ink	7.1	

Summarizing this section allows the study of the morphology of the modified inks, remarking the metals inside the graphite flakes and the calculation of the active area after modifying is also evaluated for an overview of the material used to perform modification surface.

3. Square Wave Voltammetric Response

This work reports the study of three common drugs of abuse (codeine, heroin, and morphine) and two commonly used cutting agents (paracetamol and caffeine). This section has an aim to assure if the signals obtained for the different analytes are enough different to carry out further electronic tongue experiments.

As a result, individual stock solutions of 300 μM of caffeine, codeine, heroin, morphine, and paracetamol were monitored using the SWV technique in PBS at pH 7. Some studies in the literature reported that morphine and heroin present some reactions of hydrolysis at alkaline pH^{6,7}. This factor was considered crucial while electrochemical measurements were done, favouring the choice of neutral pH for working with the desired compounds. For each substance, four replicates were achieved measuring randomly to avoid any periodic trend in the signal.

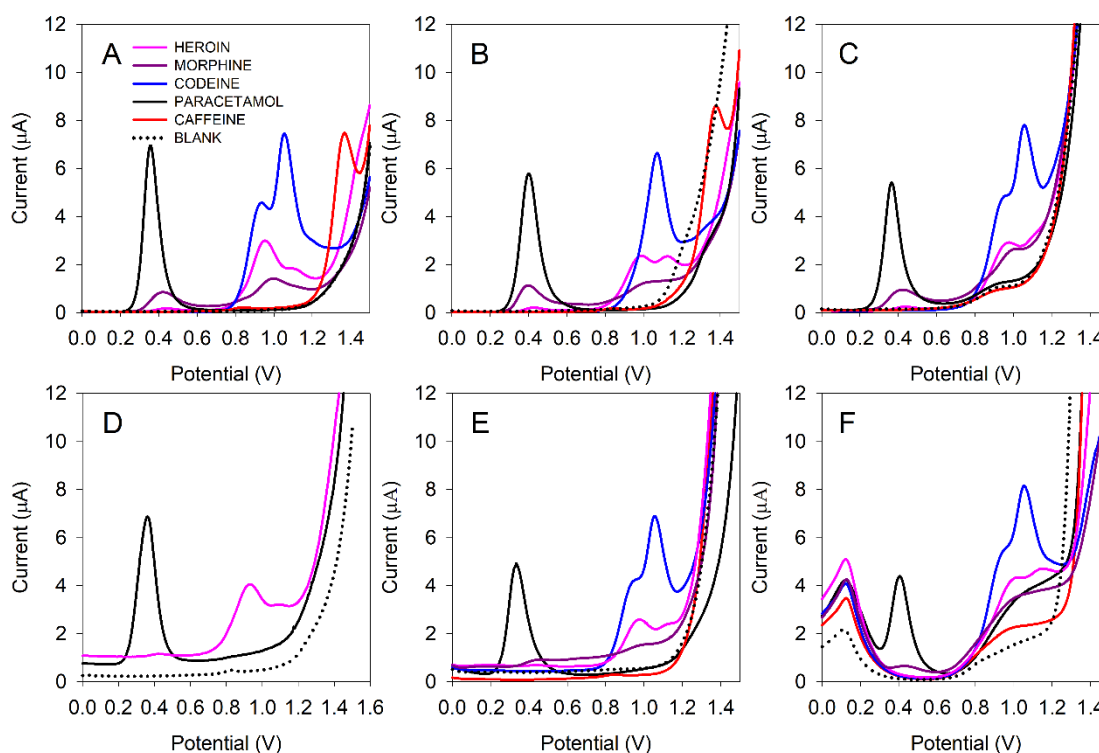


Figure IV - 12. Square wave voltammograms were obtained for the five compounds under study and a blank using the six modified sensor array. A) graphite/SPCE-Ink, B) CoPc/SPCE-Ink, C) Pd/SPCE-Ink, D) PP/SPCE-Ink, E) CuO/SPCE-Ink, F) PB/SPCE-Ink. 50 μL were dropped on the electrode surface. Potential range: 0-1.2 V, step potential: 5 mV, scan rate: 50 $\text{mV}\cdot\text{s}^{-1}$, amplitude: 25 mV and frequency: 10 Hz. The concentration used of all the analytes was 300 μM .

Results about the responses obtained are shown in Figure IV - 12. In the case of heroin, an irreversible oxidation split peak located at +0.81 V can be observed coming from the oxidation of the amino group. This fact is in agreement with some works reported in the literature⁷⁻¹⁰. Oxidation of the phenol group of 6-monoacetylmorphine (6-MAM) is observed at +0.40 V. This compound is an impurity coming from the synthesis of heroin, specifically, when the incomplete acetylation of morphine is done and/or a product of hydrolysis is originated¹¹. Furthermore, the peak coming from the phenol group from 6-MAM is overlapped with morphine and paracetamol peaks. If the analysis is performed at a higher potential, difficult signal resolution can be observed between second oxidation peaks of morphine and heroin with codeine.

Therefore, the whole voltammograms present a high degree of overlap between the signals, which can represent a restriction for the alone identification of the substances. Chemometric analysis was further done for better assessment. In this case, PCA was done to evaluate mathematically the complementarities and similarities between the fingerprint of each studied analyte.

4. Principal Component Analysis as a Selection Tool

Four replicates were measured for each sample in random order to discard any memory effect in the collected data. In this case, the whole voltammogram was selected per each electrode and each sample to perform PCA analysis. This strategy allows the search for differences and similarities in the different samples using the selected modified sensor array. According to the theoretical concepts, redundant electrodes will superimpose in the representation, meanwhile, different electrodes will be placed separately.

As can be imagined, in our case, the most interesting is to find this commented distinction. This is the only way to ensure that non-redundant information is used to analyse the case under study. Furthermore, through PCA it will be possible to observe how the electrodes can discriminate the analytes, as well as to evaluate how similar the replicates of each sample are. Results are plotted in Figure IV - 13, where the two principal components are shown. If attention is focused on Figure IV - 13A, it can be seen how the maximum variability among the samples is explained by PC1 with a value of 81.1%.

In this case, the presence of PP distorts the system showing dispersion between replicates. For this reason, this argument was used to remove it from the sensor array. This information can be related to that shown in Figure IV - 12, where discrepancies in the voltammetric response are also observed, showing no different shapes are obtained for the different compounds under study.

All these reasons make it necessary to reconsider repeating the calculation by eliminating the information given by this modified sensor. Results can be observed in Figure IV - 13B.

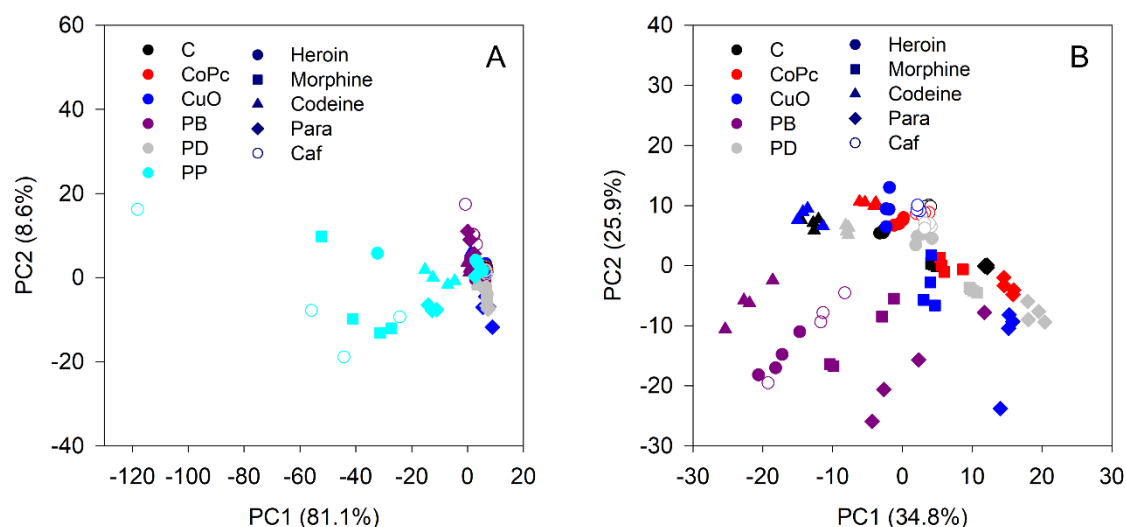


Figure IV - 13. Score plot of the two components obtained. Four replicates for each sensor and compound using a 300 μ M.

In this case, relevant information can be explained through PC1 and PC2 adding up to a total of 60.7% of the total variability. Furthermore, the most relevant of the plot is the behaviour of the PB sensor (in purple). In detail, it looks different from the other sensors, shown apart in the diagram. However, large dispersion can be observed in comparison with the others. One explanation for this dispersion could be associated with a lack of stability in the voltammetric response. Due to these observations, it was decided to discard the purple sensor from the set. All of the above characteristics can be seen in Figure IV - 13B. Therefore, the next step was to calculate a new PCA with the four remaining modifiers: graphite, CoPc, CuO, and Pd (Figure IV - 14A). This graph was interpreted based on the same criteria as the previous graphs. Therefore, the CuO modifier was discarded from the group due to the drift and distortion of the pure analyte clusters.

However, if the aim of this work were not to meticulously optimize the array, the selection of these four sensors would be suitable for the identification of the present drugs of abuse and their corresponding cutting agents. Figure IV - 14B shows the final selection with the three selected candidates (graphite, CoPc, Pd). These three modifiers present a differentiated response for each compound, as well as a moderating dispersion, allowing each substance to be assigned to the corresponding class.

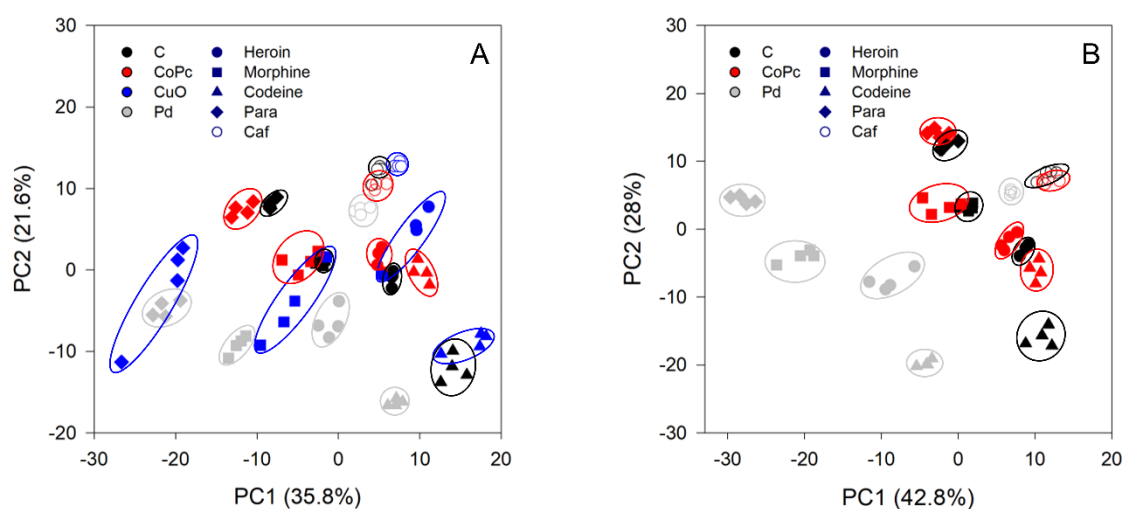


Figure IV - 14. Scores plot of the two components after PCA. Four replicates for each sensor with the five analytes: heroin, morphine, codeine, paracetamol, and caffeine. A) four SPCE array: graphite/SPCE-ink, CoPc/SPCE-ink, Pd/SPCE-ink and CuO/SPCE-ink. B) three SPCE array: graphite/SPCE-ink, CoPc/SPCE-ink and Pd/SPCE-ink.

5. Optimization through Silhouette Parameter

A first criteria was achieved with the help of the PCA to choose the best set of sensors to form the array. However, a further step in the study was desired. For the first time in the group, a methodology was developed to refine the selection based on the calculation of the Silhouette parameter. This numeric criterion makes it possible to evaluate the degree of clustering to ensure the best selection.

In this case, a different representation of the data collected was made. Specifically, it proceeded to the *unfolding* of the data. As discussed in previous sections of this thesis, this transformation of the data is based on grouping the different voltammograms of a sample into a single column or vector and using this information for processing.

Therefore, once the data was split, a PCA was performed as a first approximation to have an initial unsupervised clustering of the data according to their similarity in the multivariate space. Subsequently, the Silhouette parameter was calculated to assess the goodness of clustering. The better the clustering, the easier the identification of the desired sample.

The Silhouette calculation is defined by two parameters $a(i)$ and $b(i)$ for each sample. These parameters reflect a comparison between intra and inter-cluster variability. This strategy allows the quantification of which cluster is better discriminated compared to the other clusters participating in the system. To perform these calculations, the first two principal components (PC1 and PC2) obtained in the PCA from the *unfolding* of the data were used. With this methodology it is possible to go from a 3D matrix to a 2D matrix by simplifying and condensing the information, thus reducing the dimensionality in the case of voltammetric data.

To deal with the case study in detail, first of all, the calculation was carried out for each sensor individually, i.e., from the six initially prepared sensors.

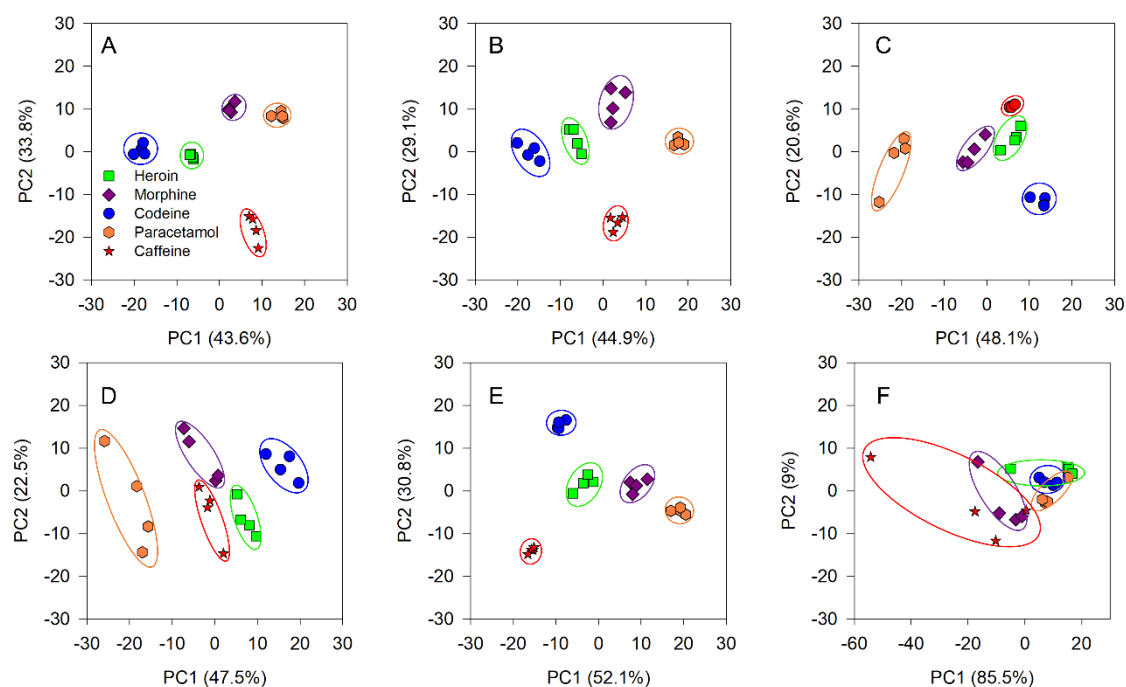


Figure IV - 15. Scores plot obtained after PCA analysis. Four replicates of 300 μ M of each compound were analysed. A) graphite, B) CoPc, C) CuO, D) PB, E) Pd and F) PP.

Figure IV - 15 clearly shows that the sensors that produce the worst clustering are PB, PP, and CuO.

These observations are supported by the Silhouette calculations obtained in Table IV - 7, when values of +0.328 for PB, +0.041 for PP, and +0.640 for CuO can be observed. In a conclusion, if each sensor is evaluated separately, the best option is graphite ink, showing an average of Silhouette parameter of +0.849. In the case of graphite, CoPc, and Pd.

In the case of graphite, CoPc, and Pd, the silhouette parameter is considered acceptable. However, the main objective of this research focuses on complementing the information given by each sensor to improve its performance and thus have a better degree of clustering. Therefore, from the three selected candidates: C, CoPc, and Pd unfolded data of the binary combinatorics of the three sensors were made and the Silhouette was evaluated. Results can be observed in Figure IV - 16.

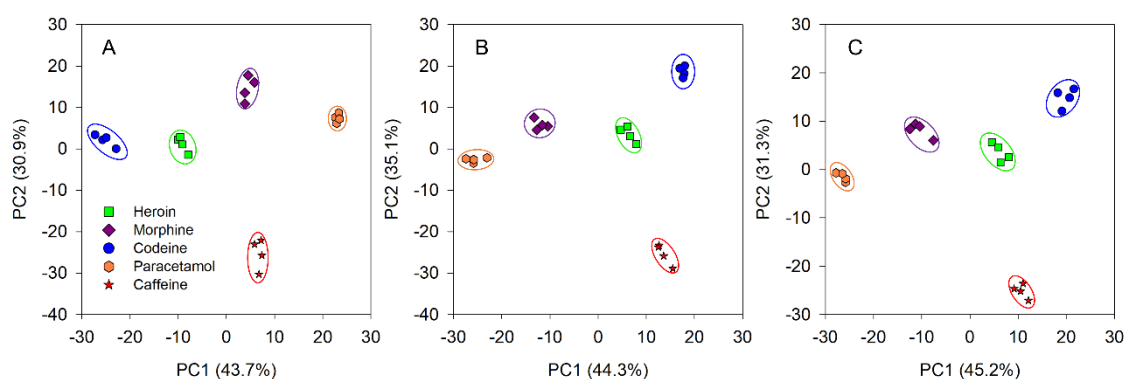


Figure IV - 16. Score plots after PCA analysis. A) C-CoPc, B) C-Pd and C) CoPc-Pd. All the combinations were tested with the five compounds under study.

Table IV - 7. Average of Silhouette parameter for the stepwise optimization of the sensor array.

Number of SPCE	Modified SPCE	Silhouette parameter
1	C	+0.849*
	CoPc	+0.735
	CuO	+0.640
	PB	+0.328
	Pd	+0.817
	PP	+0.041
2	C-CoPc	+0.841
	C-Pd	+0.863*
	CoPc-Pd	+0.848
3	C-CoPc-Pd	+0.877*

*Optimal configuration obtained after systematic evaluation on each step.

In general trends, the three combinations show a clear visualization of the clusters for the different compounds. Therefore, the choice of the best combination was made based on the Silhouette parameter. As shown in Figure IV - 16, the degree of clustering in the three cases is similar, showing an improvement with the combination C+Pd (Figure IV - 16B) with a value of +0.863. At this point of the investigation, the last possible combination to evaluate is the one formed by the three sensors. PCA representation is shown in Figure IV - 17B, with a Silhouette calculation of +0.877.

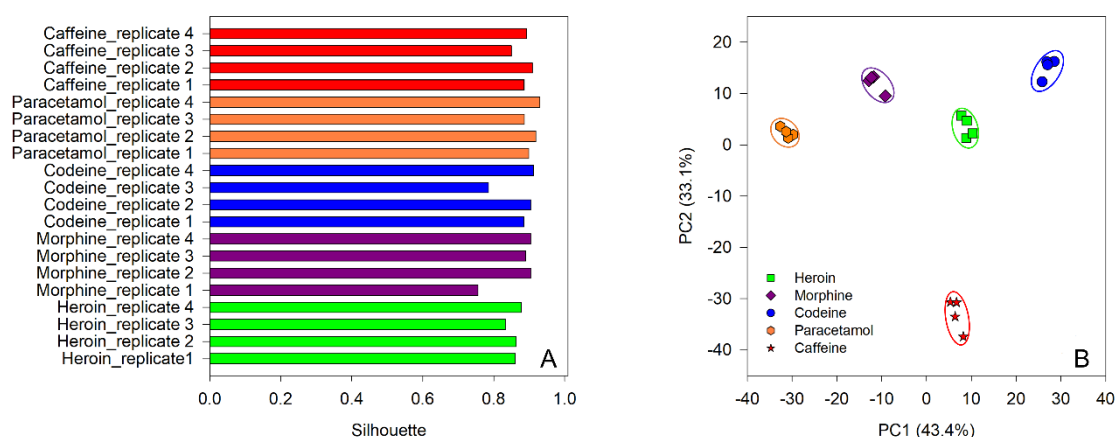


Figure IV - 17. A) Silhouette plot employing C, CoPc, and Pd sensors. B) Score plot after PCA analysis using the mentioned sensor array.

When the study is finished, it can be determined that the combination of the three modifier inks (C, CoPc, and Pd) is the best for the individual determination of the analytes. Figure IV - 17B clearly shows how the sensors have different responses to the compounds resulting in five well-defined clusters with clear differentiation and a good degree of grouping between the replicates. In addition, a total variance value of 76.5% was obtained considering PC1 and PC2, which is more than appropriate for the case study. If Figure IV - 17A is analysed, the corresponding Silhouette shows a high value (+0.877) very close to the maximum value which is one. As a summary, this result leads to easy identification of the compounds studied.

As a result of the study, it can also be concluded that the selected option of combining the three sensors gives similar results to the combination of graphite with Pd, with a Silhouette value of +0.863 using a simpler configuration of two working electrodes.

This fact can already be seen in Figure IV - 14B, where each compound is identified differently (grey dots in a separate region) compared to the other modifiers. CoPc sensor was ruled out as a stand-alone use due to the Silhouette global parameter of +0.735. Finally, the study concludes the optimization of the best working electrodes for the desired compounds, providing the benefit of using more than one electrode for their identification.

6. Machine Learning Algorithms

To take the study a step further, different “*Machine Learning Algorithms*” were tested as classifier methods to achieve an automated and intelligent final operation. Random Forest, Naive Bayes, SVM, and kNN were some examples. Results can be collected in Table IV - 8, where indicators of precision, accuracy, specificity, and sensitivity can be shown.

Table IV - 8. Results of the statistical calculation using some machine learning strategies such as kNN (k=4), Random Forest, Naive Bayes, and SVM employing leave-one-out cross-validation.

Model	Compound	Classification accuracy	Precision	Sensitivity	Specificity
kNN	Heroin	1.0	1.0	1.0	1.0
	Morphine	1.0	1.0	1.0	1.0
	Codeine	1.0	1.0	1.0	1.0
	Paracetamol	1.0	1.0	1.0	1.0
	Caffeine	1.0	1.0	1.0	1.0
Random Forest	Heroin	1.0	1.0	1.0	1.0
	Morphine	1.0	1.0	1.0	1.0
	Codeine	1.0	1.0	1.0	1.0
	Paracetamol	1.0	1.0	1.0	1.0
	Caffeine	1.0	1.0	1.0	1.0
Naive Bayes	Heroin	1.0	1.0	1.0	1.0
	Morphine	1.0	1.0	1.0	1.0
	Codeine	1.0	1.0	1.0	1.0
	Paracetamol	1.0	1.0	1.0	1.0
	Caffeine	1.0	1.0	1.0	1.0

Model	Compound	Classification accuracy	Precision	Sensitivity	Specificity
SVM	Heroin	0.8	0.0	0.0	0.0
	Morphine	0.8	0.5	0.4	0.8
	Codeine	1.0	1.0	1.0	1.0
	Paracetamol	1.0	1.0	1.0	1.0
	Caffeine	1.0	1.0	1.0	1.0

In general, all classification models gave good results, except for some misclassification in the case of the SVM, concretely in heroin and morphine samples.

Finally, the study focused on kNN is considered a simple and fundamental unsupervised classification method¹². It performs the classification of new data based on similarity measures. The only parameter to optimize is the variable k , which is related to the number of closest neighbours. The optimal value of k is obtained when the best performance is achieved. Specifically, in this case, the number of integrants in the cluster is known in advance, as it corresponds to the number of replicates of each substance tested, $k=4$. So, it is not needed to optimize this parameter.

The parameter analysed, in this case, was the confusion matrix (Table IV - 9). Leave and out was used as cross-validation methods, due to the low number of samples in the data set. The goodness of identification performance was excellent with 100% in all the indicators (accuracy, precision, sensitivity, and specificity), Table IV - 8.

Table IV - 9. Confusion matrix after applying the kNN algorithm, using leave-one-out cross-validation and $k=4$.

		PREDICTED					
		Heroin	Morphine	Codeine	Paracetamol	Caffeine	Σ
ACTUAL	Heroin	4	0	0	0	0	4
	Morphine	0	4	0	0	0	4
	Codeine	0	0	4	0	0	4
	Paracetamol	0	0	0	4	0	4
	Caffeine	0	0	0	0	4	4
	Σ	4	4	4	4	4	20

Hence, the promising clustering of degrees observed in the PCA diagram allows the good performance of the classificatory models used. Summary, this work reports the accurate optimization of a modified sensor array to identify and classify some drugs of abuse and their corresponding cuttings agents using some machine learning algorithms.

ARTICLE 3

Resolution of opiate illicit drugs signals in the presence of some cutting agents with use of a voltammetric sensor array and machine learning strategies

Dionisia Ortiz-Aguayo, Xavier Cetó, Karolien De Wael and Manel del Valle

Sensors and Actuators B: Chemical, 2022, 357, 13134

1. Outline

The present work is a continuation of the previous one in which a quantitative application is sought. For this purpose, the resolution of different opiates (heroin, morphine, and codeine) in the presence of common cutting agents (paracetamol and caffeine) was carried out using electronic tongue principles. The array used is based on the previous optimisation of **article 2**, where polystyrene inks with graphite modifiers such as bare, CoPc and Pd were chosen. The study was approached in two ways: first, a model involving mixtures of the opioids only was performed. Then, a second model was evaluated with all five compounds to assess their quantification in the presence of the cutting agents. In both cases, PLS was used as the chemometric modelling tool. The results were promising, showing low NRMSE errors, good detection limits and correct stability of the sensors.

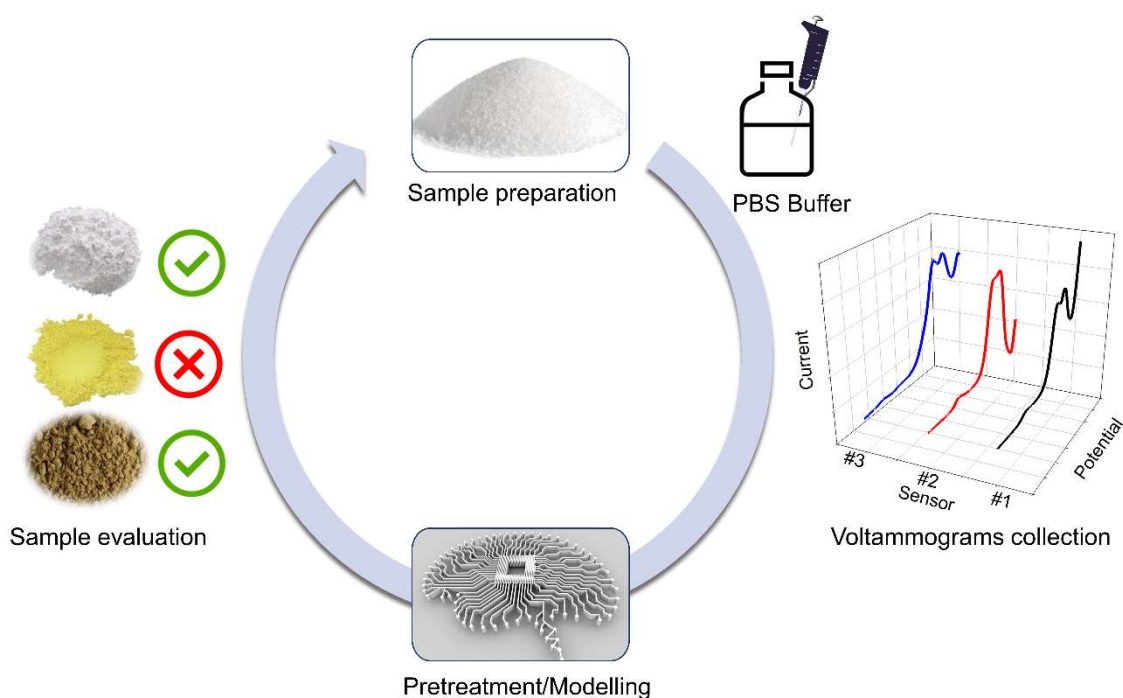


Figure IV - 18. Simulation of the analytical performance from sample preparation to sample evaluation.

2. Sensor Array Characterization

In the literature there are different methodologies for the preparation of modified electrodes^{13,14}. In this case, the procedure described in **article 2** was followed, where the electrodes were modified using a composite material (with different modifiers) by forming a graphite and polystyrene ink. This ink was deposited on the sensor surface generating a new surface suitable for electrochemical measurements. The simplicity of this methodology, together with its low cost, makes it a good candidate for obtaining chemically modifying transducers.

Throughout the group's career, different electrochemical modifiers were used in previous studies with electronic tongues^{15–19}. This information, together with the work carried out in **article 2**, allowed us to select a three-sensor array using bare graphite, CoPc and Pd as the best option for the present case study²⁰.

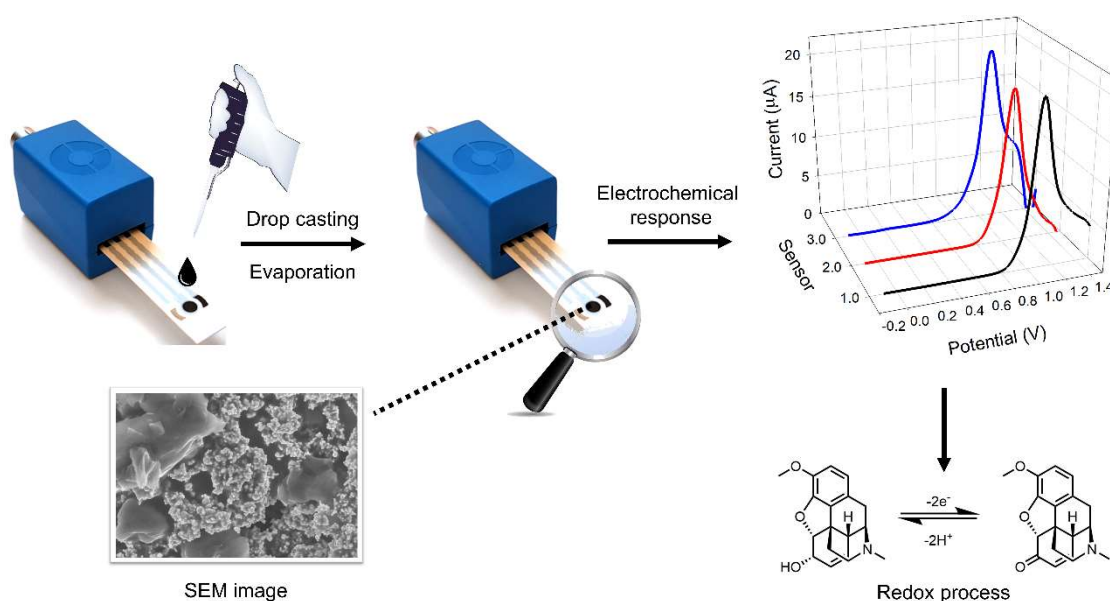


Figure IV - 19. Scheme of the experimental procedure for the electrode surface modification. Firstly, an ink-like solution was prepared incorporating the corresponding modifier. Then, 1 μ L was dropped on the surface and dried at 40°C.

The use of graphite as bare allows a direct comparison with the introduced modifiers. In the case of Pd nanoparticles, this option is increasingly used compared to the use of bulk metals, providing a higher surface to mass ratio, and improving the electrochemical properties. In addition, Pd shows good electrocatalytic activity against different electrochemical reactions.

In the case of CoPc, this family of compounds presents an efficient electrocatalysis in the determination of many biological, inorganic, and organic compounds, which makes it an excellent candidate to improve the signals in electrochemistry.

The present work is based on the resolution of mixtures including the cutting agents. However, prior physical and chemical characterisation of the modified electrodes is needed before the study can be undertaken.

The electrodes were modified following the protocol described in § 5 of experimental (Figure III-6), and their characterisation was performed by SEM studies. Studies confirmed an acceptable distribution of the modifiers among the graphite flakes. EDX verified the presence of cobalt and palladium as metals in the ink.

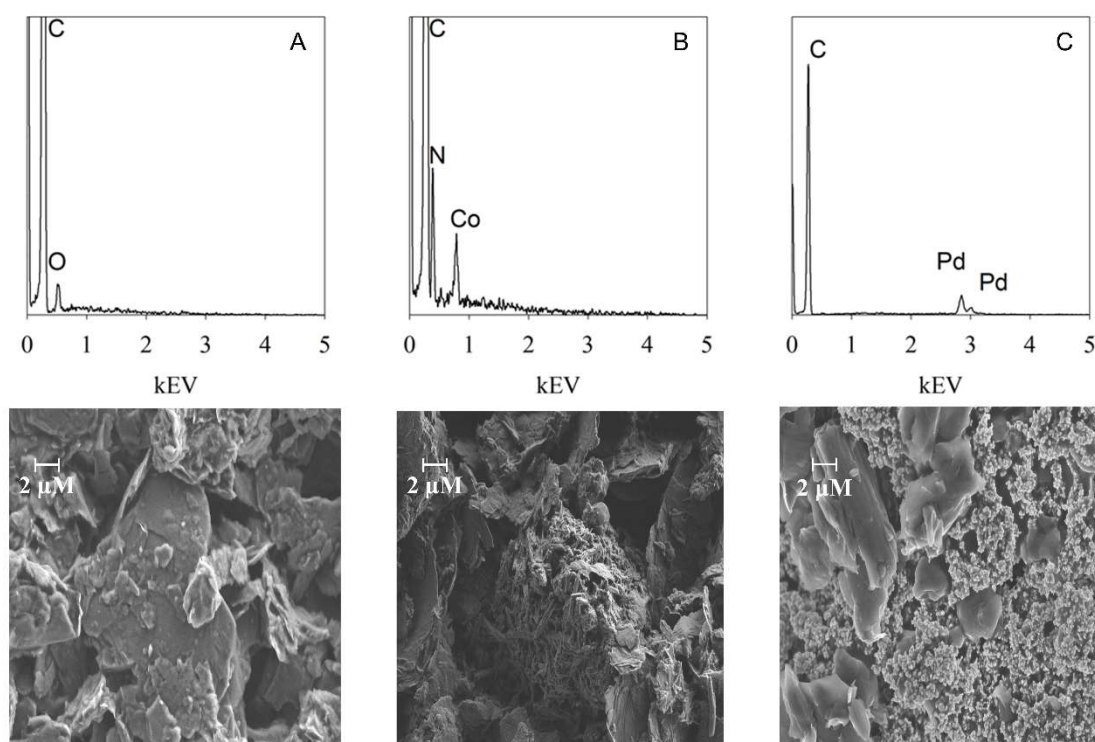


Figure IV - 20. EDX (top) and SEM (bottom) characterization of A) graphite/SPCE-Ink, B) CoPc/SPCE-Ink and C) Pd/SPCE-Ink.

The next step was the identification and evaluation of the voltammetric signals obtained from each sensor for each compound individually. SWV was used due to its fast-scanning speed and high sensitivity and compact, low-cost instrumentation^{21,22}.

Normally, in the standard working procedure, the aim is to look for different sensor response to the compound, without entering the electrochemical reaction mechanism, as this information is not relevant to carry out the chemometric treatment. However, due to the electrochemical interest of these drugs of abuse, an attempt was made to identify each peak and to superficially evaluate the reaction mechanism. All this information is shown in the following sections.

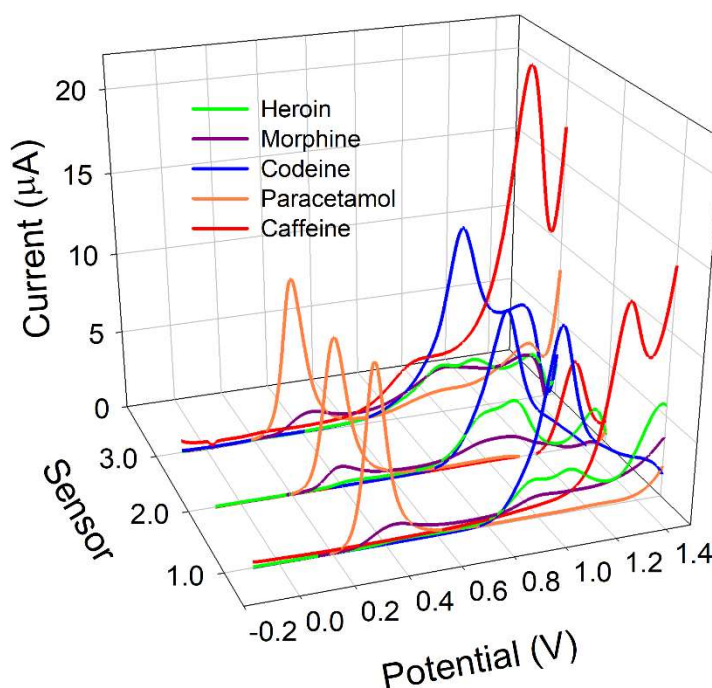


Figure IV - 21. Electrochemical fingerprint of 300 μM solutions of the five substances under study using 1) graphite, 2) CoPc and 3) Pd.

As can be seen in Figure IV - 21, different overlapped peaks can be highlighted. Regarding heroin's case, an irreversible split peak is shown at around 0.97 V, which corresponds to the oxidation of the tertiary amine group, giving rise to a secondary amine that is subsequently oxidised²³. The proposed mechanism can be observed in detail in Figure IV - 22. Furthermore, an additional smaller peak appeared at 0.40 V, which is observed more clearly in Figure IV - 27. This peak corresponds to the oxidation of the phenolic group of 6-MAM present at 3% wt/wt in the sample. This molecule is an impurity, commonly found in the synthesis of heroin, which comes from both the incomplete acetylation of morphine and the hydrolysis of heroin.

Likewise, morphine also shows an oxidation peak corresponding to the phenol group of 6-MAM at 0.40 V²⁴ but being more notable in this case. The second peak corresponds to the oxidation of the tertiary amine group, which in this case is not further oxidised.

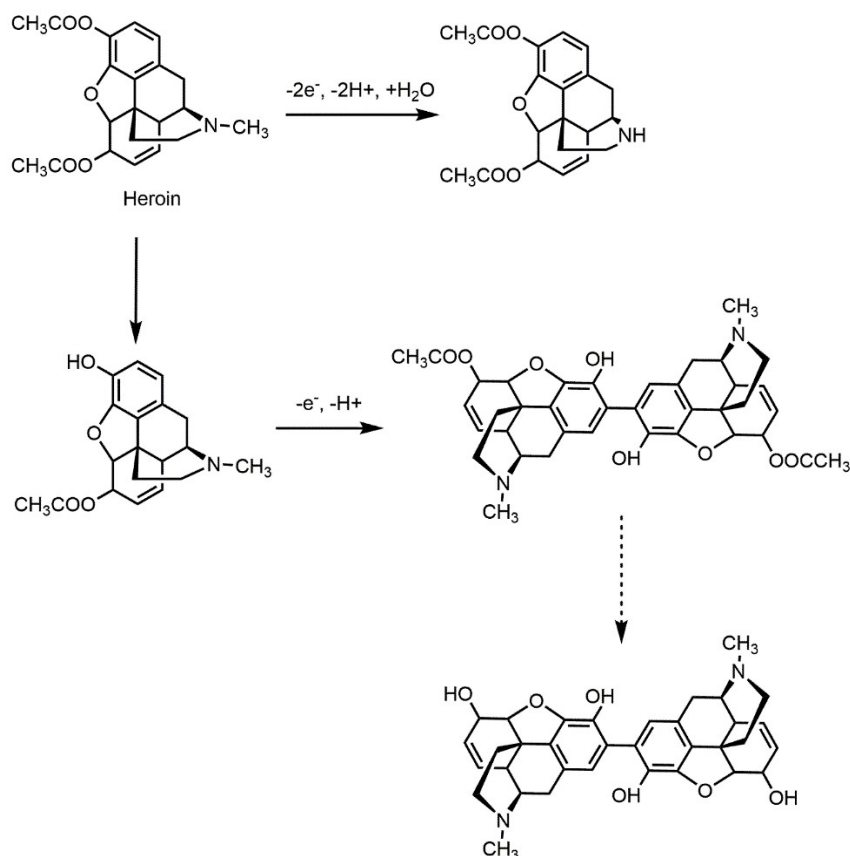


Figure IV - 22. Electrochemical oxidation mechanism of heroin proposed by Garrido,J et al.⁹.

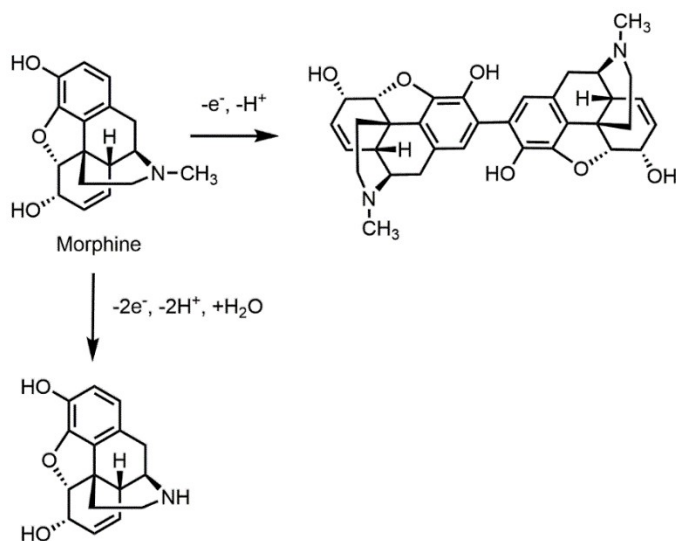


Figure IV - 23. Electrochemical oxidation mechanism of morphine proposed by Garrido,J et al.²⁴.

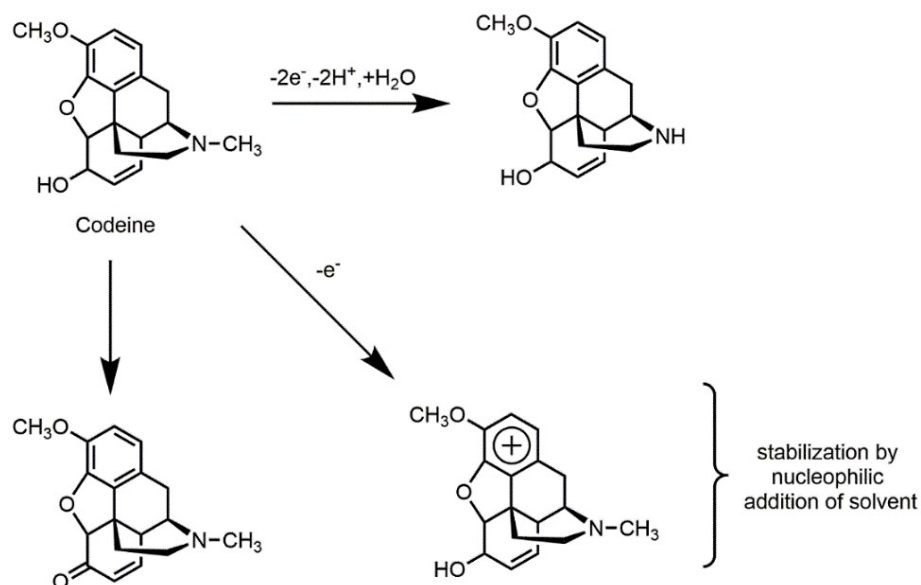


Figure IV - 24. Electrochemical oxidation mechanism of codeine proposed by Garrido, J *et al.*²⁵.

In codeine's case, one broad peak is remarked associated to the oxidation of the tertiary amine again (Figure IV - 24). If Figure IV - 21 is analysed in detail a small shoulder can be observed, which is almost superimposed and that is attributed to the oxidation of the 6-hydroxy groups²⁵. Finally, the case of the cutting agents, paracetamol, and caffeine, remains to be analysed. In the case of paracetamol, a single well-defined peak is observed at 0.40 V corresponding to the oxidation of the amide group. In the case of caffeine, there is also a single peak at 1.33 V corresponding to the oxidation of the C-8 to N-9 bond to give the substituted uric acid. Mechanisms found in the literature on the proposed electrochemical reactions are shown in Figure IV - 25 and Figure IV - 26.

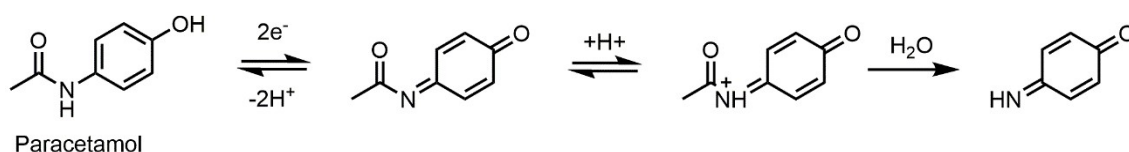


Figure IV - 25. Electrochemical oxidation mechanism of paracetamol proposed by Khairy, M *et al.*²⁶

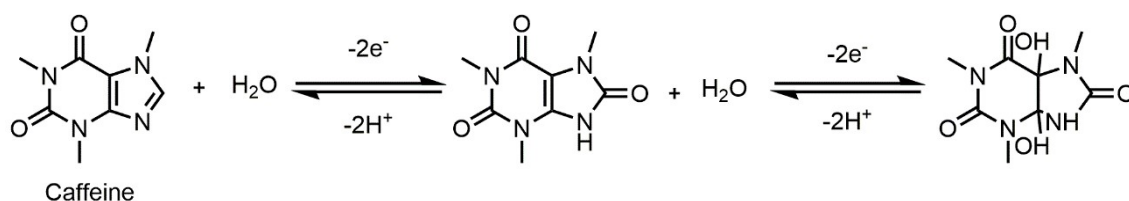


Figure IV - 26. Electrochemical oxidation mechanism of caffeine proposed by Tadesse, Y *et al.*²⁷

Therefore, the scenario is challenging as voltammograms present some overlapping peaks. For example, phenol group is overlapped with paracetamol and same situation occurs with the second oxidation peak of morphine and heroin with codeine. Nevertheless, this is not an obstacle for the study, as each analyte shows a different voltammetric profile as well as different sensitivities.

Once the general behaviour of each analyte had been evaluated, calibration curves were constructed to identify the linear range of each substance. The concentrations ranged from 25 to 750 μM . This stage of identifying the working range is very important for further construction of the model.

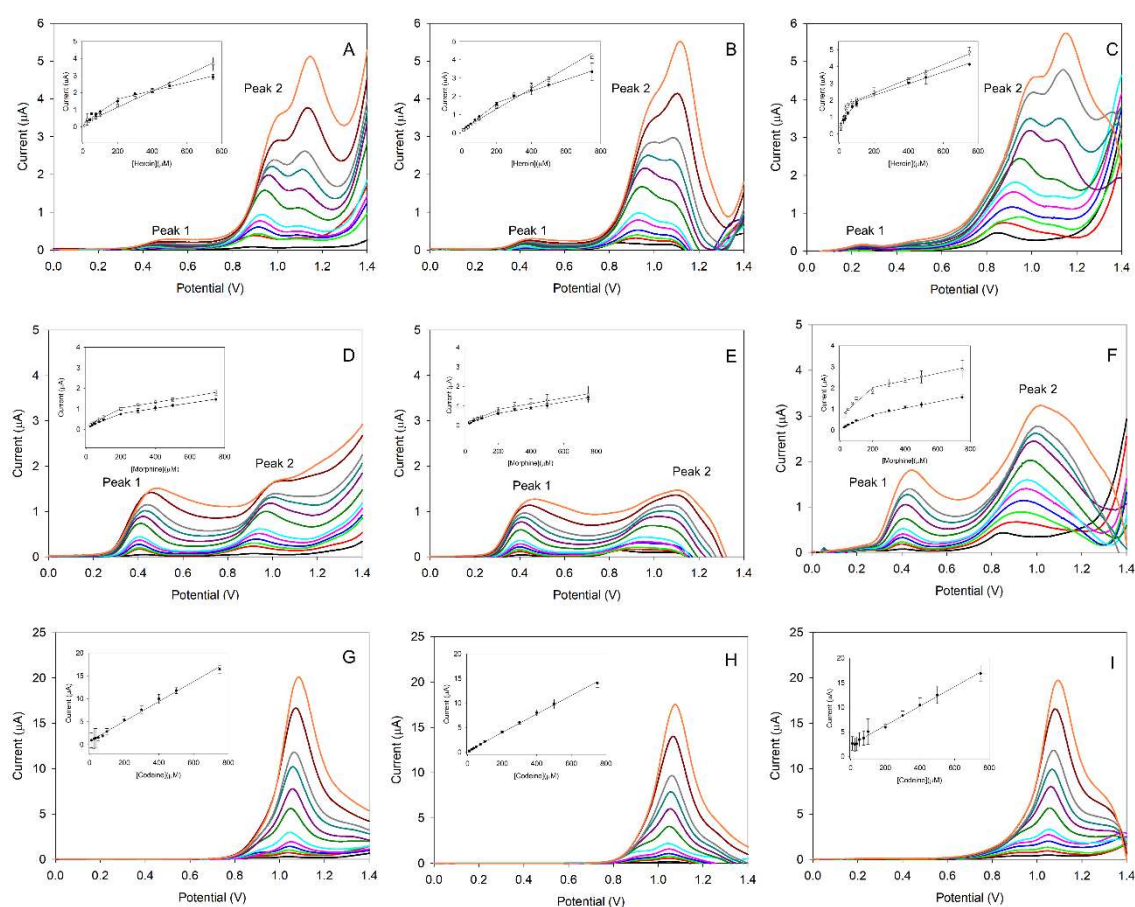


Figure IV - 27. Square wave voltammograms obtained for (A-C; top row) heroin, (D-F; middle row) morphine and (G-I; bottom row) codeine using (A, D, G; left column) graphite, (B, E, H; middle column) CoPc and (C, F, I; right column) Pd, respectively. Series of plots correspond to increasing concentrations from 10 to 1000 μM . Insets correspond to the linear regressions of peak height (at the observed potential maximum) vs. concentration, excluding the point 1000 μM as saturation of the voltammetric signal was reached for certain compounds.

Another important parameter for carrying out electrochemical measurements is the selection of the working pH.

In the present study, it was decided to work at neutral pH, because bibliographic sources^{6,7} show hydrolysis reactions of heroin and morphine at alkaline pH.

The analytical parameter chosen to examine data were the peak's height corresponding to the maximum of the oxidation response. Broadly, the responses obtained were linear for most cases with $r > 0.99$ for the ranges studied. Depending on the compound, one or two peaks were found. Calibration curves were shown in Figure IV - 27.

In heroin's case, two peaks were observed. Graphite and CoPc inks showed two linear ranges for the peak one (black), associating the oxidation of the phenol group from 6-MAM. The high range is from 200 to 750 μM , whereas the lower range is defined from 25 to 200 μM . In the case of peak two (red), only one peak is visualized from 25 to 750 μM corresponding to the oxidation of the amide group (Figure IV - 27AB). Pd behaves differently from the others, showing two linear ranges for peak 1 and peak 2 (Figure IV - 27C).

As could be expected, morphine had a similar behaviour than heroin. It can show two peaks and two linear ranges (Figure IV - 27D-F). The high came from 200 to 750 μM and low from 25 to 200 μM .

Paracetamol and codeine showed an individual peak over all the range (25 to 750 μM) (Figure IV - 27G-I and Figure IV - 28J-L). In the case of caffeine, single peak is obtained with different linear range depending on the modified electrode. Graphite and CoPc came from 50 to 750 μM , meanwhile Pd the linear range is narrow from 200 to 750 μM .

Finally, it can be concluded that the linear working range determined comes from 0 to 750 μM for heroin, morphine, codeine, paracetamol, and caffeine. All analytical parameters from the calibration curves are listed in Table IV - 10.

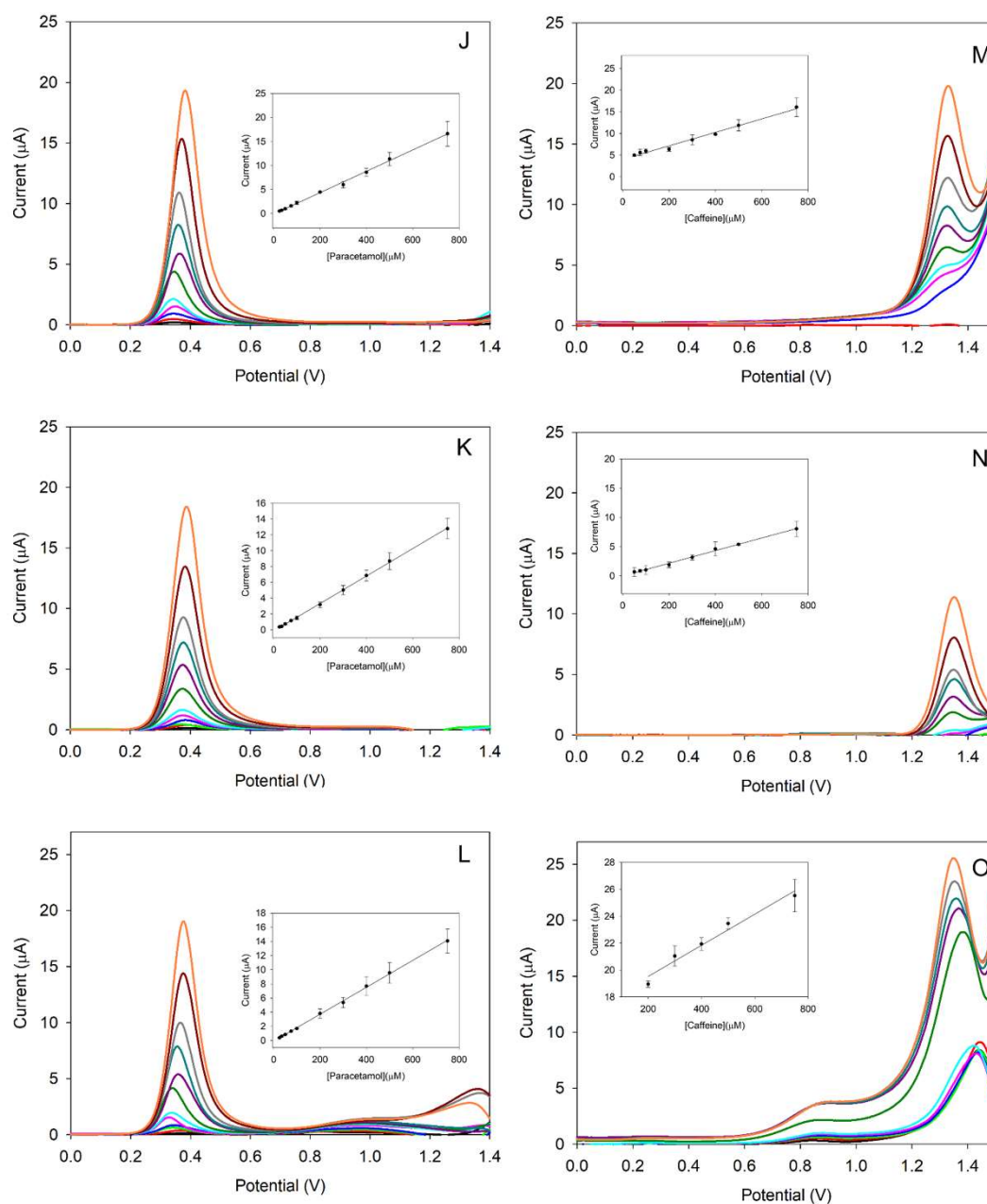


Figure IV - 28. Square wave voltammograms obtained for (J-L; left column) paracetamol and (M-O; right column) caffeine using (J, M; top row) graphite, (K, N; middle row) CoPc and (L, O; bottom row) Pd modified sensors, respectively. Series of plots correspond to increasing concentrations from 10 to 1000 μM . Insets correspond to the linear regressions of peak height vs. concentration, excluding the point 1000 μM as saturation of the voltametric signal was reached for certain compounds.

RESULTS AND DISCUSSION

Table IV - 10. Calibration data (y vs. x) for the separate determination of heroin, morphine, codeine, paracetamol, and caffeine employing the sensor array proposed.

Sensor 1: Carbon						
Compound	Potential (V)	Sensitivity (nA· μ M ⁻¹)	Intercept (μ M)	r	LOD (μ M)	Linear Range (μ M)
Heroin	0.49	6.1	0.28	0.986	3.33	25-200
		2.5	1.13	0.985		200-750
	1.16	4.7	0.21	0.997	31.8	25-750
Morphine	0.43	3.3	0.10	0.996	5.33	25-200
		1.3	0.51	0.997		200-750
	0.99	4.2	0.16	0.995	8.65	25-200
		1.4	0.76	0.994		200-750
Codeine	1.11	21.7	0.72	0.998	1.80	25-750
Paracetamol	0.39	22.3	0.12	0.999	0.82	25-750
Caffeine	1.33	15.6	4.02	0.993	44.0	50-750
Sensor 2: CoPc						
Compound	Potential (V)	Sensitivity (nA· μ M ⁻¹)	Intercept (μ M)	r	LOD (μ M)	Linear Range (μ M)
Heroin	0.43	7.2	0.15	0.999	3.95	25-200
		3.1	1.03	0.996		200-750
	1.14	5.5	0.22	0.994	83.3	25-750
Morphine	0.40	2.8	0.0709	0.994	2.88	25-200
		1.5	0.32	0.995		200-750
	1.11	3.4	0.11	0.994	96.6	25-200
		1.5	0.53	0.994		200-750
Codeine	1.09	18.9	0.21	0.999	4.29	25-750
Paracetamol	0.40	17.4	-0.16	0.999	0.75	25-750
Caffeine	1.36	10.8	0.0069	0.998	65.0	50-750

Sensor 3: Pd						
Compound	Potential (V)	Sensitivity (nA·μM ⁻¹)	Intercept (μM)	r	LOD (μM)	Linear Range (μM)
Heroin	0.27	14.3	0.41	0.988	5.31	25-200
		3.5	1.59	0.991		200-750
	1.01	34.8	0.12	0.975	14.8	25-200
		4.2	1.57	0.966		200-750
Morphine	0.46	3.2	0.0858	0.985	25.9	25-200
		1.5	0.44	0.993		200-750
	1.01	6.9	0.62	0.954	60.7	25-200
		1.7	1.68	0.961		200-750
Codeine	1.11	19.8	2.31	0.997	11.7	25-750
Paracetamol	0.38	19.0	-0.11	0.999	3.33	25-750
Caffeine	1.35	11.6	17.2	0.983	104	200-750

3. Repeatability and Reproducibility Studies

Once the characterization stage was completed, a stability study was performed to assess the number of measurements supported by the working electrodes. The variation of the voltammetric response was carried out by measuring a codeine standard solution of 450 μM concentration for 25 consecutive times. The measurements were carried out with the same electrodes and exchanging a measurement of the blank (PBS) between each measurement to check the repeatability of the devices. Therefore, each sensor was subjected to 50 consecutive measurements, a very meaningful number given the disposable nature of the screen-printed electrodes. All measurements made in the experiment are shown in Figure IV - 29.

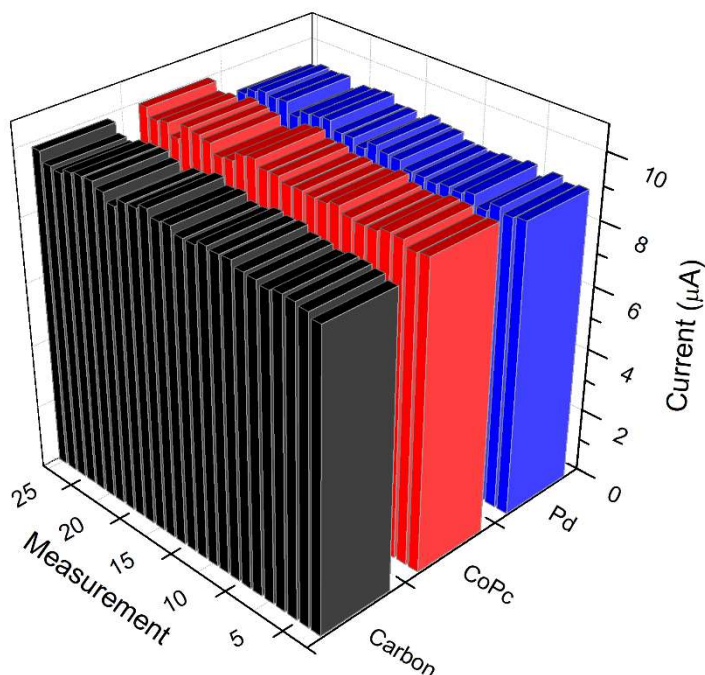


Figure IV - 29. Evaluation of the stability studied for the three modified screen-printed sensors. A total of 25 measurements were performed inserting a black solution of PBS between each measure. A stock solution of 450 μM was used. The RSD (%) for Carbon, CoPc and Pd was 1.84%, 2.01% and 2.14%, respectively.

Once the experimental part was finished, the results obtained through the calculation of the RSD (%) were evaluated. The values obtained for the present modified sensors were 1.84% (graphite), 2.01% (CoPc) and 2.14% (Pd). No fouling or drift effects were observed with the proposed sensors during the study. Therefore, it can be concluded that any possible adsorption of the oxidized form of the studied analytes did not considerably affect the stability of the sensors, as no differences were observed throughout the measurements. The same fact can be associated with the applied potentials, if there is any doubt about the high value used.

To complete the study, the reproducibility of the construction of the ink-modified printed sensors was also evaluated. The experiment was performed by preparing each modified ink by triplicate and measuring consecutively with a heroin stock solution. The results for each sensor show good construction reproducibility with RSD (%) values of 3.97%, 6.95% and 5.67% for carbon, CoPc and Pd inks, respectively.

4. Quantitative Analysis of Drug Mixtures using Partial Least Squares Regression

So far, voltammetric responses of the studied analytes have been analysed individually showing differences in their voltammetric profiles depending on the specific sensor used. However, the aim of this study is to quantify mixtures of the compounds. Therefore, it is evident that an overlapping of signals will be observed, which can be seen in Figure IV - 30 and Figure IV - 31.

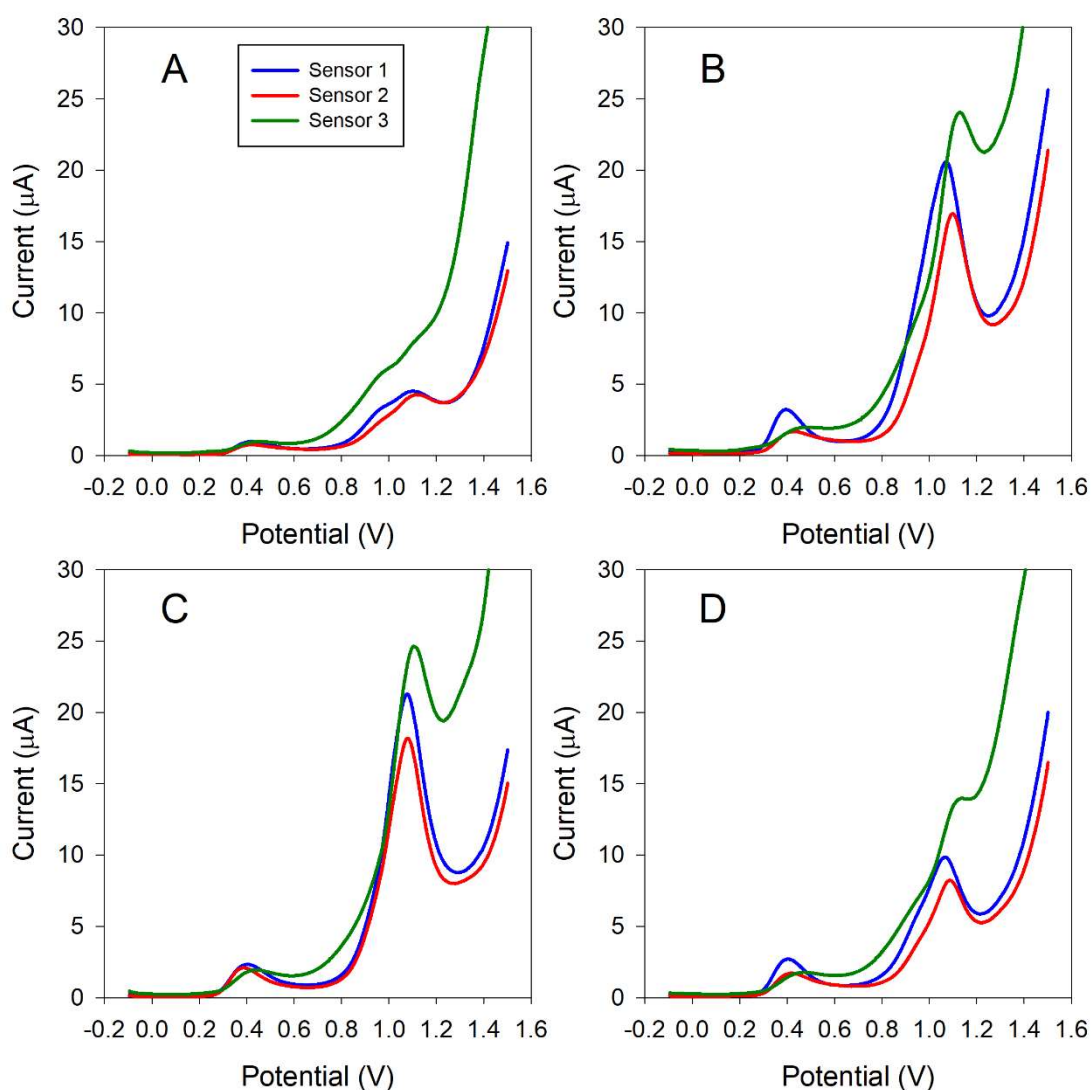


Figure IV - 30. Example of the voltammograms obtained for certain arbitrary mixtures of heroin, morphine, and codeine with concentrations for the three compounds of (A) 560 μM , 239 μM , 28 μM , (B) 627 μM , 577 μM , 435 μM , (C) 180 μM , 617 μM , 626 μM and (D) 156 μM , 531 μM , 156 μM . The samples were prepared in PBS pH 7. The three colours represent the sensor array: Graphite/SPCE-Ink (blue), Cobalt (II) phthalocyanine/SPCE-Ink (red) and Palladium/SPCE-Ink (green).

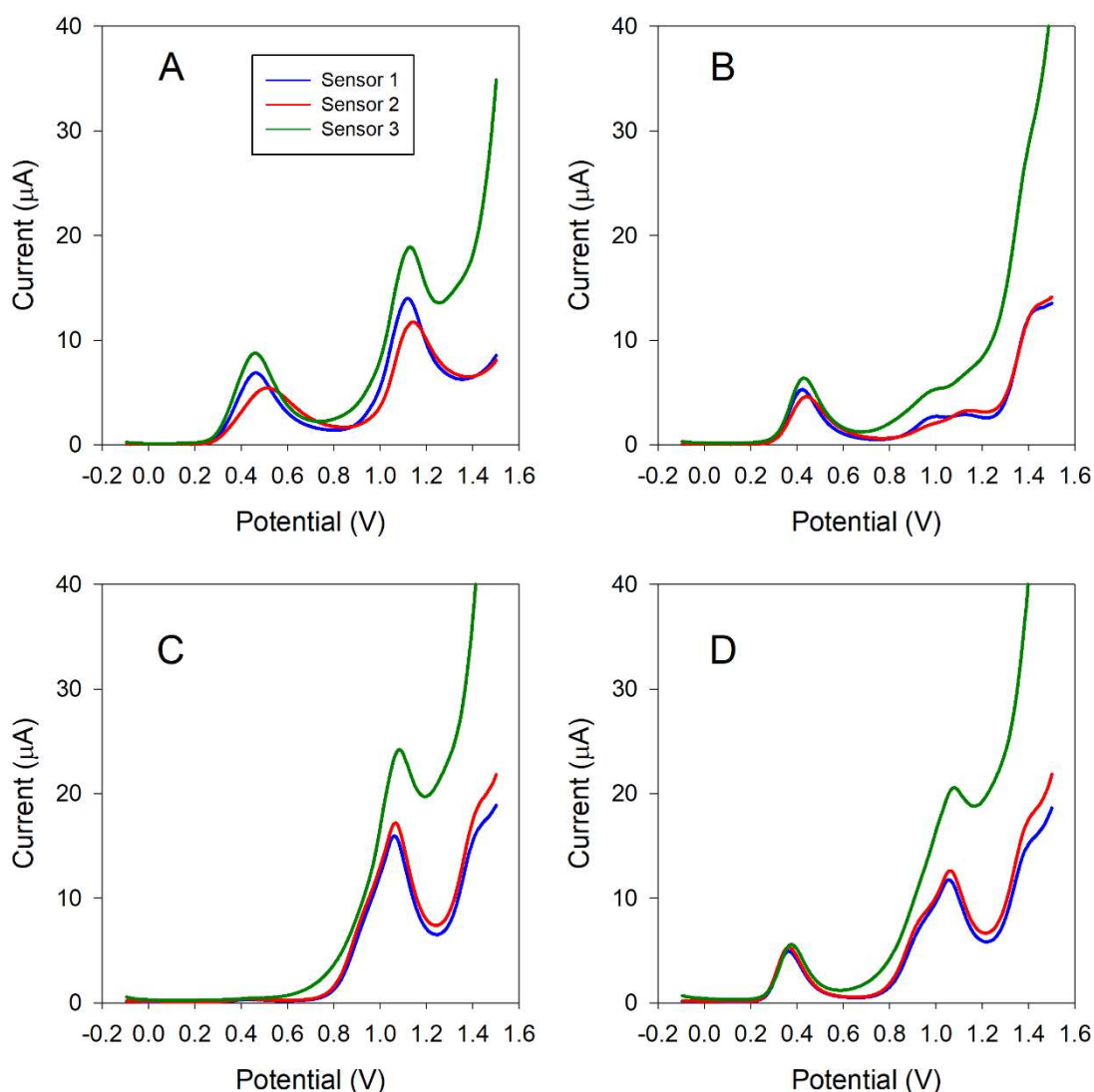


Figure IV - 31. Example of the voltammograms obtained for certain arbitrary mixtures of heroin, morphine, codeine, paracetamol, and caffeine with concentrations for the five compounds of. (A) 0 μM , 623 μM , 623 μM , 623 μM , 0 μM (B) 623 μM , 0 μM , 0 μM , 623 μM , 623 μM , (C) 623 μM , 0 μM , 623 μM , 0 μM , 623 μM and (D) 438 μM , 82 μM , 384 μM , 384 μM , 493 μM . The samples were prepared in PBS pH 7. The three colours represent the sensor array: Graphite/SPCE-Ink (blue), Cobalt (II) phthalocyanine/SPCE-Ink (red) and Palladium/SPCE-Ink (green).

Therefore, to accomplish the single quantification of each compound, the application of chemometric methods is needed, due to the fact that quantification cannot be performed by univariate regression (peak height or peak area).

In this sense, the ET strategy is based on the combination of an array of electrodes that show complementary responses to the substances of interest, with a multivariate calibration method that enables the construction of a model that associates the different sensors' response to the concentration of each analyte^{28,29}.

Next further step before building the quantitative model is the selection of the best chemometric tool. The model enables the identification and subsequently quantification of the individual compounds from the overlapped voltammograms.

As mentioned in previous sections of this doctoral thesis, the reported works are involved in the **Bordersens** project, which has as a final aim, the development of a device capable of detect different illicit drugs. To achieve this goal, the simplest instrumentation and modelling tools must be selected. For this reason, PLS1 was selected as a modelling tool to attain multivariate calibration, due to its simplicity in comparison with other techniques such as ANNs³⁰. As it well known in the literature²⁹, PLS does not require a pre-processing reduction step based on number of input variables. However, the use of it gives an improvement in terms of generalization ability and model's prediction. Once again, GAs was used as feature selection tool to simplify the model. This approach allows the identification of the most relevant feature selection, simplifying the calculation and no further computer processing shall be required for each new measurement taken. As summary, the relevant features were selected with GAs and then they were used as input into the PLS model.

The results of the GAs optimisation are shown in Figure IV - 32, where the raw voltammetric responses for 300 μM solutions of each of the compounds considered are plotted, with cross marks underneath corresponding to the selected features.

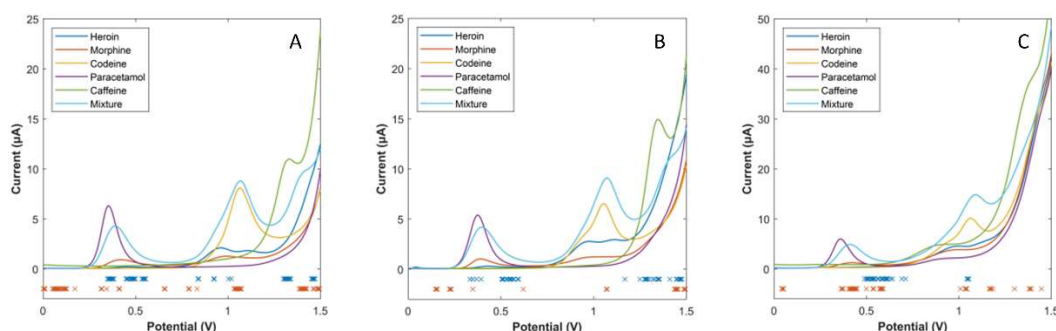


Figure IV - 32. Outcome of the feature selection step using GAs. Square wave voltammograms obtained using (A) graphite, (B) CoPc and (C) Pd sensor for pure solutions of the different compounds under study at 300 μM as well as for an arbitrary mixture of those are plotted, and underneath the features selected for the mixtures of the (x) 3 compounds and (x) 5 compounds.

As it can be observed in Figure IV - 32, the algorithm not only select the points corresponding to the maximum of the peaks but rather the points where less overlapping is observed. Concretely, points in back and front of the peak.

Specifically, two different sets of samples were prepared as already indicated in the experimental section. The first is based on ternary mixtures of the drugs considered, while the second set also considered the presence of two different cutting agents. The goal of the first set was to confirm the capability of the chosen ET to perform individual quantification, while the second set aims to confirm that the ET is even able to counterbalance the interferences of the cutting agents and successfully perform quantification.

In both situations, the coupling GA-PLS was employed to construct the model using the data from the training subset, and their performance was evaluated with respect to the samples from the test subset by selecting the number of LVs leading to the lowest RMSE value for the latter.

4.1. Three Drugs' Mixtures

From the raw data, 318 current values for three sensors were obtained. A total of 103 features were selected by using GA and PLS1 to construct the model. The optimized value of LVs for the different compounds were 7 for heroin, 8 for morphine and 15 for codeine. Then, predicted vs. expected comparison graphs were built (Figure IV - 33) with the corresponding linear regression of the comparison lines fitted (Table IV - 11) for the three drugs.

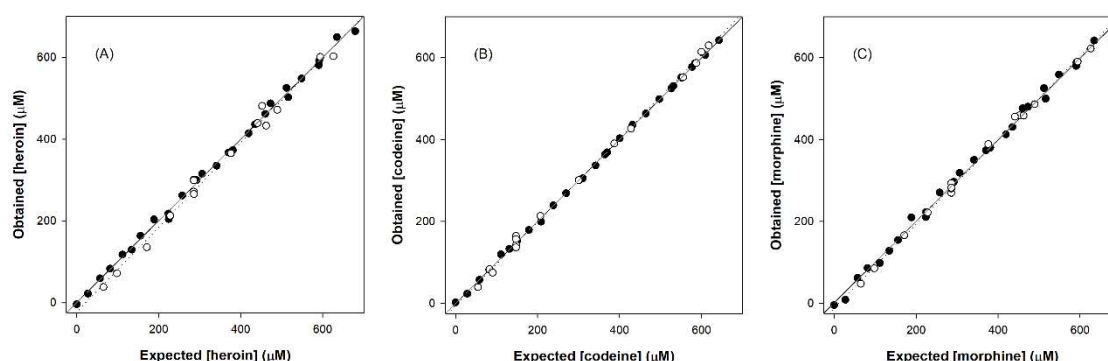


Figure IV - 33. Modelling ability of the optimized GA-PLS model for the 3 compounds case. Comparison graphs of obtained vs. expected concentrations for (A) heroin, (B) morphine and (C) codeine, for both the train (\bullet , solid line) and test subsets (\circ , dotted line). The dashed line corresponds to the ideal comparison line ($y = x$).

Table IV - 11. Fitted regression lines for the comparison between obtained vs. expected values for the different sets of samples and the three considered drugs.

Compound	Slope	Intercept (μM)	r	RMSE (μM)	NRMSE	Total NRMSE
train subset (n=27)						
Heroin	0.998 \pm 0.019	0.7 \pm 7.5	0.999	9.39	0.014	
Morphine	1.000 \pm 0.007	0.1 \pm 2.7	1.000	3.35	0.005	0.014
Codeine	0.996 \pm 0.026	1.3 \pm 10.0	0.998	12.5	0.019	
test subset (n=15)						
Heroin	1.035 \pm 0.064	-22.5 \pm 24.3	0.995	20.6	0.030	
Morphine	1.020 \pm 0.026	-5.1 \pm 9.4	0.999	10.1	0.016	0.026
Codeine	1.026 \pm 0.030	-11.3 \pm 11.5	0.999	11.1	0.016	

Intervals are calculated at the 95% confidence level. RMSE: root mean square error; NRMSE: normalized root mean square error.

As can be observed in Figure IV - 33, satisfactory results were obtained showing regression lines close to the ideal one ($y=x$) in all the cases. What is more, results provided by Table IV - 11 showed values of slope and correlation coefficient of one, and intercept value of zero, values very close to the ideal ones, all of them being within the intervals calculated at the 95% confidence level. The information about the joint confidence intervals is showed in Figure IV - 34, which clearly demonstrate that the obtained values are within the expected behaviour.

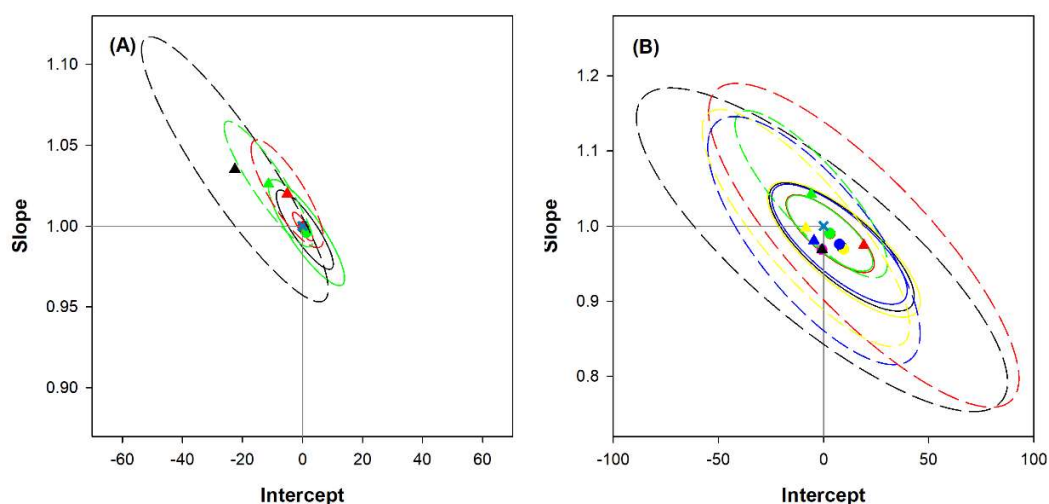


Figure IV - 34. Joint confidence intervals for (A) the three drugs, and (B) the three drugs and the two cutting agents: (black) heroin, (red) codeine, and (green) morphine, (yellow) paracetamol and (blue) caffeine, both for the training (●, solid line) and testing (▲, dashed line) subsets. Also, the ideal point (1,0) is plotted (x); intervals are calculated at the 95% confidence level.

Although the trend is satisfactory, it should be noted that a slightly higher performance is obtained for the train subset, because the data from the test subset is not used during the modelling phase, thus providing a realistic metric of the model's performance. However, if the RMSE values obtained for both subsets are compared, it can be noticed how the differences are not actually that high, confirming the ability of the proposed ET to achieve simultaneous quantification of all three drugs and the goodness of the model. Hence, the following step was to confirm whether using the same approach it is able not only to quantify the mixtures of the pure drugs, but also to quantify and to detect the considered cutting agents, which would provide a more realistic scenario of the proposed strategy.

4.2. Three Drugs and the Two Cutting Agents' Mixtures

In this section, the same conditions as above were used only changing the experimental design due to the larger number of substances that needed to be in consideration. For that, a new set of samples was prepared and measured using the optimized array.

As the previous situations, the construction of GA-PLS models were used to quantify the concentration of each of the substances present in the mixtures. In this case, 114 feature from the raw data were selected (Figure IV - 32). The optimized LVs were 13 for heroin, 10 for morphine and 18 for codeine, 12 for caffeine and 6 for paracetamol.

Again, comparison plots of predicted versus expected concentrations were constructed for each of the substances (Figure IV - 35), and linear regression parameters were calculated (Table IV - 12). As in the previous case, an acceptable trend is observed for both subsets, having a better behaviour for the train subset as mentioned above, but with RMSE values comparable in terms of magnitude.

It should be noted that the performance of the model metrics are slightly worse for the five compounds case than for the three compounds case (total NRMSE for the three drugs of 0.084 versus 0.026 for the test subset), but the higher complexity of the case has to be taken into account.

That is, on the one hand, the use of a fractional experimental design to keep the number of samples needed to build the model reasonable. On the other hand, as already reported, the scope of certain cutting agents can affect the voltammetric response, to the extent that the voltammetric peak observed for the pure analyte may not be seen in the presence of the adulterant^{31,32}.

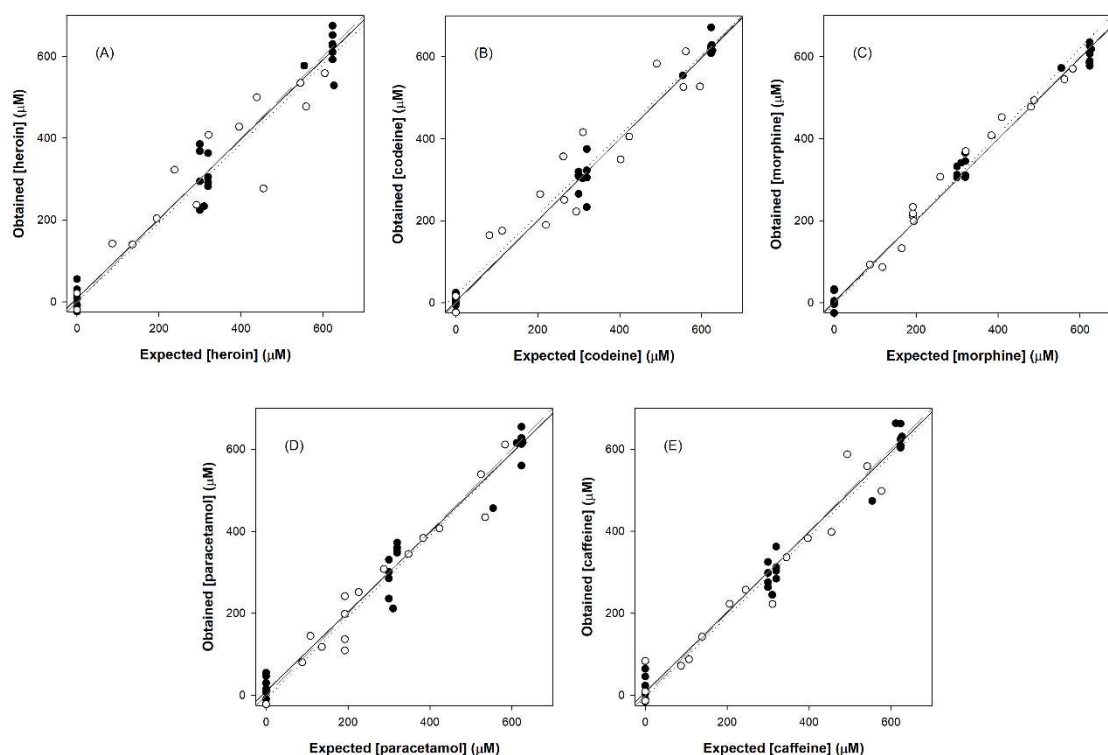


Figure IV - 35. Modelling ability of the optimized GA-PLS model for the 5 Compounds case. Comparison graphs of obtained vs. expected concentrations for (A) heroin, (B) morphine, (C) codeine, (D) paracetamol and (E) caffeine, for both the train (●, solid line) and test subsets (○, dotted line). The dashed line corresponds to the ideal comparison line ($y = x$).

Regarding the latter, this works demonstrates that with the use of an appropriate set of samples, the model can correctly quantify both drugs and cutting agents. In parallel, the same approach can be applied to the identification and quantification of other mixtures. Furthermore, multi-way processing methods allow the correction of interfering species not initially considered in the response model instead of PLS models. This gain can be done thanks to their “second order advantage”^{33,34}.

RESULTS AND DISCUSSION

Hence, considering all the points, results show the power of the proposed approach with the use of a voltammetric ET to identify and subsequently quantify seized drug samples, either in its pure form or mixed with other drugs or cutting agent.

Table IV - 12. Fitted regression lines for the comparison between obtained vs. expected values for the different sets of samples and the five considered compounds.

Compound	Slope	Intercept (μM)	r	RMSE (μM)	NRMSE	Total NRMSE
train subset (n=27)						
Heroin	0.972 \pm 0.068	8.7 \pm 27.3	0.986	43.5	0.061	
Morphine	0.990 \pm 0.041	3.1 \pm 16.6	0.995	26.2	0.037	
Codeine	0.990 \pm 0.040	3.0 \pm 16.2	0.995	25.5	0.036	0.053
Paracetamol	0.969 \pm 0.071	9.7 \pm 28.8	0.984	45.9	0.065	
Caffeine	0.976 \pm 0.063	7.5 \pm 25.5	0.987	40.6	0.057	
test subset (n=17)						
Heroin	0.968 \pm 0.169	-0.7 \pm 69.3	0.953	76.3	0.107	
Morphine	0.974 \pm 0.169	19.2 \pm 58.0	0.954	63.3	0.089	
Codeine	1.042 \pm 0.087	-5.9 \pm 28.5	0.989	30.1	0.043	0.077
Paracetamol	0.997 \pm 0.124	-8.4 \pm 38.8	0.975	41.8	0.059	
Caffeine	0.981 \pm 0.130	-4.5 \pm 39.7	0.972	50.1	0.070	

Intervals are calculated at the 95% confidence level. RMSE: root mean square error; NRMSE: normalized root mean square error

Finally, it was proceeded to assess whether the proposed model was over-fitted or not, highlighting that it has taken the precaution to use a separate validation data subset (test subset). To do so, a permutation test or “target shuffling process” was used to demonstrate that neither the high dimensionality of the data nor the coupling GAs-PLS1 were leading to overfitted models. The mentioned test permits the identification of incorrectly perceived cause and effect relationships in modelling, term which is called “chance correlation”. The process is done considering as null hypothesis that samples labels are exchangeable.

In short, this test involves randomly reordering and repeatedly of the response variables (Y), continued by the construction of a new model by shuffling the labels of the data. This means that a new model is constructed from the assignment of an "incorrect" Y-value to each sample corresponding to that of another sample.

This procedure is repeated many times to ensure that the calculated statistics are significant, in our case up to 1000 times. For each of the permutations, the different performance metrics were calculated and compared to the real model with the appropriate labels. The results obtained for this test are shown in Figure IV - 36, where the RMSE values for the different models for the three drugs plus paracetamol and caffeine are observed. The results clearly show that the model is not overtrained.

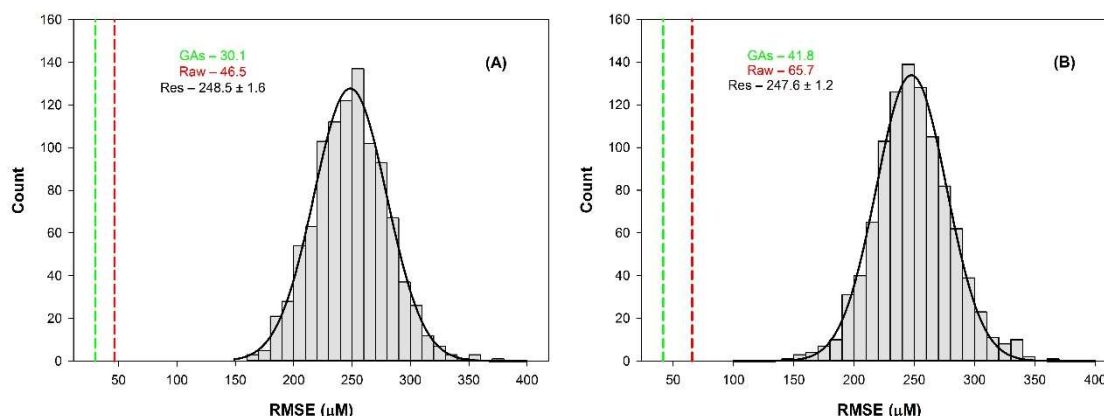


Figure IV - 36. Histogram comparing the success of PLS1 models with raw data (red) and GAs-PLS1 (green) to that of shuffled models (1000 iterations) for (A) codeine and (B) paracetamol, for the set of samples corresponding to mixtures of the 5 compounds. For the shuffled models, the data was fitted to a 3 parameter Gaussian curve and the RMSE values compared to the former.

As summary, this work reports a quantitative application for the detection of heroin, morphine, and codeine in the presence of paracetamol and caffeine simultaneously. The fusion between chemometric tools (GAs-PLS1) and voltammetry allows its resolution and quantification, verifying the non-overfitting of the proposed model by “target shuffling process”. This work has made great progress for the **Bordersens** project.

ARTICLE 4

Novel Integrated Inkjet Sensor Array for Detecting Simultaneously Some Adulterants Present in Drug of Abuse Field using Chemometrics

Dionisia Ortiz-Aguayo, Xavier Cetó, Gemma Gabriel and Manel del Valle

Sensors and Actuators B: Chemical, submitted

1. Outline

The last work of this dissertation is based on the use of a novel sensor array platform printed by inkjet printing technique. The goal in this case is the detection of three common adulterants found in cocaine seized samples, which are benzocaine, paracetamol, and phenacetin. In this case, the modification of the surface was done using previous knowledge acquired during the other works (**article 1,2 and 3**). In the reported case, CNT, CoPc, CuO, graphite and Pd was chosen as modifiers to incorporate in the ink. SWV was chosen as voltammetric technique. Since overlapping peaks needed chemometric tools to separate them, DWT was used as compression step, followed by ANNs, commonly used in the group to build the model. The results were promising showing their resolution and quantification of the analytes under study. This work was done in collaboration with the Instituto de Microelectrónica de Barcelona (IMB-CNM, CSIC), specifically with the *Centro de Investigación Biomédica en Red, Biomateriales y Nanomedicina* (CIBER-BBN).

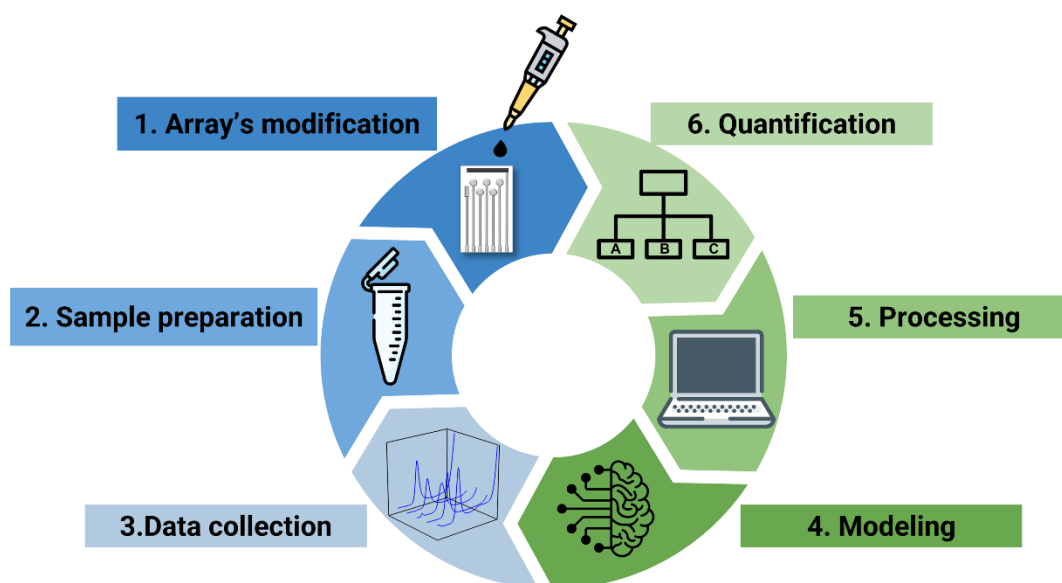


Figure IV - 37. Experimental set up of all the steps involved in the analysis. From array's modification to quantification of the desired substances.

2. Electrochemical Characterization

2.1. Effective Area Calculation

To compare the advantages of modify the surface of IPE in terms of effective area, an study with different scan rates were done following the Randles–Sevcik equation, where n is the number of transferred electrons for the redox reaction (in this case 1), F is the Faraday's constant ($96485 \text{ C}\cdot\text{mol}^{-1}$), c the concentration of electroactive substance ($\text{mol}\cdot\text{cm}^{-3}$), A is the effective area in cm^2 , v the scan rate ($\text{V}\cdot\text{s}^{-1}$), R the gas constant ($8.314 \text{ J}\cdot\text{mol}^{-1}\cdot\text{K}^{-1}$), T the temperature in K and D is the diffusion coefficient for ferrocyanide ($6.32\cdot 10^{-6} \text{ cm}^2\cdot\text{s}^{-1}$). For that, cyclic voltammetry experiments using 50 mM phosphate buffer and 0.1 M KCl containing 5 mM $[\text{Fe}(\text{CN})_6]^{3-}/[\text{Fe}(\text{CN})_6]^{4-}$ solution in the potential range of -0.4 to 0.8 V were performed. Applying 7 different scan rates (0.01, 0.025, 0.05, 0.1, 0.2, 0.3 and 0.5 $\text{V}\cdot\text{s}^{-1}$) it could be calculated the active area of each WE from the slope of the regression line of $v^{1/2}$ ($\text{V}\cdot\text{s}^{-1}$) vs. $I_p\cdot c^{-1}$ ($\text{A}\cdot\text{cm}^3\cdot\text{mol}^{-1}$). One example dealing with the details of the performed voltammograms can be found in Figure IV - 38. Concerning the calculated active areas, these were: 2.9 mm^2 for the bare electrode, 8.2 mm^2 for Graphite/IPE-Ink, 3.3 mm^2 for CNT/IPE-Ink, 3.2 mm^2 for CoPc/IPE-Ink, 3.9 mm^2 for CuO/IPE-Ink and 2.9 mm^2 for Pd/IPE-Ink, whereas the geometric area was 0.8 mm^2 ($\varnothing=1 \text{ mm}$).

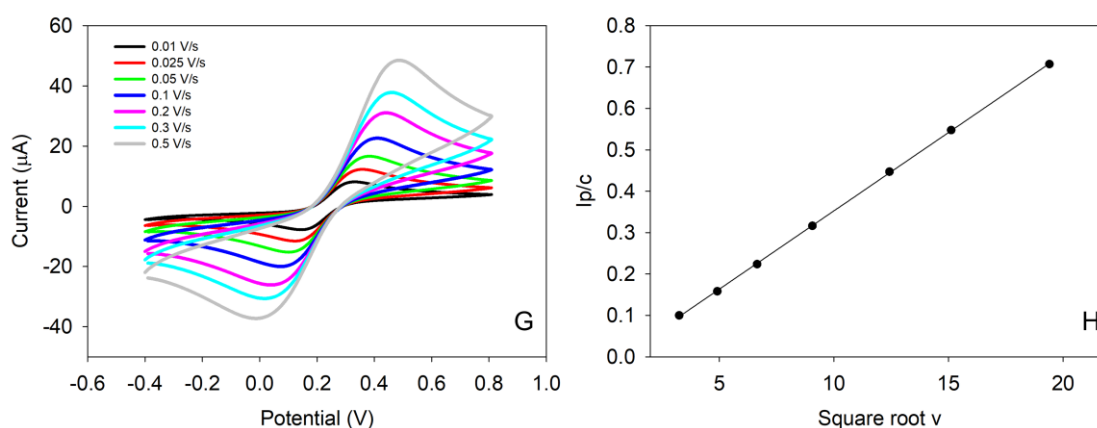


Figure IV - 38. G) Cyclic voltammetry of 5 mM $\text{K}_3\text{Fe}(\text{CN})_6/\text{K}_4\text{Fe}(\text{CN})_6$ redox couple in 0.1 M KCl varying scan rate from 0.01 V/s to 0.5 V/s using CuO/IPE-Ink. The range potential was from -0.4 V to 0.4 V with a step potential of 0.005 V. (H) Regression line of $v^{1/2}$ ($\text{V}\cdot\text{s}^{-1}$) vs. $I_p\cdot c^{-1}$ ($\text{A}\cdot\text{mol}^{-1}\cdot\text{cm}^3$).

Summarizing, the results show a significant increase of the effective area responsible of the application of the modified ink on the surface of the electrode. The most remarkable case is shown in the case of CuO-ink, giving an increase of almost four times compared to the geometric area of the sensor. Also, it is interesting to evaluate the improvement of our material in comparison with the bare surface. In the case of our ink of reference, which is carbon, a notable increment of area is done, demonstrating the suitable use of our material in the modification of the IPE surface.

3. Evaluation of the Linear Response

In the proposed work, there is a problem of similarities in the fingerprint of benzocaine and phenacetin, key point which make them attractive to analyse in the case of study. Chemometrics helps to us to separate them, but it is needed slightly different responses between sensors to discriminate them. One solution that we propose is the modification of the electrodes with the use of a composite material which contains different modifiers. With this proposal, it is quick simple to obtain new suitable surfaces for electrochemical detection methods. What it is more, an optimized way to create new chemically modified transducer is developed gaining advantages such as simplicity and low-cost approach. Many works in the group reported the benefits given by these self-formulated carbon inks^{20,35,36}. For many previous works in studies with ETs^{37,38}, remarkable results were obtained with the use of phthalocyanines, metal nanoparticles, metal oxides, and a current material very commonly used nowadays such as carbon nanotubes. All of them were considered good candidates as modifiers in the case of study. For this reason, the fifth proposed sensor array in the current work was composed by CoPc, CuO, Pd and CNT. It is decided also include a carbon ink formulation, as control, to compare with the positive aspects given by the rest of modifiers.

Once the array was defined, the evaluation of the square wave voltammograms responses of each the modified towards the different compounds individually was done to observed differentiated signals generated by them.

As can be observed in Figure IV - 39, two overlapping peaks can be remarked corresponding to the oxidation of amines presents in the skeleton of benzocaine and phenacetin. In the case of benzocaine, an irreversible oxidation peak is shown around 0.9 V, corresponding to the oxidation of the primary aniline group to a secondary amine. In the redox reaction, two electrons and two protons are released. Similarly, phenacetin also shows the oxidation peak ca. 0.9 V. Finally, in the case of paracetamol, only a well-defined Gaussian peak corresponding to the oxidation of the amide group is observed ca. 0.40 V.

After analysing this first general overview of the square wave responses, the calibration curves for the three adulterants were constructed by performing measurements from 10 to 750 μM in the case of phenacetin and paracetamol for all the modified IPEs. However, the concentration range is narrower in the case of benzocaine because of its saturation problems. For graphite and CoPc, the linear range was from 10 to 200 μM , for CNT and CuO from 10 to 300 μM and for Pd from 10 to 400 μM (Figure IV - 40). Analytical parameters of the calibration curves for each sensor are presented in Table IV - 13.

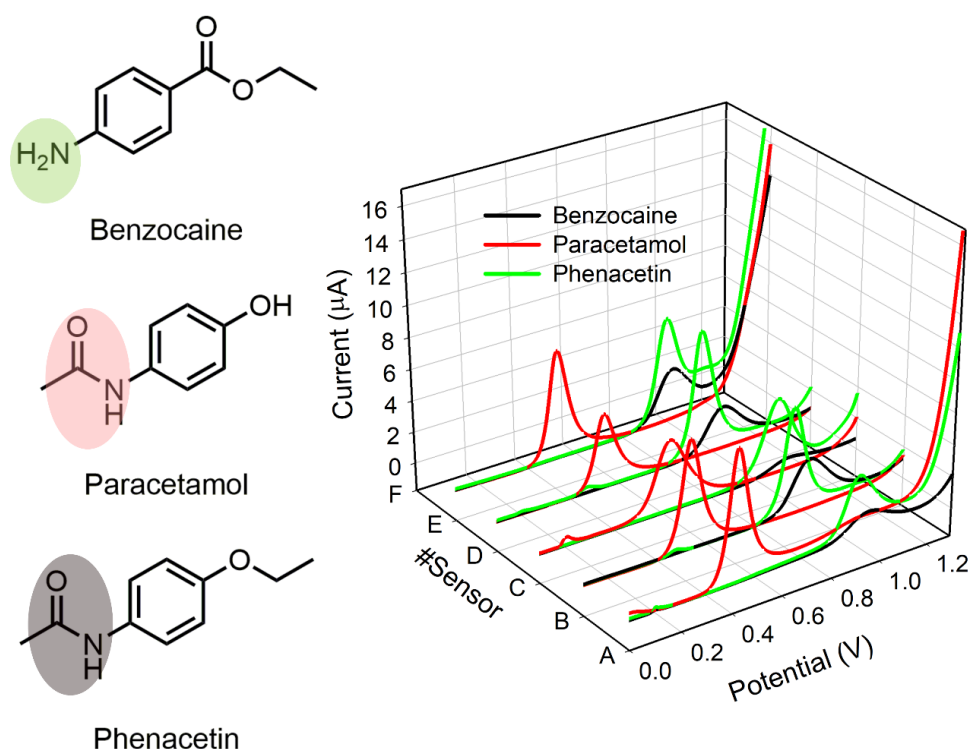


Figure IV - 39. On the right side: electrochemical fingerprint of 200 μM corresponding to the three substances under studied (benzocaine, paracetamol, and phenacetin) using the fifth sensor array selected: A) Graphite, B) CNT, C) CoPc, D) CuO and E) Pd. On the left side:

the skeleton of the adulterant studied remarking the oxidable functional group of the molecule.

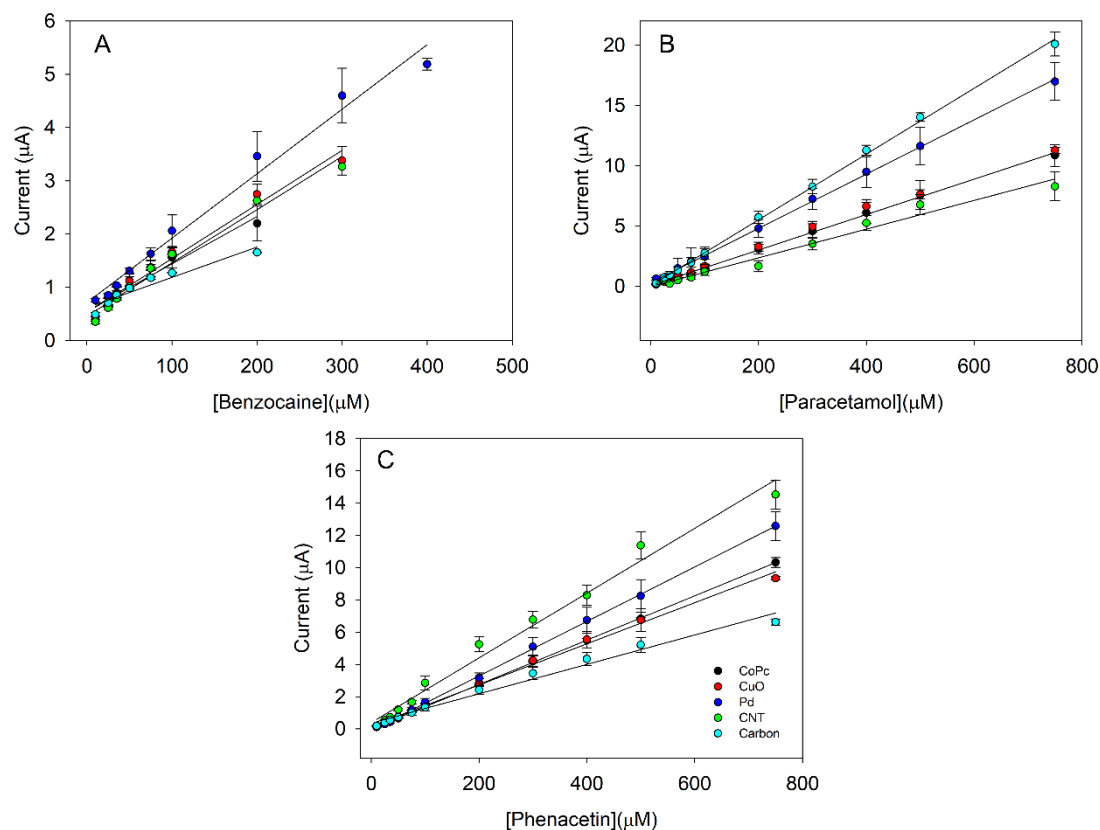


Figure IV - 40. Calibration curves of benzocaine, paracetamol and phenacetin of peak height (at the observed maximum potential) vs. concentration using the selected sensor array.

Table IV - 13. Calibration data (y vs. x) for the separate determination of benzocaine, paracetamol, and phenacetin.

Graphite						
Compound	Potential (V)	Sensitivity (nA·μM ⁻¹)	Intercept (μM)	r	LOD (μM)	Linear Range (μM)
Benzocaine	0.94	5.70·10 ⁻³	0.62	0.95	5.5	10-200
Paracetamol	0.45	2.7310 ⁻²	0.05	0.99	4.6	10-750
Phenacetin	0.91	9.10·10 ⁻³	0.36	0.99	10.6	10-750
CNT						
Compound	Potential (V)	Sensitivity (nA·μM ⁻¹)	Intercept (μM)	r	LOD (μM)	Linear Range (μM)
Benzocaine	0.85	1.00·10 ⁻²	0.46	0.99	5.5	10-300
Paracetamol	0.44	1.19·10 ⁻²	0.03	0.99	14.1	10-750
Phenacetin	0.83	2.01·10 ⁻²	0.39	0.99	14.1	10-750

CoPc						
Compound	Potential (V)	Sensitivity (nA·μM ⁻¹)	Intercept (μM)	r	LOD (μM)	Linear Range (μM)
Benzocaine	0.89	8.90·10 ⁻³	0.55	0.97	5.4	10-200
Paracetamol	0.52	1.47·10 ⁻²	0.06	0.99	3.3	10-750
Phenacetin	0.96	1.38·10 ⁻²	0.00	0.99	1.0	10-750
CuO						
Compound	Potential (V)	Sensitivity (nA·μM ⁻¹)	Intercept (μM)	r	LOD (μM)	Linear Range (μM)
Benzocaine	0.84	1.02·10 ⁻²	0.52	0.99	5.3	10-300
Paracetamol	0.44	1.52·10 ⁻²	0.11	0.99	5.5	10-750
Phenacetin	0.83	1.28·10 ⁻²	0.22	1.00	6.3	10-750
Pd						
Compound	Potential (V)	Sensitivity (nA·μM ⁻¹)	Intercept (μM)	r	LOD (μM)	Linear Range (μM)
Benzocaine	0.85	1.21·10 ⁻²	0.71	0.99	6.9	10-400
Paracetamol	0.43	2.25·10 ⁻²	0.29	0.99	3.5	10-750
Phenacetin	0.86	1.69·10 ⁻²	0.09	0.99	2.1	10-750

4. Repeatability and Reproducibility Studies

Once the calibration curves were completed, a stability study was done in order to verify that sensors can support many consecutive measurements, requirement needed when electronic tongues approach is done. To deal with this issue, benzocaine was chosen for the study, assuming comparable results for the rest of adulterants.

It is important to analyse the electrochemical behaviour of benzocaine because it provokes peak suppression signal, among others, in the fingerprint of cocaine electrochemical profile changing experimental conditions³⁹. Furthermore, this adulterant presents some fouling effect when the concentration increases, verifying their adsorption on the surface.

Specifically, a stock solution of benzocaine of 150 μM was measured for 10 consecutive measurements without changing the electrode. The results obtained

displayed an impressive decrease of the signal, suggesting that sensor surface is being blocked. At this point, some cleanings must be performed to improve the stability of the signal. Experiments with electrochemical cleaning using acid and alkaline media were incorporated between each measurement, without showing any improvement. Finally, an electrochemical cleaning (+1.35 V) for 30 s using phosphate buffer with 0.1 M KCl was tested. This soft cleaning allows to maintain the surface most stable and achieve to perform 10 consecutive measurements with relative standard deviation (RSD (%)) of 4.3%, which attempt promising results for next applying the electronic tongue approach. Results of these experiments can be found Figure IV - 41.

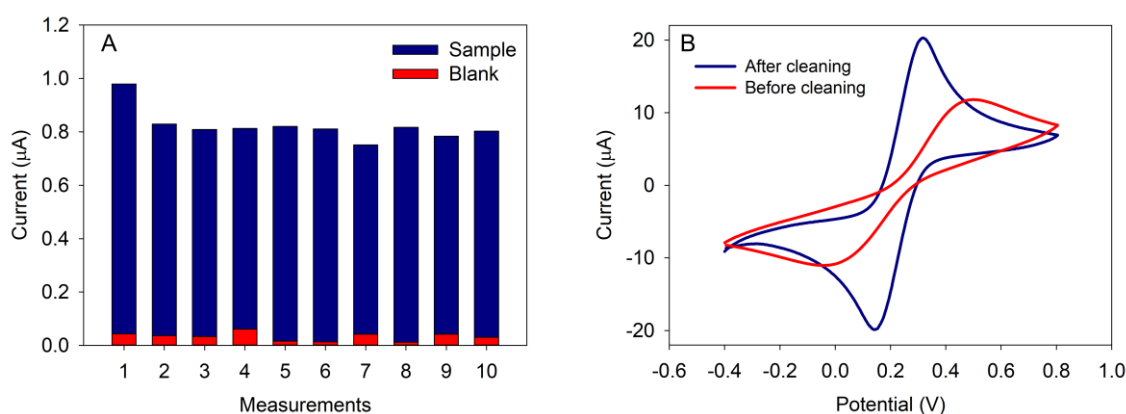


Figure IV - 41. A) Evaluation of the stability studied for the five modified IPE sensor array. A total of 10 measurements were performed inserting a blank solution of PBS between each measure. A paracetamol stock solution of 200 µM was used. B) Cyclic voltammogram using 5 mM $K_3Fe(CN)_6/K_4Fe(CN)_6$ redox couple in 0.1 M KCl.

IPEs sensors are mainly focused to be used with a single use or a few numbers of measurements, because its easy way to manufacture once the set-up is optimized⁴⁰.

This issue is in contrast with the philosophy of electronic tongue, which try to always use the same sensor to avoid drifts and/or periodic trends. Therefore, it was challenging to couple these two concepts to finally get consistent results maintaining the principles of both strategies.

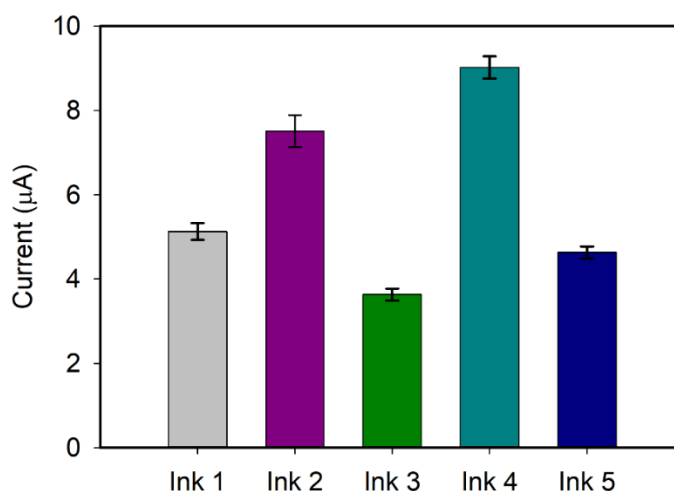


Figure IV - 42. Construction reproducibility of sensors with the fifth modified ink under study using a stock solution of paracetamol 150 μM . Graphite (ink 1), CoPc (ink 2), CuO (ink 3), Pd (ink 4) and CNT (ink 5).

Next, as sensors must be changed during the final experiment, the reproducibility of construction of the ink-modified IPE was also evaluated. The experiment was carried out preparing each modified ink by triplicate ($n=3$) (Figure IV - 42) and measuring consecutively with a paracetamol stock solution. All the sensors present good fabrication reproducibility with RSD (%) values of 3.9% for Graphite, 5.1% for CoPc, 4.0% for CuO, 2.9% for Pd and 3.0% for CNT, highlighting the best result for Pd ink, respectively.

5. Surface Electrode Characterization

5.1. Morphology Studies

The morphology of the modified electrodes was observed by SEM. The different electrochemical behaviour of the studied modified can be justified accordingly to the morphology. As it can be observed in Figure IV - 43, different shapes can be observed depending on the modified employed. Furthermore, microscopy studies show clearly the different modifiers distributed quasi homogeneously through the graphite flakes.

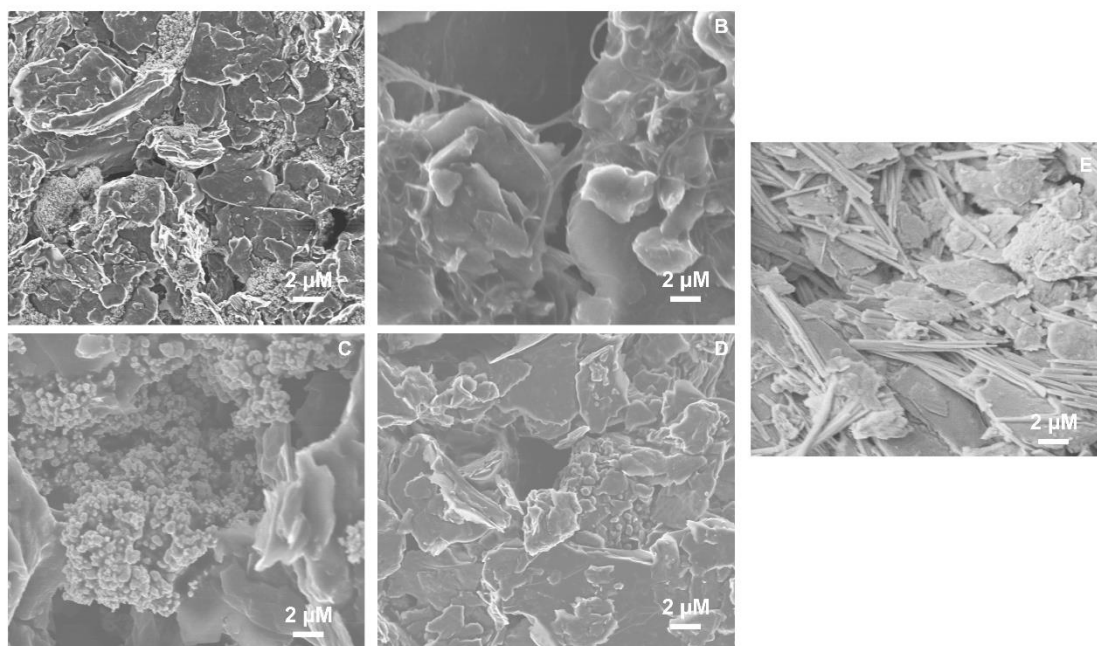


Figure IV - 43. SEM images. A) Graphite/IPE-Ink, B) CNT/IPE-Ink, C) Pd/IPE-Ink, D) CuO/IPE-Ink and E) CNT/IPE-Ink.

More in detail, a cross-section was done to the CNT modified electrode to show the different zones. This information is summarized in Figure IV - 44. Indeed, two remarkable zones can be observed in the picture. The first corresponds to the cross-section zone, in which the silver material that forms the working electrode can be observed clearly, whereas the enlarged area, the modified graphite ink, which shows uplift due to the cross-section produced.

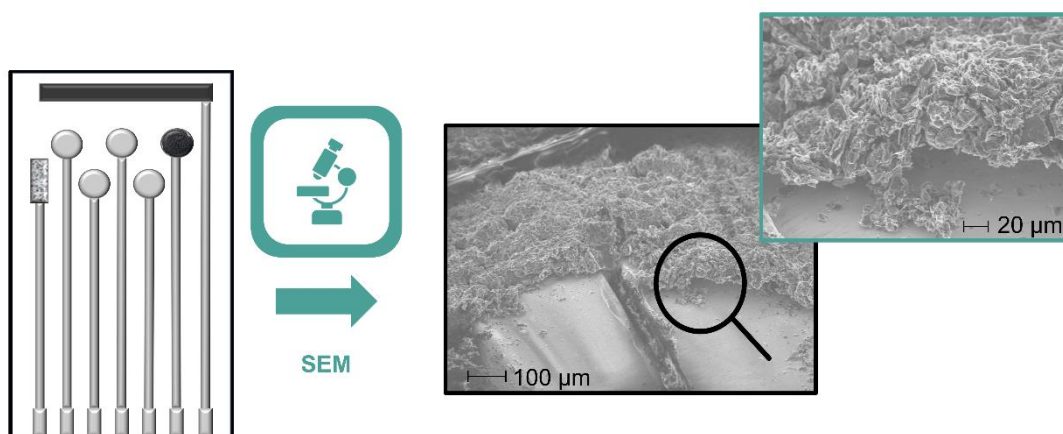


Figure IV - 44. Cross-section of the CNT modified electrode to observe the remarkable zones.

5.2. Impedance Measurements

Impedimetric measurements were carried out to analyse the morphology of the IPE modified electrode surface. To achieve that, measurements in $K_3[Fe(CN)_6]/K_4[Fe(CN)_6]$ (1:1) mixture solution were done. Firstly, the unmodified electrode was checked it, following by the fifth modified inks. As it can be observed in Figure IV - 45, Nyquist Plot shows that the charge-transfer resistance (R_{ct}) increased in all the cases, showing the smallest value for the case of the unmodified electrode, as expected.

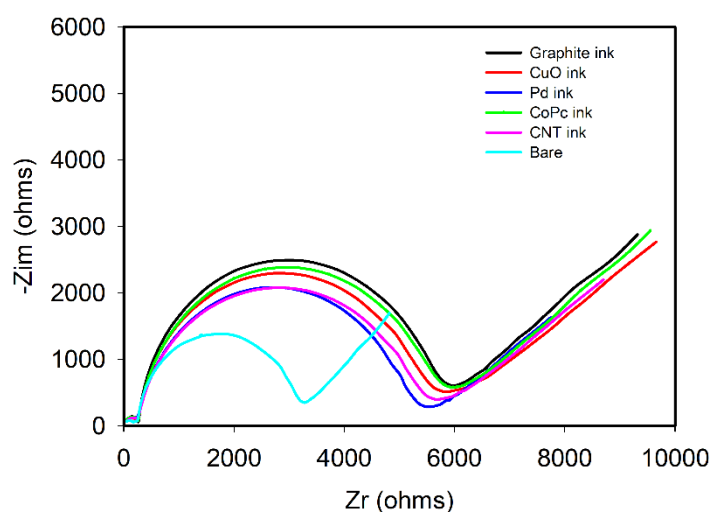


Figure IV - 45. Nyquist Plot of the fifth modified inks including the bare electrode. Measurements were carried out in PBS buffer containing 0.01 M $K_3[Fe(CN)_6]/K_4[Fe(CN)_6]$ (1:1) mixture as redox marker.

More in detail, there are not many significances differences between all the modified inks. Specifically, the highest value of R_{ct} corresponds to carbon ink very close to CoPc. Lower values of resistance can be observed in the case of CNT and Pd nanoparticles.

6. Chemometric Analysis

Voltammetric responses for each compound were analysed individually, showing different response for the different compounds under study. However, the profiles shows clearly that there will be an overlap on the square wave voltammograms when mixtures of those are to be analysed. Therefore, to achieve the individual quantification of each of the substance, the use of chemometric techniques is required.

Depending on the final application (qualitative or quantitative), it is possible to choose the best chemometric method to afford the problem. In this work, both approximations were done, which will be discussed in the detail in the following sections.

6.1. Qualitative Analysis: Principal Component Analysis

PCA is a chemometric tool which allows the search of similarities between samples. In this case, this tool was used to verify the good performance of the sensors in front of the studied substances. With PCA it is expected that redundant sensors (sensors than contribute with the same information) would appear superimposed in the scores space, meanwhile sensors with different responses will manifest in distinction in it. As it can be observed in Figure IV - 46, the relevant information of the samples using the two first PCs made 58.3% of the total variability. In general trends, the proposed modified inks showed different response towards the studied molecules, and with limited dispersion in some cases, facilitating the assignment of substances to its class. Previous representation showed the information divided by sensor and substance. However, there is another kind of representation, where voltammetric responses of the fifth electrodes were combined into a single vector. Figure IV - 47 displays this content. As it can be observed three clusters can be remarked corresponding to the three compounds under study. In this case, three PCs represents 86.4% of the total variability. This value is more than acceptable because it was reduced from a large number de variables to only PC1, PC2 and PC3.

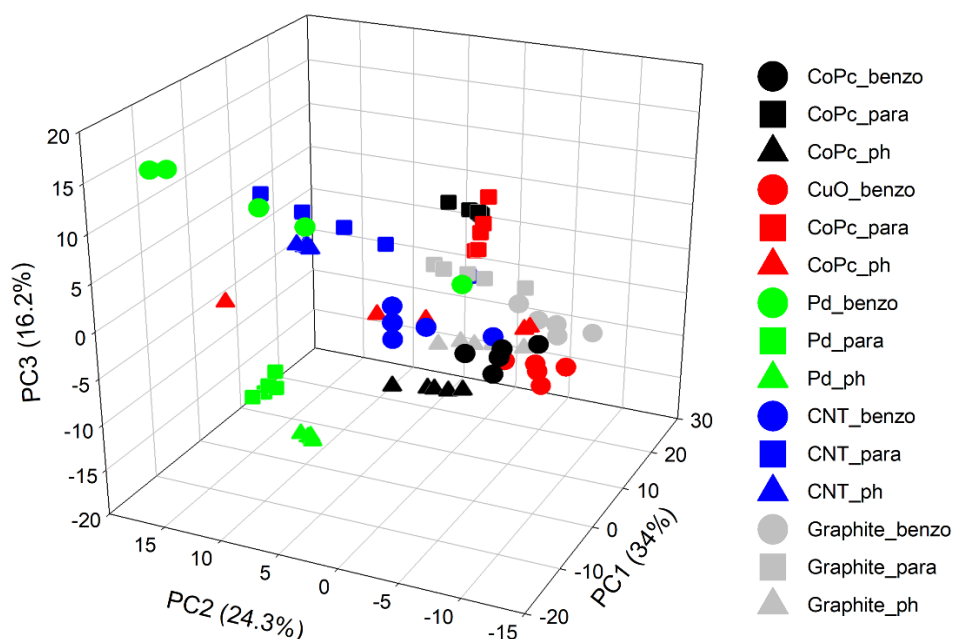


Figure IV - 46. Score plot of the three components obtained after PCA analysis. 4 replicates for each sensor were done determining the three compounds of interest: benzocaine, phenacetin, and paracetamol of 200 μ M. The array used was CoPc/IPE-Ink, CuO/IPE-Ink, Pd/IPE-Ink, CNT/IPE-Ink, and graphite/IPE-ink.

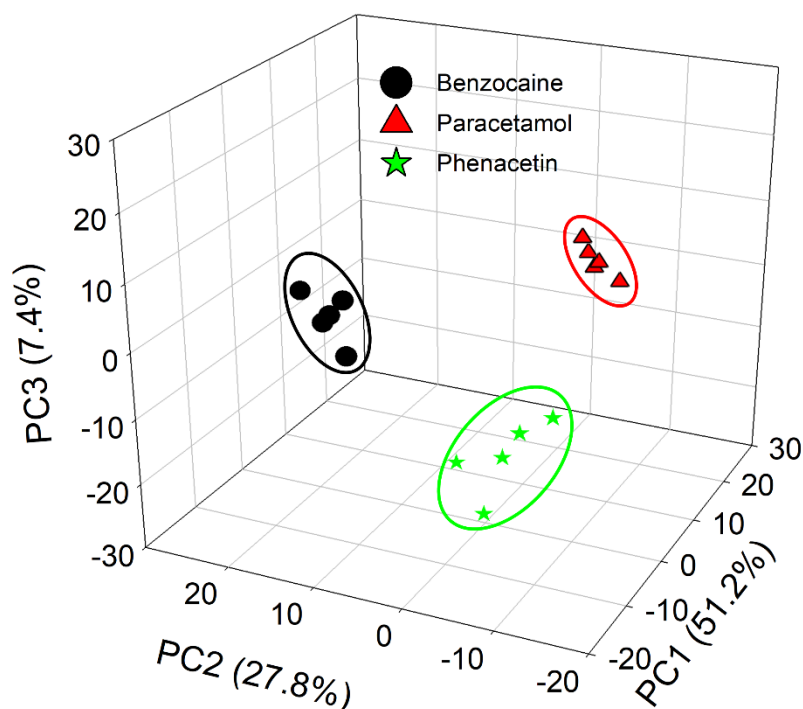


Figure IV - 47. Scores plot for the three first principal components for the analytes benzocaine, paracetamol and phenacetin, common adulterants present in cocaine seizures samples.

As conclusion, the proposed array is suitable to study the mixtures under study, showing differentiated response in front of the three studied adulterants.

7. Quantification Analysis

A DWT pre-processing stage was performed employing Daubechies wavelet and a fourth decomposition level, the best choice from preliminary tests and previous experience.

The DWT allowed compressing the original data set information up to 91.4% without any loss of relevant information. From the proposed 5-sensor array, the corresponding voltammograms were compressed, and the obtained coefficients were fed into.

An ANN model was used to achieve the simultaneous determination of the three cutting agents studied. The model was built employing the data of the train subset, using the data of the test subset to assess its performance.

After a systematic evaluation of topologies, the final DWT-ANN architecture model had 120 input neurons (corresponding to the 24 wavelet approximation coefficients obtained from wavelet analysis of each of the 5 sensor signals, 8 neurons and *logsig* function in the hidden layer and 2 output neurons and *satlins* function in the output layer.

To visualize the performance of the model, the comparison graphs of obtained vs. expected concentrations were built for each of the analytes demonstrating the feasibility of the model obtained (Figure IV - 48).

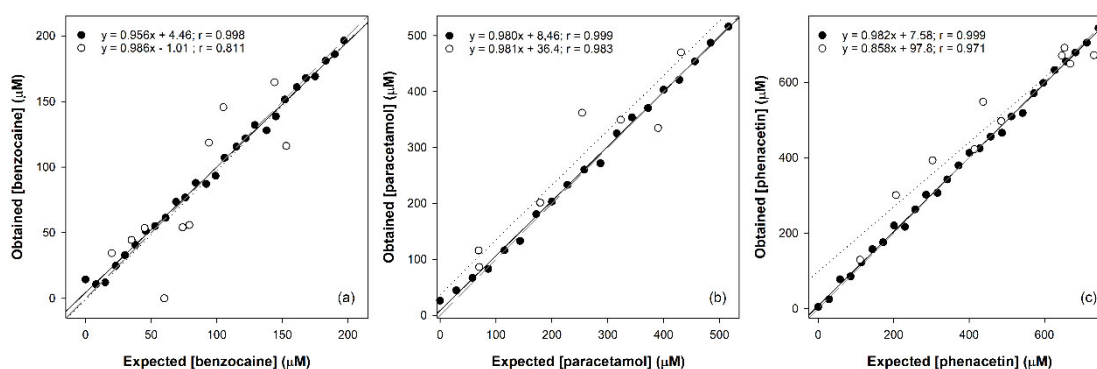


Figure IV - 48. Comparison graphs obtained vs. expected for benzocaine, phenacetin, and paracetamol.

8. References

- (1) Bayne, C. K.; Haswell, S. J. *Practical Guide to Chemometrics*; 1995; Vol. 37. <https://doi.org/10.2307/1269627>.
- (2) Abdi, H. Partial Least Squares Regression and Projection on Latent Structure Regression (PLS Regression). *WIREs Comput. Stat.* **2010**, 2 (1), 97–106. <https://doi.org/10.1002/wics.51>.
- (3) Gutes, A.; Calvo, D.; Céspedes, F.; del Valle, M. Automatic Sequential Injection Analysis Electronic Tongue with Integrated Reference Electrode for the Determination of Ascorbic Acid, Uric Acid and Paracetamol. *Microchim. Acta* **2007**, 157 (1–2), 1–6. <https://doi.org/10.1007/s00604-006-0660-4>.
- (4) Alegret, S.; Alonso, J.; Bartrolí, J.; Céspedes, F.; Martínez-Fàbregas, E.; Valle, M. Del. Amperometric Biosensors Based on Bulk-Modified Epoxy Graphite Biocomposites. *Sensors Mater.* **1996**, 8 (3), 147–153.
- (5) Wang, J. *Analytical Electrochemistry*, 3ed Editio.; John Wiley & Sons: Hoboken, New Jersey, 2006.
- (6) Broséus, J.; Gentile, N.; Esseiva, P. The Cutting of Cocaine and Heroin: A Critical Review. *Forensic Sci. Int.* **2016**, 262, 73–83. <https://doi.org/10.1016/j.forsciint.2016.02.033>.
- (7) Rodríguez, J. R. B.; Díaz, V. C.; García, A. C.; Blanco, P. T. Voltammetric Assay of Heroin in Illicit Dosage Forms. *Analyst* **1990**, 115 (2), 209–212. <https://doi.org/10.1039/AN9901500209>.
- (8) Navaee, A.; Salimi, A.; Teymourian, H. Graphene Nanosheets Modified Glassy Carbon Electrode for Simultaneous Detection of Heroine, Morphine and Noscapine. *Biosens. Bioelectron.* **2012**, 31 (1), 205–211. <https://doi.org/10.1016/j.bios.2011.10.018>.
- (9) Garrido, J. M. P. J.; Delerue-Matos, C.; Borges, F.; Macedo, T. R. A.; Oliveira-Brett, A. M. Voltammetric Oxidation of Drugs of Abuse III. Heroin and Metabolites. *Electroanalysis* **2004**, 16 (18), 1497–1502. <https://doi.org/10.1002/elan.200302975>.
- (10) Garrido, J. M. P. J.; Delerue-Matos, C.; Borges, F.; Macedo, T. R. A.; Oliveira-Brett, A. M. Electrochemical Analysis of Opiates - An Overview. *Anal. Lett.* **2004**, 37 (5), 831–844. <https://doi.org/10.1081/AL-120030282>.
- (11) Kaa, E. Impurities, Adulterants and Diluents of Illicit Heroin. Changes during a 12-Year Period. *Forensic Sci. Int.* **1994**, 64 (2–3), 171–179. [https://doi.org/10.1016/0379-0738\(94\)90228-3](https://doi.org/10.1016/0379-0738(94)90228-3).
- (12) R.G Brereton. *Applied Chemometrics for Scientists*; John Wiley & Sons, Ed.; Chichester, 2007.
- (13) Cetó, X.; Céspedes, F.; Pividori, M. I.; Gutiérrez, J. M.; Del Valle, M. Resolution of Phenolic Antioxidant Mixtures Employing a Voltammetric Bio-Electronic Tongue. *Analyst* **2012**, 137 (2), 349–356. <https://doi.org/10.1039/c1an15456g>.
- (14) Bard, A. J. Chemical Modification of Electrodes. *J. Chem. Educ.* **1983**, 60 (4), 302. <https://doi.org/10.1021/ed060p302>.
- (15) Ortiz-Aguayo, D.; Bonet-San-Emeterio, M.; del Valle, M. Simultaneous Voltammetric Determination of Acetaminophen, Ascorbic Acid and Uric Acid by Use of Integrated Array of Screen-Printed Electrodes and Chemometric Tools. *Sensors* **2019**, 19 (15), 3286. <https://doi.org/10.3390/s19153286>.

-
- (16) Gutiérrez, J. M.; Moreno-Barón, L.; Pividori, M. I.; Alegret, S.; del Valle, M. A Voltammetric Electronic Tongue Made of Modified Epoxy-Graphite Electrodes for the Qualitative Analysis of Wine. *Microchim. Acta* **2010**, *169* (3–4), 261–268. <https://doi.org/10.1007/s00604-010-0351-z>.
- (17) Rodríguez-Mendez, M. L.; García-Hernández, C.; Medina-Plaza, C.; García-Cabezón, C.; de Saja, J. A. Multisensor Systems Based on Phthalocyanines for Monitoring the Quality of Grapes. *J. Porphyr. Phthalocyanines* **2016**, *20* (08n11), 889–894. <https://doi.org/10.1142/S1088424616500796>.
- (18) Metters, J. P.; Kadara, R. O.; Banks, C. E. New Directions in Screen Printed Electroanalytical Sensors: An Overview of Recent Developments. *Analyst* **2011**, *136* (6), 1067. <https://doi.org/10.1039/c0an00894j>.
- (19) Tsakova, V.; Seeber, R. Conducting Polymers in Electrochemical Sensing: Factors Influencing the Electroanalytical Signal. *Anal. Bioanal. Chem.* **2016**, *408* (26), 7231–7241. <https://doi.org/10.1007/s00216-016-9774-7>.
- (20) Ortiz-Aguayo, D.; Wael, K. De; Valle, M. del. Voltammetric Sensing Using an Array of Modified SPCE Coupled with Machine Learning Strategies for the Improved Identification of Opioids in Presence of Cutting Agents. *J. Electroanal. Chem.* **2021**, *902*, 115770. <https://doi.org/10.1016/j.jelechem.2021.115770>.
- (21) Galik, M.; O'Mahony, A. M.; Wang, J. Cyclic and Square-Wave Voltammetric Signatures of Nitro-Containing Explosives. *Electroanalysis* **2011**, *23* (5), 1193–1204. <https://doi.org/10.1002/elan.201000754>.
- (22) O'Mahony, A. M.; Windmiller, J. R.; Samek, I. A.; Bandodkar, A. J.; Wang, J. "Swipe and Scan": Integration of Sampling and Analysis of Gunshot Metal Residues at Screen-Printed Electrodes. *Electrochem. commun.* **2012**, *23*, 52–55. <https://doi.org/10.1016/j.elecom.2012.07.004>.
- (23) Moros, J.; Galipienso, N.; Vilches, R.; Garrigues, S.; De La Guardia, M. Nondestructive Direct Determination of Heroin in Seized Illicit Street Drugs by Diffuse Reflectance Near-Infrared Spectroscopy. *Anal. Chem.* **2008**, *80* (19), 7257–7265. <https://doi.org/10.1021/ac800781c>.
- (24) Garrido, J. M. P. J.; Delerue-Matos, C.; Borges, F.; Macedo, T. R. A.; Oliveira-Brett, A. M. Voltammetric Oxidation of Drugs of Abuse I. Morphine and Metabolites. *Electroanalysis* **2004**, *16* (17), 1419–1426. <https://doi.org/10.1002/elan.200302966>.
- (25) Garrido, J. M. P. J.; Delerue-Matos, C.; Borges, F.; Macedo, T. R. A.; Oliveira-Brett, A. M. Voltammetric Oxidation of Drugs of Abuse II. Codeine and Metabolites. *Electroanalysis* **2004**, *16* (17), 1427–1433. <https://doi.org/10.1002/elan.200302967>.
- (26) Khairy, M.; Mahmoud, B. G.; Banks, C. E. Simultaneous Determination of Codeine and Its Co-Formulated Drugs Acetaminophen and Caffeine by Utilising Cerium Oxide Nanoparticles Modified Screen-Printed Electrodes. *Sensors Actuators B Chem.* **2018**, *259*, 142–154. <https://doi.org/10.1016/j.snb.2017.12.054>.
- (27) Tadesse, Y.; Tadese, A.; Saini, R. C.; Pal, R. Cyclic Voltammetric Investigation of Caffeine at Anthraquinone Modified Carbon Paste Electrode. *Int. J. Electrochem.* **2013**, *2013*, 1–7. <https://doi.org/10.1155/2013/849327>.
- (28) del Valle, M. Electronic Tongues Employing Electrochemical Sensors. *Electroanalysis* **2010**, *22* (14), 1539–1555.
-

- <https://doi.org/10.1002/elan.201000013>.
- (29) Cetó, X.; Céspedes, F.; del Valle, M. Comparison of Methods for the Processing of Voltammetric Electronic Tongues Data. *Microchim. Acta* **2013**, *180* (5–6), 319–330. <https://doi.org/10.1007/s00604-012-0938-7>.
- (30) Richards, E.; Bessant, C.; Saini, S. Multivariate Data Analysis in Electroanalytical Chemistry. *Electroanalysis* **2002**, *14* (22), 1533–1542. [https://doi.org/10.1002/1521-4109\(200211\)14:22<1533::AID-ELAN1533>3.0.CO;2-T](https://doi.org/10.1002/1521-4109(200211)14:22<1533::AID-ELAN1533>3.0.CO;2-T).
- (31) Florea, A.; Schram, J.; de Jong, M.; Eliaerts, J.; Van Durme, F.; Kaur, B.; Samyn, N.; De Wael, K. Electrochemical Strategies for Adulterated Heroin Samples. *Anal. Chem.* **2019**, *91* (12), 7920–7928. <https://doi.org/10.1021/acs.analchem.9b01796>.
- (32) de Jong, M.; Florea, A.; Eliaerts, J.; Van Durme, F.; Samyn, N.; De Wael, K. Tackling Poor Specificity of Cocaine Color Tests by Electrochemical Strategies. *Anal. Chem.* **2018**, *90* (11), 6811–6819. <https://doi.org/10.1021/acs.analchem.8b00876>.
- (33) Escandar, G. M.; Goicoechea, H. C.; Muñoz de la Peña, A.; Olivieri, A. C. Second- and Higher-Order Data Generation and Calibration: A Tutorial. *Anal. Chim. Acta* **2014**, *806*, 8–26. <https://doi.org/10.1016/j.aca.2013.11.009>.
- (34) Mimendia, A.; Gutiérrez, J. M.; Opalski, L. J.; Ciosek, P.; Wróblewski, W.; del Valle, M. SIA System Employing the Transient Response from a Potentiometric Sensor Array—Correction of a Saline Matrix Effect. *Talanta* **2010**, *82* (3), 931–938. <https://doi.org/10.1016/j.talanta.2010.05.061>.
- (35) Cipri, A.; del Valle, M. Pd Nanoparticles/Multiwalled Carbon Nanotubes Electrode System for Voltammetric Sensing of Tyrosine. *J. Nanosci. Nanotechnol.* **2014**, *14* (9), 6692–6698. <https://doi.org/10.1166/jnn.2014.9370>.
- (36) Ortiz-Aguayo, D.; Cetó, X.; De Wael, K.; del Valle, M. Resolution of Opiate Illicit Drugs Signals in the Presence of Some Cutting Agents with Use of a Voltammetric Sensor Array and Machine Learning Strategies. *Sensors Actuators B Chem.* **2021**, 131345. <https://doi.org/10.1016/j.snb.2021.131345>.
- (37) De Sá, A. C.; Cipri, A.; González-Calabuig, A.; Stradiotto, N. R.; Del Valle, M. Resolution of Galactose, Glucose, Xylose and Mannose in Sugarcane Bagasse Employing a Voltammetric Electronic Tongue Formed by Metals Oxy-Hydroxide/MWCNT Modified Electrodes. *Sensors Actuators, B Chem.* **2016**, *222*, 645–653. <https://doi.org/10.1016/j.snb.2015.08.088>.
- (38) Sarma, M.; Romero, N.; Cetó, X.; Valle, M. Del. Optimization of Sensors to Be Used in a Voltammetric Electronic Tongue Based on Clustering Metrics. *Sensors* **2020**, *20* (17), 4798. <https://doi.org/10.3390/s20174798>.
- (39) Jong, M.; Slegers, N.; Schram, J.; Daems, D.; Florea, A.; De Wael, K. A Benzocaine-Induced Local Near-Surface PH Effect: Influence on the Accuracy of Voltammetric Cocaine Detection. *Anal. Sens.* **2021**, *1* (1), 54–62. <https://doi.org/10.1002/anse.202000012>.
- (40) Moya, A.; Gabriel, G.; Villa, R.; Javier del Campo, F. Inkjet-Printed Electrochemical Sensors. *Curr. Opin. Electrochem.* **2017**, *3* (1), 29–39. <https://doi.org/10.1016/j.coelec.2017.05.003>.

V. CONCLUSIONS

Once the end of the road is reached, it is necessary to draw conclusions, applying all the knowledge acquired along the way.



1. Conclusions

The present doctoral thesis has led to the following conclusions. Overall, the general objective of the development of electronic tongues for forensic and security applications has been completed. For this purpose, different printed sensor platforms have been tested for different fields of application showing good results. In more detail, it can be concluded that:

1. The design, evaluation and characterization of the different printed sensor platforms were successfully achieved. For that, techniques based on serigraphy and inkjet printing were selected.

1.1. After evaluating and characterizing the integrated array of screen-printed electrodes provided by DropSens, it could be demonstrated the feasibility of the device showing enhanced results in comparison with previous studies in the group.

1.2. In addition, ItalSens single electrodes showed proper results and for this it could be considered as an approach to afford the problematic that imply the opioids case study.

1.3. The inkjet printed platform array tested in this work provides promising results to consider this new emergent technology as a candidate to be applied in the cocaine cutting agents determination.

In all cases, an electrochemical and morphological characterisation have been carried out. Calculations on the effective area of the working electrodes and their analytical parameters were also determined.

2. The development of a composite based on a polystyrene/graphite ink was successfully carried out as a first approach for the modification of electrochemical sensors. The methodology proposed for the modification has been a good strategy to solve the problem of overlapping of the mixtures studied throughout the doctoral thesis.

Moreover, it is a simple, economical, and stable approach that allows many measurements thanks to the polystyrene matrix. Therefore, the method has been validated due to its application in different sensor platforms.

3. A validation of the materials and methods was carried out using a reference mixture, commonly known in the laboratory. The work from **article 1** provided for the first time in our group the simultaneous detection of the reference mixture: AA, UA and PA using a multi screen-printed electrodes integrated array. This project provided improved results thanks to the applicability of electronic tongues and chemometrics. In this case, PCA and PLS were used as data processing and modelling tools. Therefore, this work not only validated the surface modification technology, but also demonstrated the advantages of screen-printed electrodes for on-site analysis as an alternative to classical methods.
4. A strategy to identify heroin, morphine, and codeine in the presence of cuttings agents such as caffeine and paracetamol was developed with surprising results. This work is drawn from **article 2**.
 - 4.1. For a first time, the qualitative analysis of the presented drugs of abuse in the presence of the cutting agents were achieved successfully thanks to the use of modified screen-printed electrodes. The work was also a progress in our research group. For the first time, a methodology was developed to optimize the selection of the number of sensors to be used. This strategy would not have been possible without the use of PCA as a visualisation tool and Silhouette calculation as a clustering metrics. Regarding the results obtained, the best candidate array was based on graphite, CoPc and Pd.
 - 4.2. In addition, the study was completed with the creation of a classification model. Among all the algorithms checked, it can be concluded that kNN allows the simplest identification of the samples with excellent results thanks to the clear distinction of the samples with the selected array.

5. The promising results obtained in **article 2** led to the development of a quantitative application (**article 3**). Two works are represented in the article: on the one hand, the generation of a chemometric model allowing the distinction of the three drugs of abuse heroin, morphine, and codeine. For this purpose, a tilted factorial model was used for the design of the electronic tongue. On the other hand, the generation of a five-compound chemometric model, which allowed the incorporation of two cutting agents commonly present in illicit heroin samples such as paracetamol and caffeine. The preparation of this electronic tongue was carried out using a CCF design, due to the large number of samples.
 - 5.1. The two models showed satisfactory performance demonstrating the power of the proposed voltammetric tongue for identification of seized drug street samples, both in their pure form and mixed with different cutting agents.
 - 5.2. Data processing was aided using GAs to reduce the number of inputs and PLS as a multivariate calibration model. As a summary of this work, the combination of the ET with the modification employed and the chemometric tools demonstrate the potential of these strategies to be used as analytical tools for the detection of illicit drugs from street samples offering cheap measurement systems with rapid response, simple use and high portability, important topic for law-enforcement applications or point-of-use forensic.
6. A strategy to quantify benzocaine, phenacetin and paracetamol were developed successfully using IJP as emergent technology. The design and printing of the sensor platform was done properly. The electrochemical part coupled with the chemometrics, in this case, DWT+ANNs showed promising results for the simultaneous determination of these cuttings agents from cocaine seizures samples.

2. Futures Perspectives

In a research work, such as a doctoral thesis, it is always difficult to put an end to the topic under study. That is why there are always new ideas and improvements that can be implemented in the processes. The key points I would address are as follows:

1. To explore new, more environmentally friendly substrates. Different studies referenced in the introduction of this thesis demonstrate the potential of this material and the good results obtained from the electrochemical point of view.
2. To develop more aqueous inks that comply with the current term of "*Green Chemistry*". The use of organic solvents is far from this purpose. For this reason and taking advantage of the fact that electrochemical processes are relatively clean, the formulation of more aqueous inks would solve the problem under study. In addition, alternatives to drop casting, such as electro-polymerisation techniques, could be tested.
3. To generate more complex models for the identification of more analytes in the sample. This would be very useful in the forensic field for the detection of more than one drug of abuse.
4. Taking advantage of the recent purchase of a 3D printer in the group, try to find different filaments combining materials for printing electrochemical sensors to develop in the field of electronic tongues.

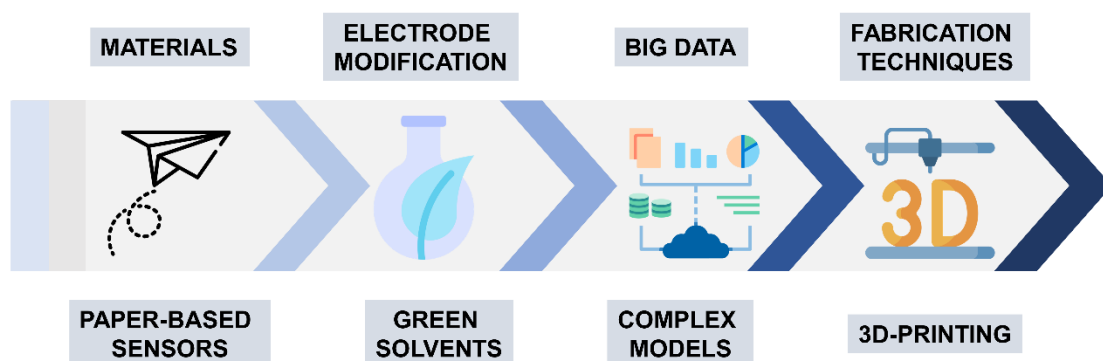
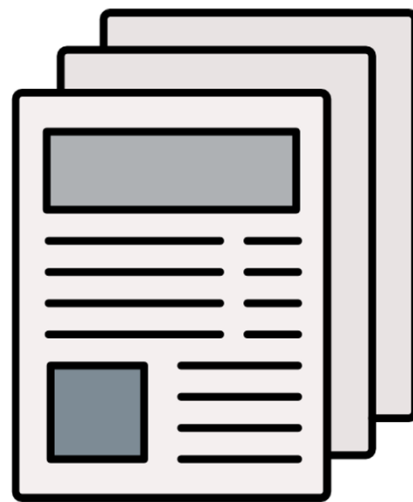


Figure V - 1. Some key ideas as a starting point for future works.

ANNEX 1: PUBLICATIONS



ARTICLE 1

Simultaneous Voltammetric Determination of Acetaminophen, Ascorbic Acid, and Uric Acid by Use of Integrated Array of Screen-Printed Electrodes and Chemometric Tools

Dionisia Ortiz-Aguayo, Marta Bonet-San-Emeterio and Manel del Valle

Sensors, 2019, 19(15), 3286

Article

Simultaneous Voltammetric Determination of Acetaminophen, Ascorbic Acid and Uric Acid by Use of Integrated Array of Screen-Printed Electrodes and Chemometric Tools

Dionisia Ortiz-Aguayo , Marta Bonet-San-Emeterio  and Manel del Valle * 

Sensors and Biosensors Group, Department of Chemistry, Universitat Autònoma de Barcelona, 08193 Bellaterra, Spain

* Correspondence: manel.delvalle@uab.es; Tel.: +34-93-581-3235

Received: 28 June 2019; Accepted: 24 July 2019; Published: 26 July 2019



Abstract: In the present work, ternary mixtures of Acetaminophen, Ascorbic acid and Uric acid were resolved using the Electronic tongue (ET) principle and Cyclic voltammetry (CV) technique. The screen-printed integrated electrode array having differentiated response for the three oxidizable compounds was formed by Graphite, Prussian blue (PB), Cobalt (II) phthalocyanine (CoPc) and Copper oxide (II) (CuO) ink-modified carbon electrodes. A set of samples, ranging from 0 to 500 $\mu\text{mol}\cdot\text{L}^{-1}$, was prepared, using a tilted (3°) factorial design in order to build the quantitative response model. Subsequently, the model performance was evaluated with an external subset of samples defined randomly along the experimental domain. Partial Least Squares Regression (PLS) was employed to construct the quantitative model. Finally, the model successfully predicted the concentration of the three compounds with a normalized root mean square error (NRMSE) of 1.00 and 0.99 for the training and test subsets, respectively, and $R^2 \geq 0.762$ for the obtained vs. expected comparison graphs. In this way, a screen-printed integrated electrode platform can be successfully used for voltammetric ET applications.

Keywords: electronic tongue; modifiers; acetaminophen; ascorbic acid; uric acid; partial least squares regression

1. Introduction

Acetaminophen, Ascorbic acid and Uric acid (Figure 1) play an important role in humans' life. Acetaminophen (N-acetyl-p-aminophenol or paracetamol (PA)) is an antipyretic and analgesic drug commonly used against arthritis, headache, muscle aches, menstrual cramps and fevers [1]. A high amount of PA can cause the accumulation of toxic metabolites, leading to severe and sometimes fatal hepatotoxicity and nephrotoxicity [2]. Ascorbic acid (AA) is a vitamin commonly present in many biological systems and in multivitamin formulations. It is widely employed to provide an adequate dietary intake and as an antioxidant [3]. Its excessive dose may cause headache, trouble sleeping, gastrointestinal discomfort and flushing of the skin [4]. Uric acid (UA) is the primary product of purine metabolism [5]. Continuous monitoring of UA in the body fluid is essential since its abnormal concentration levels lead to several diseases, such as hyperuricemia and gout [6]. Other diseases, such as leukemia and pneumonia are also associated with enhanced urate levels.

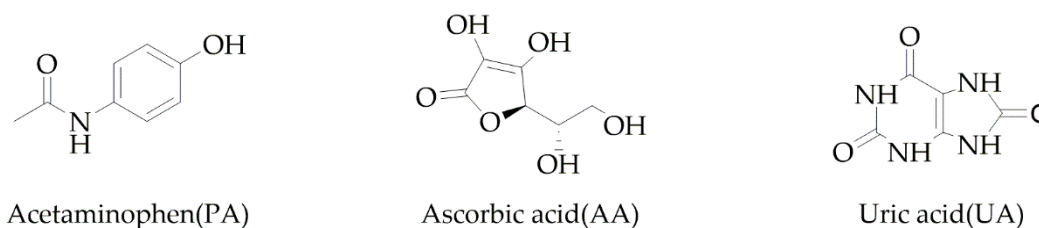


Figure 1. Chemical structure of three studied compounds in this report (Acetaminophen, Ascorbic acid and Uric acid).

Several analytical methods for individual or simultaneous determination of PA, AA and UA have been reported in the literature such as spectrofluorometry [7,8], spectrophotometry [9,10], chromatography [11,12], and capillary zone electrophoresis [13,14]. The problem is that these methods can be expensive and need complex procedures. For these reasons, the development of rapid, cheap and effective determination procedures is needed. One proposal to overcome this can be the development of electrochemical sensors [15]. This kind of devices provide some advantages, such as, low detection limits, wide linear response range, good stability and reproducibility.

However, certain difficulties arise when the simultaneous determination of these three compounds is attempted. The oxidation peaks of PA, AA and UA are almost overlapping on traditional electrodes [16], which make their simultaneous determination highly difficult. One solution to solve the main drawback is the use of methods based on modified electrodes, which have fascinated many researchers due to their simplicity, high sensitivity, and low cost. In addition, this strategy allows some improvement based on electrocatalysis, liberation from surface fouling and prevention of undesirable reactions competing kinetically with the desired electrode process [17].

Modified electrodes [18] can be prepared by several different techniques based on adsorbing, attaching specific molecules (e.g., peptides [19] or complexing agents [20,21]) to the surface by self-assembled monolayer [22], coating and entrapment, e.g., in the form of conductive ink [23]. The last strategy has become interesting for electrochemists in recent times, because this deliberate and controlled modification of the electrode surface can produce new surfaces with interesting properties employed for new devices and applications in electrochemistry.

Nature has developed and optimized an impressive variety of sensing systems used for navigation, spatial orientation, prey detection, object inspection, peer interaction, etc. which provide technologists with inspiring ideas for new concepts for sensors or improvements within the field [24,25]. Illustrating examples in chemical sensing is the development of electronic noses (EN) and electronic tongues (ET), both sharing the concept of preferring a number of sensors (a sensor array) with broad selectivity pattern, instead of a single, highly selective sensor. The use of this number of receptors in a combinatorial way is what permits to the animal senses to be effective in detecting thousands of different compounds or situations. In the field of chemical analysis, the main bioinspired systems take after three mammal senses: smell, taste and sight. Therefore, there have been reported electronic noses (EN) [26], eyes (EE) and tongues (ET) [27]. From these principles, the EN, formed by an array of sensors with slightly different response to generic compounds has been used for analysis in the gas phase and stands out for its closeness to artificial olfaction. In the case of EE, there are also interesting advances reported in the literature. An example is the development of a bioinspired electronic white cane for blind people using whiskers multiple sensor principle for short-range navigation and exploration [28].

Similar to the EN is the ET that, according to IUPAC [29], is defined as a multisensor system, which consists of a number of low-selective sensors and uses advanced mathematical procedures for signal processing based on pattern recognition and/or multivariate data analysis. This analytical system applied to liquid analysis allows the generation of multidimensional information in combination with chemometric processing, which allows extracting the maximum chemical information from these complex data.

In this way, biomimetic systems, in opposition of classical approaches, use the combination of low selective and/or cross-responsive sensors to obtain rich and complementary analytical information. Next, this complex, multi-dimensional information needs to be processed with proper data treatment tools, which is accomplished with chemometrics. This coupling has been declared one of the ways of progress in developing new sensing schemes [30]. There are different data processing tools depending on the final application needed. If this is a qualitative goal, PCA is a suitable linear visualization/pattern recognition method. This tool allows the reduction of the dimensionality of a multivariate problem and facilitates the visualization of different categories of the multivariate profiles by remarking similarities and differences between sample clusters. When the purpose is quantitative, different tools are available, given the numeric information is the end result. Some of these are Principal Component Regression (PCR), which departs from a first PCA transformation to build a multivariate regression, Partial Least Squares Regression (PLS), or Artificial Neural Networks (ANNs) [31].

In the present work, an eight sensor integrated array of screen-printed electrodes has been developed in base of a multiple screen-printed carbon electrode (SPCE) platform. The voltammetric array, consisting of Graphite/SPCE-Ink, Prussian blue/SPCE-Ink, Cobalt (II) phthalocyanine/SPCE-Ink and Copper oxide (II)/SPCE-Ink was employed for the simultaneous determination of the three aforementioned compounds (PA, AA and UA) by using the Cyclic voltammetry (CV) technique. This represents an example of resolving a mixture where heavily interfering signals are generated and resolving its components is difficulted. In other words, it is shown how to detect simultaneously the different analytes in presence of their interferents, which redox signals overlap. For showing these aspects, firstly, the behavior of the sensors was evaluated separately for each compound; secondly, peak current responses showed that all sensors had differentiated response for the three oxidizable compounds of clinical interest. Finally, a response model was developed to determine mixtures of PA, AA and UA at the $\mu\text{mol}\cdot\text{L}^{-1}$ level.

2. Materials and Methods

2.1. Chemicals and Reagents

All solutions were made up using sterilized Milli-Q water (Millipore, Billerica, MA, USA). Cobalt (II) phthalocyanine (CoPc), Copper (II) oxide (CuO) nanopowder (<50 nm), Polypyrrole doped (PP) and Palladium, powder submicron 99.9+% (Pd), which were used as modifiers, were purchased from Sigma-Aldrich (St. Louis, MO, USA). Prussian blue was from Acros Organics (Geel, Belgium). The preparation of the ink composite was done using mesitylene and polystyrene, obtained from Sigma-Aldrich (St. Louis, MO, USA). Graphite powder (particle size < 50 μm) was received from BDH (BDH Laboratory Supplies, Poole, UK). Potassium chloride was purchased from Merck (Darmstadt, Germany).

Acetaminophen (PA), Ascorbic acid (AA), Uric acid (UA) and hydrogen peroxide (H_2O_2) solution were purchased from Sigma-Aldrich (St. Louis, MO, USA).

All the measurements were carried out using 50 mM phosphate buffer (PBS) solution and 0.1 M KCl solution at pH 7.

2.2. Electronic Tongue

The voltammetric ET was formed by an integrated array of eight screen-printed electrodes as working electrodes (8W110 Electrodes, ceramic substrate: $50 \times 27 \times 1$ mm. and electric contacts composed of silver) from DropSens (Oviedo, Spain). The electrochemical cell consisted on: 8 working electrode (carbon, 2.95 mm diameter), auxiliary electrode (carbon) and pseudo reference electrode (Silver) [32].

Electrochemical measurements were performed at room temperature (25 °C), using a portable Multi Potentiostat/Galvanostat μStat 8000 from DropSens controlled through its Dropview Multichannel 5.5 software package. A complete Cyclic voltammogram was recorded for each sample and for each

electrode by cyclic the potential between -1.5 and $+1.5$ V with a step potential of 9 mV and a scan rate of $50 \text{ mV}\cdot\text{s}^{-1}$.

2.3. Modification of the Electrode Surface

The nanomaterial SPCE/modifier was produced in the form of a conductive ink-like composite. The corresponding modifier, graphite and polystyrene were thoroughly mixed with mesitylene for 2 h (Figure 2) using a magnetic stirrer. After that, 2 min of sonication was performed in order to obtain a medium thick solution. The ink-like composite was dropped $5 \mu\text{L}$ onto the surface of a screen-printed carbon electrodes (SPCE) and dried at 40°C for at least 1 h in order to remove the solvent. Once the sensor was prepared, the next step is an activation [33,34] in order to enhance sensing performances of modified ink (Figure 3 displays the typical gain achieved after activation). Electrochemical activation consisted of 10 repetitive voltammetric cycles at $50 \text{ mV}\cdot\text{s}^{-1}$ between 1.5 and -1.5 V using $10 \text{ mM H}_2\text{O}_2$ in phosphate buffer (pH 7). After activation, electrodes were rinsed with deionized water and dried in air.

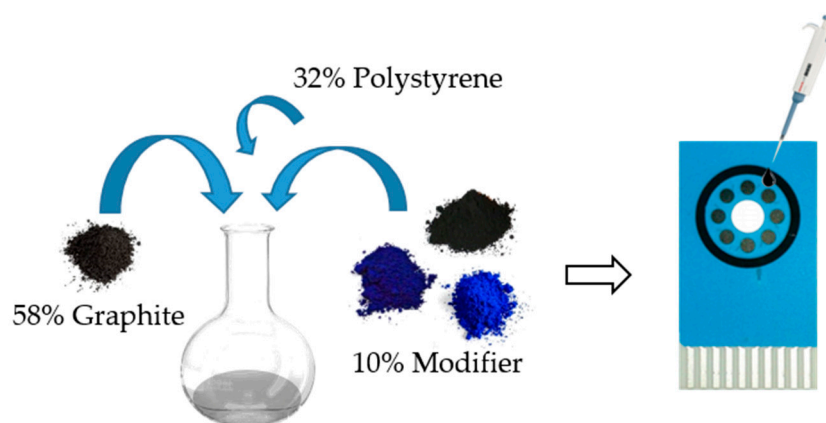


Figure 2. Scheme of the experimental procedure for the electrode surface modification. Firstly, an ink-like solution was prepared incorporating the corresponding modifier. Then, $5 \mu\text{L}$ was dropped on the electrode surface and dried a 40°C . An activation step is done with hydrogen peroxide to finally record the voltammetric signal.

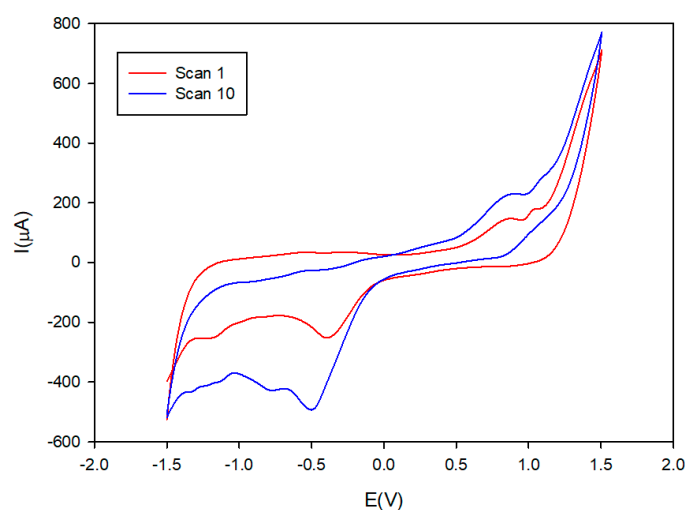


Figure 3. Comparison of the Cobalt (II) phthalocyanine/SPCE-Ink before (scan 1) and after (scan 10) the activation. Electrochemical activation consists of 10 repetitive voltammetric cycles at $50 \text{ mV}\cdot\text{s}^{-1}$ between 1.5 and -1.5 V using $10 \text{ mM H}_2\text{O}_2$ in phosphate buffer (pH 7). After activation, electrodes were rinsed with deionized water and dried in air.

2.4. Characterization by Scanning Electron Microscopy

The morphological characterization of the modified screen-printed electrode was performed by Scanning Electron Microscopy (SEM). A scanning electron microscope with field emission gun (FEG-SEM) of Zeiss, model MERLIN SM0087 was used.

2.5. Sample Preparation

According to the European Pharmacopoeia [35] the size of the data set needed for building the calibration is dependent on interfering properties and the number of analytes that needs to be handled in the model. In the majority of the cases, the size of the learning data set for calibration needs to be large when the interfering variations are acquired randomly. However, when the major interferences can be controlled they can be varied according to a statistical experimental design.

In this case, the second option was accomplished using a tilted factorial experimental design [36] 3^3 (27 samples) for the train subset. This tilted model consisted of a factorial design with a 45° rotation in each axis. With this approach it is possible to avoid the repetition of numeric values. Meanwhile, the validation of the constructed model was done with an external test set (12 samples), these were distributed randomly within the experimental domain (0 to 500 $\mu\text{mol}\cdot\text{L}^{-1}$) for each compound (Figure 4).

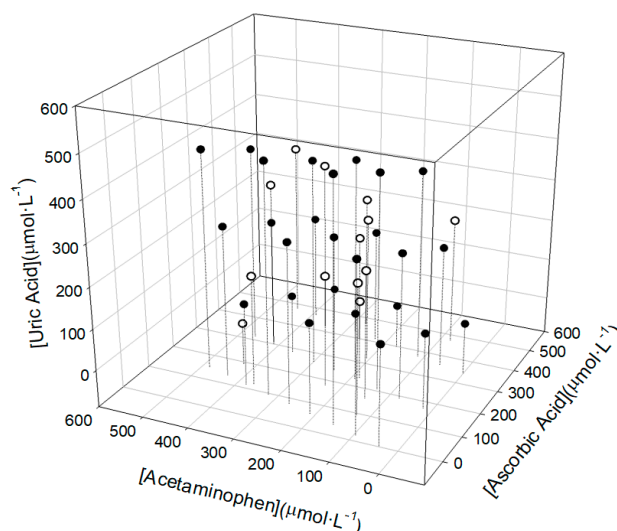


Figure 4. Representation of the tilted factorial experimental design employed (3^3) where it can be observed how the test samples (in white) are distributed covering all the space of the training samples (in black).

Samples were prepared in buffer solution (50 mM phosphate buffer solution at pH 7 containing 0.1 M KCl). Fresh stock solutions of pharmaceutical compounds were prepared the same day of the measurements, in order to avoid/reduce the day-to-day variability.

2.6. Data Processing

The statistical treatment and data analysis were performed using routines developed by the authors using MATLAB R2017a (MathWorks, Natick, MA, USA); in particular, the functionalities “plsregress” from the Statistics and Machine Learning Toolbox, was the one employed for the response model; the web page Clustvis [37] was the one used for PCA calculation; Sigmaplot (Systat Software Inc., San Jose, CA, USA) was used to graphically represent and analyze the results.

3. Results and Discussion

3.1. Characterization of the Surface

A SEM characterization was performed in order to investigate the spatial distribution of the ink-nanoparticles and to verify if the particles were all on the external surface or in the inner layers. As can be observed in Figure 5, the different modifiers are distributed quasi-homogeneous between the graphite layers. The size of the nanoparticles is below 1 μm .

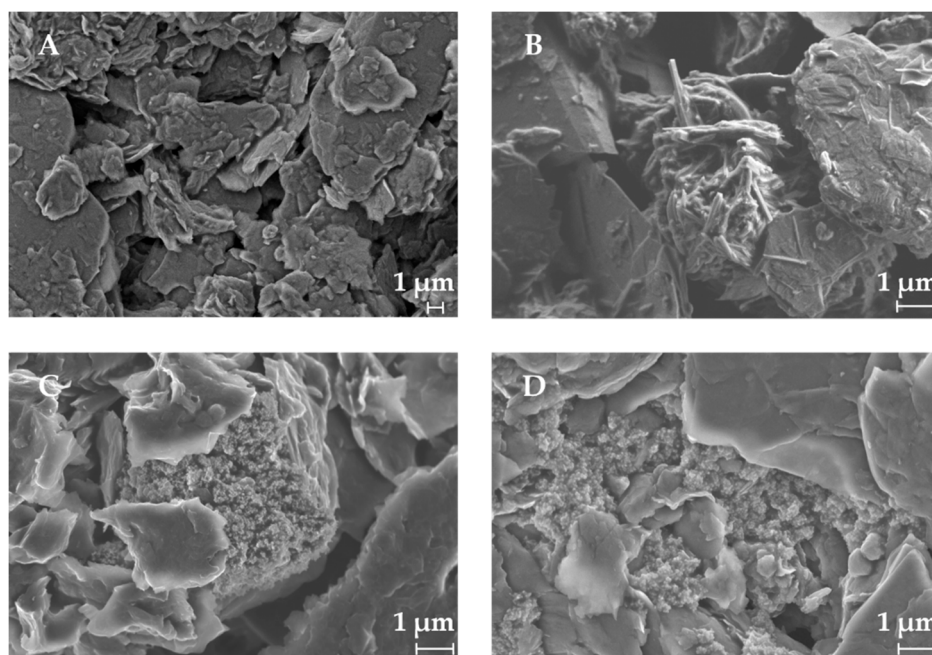


Figure 5. Scanning Electron Microscopy (SEM) characterization of (A) Graphite/SPCE-Ink, (B) Cobalt (II) phthalocyanine/SPCE-Ink, (C) Copper oxide (II)/SPCE-Ink and (D) Prussian blue/SPCE-Ink.

3.2. Voltammetric Array Response

The four aforementioned modifications used to perform this work, were selected among six modifications candidates (Graphite, Cobalt(II) phthalocyanine, Copper oxide (II), Prussian blue, Polypyrrole doped and Palladium) to construct the sensor array. This selection facilitates the modification in form of an ink. In addition, these nanomaterials are the ones with extended experience in the laboratory (although used in a different electrode format, the epoxy-graphite composites [38]). The behaviors of these sensors for each compound were evaluated individually. Once the voltammograms were collected, a preliminary qualitative analysis was performed in order to evaluate the complementarity of the sensors. The chemometric tool used was PCA. The information collected in this case to perform the PCA calculation was the unfolded data. If electrodes are redundant they would appear superimposed in the PCA graph, while a different response will manifest in their separation. As can be seen in Figure 6, each sensor showed performance in different regions. This fact accomplishes a relevant role in the execution of the electronic tongue, justifying the good contribution of the four prepared electrodes in the sensor array. In addition, this analysis made us discard from the sensor array system the Palladium and Polypyrrole sensors, because they were not able to provide distinction between the different substances (Figure 6). According to these criteria, the other modifiers could be classified as good candidates because they provided a wide range of variability between the substances. In addition, the vast majority of the signals were far away from zero, meaning they provide useful information to the system.

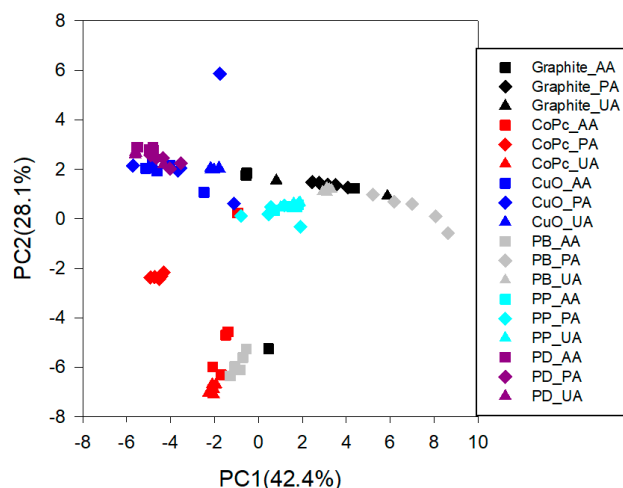


Figure 6. Score plot of the two components obtained after Principal Component Analysis (PCA) analysis. Five replicates for each sensor were done determining the three compounds of interest: Acetaminophen, Ascorbic acid and Uric acid.

After this pre-selection step, voltammograms for each of the selected electrodes towards individual compounds were secondly evaluated. Two scans were performed choosing the second one to represent the voltammetric response.

Therefore, following the conditions described in Section 2.1, a stock solution of $300 \mu\text{mol}\cdot\text{L}^{-1}$ of these compounds was evaluated. As can be observed in Figure 7, slightly different signals were obtained for the different compounds of interest, a necessary requirement for the performance of the electronic tongue.

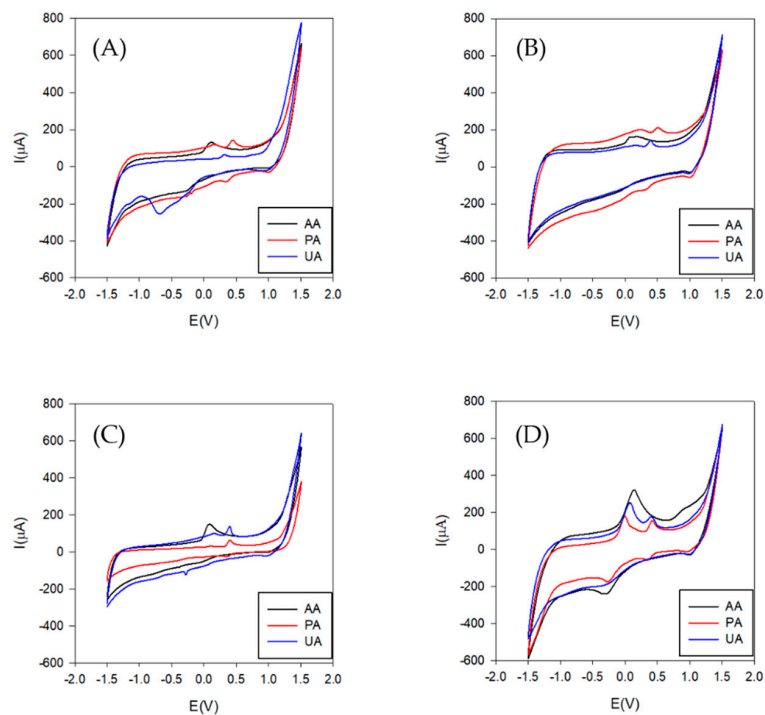


Figure 7. Voltammetric response for Acetaminophen (PA), Ascorbic acid (AA) and Uric acid (UA) using the four finally selected inks. (A) Cobalt (II) phthalocyanine/SPCE-Ink; (B) Prussian blue/SPCE-Ink; (C) Graphite/SPCE-Ink; (D) Copper oxide (II)/SPCE-Ink. The range of potential was from -1.5 to 1.5 V. The scan rate was $50 \text{ mV}\cdot\text{s}^{-1}$ and step rate of 9 mV . A $300 \mu\text{mol}\cdot\text{L}^{-1}$ individual solution was employed for the four modified screen-printed electrodes.

3.3. Characterization of the Modified Integrated Screen-Printed Electrodes

3.3.1. Calibration Curves

To evaluate the behavior of each sensor for each compound separately, some calibration curves were performed using Cyclic voltammetry (CV) technique representing the peak height which corresponds to the maximum of the oxidation signal. This kind of experiment is important to determine the linear range and the maximum concentration of each compound for the final experiment (electronic tongue).

As can be observed in Figure 8, the studied ranges were linear for all the compounds. Therefore, for the ET development the concentration working range was from 0 to 500 $\mu\text{mol}\cdot\text{L}^{-1}$ for Acetaminophen, Ascorbic acid and Uric acid. The linear relationship and the calibration equations for each sensor are represented in Table 1.

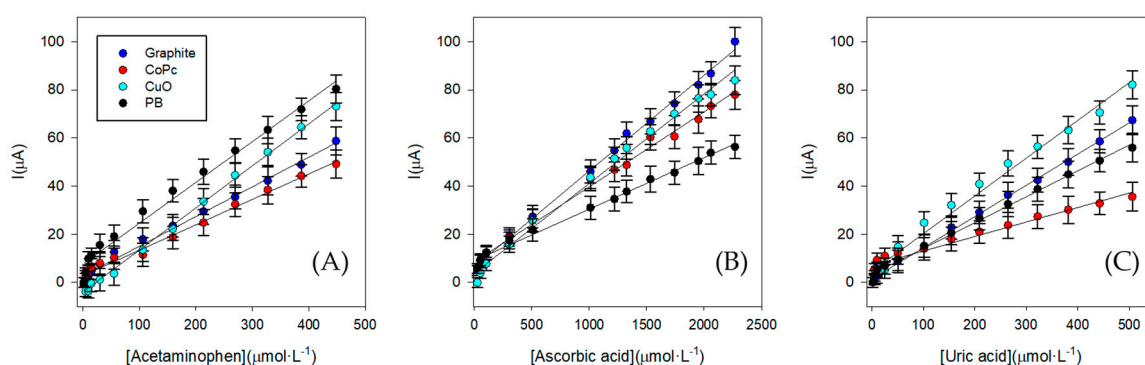


Figure 8. Calibration curves for three replicates ($n = 3$) to determine the concentration working range for the three compounds under study for the four modified screen-printed electrodes. (A) Acetaminophen, (B) Ascorbic acid, (C) Uric acid.

Table 1. Calibration data (y vs. x) for the separate determination of Acetaminophen, Ascorbic acid and Uric acid employing the integrated sensor array chosen.

Compounds	Graphite	Cobalt (II) Phthalocyanine	Copper Oxide (II)	Prussian Blue
Acetaminophen	$y = 0.1234x + 2.6656$ $R^2 = 0.993$	$y = 0.1057x + 2.7753$ $R^2 = 0.991$	$y = 0.1749x - 4.0453$ $R^2 = 0.997$	$y = 0.1696x + 7.5897$ $R^2 = 0.984$
Ascorbic Acid	$y = 0.0398x + 6.5307$ $R^2 = 0.997$	$y = 0.0311x + 8.5678$ $R^2 = 0.993$	$y = 0.0372x + 3.8868$ $R^2 = 0.992$	$y = 0.0214x + 9.0457$ $R^2 = 0.992$
Uric Acid	$y = 0.1298x + 4.6275$ $R^2 = 0.999$	$y = 0.0534x + 9.3828$ $R^2 = 0.996$	$y = 0.1569x + 15.231$ $R^2 = 0.988$	$y = 0.1074x + 7.6534$ $R^2 = 0.995$

3.3.2. Stability and Reproducibility Studies

After the calibration characterization, a stability and reproducibility study was done in order to verify that the sensors were capable of supporting the number of measurements necessary for the Electronic tongue (ET) development. The procedure used to analyze the durability/stability of the sensors consisted on measuring a stock solution of Acetaminophen ($165 \mu\text{mol}\cdot\text{L}^{-1}$) 30 times. A blank, in PBS solution, was inserted between each measurement to evaluate if the system was presenting fouling effect.

In all cases, the four sensors showed stable responses with Relative Standard Deviation (%RSD) of 3.9%, 6.3%, 5.5% and 8.2% for Graphite, Copper oxide (II), Prussian blue and Cobalt (II) phthalocyanine electrodes, respectively. No fouling effect was either observed in this study, when examining any trend among the blanks.

The next step was to study the reproducibility of construction of the ink-modified SPCE sensor. The experiment was done preparing four sensors by triplicate ($n = 3$) and measuring consecutively with an acetaminophen stock solution. The results for each sensor present a good reproducibility, showing the best for the Prussian blue with a relative standard deviation (RSD) of 0.8% (Table 2).

Table 2. Reproducibility of construction of each sensor with the results of the relative standard deviation (RSD).

Sensor	RSD%
Graphite/SPCE-Ink	2.9
Cobalt (II) phthalocyanine/SPCE-Ink	7.5
Copper oxide (II)/SPCE-Ink	1.3
Prussian blue/SPCE-Ink	0.8

3.4. Qualitative Analysis: Principal Component Analysis (PCA)

Once the characterization was accomplished, a PCA was performed in order to evaluate the discrimination power of the sensors (Figure 9). The information collected in this case to perform the PCA calculation was the sensitivity of the calibration curves. Once it was confirmed that the different electrodes presented a differentiated electrochemical behavior towards the different compounds under study, allowing the detection for the three compounds, the next step was the characterization of the sensor array chosen.

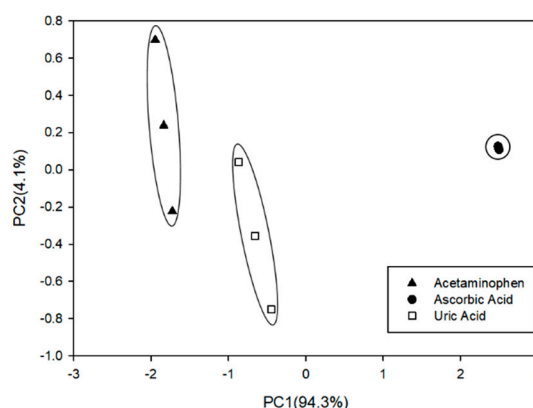


Figure 9. Score plot of the two components obtained after PCA analysis. The PCA shows three clusters across the PC1 (94.3%). These clusters correspond to the studied compounds for $n = 3$ replicates. These results were obtained using the sensor array chosen.

3.5. Quantitative Analysis: Partial Least Squares (PLS) Regression

Once the qualitative analysis was completed, the data was processed in order to build a model able to quantify each compound individually. As results of the high complexity of the data, it was mandatory to use pretreatments that leads to less noisy and more homogeneous data interpretation. Eventually, the Standard Normal Variate (SNV) [39] method was used as a pretreatment tool and the Partial Least Squares (PLS) technique for the model building. SNV method allowed to reduce the scatter effect of the measurements applying an easy mathematical process; it consists on the subtraction of the measurement mean to the measure and followed by dividing the data by its standard deviation, obtaining in this way a normalized base line for all the samples. A PLS1 approach was next employed, in which one model with single output was built for each compound. The number of the latent variables (LVs) [40] for each model were also optimized to achieve the lowest error possible and to avoid the overfitting. The final PLS models were defined for eight components or latent variables (LVs) for Acetaminophen and 7 LVs for the other two.

In Figure 10 it can be observed the comparison of the obtained vs. expected results for training sample set (dark dots), for each compound. In the same graph for each compound the testing sample set (white dots) were projected, allowing the visualization of the feasibility of each model.

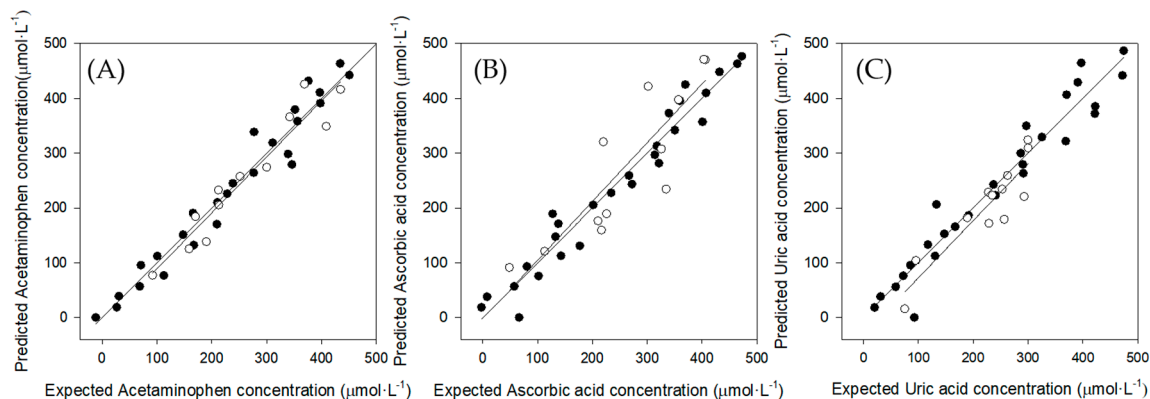


Figure 10. Obtained vs. expected concentrations results plots for the training set (black dots) and the testing set (white dots) for (A) Acetaminophen, (B) Ascorbic acid and (C) Uric acid.

The comparison general trend was expressed as the linear regression of the comparison line. As it can be observed in Table 3, for all the studied compounds, the y-intercept and slope of the training and testing test regressions include 0 and 1 respectively, taking into account their confidence interval (95%). Regarding the correlation coefficients for all the regressions, they are close to 1. Therefore, this satisfactory trend confirms the potential of the proposed approach.

Table 3. Results of the fitted regression curves for obtained vs. expected values, for the training and testing subsets of samples and the three considered compounds (intervals calculated at the 95% confidence level). NRMSE: normalized root mean square error.

Set	Analyte	R ²	Slope	Intercept (μmol·L ⁻¹)	NRMSE
Training Set (n = 27)	Acetaminophen	0.962	1.00 ± 0.09	0 ± 25	0.90
	Ascorbic acid	0.955	1.00 ± 0.09	0 ± 25	0.97
	Uric acid	0.940	1.00 ± 0.11	0 ± 31	1.12
Testing Set (n = 12)	Acetaminophen	0.915	1.02 ± 0.22	-13 ± 28	0.7
	Ascorbic acid	0.762	1.07 ± 0.42	-3 ± 54	1.41
	Uric acid	0.829	1.04 ± 0.33	-32 ± 36	0.85

To evaluate also the fitting degree of the models the NRMSE parameter, Normalized Root Mean Square Error, was calculated according to Equation (1).

$$\text{NRMSE} = \frac{\sqrt{\frac{\sum_i (x_{\text{expected}} - x_{\text{predicted}})^2}{j \cdot N - 1}}}{c_{\text{max}} - c_{\text{min}}} \quad (1)$$

where x_{expected} is the theoretical concentration of the sample, $x_{\text{predicted}}$ is the predicted concentration, j is the number of analytes considered, N the number of samples, c_{max} is the maximum concentration and c_{min} is the minimum concentration. All the information about the models are summarized in Table 3.

As can be observed, in practice, the test sample subset had the lowest NRMSE for the Acetaminophen and Uric acid compound, so the predictive capabilities of the models performed in satisfactory way. However, for the Ascorbic acid compound slightly larger values were obtained. Regarding to the correlation coefficients, the better values were observed for the training sample set.

Comparing these results with previous work [41] done in our group employing the same modifiers but with different technology, in this case, the bulk modification of a graphite-epoxy composite electrode (Table 4), we can highlight as a main conclusion that the results obtained are similar, showing a slight improvement in the present report in terms of slope and intercept of the comparison lines. Accordingly, the combination of the screen-printed integrated voltammetry array sensors and chemometric tools allows the possibility to determine and quantify simultaneously a substance in the presence of other ones with overlapping redox potential.

Table 4. Results of the fitted regression curves for obtained vs. expected values, for the training and testing subsets of samples and the three considered compounds (intervals calculated at the 95% confidence level) for the previous works [41].

Set	Analyte	R ²	Slope	Intercept (μmol·L ⁻¹)
Training Set (n = 33)	Acetaminophen	0.968	0.942 ± 0.031	32 ± 21
	Ascorbic acid	0.947	0.933 ± 0.040	36 ± 25
	Uric acid	0.923	0.873 ± 0.046	58 ± 25
Testing Set (n = 15)	Acetaminophen	0.848	0.895 ± 0.105	82 ± 71
	Ascorbic acid	0.908	0.919 ± 0.081	65 ± 41
	Uric acid	0.753	0.871 ± 0.138	−8 ± 86

4. Conclusions

The presented work reported for a first time in our group the simultaneous voltammetric detection of Acetaminophen, Ascorbic acid and Uric acid combining a multi screen-printed electrode integrated array with advanced chemometrics. This study clearly illustrates one of the capabilities of the biomimetic systems, concretely, ET. The ET strategy allowed the possibility, first to differentiate the compounds, next, to determine and quantify simultaneously a substance in the presence of other ones with overlapping redox potentials.

The samples were analyzed by combining the Cyclic voltammetry (CV) technique for extracting the fingerprint of the individual substances and mixtures, coupled with chemometrics strategies, which permitted the resolution of the overlapping signal and its identification.

The use of Principal Component Analysis (PCA) as qualitative tool was useful to determine the capability of the sensors to distinguish the different compounds under study, while in a further purpose resolution and quantification of ternary mixtures was achieved employing Partial Least Squares Regression (PLS) model.

Therefore, this work demonstrates the advantages of screen-printed integrated electrochemical sensors for on-field analysis results in a promising methodology that could substitute the classical time-consuming, methods. Future works will try to detect these analytes in real pharmaceutical study case.

Author Contributions: All authors contributed to this work. M.B.-S.-E. performed the Partial Least Squares (PLS) calculations. M.d.V. planned, got the funding and supervised the experiments. D.O.-A. performed the experiments, prepared the graphs and wrote the first version of the manuscript.

Funding: This research was funded by the Spanish Government (Ministerio de Economía y Competitividad) grant number CTQ2016-80170-P. M.B.-S.-E. was funded by Secretaria d'Universitats i Recerca del Departament d'Empreses i Coneixement de la Generalitat de Catalunya and to European Social Fund, European Union through a FI fellowship. D.O.-A. was funded by Universitat Autònoma de Barcelona through a PIF fellowship. M.d.V. was funded by program ICREA Academia.

Conflicts of Interest: The authors declare no conflict of interest.

References

1. Sanghavi, B.J.; Srivastava, A.K. Simultaneous voltammetric determination of acetaminophen, aspirin and caffeine using an in situ surfactant-modified multiwalled carbon nanotube paste electrode. *Electrochim. Acta* **2010**, *55*, 8638–8648. [\[CrossRef\]](#)
2. Madrakian, T.; Haghshenas, E.; Afkhami, A. Simultaneous determination of tyrosine, acetaminophen and ascorbic acid using gold nanoparticles/multiwalled carbon nanotube/glassy carbon electrode by differential pulse voltammetric method. *Sens. Actuators B Chem.* **2014**, *193*, 451–460. [\[CrossRef\]](#)
3. Hu, G.; Ma, Y.; Guo, Y.; Shao, S. Electrocatalytic oxidation and simultaneous determination of uric acid and ascorbic acid on the gold nanoparticles-modified glassy carbon electrode. *Electrochim. Acta* **2008**, *53*, 6610–6615. [\[CrossRef\]](#)
4. Beard, E.L. The American society of health system pharmacists. *JONA's Healthc. Law Eth. Regul.* **2001**, *3*, 78–79. [\[CrossRef\]](#)
5. Kaur, H.; Halliwell, B. Action of biologically-relevant oxidizing species upon uric acid. Identification of uric acid oxidation products. *Chem. Biol. Interact.* **1990**, *73*, 235–247. [\[CrossRef\]](#)
6. Miland, E.; Miranda Ordieres, A.J.; Tuñón Blanco, P.; Smyth, M.R.; Fágáin, C.Ó. Poly(o-Aminophenol)-Modified Bionzyme Carbon Paste Electrode for the Detection of Uric Acid. *Talanta* **1996**, *43*, 785–796. [\[CrossRef\]](#)
7. Dejaegher, B.; Bloomfield, M.S.; Smeyers-Verbeke, J.; Vander Heyden, Y. Validation of a Fluorimetric assay for 4-aminophenol in paracetamol formulations. *Talanta* **2008**, *75*, 258–265. [\[CrossRef\]](#)
8. Llorent-Martínez, E.J.; Šatínský, D.; Solich, P.; Ortega-Barrales, P.; Molina-Díaz, A. Fluorimetric SIA optosensing in pharmaceutical analysis: Determination of paracetamol. *J. Pharm. Biomed. Anal.* **2007**, *45*, 318–321. [\[CrossRef\]](#)
9. Sirajuddin; Khaskheli, A.R.; Shah, A.; Bhangar, M.I.; Niaz, A.; Mahesar, S. Simpler spectrophotometric assay of paracetamol in tablets and urine samples. *Spectrochim. Acta Part A Mol. Biomol. Spectrosc.* **2007**, *68*, 747–751. [\[CrossRef\]](#)
10. Ortega Barrales, P.; Fernández De Córdova, M.L.; Molina Díaz, A. Indirect determination of ascorbic acid by solid-phase spectrophotometry. *Anal. Chim. Acta* **1998**, *360*, 143–152. [\[CrossRef\]](#)
11. Akay, C.; Gümüşel, B.; Degim, T.; Tartilimis, S.; Cevheroglu, S. Simultaneous determination of acetaminophen, acetylsalicylic acid and ascorbic acid in tablet form using HPLC. *Drug Metabol. Drug Interact.* **1999**, *15*, 197–206. [\[CrossRef\]](#) [\[PubMed\]](#)
12. Thomis, R.; Roets, E.; Hoogmartens, J. Analysis of tablets containing aspirin, acetaminophen, and ascorbic acid by high-performance liquid chromatography. *J. Pharm. Sci.* **1984**, *73*, 1830–1833. [\[CrossRef\]](#) [\[PubMed\]](#)
13. Capella-Peiró, M.E.; Bose, D.; Rubert, M.F.; Esteve-Romero, J. Optimization of a capillary zone electrophoresis method by using a central composite factorial design for the determination of codeine and paracetamol in pharmaceuticals. *J. Chromatogr. B Anal. Technol. Biomed. Life Sci.* **2006**, *839*, 95–101. [\[CrossRef\]](#) [\[PubMed\]](#)
14. Sun, X.; Niu, Y.; Bi, S.; Zhang, S. Determination of ascorbic acid in individual rat hepatocyte cells based on capillary electrophoresis with electrochemiluminescence detection. *Electrophoresis* **2008**, *29*, 2918–2924. [\[CrossRef\]](#) [\[PubMed\]](#)
15. Švorc, L. Determination of caffeine: A comprehensive review on electrochemical methods. *Int. J. Electrochem. Sci.* **2013**, *8*, 5755–5773.
16. Zhu, X.; Xu, J.; Duan, X.; Lu, L.; Zhang, K.; Yu, Y.; Xing, H.; Gao, Y.; Dong, L.; Sun, H.; et al. Controlled synthesis of partially reduced graphene oxide: Enhance electrochemical determination of isoniazid with high sensitivity and stability. *J. Electroanal. Chem.* **2015**, *757*, 183–191. [\[CrossRef\]](#)
17. Ren, W.; Luo, H.Q.; Li, N.B. Simultaneous voltammetric measurement of ascorbic acid, epinephrine and uric acid at a glassy carbon electrode modified with caffeic acid. *Biosens. Bioelectron.* **2006**, *21*, 1086–1092. [\[CrossRef\]](#)
18. Bard, A.J. Chemical modification of electrodes. *J. Chem. Educ.* **1983**, *60*, 302. [\[CrossRef\]](#)
19. Serrano, N.; Prieto-Simón, B.; Cetó, X.; del Valle, M. Array of peptide-modified electrodes for the simultaneous determination of Pb(II), Cd(II) and Zn(II). *Talanta* **2014**, *125*, 159–166. [\[CrossRef\]](#)
20. Serrano, N.; González-Calabuig, A.; del Valle, M. Crown ether-modified electrodes for the simultaneous stripping voltammetric determination of Cd(II), Pb(II) and Cu(II). *Talanta* **2015**, *138*, 130–137. [\[CrossRef\]](#)

21. Pérez-Ràfols, C.; Serrano, N.; Díaz-Cruz, J.M.; Ariño, C.; Esteban, M. Penicillamine-modified sensor for the voltammetric determination of Cd(II) and Pb(II) ions in natural samples. *Talanta* **2015**, *144*, 569–573. [CrossRef] [PubMed]
22. Wawrzyniak, U.E.; Ciosek, P.; Zaborowski, M.; Liu, G.; Gooding, J.J. Gly-Gly-His immobilized on monolayer modified back-side contact miniaturized sensors for complexation of copper ions. *Electroanalysis* **2013**, *25*, 1461–1471. [CrossRef]
23. Cipri, A.; del Valle, M. Pd nanoparticles/multiwalled carbon nanotubes electrode system for voltammetric sensing of tyrosine. *J. Nanosci. Nanotechnol.* **2014**, *14*, 6692–6698. [CrossRef] [PubMed]
24. Del Valle, M. Bioinspired sensor systems. *Sensors* **2011**, *11*, 10180–10186. [CrossRef] [PubMed]
25. Toko, K. *Biomimetic Sensor Technology*; Cambridge University Press: Cambridge, UK, 2000.
26. Röck, F.; Barsan, N.; Weimar, U. Electronic nose: Current Status and future trends. *Chem. Rev.* **2008**, *108*, 705–725. [CrossRef] [PubMed]
27. Tahara, Y.; Toko, K. Electronic tongues—A review. *IEEE Sens. J.* **2013**, *13*, 3001–3011. [CrossRef]
28. Pallejà, T.; Tresanchez, M.; Teixidó, M.; Palacin, J. Bioinspired electronic white cane implementation based on a LIDAR, a Tri-Axial accelerometer and a tactile belt. *Sensors* **2010**, *10*, 11322–11339. [CrossRef] [PubMed]
29. Vlasov, Y.; Legin, A.; Rudnitskaya, A.; di Natale, C.; D’Amico, A. Nonspecific sensor arrays (“electronic tongue”) for chemical analysis of liquids (IUPAC technical report). *Pure Appl. Chem.* **2005**, *77*, 1965–1983. [CrossRef]
30. Lavine, B.K.; Workman, J., Jr. Chemometrics. *Anal. Chem.* **2002**, *74*, 2763–2769. [CrossRef]
31. Hanrahan, G. Computational neural networks driving complex analytical problem solving. *Anal. Chem.* **2010**, *82*, 4307–4313. [CrossRef]
32. Dropsens. 8W Screen-Printed Carbon Electrode. Available online: http://www.dropsens.com/pdfs_productos/new_brochures/8w110.pdf (accessed on 25 July 2019).
33. Daniels, J.S.; Pourmand, N. Label-free impedance biosensors: Opportunities and challenges. *Electroanalysis* **2007**, *19*, 1239–1257. [CrossRef] [PubMed]
34. González-Sánchez, M.I.; Gómez-Monedero, B.; Agrisuelas, J.; Iniesta, J.; Valero, E. Highly activated screen-printed carbon electrodes by electrochemical treatment with hydrogen peroxide. *Electrochem. Commun.* **2018**, *91*, 36–40. [CrossRef]
35. Council of Europe. *European Pharmacopoeia*, 8th ed.; Directorate for the Quality of Medicines & HealthCare: Strasbourg, France, 2013.
36. Cetó, X.; Céspedes, F.; Pividori, M.I.; Gutiérrez, J.M.; del Valle, M. Resolution of phenolic antioxidant mixtures employing a voltammetric bio-electronic tongue. *Analyst* **2012**, *137*, 349–356. [CrossRef] [PubMed]
37. Metsalu, T.; Vilo, J. ClustVis: A web tool for visualizing clustering of multivariate data using principal component analysis and heatmap. *Nucleic Acids Res.* **2015**, *43*, W566–W570. [CrossRef] [PubMed]
38. Alegret, S.; Alonso, J.; Bartolí, J.; Céspedes, F.; Martínez-Fàbregas, E.; del Valle, M. Amperometric Biosensors based on bulk-modified epoxy graphite biocomposites. *Sens. Mater.* **1996**, *8*, 147–153.
39. Gemperline, P. *Practical Guide to Chemometrics*, 2nd ed.; CRC press: Boca Raton, FL, USA, 2006.
40. Abdi, H. Partial least squares regression and projection on latent structure regression (PLS regression). *Wiley Interdiscip. Rev. Comput. Stat.* **2010**, *2*, 97–106. [CrossRef]
41. Gutés, A.; Calvo, D.; Céspedes, F.; del Valle, M. Automatic sequential injection analysis electronic tongue with integrated reference electrode for the determination of ascorbic acid, uric acid and paracetamol. *Microchim. Acta* **2007**, *157*, 1–6. [CrossRef]



ARTICLE 2

Voltammetric sensing using an array of modified SPCE coupled with machine learning strategies for the improved Identification of opioids in presence of cutting agents

Dionisia Ortiz-Aguayo, Karolien De Wael and Manel del Valle

Journal of Electroanalytical Chemistry, 902, 115770.



Voltammetric sensing using an array of modified SPCE coupled with machine learning strategies for the improved identification of opioids in presence of cutting agents

Dionisia Ortiz-Aguayo^a, Karolien De Wael^b, Manel del Valle^{a,*}

^a Sensors and Biosensors Group, Department of Chemistry, Universitat Autònoma de Barcelona, Edifici Cn, 08193 Bellaterra, Spain

^b AXES Research Group, Department of Bioscience Engineering, University of Antwerp, Groenenborgerlaan 171, 2020 Antwerp, Belgium

ARTICLE INFO

Keywords:

Opioids
Electronic tongue
Principal component analysis
Voltammetric sensors
Silhouette

ABSTRACT

This work reports the use of modified screen-printed carbon electrodes (SPCEs) for the identification of three drugs of abuse and two habitual cutting agents, caffeine and paracetamol, combining voltammetric sensing and chemometrics. In order to achieve this goal, codeine, heroin and morphine were subjected to Square Wave Voltammetry (SWV) at pH 7, in order to elucidate their electrochemical fingerprints. The optimized SPCEs electrode array, which have a differentiated response for the three oxidizable compounds, was derived from Carbon, Prussian blue, Cobalt (II) phthalocyanine, Copper (II) oxide, Polypyrrole and Palladium nanoparticles ink-modified carbon electrodes. Finally, Principal Component Analysis (PCA) coupled with Silhouette parameter assessment was used to select the most suitable combination of sensors for identification of drugs of abuse in presence of cutting agents.

1. Introduction

Heroin (3,6-diacetylmorphine, diamorphine, Fig. 1) is a potent synthetic opiate drug synthesized by acetylation of morphine, typically obtained from poppy seeds. The appearance of this illicit drug changes from white (pure form) to dark brown due to impurities formed during the manufacturing process or adulterants and cutting agents. The common impurities come from opium alkaloids or by-products from the fabrication process (morphine, monoacetylmorphine, codeine, acetyl-codeine, noscapine, papaverine or lead) [1–2]. Apart from impurities, it is frequent in illegal commerce to adulterate the narcotic with some cuttings agents; these can be pharmacologically inactive, just like sugars or starch or, otherwise, with pharmacological activity such as paracetamol, caffeine, phenobarbital, quinine, clenbuterol, procaine or levamisole, among others [3]. In this work, two mentioned examples were used as cutting agents, paracetamol and caffeine, as certain side-effects are considered for their choice. In the case of paracetamol, it simulates the analgesic effect of heroin; in the case of caffeine, it helps vaporizing heroin at lower temperature, facilitating its smoking.

Morphine (Fig. 1) is the opiate alkaloid which effectively causes disruption in the central nervous system, that is why it is pharmacologically used to relieve pain in patients [4]. The interest of analysis of

this compound relies, first, in the monitoring of therapeutic levels in patients. Secondly, the analysis of morphine is relevant for epidemiological purposes of drug abuse control and also in forensic cases; in this field it can be an evidence of heroin usage and can help identifying causes of intoxication or death in situations of clinical and pathological interest. Codeine (3-methylmorphine, Fig. 1) is a second main alkaloid separated from opium. This drug is extensively used to treat mild to moderate pain and for cough suppression in clinical practice. Despite its medical applications, the abuse of this narcotic can also create health risks.

The widespread use of illicit drugs has led to an increase effort toward developing and improving methods for their detection per example in a seizure of a smuggled consignment, or in biological samples, which is still a very challenging task from an analytical point of view. Several analytical methods have been developed for individual determination of these compounds such as capillary electrophoresis [5–6] chemiluminescence [7–8], diffuse reflectance near-infrared spectroscopy [9], high-performance liquid chromatography, gas chromatography [10] and surface plasmon resonance based on immunosensors [11]. Drawbacks associated are the high costs and time-consuming nature of these methods, accompanied by a need of complex procedures such as sample pre-treatment step to obtain satis-

* Corresponding author.

E-mail address: manel.delvalle@uab.cat (M.del Valle).

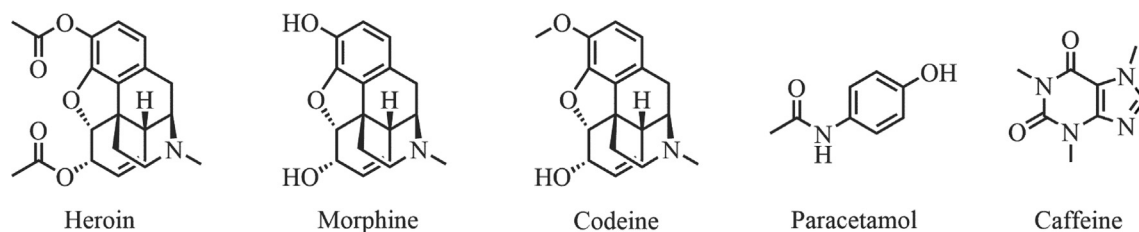


Fig. 1. Chemical structure of the three drugs of abuse considered in this study (heroin, morphine and codeine) and their corresponding cutting agents (paracetamol and caffeine).

factory results. For these reasons, the development of cheap, effective, rapid and simultaneous determination procedures in pharmaceutical and illicit samples is still a big challenge in analytical chemistry. One approach to overcome the above shortcomings can be the use of electrochemical sensors, as most of these drugs of abuse are electroactive substances. Electrochemical sensors may provide some advantages, such as a cheap and simple use, low detection limits, wide linear response ranges, good stability and reproducibility.

Electrochemical methods, in special voltammetry, have been already used for individual determination of opiate alkaloids, because of their advantages in applicability. However, certain difficulties arise when the simultaneous determination of these three compounds is attempted, due to the overlapping of the different voltammograms obtained at traditional electrodes.

In this work, the alternative proposed to tackle the problem is the use of modified electrodes [12], which have fascinated many researchers due to their simplicity, high sensitivity and low cost. This kind of devices provides improvement based on electrocatalysis, avoiding fouling effect and preventing undesirable reactions which can compete kinetically with the desired electrode process [13]. Modified electrodes can be prepared by different techniques based on adsorbing or attaching specific molecules (e.g. peptides [14] or complexing agents [15] to the surface; this may be achieved by self-assembled monolayers [16], chemical grafting, coating and entrapment, e.g. in the form of conductive ink [17]. The last strategy has become interesting in recent times, because the deliberate and controlled modification of the electrode surface can produce new surfaces with interesting properties employed for new devices and applications in electrochemistry. As a further step in electrochemical sensing, a newly, nature-inspired way to proceed, intended to enrich the usable departure information has become popularized: in this, different electrodes may be used in array form, work with them in parallel, and produce advanced applications at insignificant increase of effort or cost [18]. This approach will employ then a set of cross-sensitive, chemical sensors that will provide a complex information-rich response from a sample. This set of complex electrochemical signals generated are next processed using intelligent chemometric algorithms (e.g., machine learning strategies) to allow for the qualitative identification or the quantitative determination of the compounds [19]. As the main character of this work here is the qualitative identification of the compounds considered, firstly, the multivariate data generated was examined using Principal Component Analysis (PCA) [20]; this is normally the first strategy used to visualize similarity between samples. From this PCA analysis, a first grouping of samples could be established and a measure of clustering could be calculated using the Silhouette parameter [21].

The set of SPCE sensors to form the array considered the ensuing six modifiers: Graphite-Ink, Prussian blue-Ink, Cobalt (II) phthalocyanine-Ink, Copper (II) oxide-Ink, Palladium nanoparticles-Ink and Polypyrrole-Ink. In the procedure, these were incorporated one at a time in the array in a step way manner, for which after PCA analysis and calculation of the Silhouette parameter, the improvement of the latter determined the benefits of including the contemplated sensor. In this

way, the best combination of electrodes to form the sensor array could be defined from their actual performance in the identification of the opioids and cutting agents. Eventually, some machine learning strategies were tested and their performance examined, choosing finally a K-nearest neighbor classifier (kNN) as the preferred algorithm.

2. Experimental

2.1. Chemical and reagents

Codeine and heroin were provided by the National Institute of Criminalistics and Criminology (NICC, Belgium). Morphine hydrochloride, potassium monophosphate, potassium chloride and potassium hydroxide were purchased from Sigma-Aldrich (Overijse, Belgium). Cobalt (II) phthalocyanine (CoPc), Copper (II) oxide (CuO) nanopowder (<50 nm), Polypyrrole doped (PP) and Palladium, powder submicron 99.9+ % (Pd), which were used as modifiers, were purchased from Sigma-Aldrich (St. Louis, MO, USA). Prussian blue (PB) was obtained from Acros Organics (Geel, Belgium). The preparation of the ink composite was done using mesitylene and polystyrene, obtained from Sigma-Aldrich (St. Louis, MO, USA). Graphite powder (particle size < 50 μm) was received from BDH (BDH Laboratory Supplies, Poole, UK). Potassium chloride was purchased from Merck (Darmstadt, Germany).

All aqueous solutions were prepared using MilliQ water ($R > 18 \text{ M}\Omega\cdot\text{cm}^{-1}$). The reagents were of analytical reagent grade and used without further purification. Fresh stock solutions were prepared the same day of the measurements, to reduce day to day variability.

2.2. Instrumentation and apparatus

SWV measurements were performed using a Multi-channel Potentiostat/Galvanostat/Impedance Analyzer (MultiPalmSens4, The Netherlands) controlled by Multitrace software. ItalSens graphite screen-printed electrodes containing a graphite working electrode (3 mm diameter), a carbon counter electrode and a (pseudo)silver reference electrode (PalmSens, The Netherlands) were used for the measurements, as received or after modification.

2.3. Modification of the electrode surface

The material used for the modification of the SPCE is a graphite-based ink-like composite. The corresponding modifier, graphite and polystyrene were thoroughly dispersed with mesitylene for 2 hours [17]. After that, 2 minutes of sonication was performed in order to obtain a medium thick solution. The ink-like composite was dropped (1 μL) onto the surface (Fig. 2) of a graphite SPCE and dried at 40 $^{\circ}\text{C}$ for at least 1 hour in order to remove the solvent and let the SPCE operative.



Fig. 2. Scheme of the experimental procedure for the electrode surface modification. Firstly, an ink-like solution was prepared incorporating the corresponding modifier. Then, 1 μL of ink was dropped on the electrode surface and dried at 40 $^{\circ}\text{C}$.

2.4. Characterization of the electrodes by scanning electron microscopy

The morphological characterization of the modified SPCE electrodes was performed by Field Emission Gun-Scanning Electron Microscope (FEG-SEM) of Zeiss, model MERLIN SM0087 and Energy Dispersive X-Ray Analysis (EDX). Imaging was performed based on secondary, back-scattered electrons.

2.5. Procedure

Samples were prepared in phosphate buffer 20 mM containing 100 mM KCl (PBS). This media was used as supporting electrolyte for electrochemical measurements; its pH was adjusted to desired value using a 100 mM KOH solution using a CyberScan 510 pH-meter from Eutech Instruments (Landsmeer, The Netherlands) equipped with a HI-1131 glass bodied pH electrode from Hanna Instruments (Bedfordshire, United Kingdom). SWV measurements were performed by placing a volume of 50 μL of sample solution onto the printed part of the SPCE, which was maintained in horizontal position. The technique employed for the determination of the considered substances was Square Wave Voltammetry (SWV). The single scan SWV parameters were as follows: potential range 0 V to 1.2 V, step potential 5 mV, amplitude 25 mV and frequency 10 Hz, as employed in former studies in the laboratory [22].

2.6. Calculation of Silhouette parameter

PCA is a suitable linear visualization method of multivariate data, that allows the reduction of the dimensionality of a multivariate problem and facilitates the visualization of the groupings of the multivariate profiles by remarking similarities and differences between them, forming sample clusters. PCA is very useful to identify these clusters, but it is normally hard to interpret and to validate the grouping. For this reason, the Silhouette calculation [21] was introduced as a measure of clustering, i.e. how easy is to distinguish between the clusters associated to the different compounds. This strategy refers to a method of interpretation and validation of consistency within clusters of data, providing a numerical figure of how well each object matches its cluster.

The Silhouette is based on the calculation of two parameters: a and b . For each sample i , $a(i)$ is the average distance between i and all other samples within the same cluster. In the case of $b(i)$ is the smallest average distance of i to all samples in any other cluster, of which i is not a member. Silhouette parameter is calculated then as:

$$s(i) = \frac{b(i) - a(i)}{\max\{a(i), b(i)\}} \quad (1)$$

Which can be also written as:

$$s(i) = \begin{cases} 1 - \frac{a(i)}{b(i)}, & \text{if } a(i) < b(i) \\ 0; & \text{if } a(i) = b(i) \\ \frac{b(i)}{a(i)} - 1; & \text{if } a(i) > b(i) \end{cases} \quad (2)$$

The Silhouette value is a measure of how similar an object to its own cluster (cohesion) compared to other clusters (separation). The Silhouette ranges from -1 to $+1$, where a high value (close to $+1$) indicates that the object is well matched to its own cluster. If most samples have a high Silhouette value, then the clustering configuration is appropriate. If many points have a low or negative value, then the clustering configuration may have too many or too few clusters. The average of the Silhouette parameter for the whole set of samples can then be employed as an index to evaluate the overall clustering ability of the selected sensor configuration, in a procedure to obtain the best identification ability.

2.7. Data treatment

The web page Clustvis [23] was the tool used for online PCA calculation; Sigmaplot (Systat Software Inc., San Jose, CA, USA) was used to graphically represent and analyze the results. Microsoft Excel 2016 and Orange open source programming language (University of Ljubljana, Slovenia) [24–25] were used to perform some Silhouette calculations and to generate the identification models for which K-nearest neighbor classifier (kNN), Random Forest, Naive Bayes and Support Vector Machine (SVM) algorithms were employed and compared [26].

3. Results and discussion

This research depicts an intelligent sensor strategy, in which a given opioid is identified, with the possibility of being confounded by a cutting agent, and where the involved technique used is voltammetry. In short, the strategy combines the use of multiple sensor electrochemistry to extract the fingerprint of each compound on each sensor, followed by advanced data processing for interpreting the multi-dimensional generated data.

The study started defining a procedure for the ink modification of the SPCE with their initial characterization and operation. Next, the sensor array was optimized by step by step systematic evaluation of the incorporation of an additional sensor electrode, till maximum identification ability was achieved. To evaluate this, it was used PCA to visualize clustering of target substances and how easily these could be distinguished, together with calculation of a clustering metrics, the Silhouette parameter, to provide a numeric criterion for the optimization of the best sensor array configuration. Finally, kNN and

additional classifiers were used as pattern recognition model to perform automatic identification of the substances considered in our study case.

3.1. Characterization of the electrode surface

Characterization of the ink-modified working electrodes (WE) employed in this work was done using microscopy studies and electrochemical techniques.

A SEM characterization was performed in order to investigate the spatial distribution of the ink-nanoparticles and to verify if the nanoparticles were all on the external surface or in the inner layers. As can be observed in Fig. 3, the different modifiers are distributed quasi-homogeneously between the graphite layers verifying the presence of the expected metals, on their respective inks through their EDX spectra (Fig. 4); electrodes modified with Polypyrrole or unmodified are not shown in the manuscript because of absence of distinctive metallic signals. However, their spectra can be checked in the supplementary material.

After microscopy studies, the effective surface area of bare and modified electrodes was evaluated according to the Randles–Sevcik equation (eq (3)) [27], where n is the number of transferred electrons for the redox reaction (in this case 1), F is the Faraday's constant ($96485 \text{ C}\cdot\text{mol}^{-1}$), c the concentration of electroactive substance ($\text{mol}\cdot\text{cm}^{-3}$), A is the effective area in cm^2 , ν the scan rate ($\text{V}\cdot\text{s}^{-1}$), R the gas constant ($8.314 \text{ J}\cdot\text{mol}^{-1}\cdot\text{K}^{-1}$), T the temperature in K and D is the diffusion coefficient for ferrocyanide ($6.32\cdot 10^{-6} \text{ cm}^2\cdot\text{s}^{-1}$). For that, CV experiments using $20 \text{ mM KH}_2\text{PO}_4$ and 100 mM KCl containing $5 \text{ mM } [\text{Fe}(\text{CN})_6]^{3-}/[\text{Fe}(\text{CN})_6]^{4-}$ solution in the potential range of -0.4 to 0.8 V were performed. Applying 7 different scan rates (0.01 , 0.025 , 0.05 , 0.1 , 0.2 , 0.3 and $0.5 \text{ V}\cdot\text{s}^{-1}$) it could be calculated the active area of each WE from the slope of the regression line of $\nu^{1/2}$ ($\text{V}\cdot\text{s}^{-1}$) vs. $I_p\cdot c^{-1}$ ($\text{A}\cdot\text{cm}^3\cdot\text{mol}^{-1}$). The details of the performed voltammograms can be found in Supplementary Info. Concerning the calculated active areas, these were: 11.7 mm^2 for the bare electrode, 8.2 mm^2 for Graphite/SPCE-Ink, 8.5 mm^2 for Copper (II) oxide/SPCE-Ink and 8.1 mm^2 for Prussian blue/SPCE-Ink. 9.3 mm^2 for Cobalt (II) phthalocyanine/SPCE-Ink, 9.4 mm^2 for Pd nanoparticles/SPCE-Ink and 6.1 mm^2 for Polypyrrole/SPCE-Ink, whereas the geometric area was 7.1 mm^2 ($\varnothing = 3 \text{ mm}$).

$$I_p = 0.4463 \cdot n \cdot F \cdot c \cdot A \cdot \sqrt{\nu} \cdot \left(\frac{nDF}{RT} \right)^{\frac{1}{2}} \quad (3)$$

Summarizing, this section verifies the proper modification of the electrodes via ink-deposit, showing a quasi-homogeneous distribution of the metal nanoparticles between the graphite particles, and yielding the different prepared electrodes comparable active surfaces.

3.2. Electrochemical response

The voltammetric responses for each of the modified screen-printed electrodes were first evaluated towards the five individual compounds (three drugs and two cutting agents), to assure that the generated signals were different enough for the desired application.

As a result, and as described under conditions in Section 2.5, individual stock solutions of $300 \mu\text{mol}\cdot\text{L}^{-1}$ of heroin, morphine, codeine, paracetamol and caffeine in PBS at pH 7 were determined using SWV. It was decided to perform the electrochemical measurements at neutral pH because heroin and morphine undergo some hydrolysis reactions at alkaline pH [3,28]. Measurements were done in random sequence to avoid any structure in the signals.

Heroin gives rise to an irreversible oxidation split peak at $+0.81 \text{ V}$ on SPCE at pH 7 due to the oxidation of the amino group, which is in concordance with the literature [4,28–30]. An additional oxidation peak was observed at a lower potential $+0.40 \text{ V}$ due to the oxidation of the phenol group of 6-monoacetylmorphine (6-MAM) a trace constituent present in the sample (typical content, 3 wt%). In detail, 6-MAM is an impurity from heroin synthesis, resulting in the incomplete acetylation of morphine and also a product of hydrolysis of the alkaloid present in most heroin samples [1]. As can be seen in Fig. 5, the peak corresponding to the oxidation of the phenol group of 6-MAM and morphine is overlapped with the oxidation peak of paracetamol. The same situation occurs between the second oxidation peaks of heroin and morphine with codeine, foreseeing a case with difficult signal resolution.

As shown in Fig. 5, complex and highly overlapped signals are obtained along the whole voltammograms and with the different sensors considered. The fingerprint of each compound from a single sensor is not enough information, which can represent a limitation for the identification of the considered substances alone. For better assess-

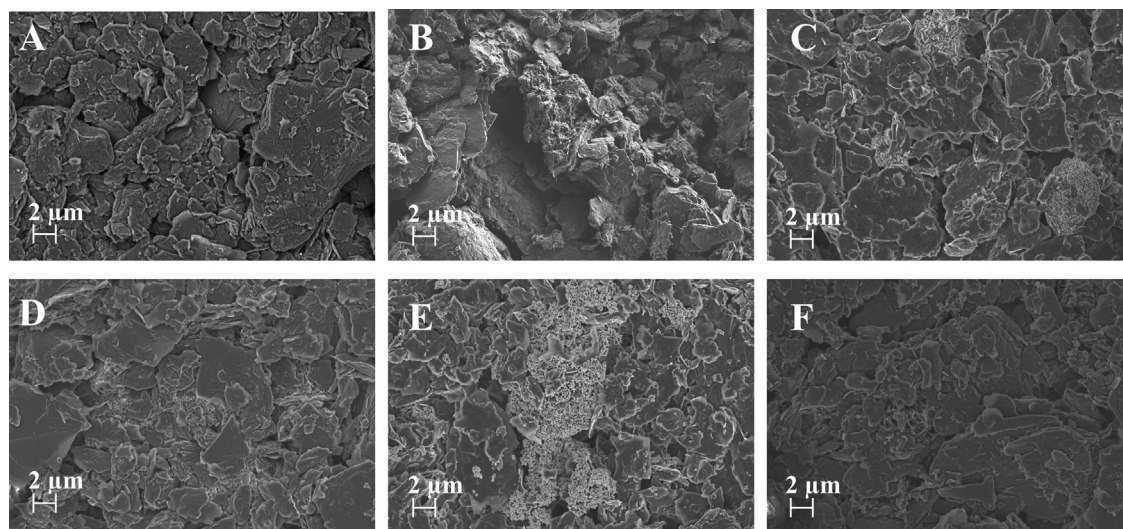


Fig. 3. SEM characterization of (A) Graphite/SPCE-Ink, (B) Cobalt (II) phthalocyanine/SPCE-Ink, (C) Copper (II) oxide/SPCE-Ink, (D) Prussian blue/SPCE-Ink (E) Pd nanoparticles/SPCE-Ink and (F) Polypyrrole/SPCE-Ink.

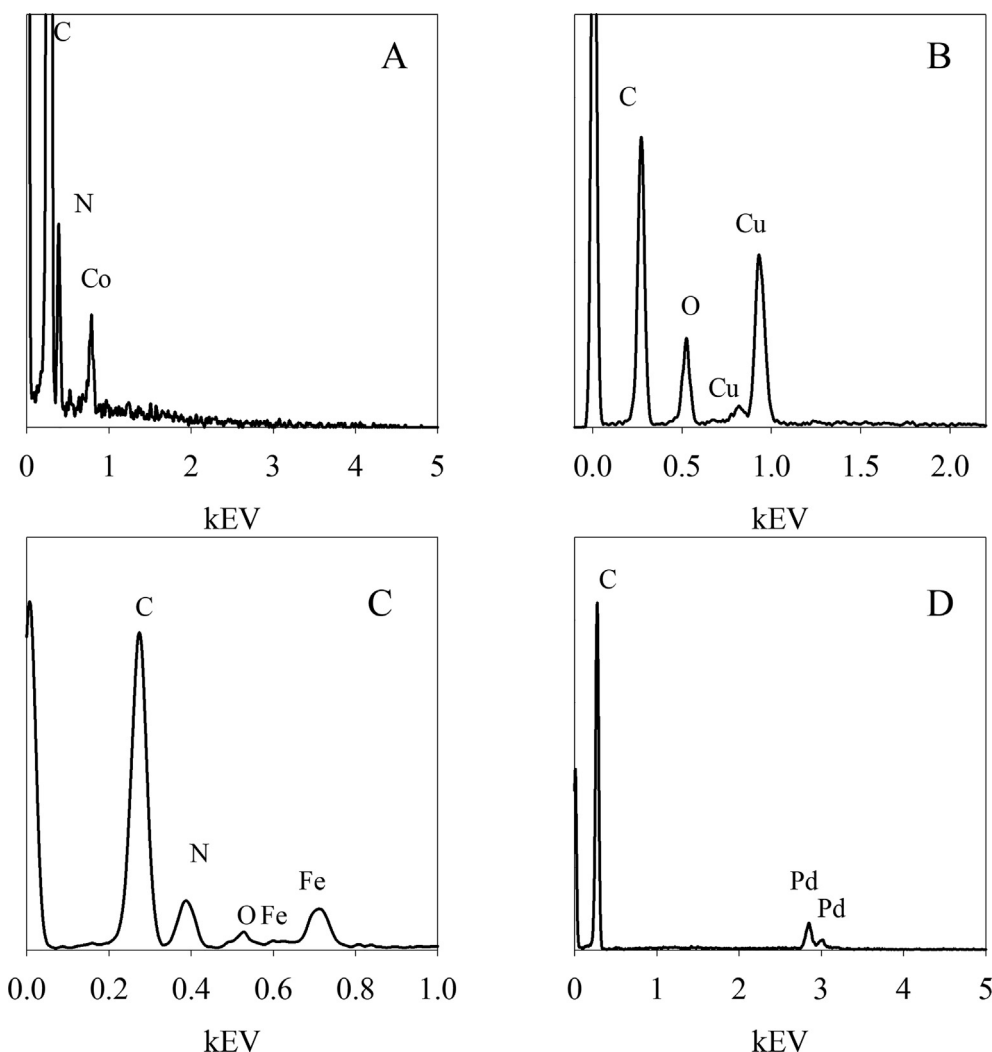


Fig. 4. EDX analysis of (A) Cobalt (II) phthalocyanine/SPCE-Ink, (B) Copper oxide (II)/SPCE-Ink, (C) Prussian blue/SPCE-Ink and (D) Pd nanoparticles/SPCE-Ink.

ment, a chemometric assay was further done: PCA was carried out to better evaluate mathematically the similarities and the complementarities between the voltammetric responses of the compounds of interest.

3.3. Selection of the working electrodes using Principal Component Analysis strategies

Once the voltammograms of the five compounds of interest under study were collected with the six modified screen-printed electrodes, a PCA was performed. Each sample was measured in four replicates to check any drift or memory effect in electrodes. The complete set of samples were measured in random order, to roll out any structure in the data. The information gathered in this case to perform the mathematical calculation was one voltammogram per each sample, and per each electrode, and strategy was to check for similarities and differences among these. With PCA strategy it is expected that the redundant electrodes (electrodes that contribute with the same information) would appear superimposed in the scores space, while electrodes with different responses will manifest in distinction in it. Moreover, this strategy may allow to detect if electrodes can discriminate the studied compounds and how similar are the replicates of one sample.

The scores of samples corresponding to the two first principal components (PC) (the coordinates of each sample/electrode combination in the new space defined by the transformation defined for the PCA) for the five compounds of interest are represented in Fig. 6. In

Fig. 6A, it can be seen that the major part of the variability among the samples, the most relevant information is explained for PC1 (81.1%). In this plot, it is clear to observe that Polypyrrole (PP) dominated the response in comparison with the other modifiers, also with a high dispersion for the replicas, distorting all the system. This argument was applied to discard it from the set of modified electrodes. The discrepancies in the voltammograms for this electrode can be also observed in Fig. 5D. In there, the voltammogram from the PP modified ink did not show very different shapes for the different compounds under study, on the contrary, a high non-specific variability, e.g. the baseline was observed. For all the mentioned reasons, a refinement of the calculation was performed removing the PP modified electrode to evaluate the rest of candidates. The results are shown in Fig. 6B. As it can be seen, the relevant information of the samples using the two first PCs made 60.7% of the total variability. Regarding to this plot, it is possible to notice that the purple sensor samples, which correspond to the Prussian blue (PB) modifier, presented large dispersion in comparison with the others, mainly a lack of stability in the voltammetric responses. Because of this inconsistency, the Prussian blue modifier was also discarded from the system. These undesired features can be observed in the different elongated purple clusters (symbol shape replicas) shown in Fig. 6B.

At this point, a new PCA was calculated with the remaining four modifier inks: Carbon, Cobalt phthalocyanine (II), Copper (II) oxide and Pd nanoparticles (Fig. 7A). Applying the previous criteria commented for the PP and PB modifiers, it was decided to remove

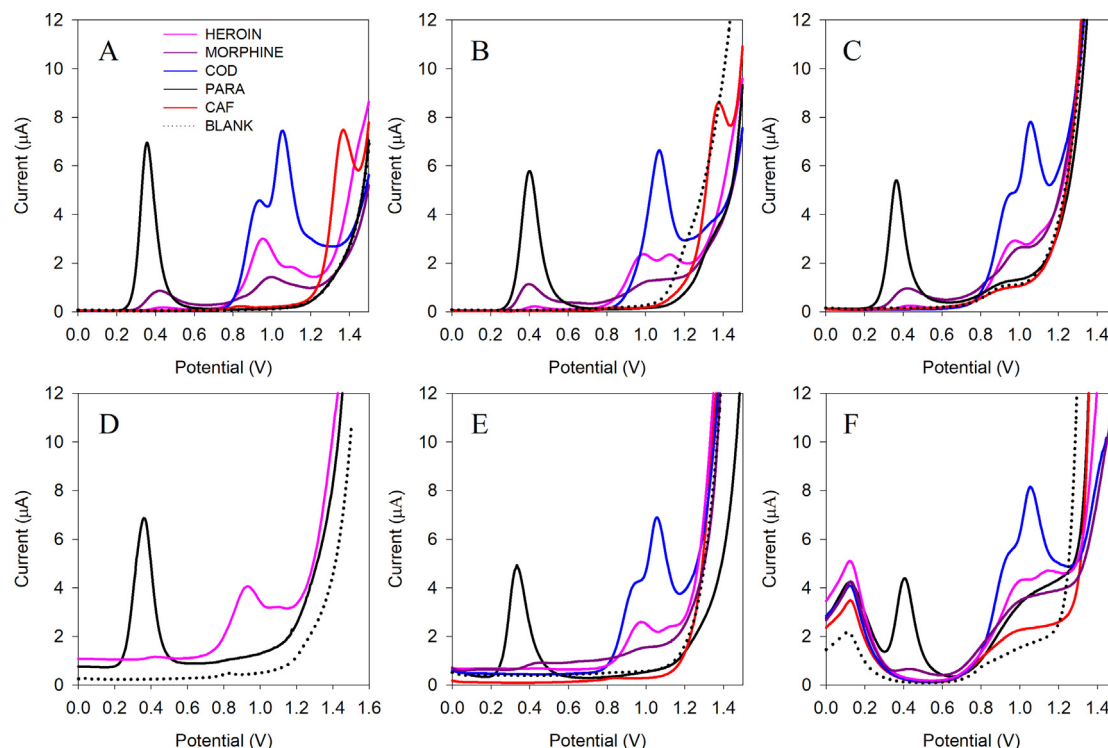


Fig. 5. Voltammetric response for Heroin (pink), Morphine (purple), Codeine (blue), Paracetamol (black) and Caffeine (red) using the six modified electrodes. (A) Graphite/SPCE-Ink; (B) Cobalt (II) phthalocyanine/SPCE-Ink; (C) Pd nanoparticles/SPCE-Ink; (D) Polypyrrole/SPCE-Ink; (E) Copper (II) oxide/SPCE-Ink; (F) Prussian blue/SPCE-Ink. SWV measurements were performed by placing 50 μL solution onto SPCE. The single scan SWV parameters were as follows: potential range 0 V to 1.2 V, step potential 5 mV, amplitude 25 mV and frequency 10 Hz. The scan rate was $50 \text{ mV}\cdot\text{s}^{-1}$. A $300 \mu\text{mol}\cdot\text{L}^{-1}$ individual solution was employed for the six modified screen-printed electrodes.

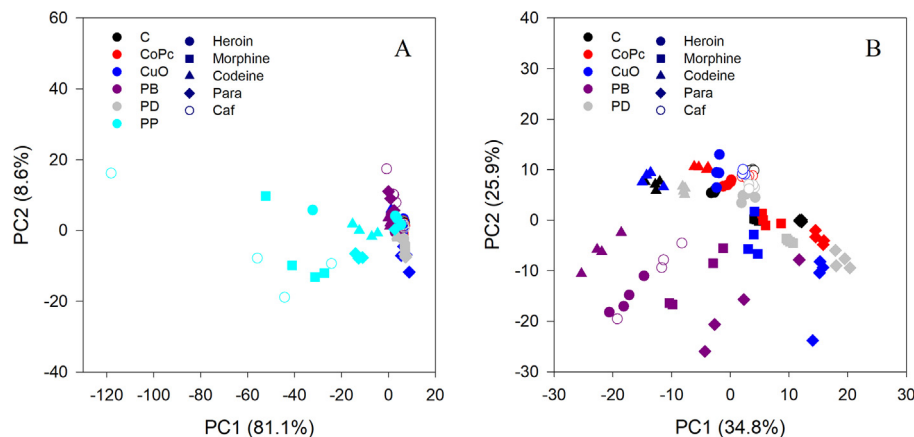


Fig. 6. Score plot of the two components obtained after PCA analysis. 4 replicates for each sensor were done determining the five compounds of interest: heroin, morphine, codeine, paracetamol and caffeine with a concentration of $300 \mu\text{mol}\cdot\text{L}^{-1}$. (A) Use of an array with six SPCEs: Graphite/SPCE-Ink; Cobalt (II) phthalocyanine/SPCE-Ink; Copper oxide (II)/SPCE-Ink; Prussian blue/SPCE-Ink; Pd nanoparticles/SPCE-Ink and Polypyrrole/SPCE-Ink. (B) Use of the optimized sensor array: Graphite/SPCE-Ink; Cobalt (II) phthalocyanine/SPCE-Ink; Copper oxide (II)/SPCE-Ink; Prussian blue/SPCE-Ink and Pd nanoparticles/SPCE-Ink.

the Copper (II) oxide electrode from the sensor array. This sensor presented some drift among the four replicates of almost all the studied compounds (like PP and PB), causing a distortion in the clusters of the pure compounds. But at this point, the PCA strategy was able to differentiate clearly the cutting agents and the drugs of abuse (see how the symbols group together in Fig. 7A and 7B). Finally, the last PCA with the three modifiers selected is shown in Fig. 7B. As it can be observed, these candidates showed different response towards the studied molecules, and with limited dispersion, facilitating the assignment of substances to its class.

3.4. Optimization of the sensor array from the Silhouette parameter

Once a first assessment of sensors was done, the final optimization was developed, in this case with use of an objective numeric criteria. This second part consisted to determine which combination of the selected sensors is more suited to obtain the best performance in the identification of the studied compounds. To reply this question, a new strategy, which was the calculation of the Silhouette parameter as a measure of the clustering degree was applied for the first time in our group to deal with the problem. And from this point here, the

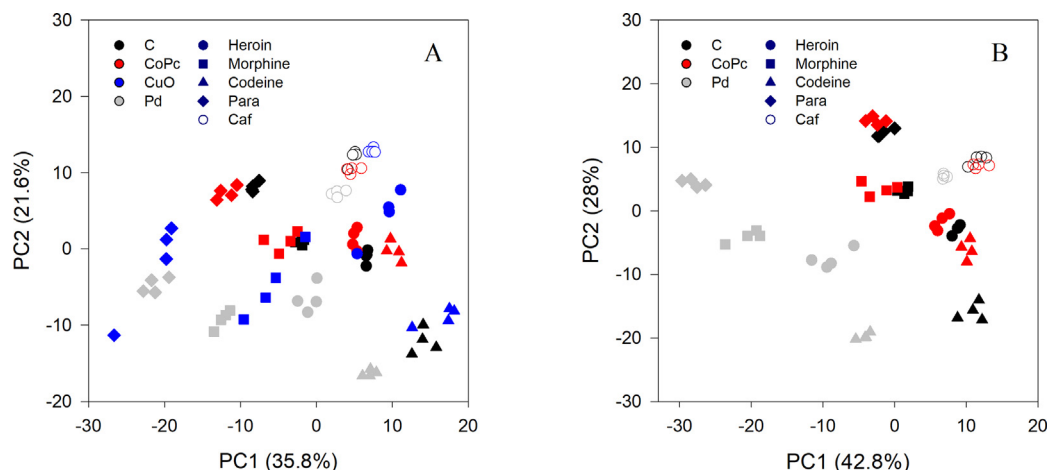


Fig. 7. Score plot of the two components obtained after PCA analysis. 4 replicates for each sensor were done determining the five compounds of interest: heroin, morphine, codeine, paracetamol and caffeine with a concentration of $300 \mu\text{mol}\cdot\text{L}^{-1}$. (A) With the 4 SPCE array: Graphite/SPCE-Ink; Cobalt (II) phthalocyanine/SPCE-Ink; Pd nanoparticles/SPCE-Ink; Copper (II) oxide/SPCE-Ink. (B) With the 3 SPCE array: Graphite/SPCE-Ink; Cobalt (II) phthalocyanine/SPCE-Ink and Pd nanoparticles/SPCE-Ink.

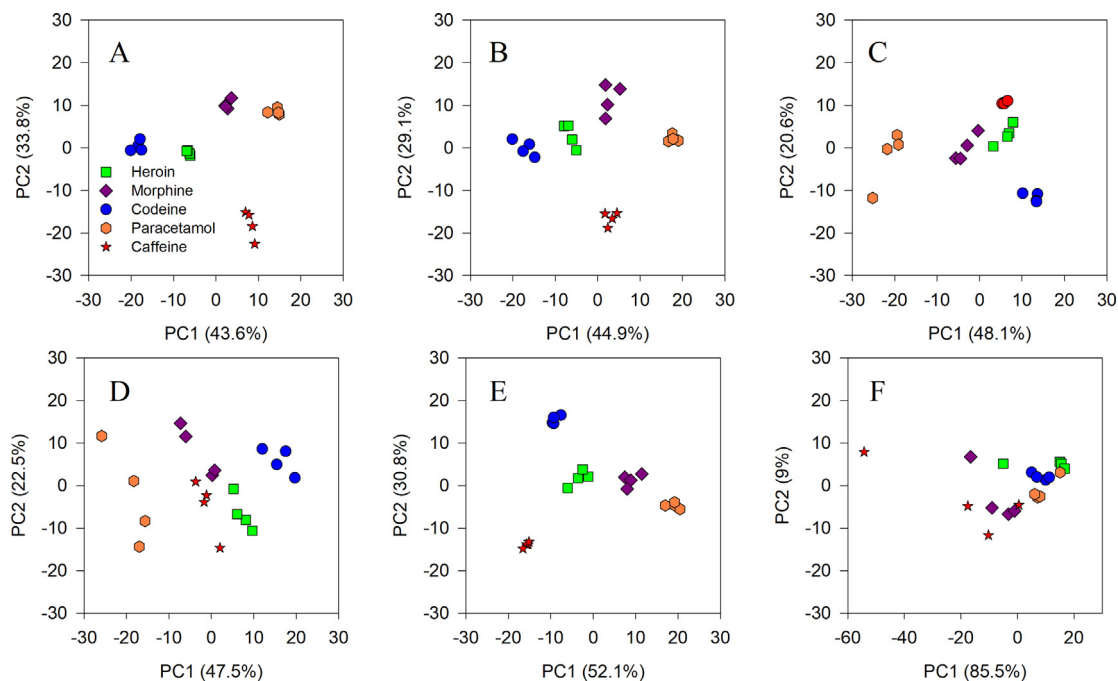


Fig. 8. Score plot of the two first components obtained after PCA analysis of information provided by each single SPCE electrode. A total of 20 samples were analyzed corresponding to quadruplicate determination of $300 \mu\text{mol}\cdot\text{L}^{-1}$ of heroin, morphine, codeine, paracetamol and caffeine, using: (A) Graphite/SPCE-Ink, (B) Cobalt (II) phthalocyanine/SPCE-Ink, (C) Copper (II) oxide/SPCE-Ink, (D) Prussian blue/SPCE-Ink, (E) Pd nanoparticles/SPCE-Ink and (F) Polypyrrole/SPCE-Ink.

complete set of voltammograms from a given sample, as determined by the specific sensors forming the array, was used for the data processing. The first step for this was to do the unfolding of the data, i.e. the different voltammograms corresponding to a sample were concatenated in a unique column and used as available information for the processing. This is the usual way to cope with this limitation of PCA, which works vectorially, not matrix-like [31]. Alternatively, there are N -way alternatives to this treatment, but are much less spread in the field, and are of more difficult use [32].

With this multiple information approach, a first PCA analysis was done, which performed an initial, unsupervised clustering of the data according to their similarity in the multivariate space. Next, the Silhouette parameter was calculated to assess the goodness of the accomplished clustering, whereas a better clustering will embrace an easier identification of a given sample. In fact, the Silhouette calculation provides a parameter for each sample, based on $a(i)$ and $b(i)$, which shows the intra-cluster compared with the inter-cluster variability. In this way, it is possible to quantify numerically which cluster is better

Table 1

Average of Silhouette parameter for the stepwise optimization of the sensor array.

Number of SPCE in the array	Modified SPCE in the array	Silhouette parameter
1	C	+0.849*
	CoPc	+0.735
	CuO	+0.640
	PB	+0.328
	Pd	+0.817
	PP	+0.041
2	C-CoPc	+0.841
	C-Pd	+0.863*
	CoPc-Pd	+0.848
3	C-CoPc-Pd	+0.877*

* Optimal configuration obtained after systematic evaluation on each step.

discriminated in comparison with all the clusters involved in the system. It is important to highlight that the data collected to perform this kind of analysis were the scores of the two first principal components (PC1 and PC2) obtained previously in the PCA score graphs from the unfolded voltammograms data. This treatment is useful to reduce the dimensionality in the case of voltammetric data; essentially it just transforms the voltammograms from a multidimensional matrix to a 2D matrix with condensed and simplified info.

Therefore, the procedure to afford this case was the calculation of the Silhouette parameter for different situations, in the stepwise strategy for the optimization of the sensor array. Firstly, the calculation was done for each sensor individually, that is, from the six sensors prepared initially.

As it can be observed in PCA score plots on Fig. 8, the sensors which produced worst clustering were CuO, PB and PP. This fact can be verified with the calculation of the Silhouette parameter, as summarized in Table 1. In this case, the three electrodes mentioned presented the worst Silhouette parameter with values of +0.640 for CuO, +0.328 for PB and +0.041 for PP. This first assessment, showing that best option with a single sensor is using the SPCE with graphite ink, yielded an average Silhouette parameter of +0.849. With this information, it is important to remark that with any of the three sensors alone (C, CoPc and Pd) the identification application could be carried out, since the Silhouette parameter can be considered acceptable. However, our primary objective is to complement the information from different sensors in an electronic tongue approach to improve final performance and reach a better degree of clustering. This may be of help in scenarios with unfavorable S/N ratio, as would be the case with lower concentration of the species sought, or with additional interference effects. Therefore, in the stepwise process, a second electrode is incorporated in the array, and the Silhouette parameter is calculated to provide the best combination of sensors from the set C, CoPc and Pd.

The results of these combinations are collected in Fig. 9. Apparently, the visualization of the clusters for the different compounds in the three cases is quite good, so the crucial argument to decide which combination is the most suitable for the case of study is the Silhouette parameter. As it can be observed in Fig. 9, the global clustering for the three cases is largely similar, showing the best combination for the couple C + Pd with a calculated s of +0.863 (Fig. 9B). To finally take the decision, the last possibility combining the three modified sensors was evaluated. The PCA obtained for the combination using three SPCE sensors, and $s = +0.877$ is shown in Fig. 10B.

As a result, it can be concluded that the use of the combination of the modifying inks with these three modifiers allowed the optimal individual determination of the compounds under study. As it can be observed in Fig. 10B, the different sensors proportionated the particular response toward the individual compounds, showing five clusters, with close grouping, and clear differentiation. The PCA obtained is appropriate, representing the relevant information between PC1 and PC2 with a variance of 76.5%. The average Silhouette parameter finally obtained, +0.877 is a high value, and close to the highest attainable value, +1.00, forecasting an easy identification in the final 'intelligent' identification of the selected compounds. It is also clear that the information provided by the combination of the three modifiers previously commented is very similar to the combination of graphite and Pd nanoparticles with a Silhouette global parameter of +0.863, and a simpler setup of only two sensors in the array. For future applications, it was decided to maintain Pd in the sensor array in order to collect the information it provided. As it can be seen in Fig. 7B, the electrochemical response proportionated by this modifier sensor supplied differentiated response (grey points in a rather separate region) in comparison with the remaining working electrodes. The performed analysis would be also a base criterion to ascertain if the application can be performed with just a single sensor (the one with graphite ink, in this case), or the complexity involved in the use of a sensor array balances the obtained gains. Lastly, the use of CoPc alone was completely discarded exhibiting a value of Silhouette global parameter of +0.735.

3.5. K-nearest neighbor classifier

To conclude the final section of this study, a kNN classifier method was used to perform the final automated and intelligent operation. KNN [33] is one of the most fundamental and simple unsupervised classification methods and should be one of the first choices for a classification study when there is little or no prior knowledge about the distribution of the data. KNN just stores all the available cases and classifies the new data or case based on a similarity measure. The only parameter to tune is the number of closest neighbors to consider (the variable k) which can be obtained examining which is the best perfor-

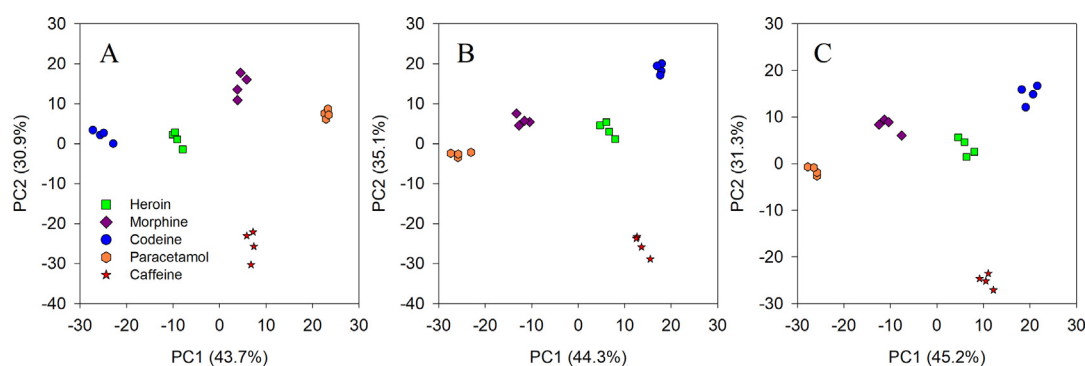


Fig. 9. Score plot of the two first components obtained after PCA analysis. A total of 20 samples were analyzed corresponding to quadruplicate determination of $300 \mu\text{mol L}^{-1}$ of heroin, morphine, codeine, paracetamol and caffeine, with pair of SPCE electrodes: (A) C-CoPc, (B) C-Pd (C) CoPc-Pd.

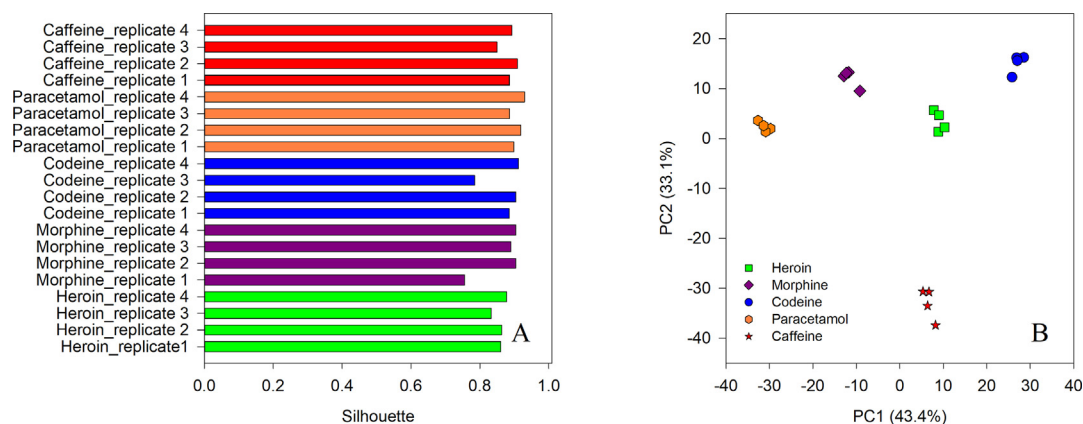


Fig. 10. (A) Silhouette plot for the different samples considered using the best combination of three SPCE sensors (C-CoPc-Pd). (B) Score plot of the two components obtained after PCA analysis. A total of 20 samples were analysed corresponding to quadruplicate determination of $300 \mu\text{mol-L}^{-1}$ of heroin, morphine, codeine, paracetamol and caffeine using the three SPCE sensors.

Table 2

Confusion matrix after applying the kNN algorithm, using leave-one-out cross-validation and $k = 4$.

		Predicted					
Actual	Heroin	Heroin	Morphine	Codeine	Paracetamol	Caffeine	Σ
	Morphine	0	4	0	0	0	4
	Codeine	0	0	4	0	0	4
	Paracetamol	0	0	0	4	0	4
	Caffeine	0	0	0	0	4	4
	Σ	4	4	4	4	4	20

Table 3

Results of the statistical calculation using some machine learning strategies as kNN ($k = 4$), Forest, Naive Bayes and SVM employing leave-one-out cross-validation.

Model	Compound	Classification accuracy	Precision	Sensitivity	Specificity
kNN	Heroin	1.0	1.0	1.0	1.0
	Morphine	1.0	1.0	1.0	1.0
	Codeine	1.0	1.0	1.0	1.0
	Paracetamol	1.0	1.0	1.0	1.0
	Caffeine	1.0	1.0	1.0	1.0
Random Forest	Heroin	1.0	1.0	1.0	1.0
	Morphine	1.0	1.0	1.0	1.0
	Codeine	1.0	1.0	1.0	1.0
	Paracetamol	1.0	1.0	1.0	1.0
	Caffeine	1.0	1.0	1.0	1.0
Naive Bayes	Heroin	1.0	1.0	1.0	1.0
	Morphine	1.0	1.0	1.0	1.0
	Codeine	1.0	1.0	1.0	1.0
	Paracetamol	1.0	1.0	1.0	1.0
	Caffeine	1.0	1.0	1.0	1.0

mance when k is varied. In this particular case, the number of intergrands in the cluster is known beforehand, as it corresponds to the number of replicas of each substance tested, $k = 4$.

Table 2 shows the confusion matrix of the identification accomplished. Cross validation of the identification model was done with the leave one out variant, as there were not many samples in the data set. With these excellent identification performance, statistic indicators of goodness of identification were also excellent in all instances, with indicators of classification accuracy, precision, sensitivity and specificity, all 100%. Additional machine learning strategies were tested in order to compare the obtained results. The identification algorithms tested were Random Forest, Naive Bayes and Support Vector Machines (SVM). As it can be observed in Table 3, Random Forest

and Naive Bayes produce proper results in all the indicators previously mentioned. In the case of SVM, certain degree of misclassification of particular samples is observed, specifically heroin and morphine. In other words, the vast majority of algorithms employed demonstrated a correct identification of the samples, thanks to the excellent degree of clustering achieved by the optimized sensor system.

4. Conclusions

The presented work reports for a first time the qualitative analysis for the determination of the following drugs of abuse: heroin, morphine and codeine and their corresponding cutting agents (caffeine

and paracetamol) combining the use of modified screen-printed electrodes with chemometrics tools, in what has been named a multisensory analysis system or electronic tongue approach.

The samples were analyzed by SWV technique for extracting the fingerprint of the individual substances, coupled with advanced data treatment such as PCA and Silhouette parameter calculation. The use of PCA allowed firstly the pre-selection of the best sensors to define the candidates for the sensor array and secondly, after calculation of the Silhouette parameter, permitted its accurate optimization, showing the most suitable combination of working electrodes. Thanks to the application of both tools, the final combination selected was with electrodes modified with Graphite, Cobalt (II) phthalocyanine and Pd nanoparticle inks. With the optimized sensor array, different identification models were tested demonstrating that kNN could be easily developed, and showing performance among the best.

The reported work demonstrates the advantages of the modification through an ink-like solution composite of screen-printed electrochemical sensors for on-field analysis results in a promising methodology that could substitute the classical time-consuming methods. Future works are directed to equivalent case studies, but with quantification purposes of arbitrary mixtures of opioids and cutting agents.

CRediT authorship contribution statement

Dionisia Ortiz-Aguayo: Conceptualization, Methodology, Investigation, Data curation, Visualization, Writing – original draft, Software. **Karolien De Wael:** Formal analysis, Funding acquisition. **Manel del Valle:** Conceptualization, Methodology, Software, Writing – review & editing.

Declaration of Competing Interest

The authors declare that they have no known competing financial interests or personal relationships that could have appeared to influence the work reported in this paper.

Acknowledgments

This research was funded by the Spanish Ministry of Science and Innovation, MCINN (Madrid) through project PID2019-107102RB-C21. This project has received funding from the European Union's Horizon 2020 Research and Innovation programme under the grant agreement No 833787, project BorderSens. Manel del Valle thanks the support from the program ICREA Academia. Dionisia Ortiz-Aguayo thanks to Universitat Autònoma de Barcelona for PIF fellowship. Karolien De Wael acknowledges the support from the University of Antwerp (IOF) and FWO (infrastructure).

References

- [1] E. Kaa, Impurities, adulterants and diluents of illicit heroin. Changes during a 12-year period, *Forensic Sci. Int.* 64 (2–3) (1994) 171–179.
- [2] C. Cole, L. Jones, J. McVeigh, A. Kicman, Q. Syed, M. Bellis, Adulterants in illicit drugs: A review of empirical evidence, *Drug Test. Anal.* 3 (2) (2011) 89–96.
- [3] J. Broséus, N. Gentile, P. Esseiva, The cutting of cocaine and heroin: A critical review, *Forensic Sci. Int.* 262 (2016) 73–83.
- [4] A. Navae, A. Salimi, H. Teymourian, Graphene nanosheets modified glassy carbon electrode for simultaneous detection of heroine, morphine and noscapine, *Biosens. Bioelectron.* 31 (1) (2012) 205–211.
- [5] R.B. Taylor, A.S. Low, R.G. Reid, Determination of opiates in urine by capillary electrophoresis, *J. Chromatogr. B Biomed. Appl.* 675 (2) (1996) 213–223.
- [6] Z. Zhang, B.o. Yan, K. Liu, Y. Liao, H. Liu, CE-MS analysis of heroin and its basic impurities using a charged polymer-protected gold nanoparticle-coated capillary, *Electrophoresis* 30 (2) (2009) 379–387.
- [7] Y. Zhuang, X. Cai, J. Yu, H. Ju, Flow injection chemiluminescence analysis for highly sensitive determination of noscapine, *J. Photochem. Photobiol. A Chem.* 162 (2–3) (2004) 457–462.
- [8] Y. Zhuang, D. Zhang, H. Ju, Sensitive determination of heroin based on electrogenerated chemiluminescence of tris(2,2'-bipyridyl)ruthenium(II) immobilized in zeolite Y modified carbon paste electrode, *Analyst* 130 (4) (2005) 534–540.
- [9] J. Moros, N. Galipienso, R. Vilches, S. Garrigues, M.d.I. Guardia, Nondestructive direct determination of heroin in seized illicit street drugs by diffuse reflectance near-infrared spectroscopy, *Anal. Chem.* 80 (19) (2008) 7257–7265.
- [10] C. Meadway, S. George, R. Braithwaite, A rapid GC-MS method for the determination of dihydrocodeine, codeine, norcodeine, morphine, normorphine and 6-MAM in urine, *Forensic Sci. Int.* 127 (1–2) (2002) 136–141.
- [11] G.o. Sakai, K. Ogata, T. Uda, N. Miura, N. Yamazoe, A surface plasmon resonance-based immunosensor for highly sensitive detection of morphine, *Sensors Actuators, B Chem.* 49 (1–2) (1998) 5–12.
- [12] J. Wang, Modified electrodes for electrochemical sensors, *Electroanalysis* 3 (4–5) (1991) 255–259.
- [13] W. Ren, H.Q. Luo, N.B. Li, Simultaneous voltammetric measurement of ascorbic acid, epinephrine and uric acid at a glassy carbon electrode modified with caffeic acid, *Biosens. Bioelectron.* 21 (7) (2006) 1086–1092.
- [14] N. Serrano, B. Prieto-Simón, X. Cetó, M. del Valle, Array of peptide-modified electrodes for the simultaneous determination of Pb(II), Cd(II) and Zn(II), *Talanta* 125 (2014) 159–166.
- [15] N. Serrano, A. González-Calabuig, M. del Valle, Crown ether-modified electrodes for the simultaneous stripping voltammetric determination of Cd(II), Pb(II) and Cu(II), *Talanta* 138 (2015) 130–137.
- [16] U.E. Wawrzyniak, P. Ciosek, M. Zaborowski, G. Liu, J.J. Gooding, Gly-Gly-His immobilized on monolayer modified back-side contact miniaturized sensors for complexation of copper ions, *Electroanalysis* 25 (6) (2013) 1461–1471.
- [17] A. Cipri, M. del Valle, Pd nanoparticles/multiwalled carbon nanotubes electrode system for voltammetric sensing of tyrosine, *J. Nanosci. Nanotechnol.* 14 (9) (2014) 6692–6698.
- [18] M. del Valle, Bioinspired sensor systems, *Sensors* 11 (11) (2011) 10180–10186.
- [19] A. Legin, D. Kirsanov, M. del Valle, Avoiding nonsense in electronic taste sensing, *TRAC Trends Anal. Chem.* 121 (2019) 115675.
- [20] L. Moreno-Barón, R. Cartas, A. Merkoçi, S. Alegret, J.M. Gutiérrez, L. Leija, P.R. Hernandez, R. Muñoz, M. del Valle, Data compression for a voltammetric electronic tongue modelled with artificial neural networks, *Anal. Lett.* 38 (13) (2005) 2189–2206.
- [21] Thinsungnoen, T., Kaoungku, N., Durongdumronchai, P., Kerdprasop, K., and Kerdprasop, N. The Clustering Validity with Silhouette and Sum of Squared Errors. *Proc. 2nd Int. Conf. Ind. Appl. Eng.* 2015, 3 (7), 44–51.
- [22] A. Florea, J. Schram, M. de Jong, J. Eliaerts, F. Van Durme, B. Kaur, N. Samyn, K. De Wael, Electrochemical strategies for adulterated heroin samples, *Anal. Chem.* 91 (12) (2019) 7920–7928.
- [23] T. Metsalu, J. Vilo, ClustVis: A web tool for visualizing clustering of multivariate data using Principal Component Analysis and heatmap, *Nucleic Acids Res.* 43 (W1) (2015) W566–W570.
- [24] M. Peker, O. Özkaraça, A. Şaşar, Use of orange data mining toolbox for data analysis in clinical decision making, *Expert Sys. Tech. Biomed. Sci. Prac.* (2018) 143–167.
- [25] A. Naik, L. Samant, Correlation review of classification algorithm using data mining tool: weka, rapidminer, tanagra, orange and knime, *Procedia Comput. Sci.* 85 (Cms) (2016) 662–668.
- [26] O. Campesato, Artificial Intelligence, Machine Learning, and Deep Learning, Dulles, VA, USA, 2020.
- [27] J. Wang, Analytical Electrochemistry, John Wiley & Sons Inc, Hoboken, NJ, USA, 2006.
- [28] J.R.B. Rodríguez, V.C. Díaz, A.C. García, P.T. Blanco, Voltammetric assay of heroin in illicit dosage forms, *Analyst* 115 (2) (1990) 209–212.
- [29] J.M.P.J. Garrido, C. Delerue-Matos, F. Borges, T.R.A. Macedo, A.M. Oliveira-Brett, Voltammetric oxidation of drugs of abuse III Heroin and metabolites, *Electroanalysis* 16 (18) (2004) 1497–1502.
- [30] J.M.P.J. Garrido, C. Delerue-Matos, F. Borges, T.R.A. Macedo, A.M. Oliveira-Brett, Electrochemical analysis of opiates - an overview, *Anal. Lett.* 37 (5) (2004) 831–844.
- [31] A. González-Calabuig, M. del Valle, Voltammetric electronic tongue to identify Brett character in wines. On-site quantification of its ethylphenol metabolites, *Talanta* 179 (2018) 70–74.
- [32] R. Bro, Review on multiway analysis in chemistry—2000–2005, *Crit. Rev. Anal. Chem.* 36 (3–4) (2006) 279–293.
- [33] R.G. Brereton, Applied chemometrics for scientists, John Wiley & Sons, Chichester, 2007.

Voltammetric Sensing Using an Array of modified SPCE Coupled with Machine Learning Strategies for the Improved Identification of Opioids in Presence of Cutting Agents

Dionisia Ortiz-Aguayo^a, Karolien De Wael^b and Manel del Valle^{a*}

^a Sensors and Biosensors Group, Department of Chemistry, Universitat Autònoma de Barcelona, Carrer dels Til·lers, 08193 Bellaterra, Spain.

^bAXES Research Group, Department of Bioscience Engineering, University of Antwerp, Groenenborgerlaan 171, 2020 Antwerp, Belgium.

Supplementary Material

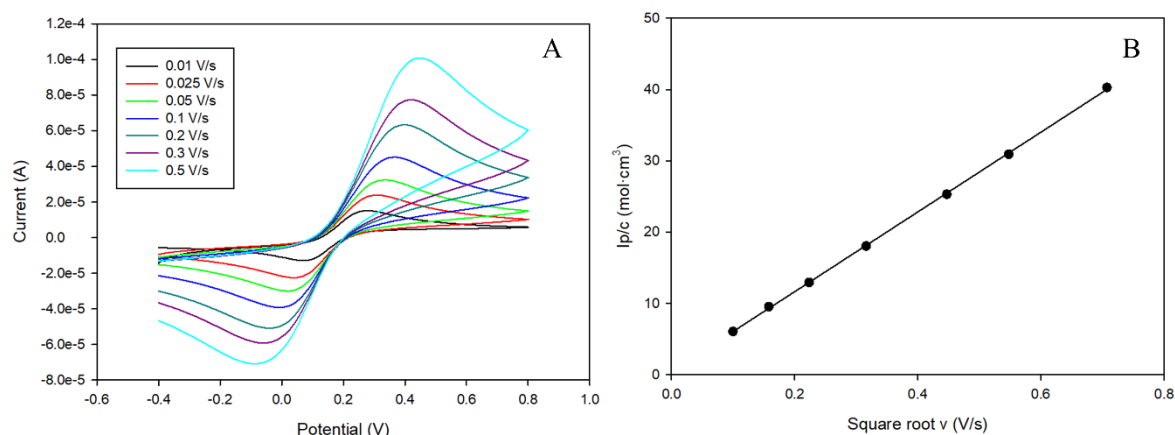


Figure S 1. (A) Cyclic voltammetry of 5 mM $\text{K}_3\text{Fe}(\text{CN})_6/\text{K}_4\text{Fe}(\text{CN})_6$ redox couple in 0.1 M KCl varying scan rate from 0.01 V/s to 0.5 V/s using Graphite/SPCE-Ink. The range potential was from -0.4 V to 0.4 V with a step potential of 0.005 V. (B) Regression line of $v^{1/2}$ ($\text{V} \cdot \text{s}^{-1}$) vs. $I_p \cdot c^{-1}$ ($\text{mol} \cdot \text{cm}^3$).

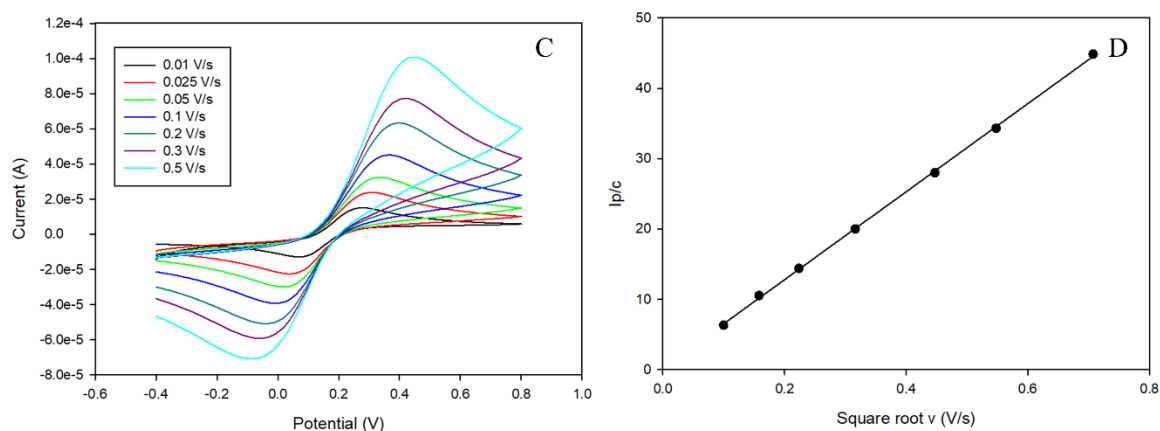


Figure S 2. (C) Cyclic voltammetry of 5 mM $\text{K}_3\text{Fe}(\text{CN})_6/\text{K}_4\text{Fe}(\text{CN})_6$ redox couple in 0.1 M KCl varying scan rate from 0.01 V/s to 0.5 V/s using Copper oxide (II)/SPCE-Ink. The range potential was from -0.4 V to 0.4 V with a step potential of 0.005 V. (D) Regression line of $v^{1/2}$ ($\text{V} \cdot \text{s}^{-1}$) vs. $I_p \cdot c^{-1}$ ($\text{mol} \cdot \text{cm}^3$).

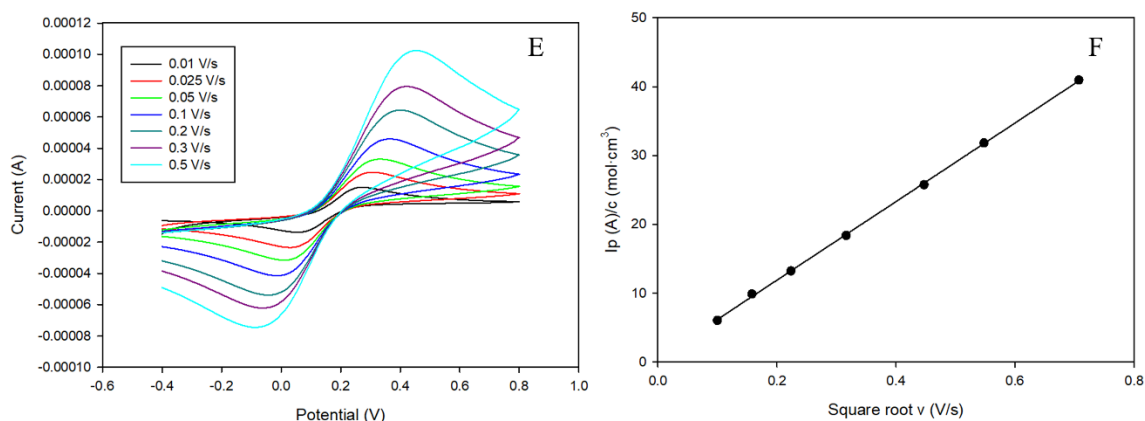


Figure S 3. (E) Cyclic voltammetry of 5 mM $\text{K}_3\text{Fe}(\text{CN})_6/\text{K}_4\text{Fe}(\text{CN})_6$ redox couple in 0.1 M KCl varying scan rate from 0.01 V/s to 0.5 V/s using Prussian blue/SPCE-Ink. The range potential was from -0.4 V to 0.4 V with a step potential of 0.005 V. (F) Regression line of $v^{1/2} (\text{V}\cdot\text{s}^{-1})$ vs. $I_p\cdot c^{-1}(\text{mol}\cdot\text{cm}^3)$.

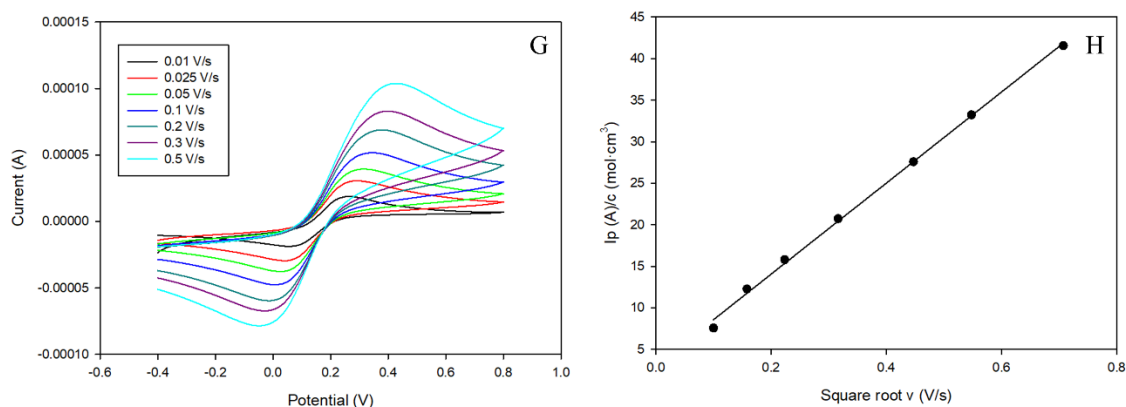


Figure S 4. (G) Cyclic voltammetry of 5 mM $\text{K}_3\text{Fe}(\text{CN})_6/\text{K}_4\text{Fe}(\text{CN})_6$ redox couple in 0.1 M KCl varying scan rate from 0.01 V/s to 0.5 V/s using Cobalt (II) phthalocyanine/SPCE-Ink. The range potential was from -0.4 V to 0.4 V with a step potential of 0.005 V. (H) Regression line of $v^{1/2} (\text{V}\cdot\text{s}^{-1})$ vs. $I_p\cdot c^{-1}(\text{mol}\cdot\text{cm}^3)$.

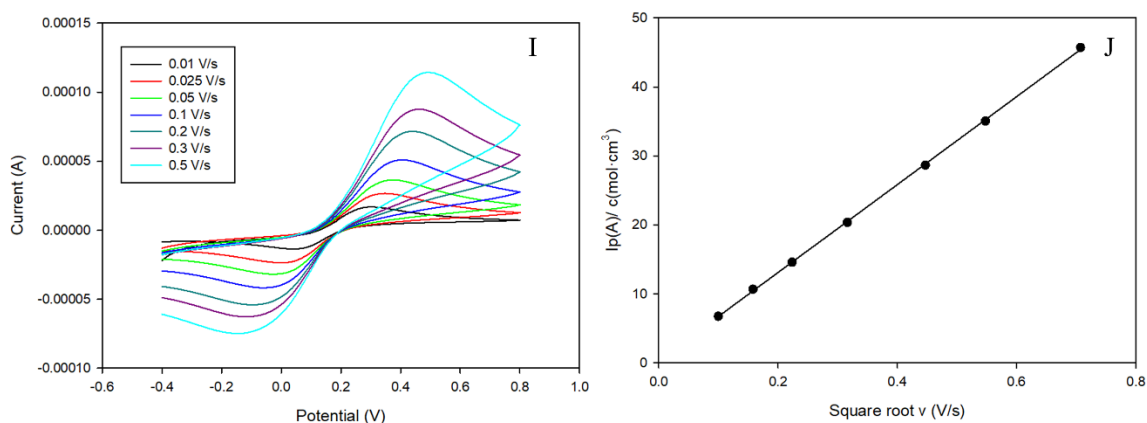


Figure S 5. (I) Cyclic voltammetry of 5 mM $\text{K}_3\text{Fe}(\text{CN})_6/\text{K}_4\text{Fe}(\text{CN})_6$ redox couple in 0.1 M KCl varying scan rate from 0.01 V/s to 0.5 V/s using Pd nanoparticles/SPCE-Ink. The range potential was from -0.4 V to 0.4 V with a step potential of 0.005 V. (J) Regression line of $v^{1/2}$ ($\text{V}\cdot\text{s}^{-1}$) vs. $I_p\cdot c^{-1}(\text{mol}\cdot\text{cm}^3)$.

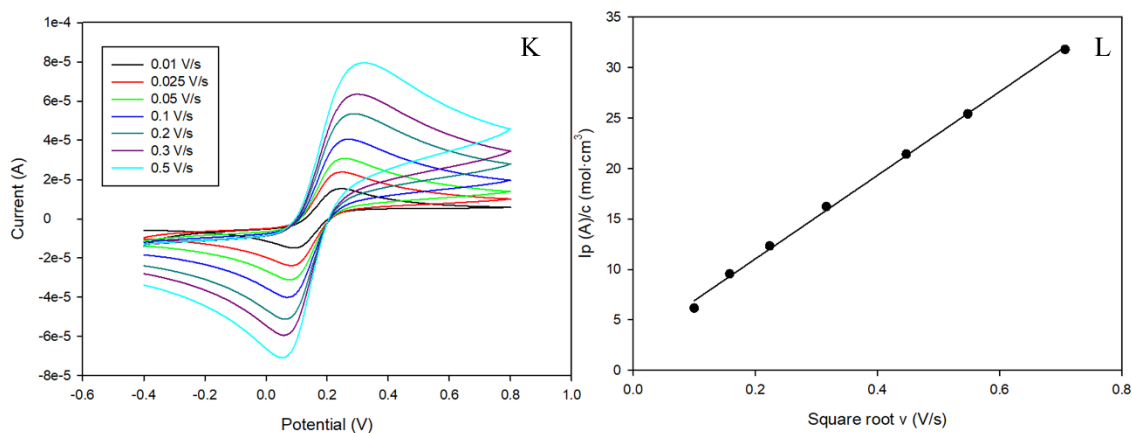


Figure S 6. (K) Cyclic voltammetry of 5 mM $\text{K}_3\text{Fe}(\text{CN})_6/\text{K}_4\text{Fe}(\text{CN})_6$ redox couple in 0.1 M KCl varying scan rate from 0.01 V/s to 0.5 V/s using Polypyrrole/SPCE-Ink. The range potential was from -0.4 V to 0.4 V with a step potential of 0.005 V. (L) Regression line of $v^{1/2}$ ($\text{V}\cdot\text{s}^{-1}$) vs. $I_p\cdot c^{-1}(\text{mol}\cdot\text{cm}^3)$.

Table 1. Composition of A

Element	App Conc.	Intensity Corrn.	Weight%	Weight% Sigma	Atomic%
C K	99.84	2.0878	77.10	1.50	84.05
N K	4.17	0.4414	15.25	1.28	14.25
Co L	3.07	0.6480	7.65	1.13	1.70
Totals			100.00		

Table 2. Composition of B

Element	App Conc.	Intensity Corrn.	Weight%	Weight% Sigma	Atomic%
C K	35.10	1.7012	38.89	1.06	67.91
O K	15.02	2.3300	12.15	0.67	15.93
Cu L	20.20	0.7779	48.96	1.13	16.16
Totals			100.00		

Table 3. Composition of C

Element	App Conc.	Intensity Corrn.	Weight%	Weight% Sigma	Atomic%
C K	71.40	1.9474	41.90	1.06	60.62
N K	11.43	0.6381	20.48	0.95	25.41
O K	5.01	1.9559	2.93	0.35	3.18
Fe L	21.59	0.7112	34.70	1.34	10.80
Totals			100.00		

Table 4. Composition of D

Element	App Conc.	Intensity Corrn.	Weight%	Weight% Sigma	Atomic%
C K	3.27	2.2516	58.12	1.50	92.48
Pd L	0.80	0.7701	41.88	1.50	7.52
Totals			100.00		

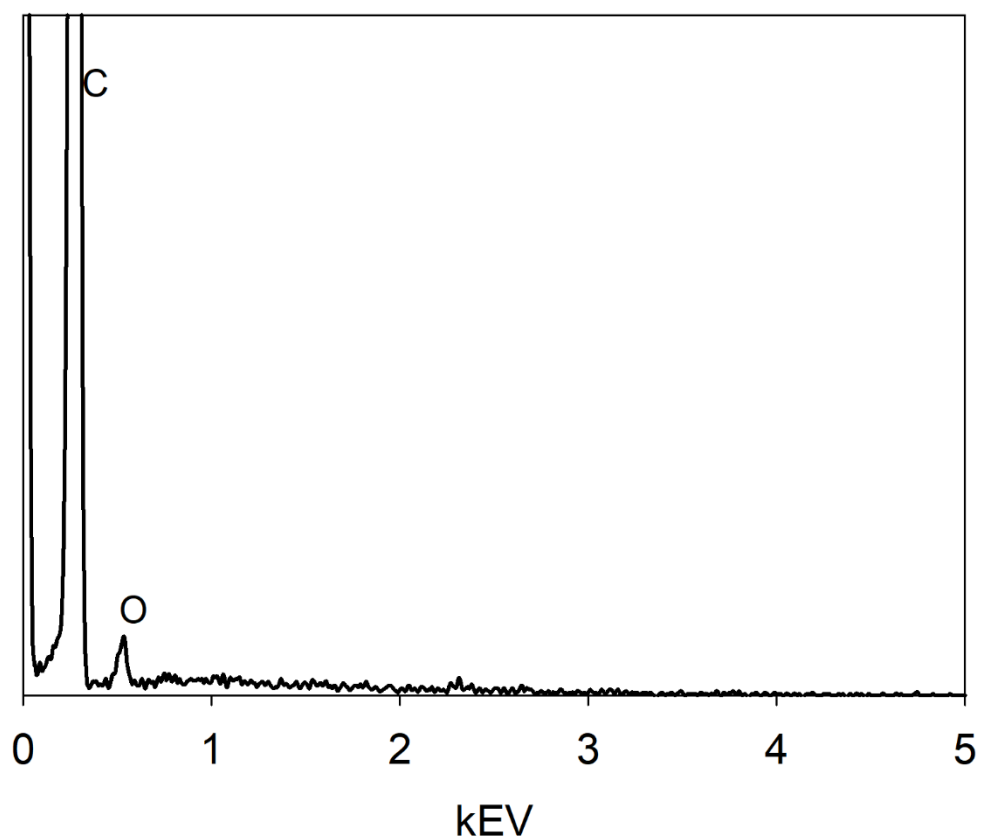


Figure S 8. EDX for polypyrrole.

Table 5. Composition of polypyrrole.

Element	App Conc.	Intensity Corrn.	Weight%	Weight% Sigma	Atomic%
C K	105.87	2.1568	97.99	0.37	98.49
O K	1.56	1.5539	2.01	0.37	1.51
Totals			100.00		

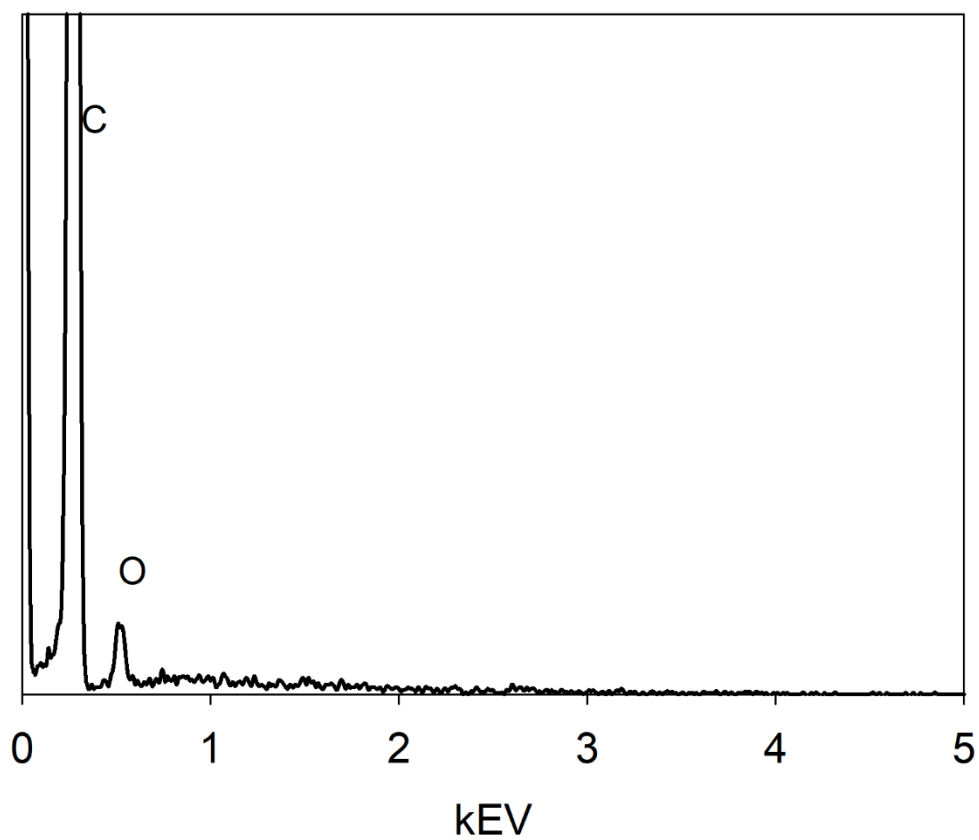


Figure S 9. EDX for unmodified electrode.

Table 6. Composition of unmodified electrode.

Element	App Conc.	Intensity Corrn.	Weight%	Weight% Sigma	Atomic%
C K	141.10	2.1528	96.81	0.44	97.59
O K	3.38	1.5638	3.19	0.44	2.41
Totals			100.00		

ARTICLE 3

Resolution of opiate illicit drugs signals in the presence of some cutting agents with use of a voltammetric sensor array and machine learning strategies

Dionisia Ortiz-Aguayo, Xavier Cetó, Karolien De Wael and Manel del Valle

Sensors and Actuators B: Chemical, 2022, 357, 13134



Resolution of opiate illicit drugs signals in the presence of some cutting agents with use of a voltammetric sensor array and machine learning strategies

Dionisia Ortiz-Aguayo^a, Xavier Cetó^a, Karolien De Wael^b, Manel del Valle^{a,*}

^a Sensors and Biosensors Group, Department of Chemistry, Universitat Autònoma de Barcelona, Edifici Cn, 08193 Bellaterra, Spain

^b AXES Research Group, Department of Bioscience Engineering, University of Antwerp, Groenenborgerlaan 171, 2020 Antwerp, Belgium

ARTICLE INFO

Keywords:

Electronic tongue

Voltammetric sensors

Opioids

Partial-least squares regression

ABSTRACT

In the present work, the resolution and quantification of mixtures of different opiate compounds in the presence of common cutting agents using an electronic tongue (ET) is evaluated. More specifically, ternary mixtures of heroin, morphine and codeine were resolved in the presence of caffeine and paracetamol. To this aim, an array of three carbon screen-printed electrodes were modified with different ink-like solutions of graphite, cobalt (II) phthalocyanine and palladium, and their responses towards the different drugs were characterized by means of square wave voltammetry (SWV). Developed sensors showed a good performance with good linearity at the μM level, LODs between 1.8 and 5.3 μM for the 3 actual drugs, and relative standard deviation (RSD) ca. 2% for over 50 consecutive measurements. Next, a quantitative model that allowed the identification and quantification of the individual substances from the overlapped voltammograms was built using partial least squares regression (PLS) as the modeling tool. With this approach, quantification of the different drugs was achieved at the μM level, with a total normalized root mean square error (NRMSE) of 0.084 for the test subset.

1. Introduction

The consumption and trafficking of illicit drugs have increased significantly over the last years, creating a negative impact in people's health and in the economy, while contributing to an increase of criminality [1]. The increase in consumption and trafficking has also enriched the illicit drug markets, which are powerful systems of production and distribution that generate large amount of unwanted activities [2]. In this direction, the rapid detection of illicit drugs to disarticulate such markets and safeguard the public still remains a challenge for authorities.

The main drawbacks posed by currently used on-site methods for the detection of illicit drugs and their precursors are the low accuracy of color tests, or the high cost and low portability of spectroscopic tests. In the light of the pressing need for better drug test systems at border controls, BorderSens project [3] aims to establish the basis for the development of a portable device capable to quickly test for different drugs, precursors and cutting agents, with outstanding accuracy and reduced false positives and false negatives. However, given the challenge that such a task represents, the quantitative analysis of opiates

mixtures is investigated herein as a proof-of-concept of what can be achieved.

In the USA, the Controlled Substances Act (CSA) defines five classes of drugs: narcotics, depressants, stimulants, hallucinogens and anabolic steroids [4]. Among those, narcotics (also known as "opioids") represent one of the biggest health and economic burden, accounting 63% of deaths by drug overdose in the USA in 2015 and nearly 70% in 2018 [5, 6]. A particular class of opioids are opiates, which originate or are derived from naturally occurring alkaloids found in certain poppy species, specifically *Papaver somniferum* [7]. Common opiates include opium, heroin, morphine and codeine.

Several alternate methods for the individual and simultaneous determination of opiates have been reported in the literature. Those are based on common analytical techniques such as chromatography [8,9], capillary electrophoresis [10,11], chemiluminescence [12,13], diffuse reflectance near-infrared spectroscopy [14] or surface plasmon resonance (SPR) based immunosensors [15]. Despite being powerful, these techniques present some disadvantages that hinder their application for the on-site drug monitoring, like requiring a sample pre-treatment step and/or laboratory facilities (low portability), being time-consuming and

* Corresponding author.

E-mail address: manel.delvalle@uab.cat (M. del Valle).

<https://doi.org/10.1016/j.snb.2021.131345>

Received 30 July 2021; Received in revised form 13 December 2021; Accepted 29 December 2021

Available online 31 December 2021

0925-4005/© 2021 The Author(s).

Published by Elsevier B.V. This is an open access article under the CC BY-NC-ND license

(<http://creativecommons.org/licenses/by-nc-nd/4.0/>).

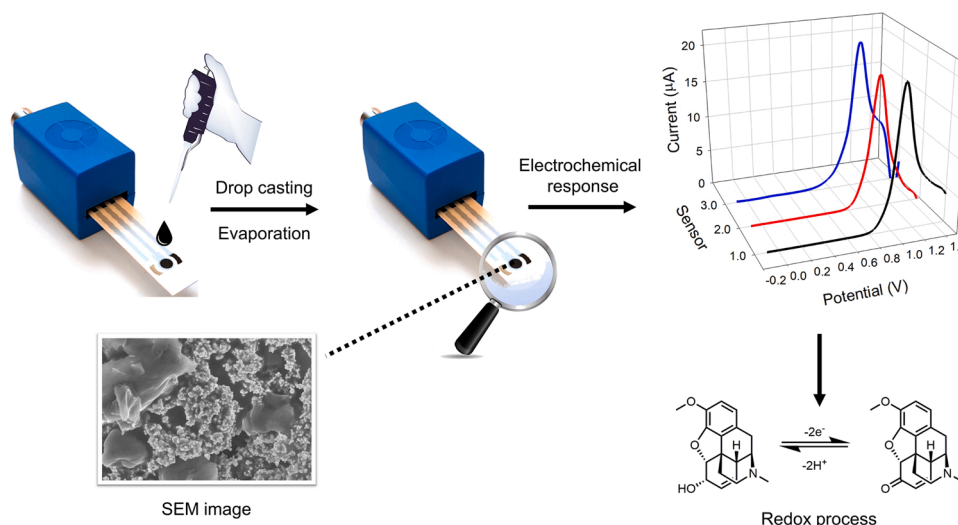


Fig. 1. Scheme of the experimental procedure for the electrode surface modification. Firstly, an ink-like solution was prepared incorporating the corresponding modifier. Then, 1 μL was dropped on the surface and dried at 40 $^{\circ}\text{C}$.

quite costly (both from the equipment and reagents side).

In this regard, the use of electrochemical sensors represents a promising alternative which may allow to overcome these limitations. These devices can be used as powerful analytical tools for the analysis of illicit substances from street and biological samples as they offer low-cost measurement systems with rapid response, simple usage and high portability; all of them required characteristics for point-of-use forensic applications. Despite the advantages that electrochemical methods may offer, the simultaneous determination of the aforementioned compounds can be challenging given their similar electrochemical response and the complexity of the samples [16]. Precisely, the main drawback is that, when using bare electrodes, there might be some overlapping between peaks, or even peak suppression [17]. Actually, the most complicated situation is the discrimination between heroin and morphine, since both molecules present the same functional groups in their skeleton and consequently, their corresponding fingerprint is quite similar. To overcome this difficulty, modification of the electrochemical sensors may be required, but it might also be necessary to couple these techniques with other strategies such as the use of chemometrics; a combination that is known as electronic tongue (ET) [18,19].

According to the IUPAC [20], an ET is defined as “a multisensor system, which consists of a number of low selective sensors and uses advanced mathematical procedures for signal processing based on pattern recognition and/or multivariate data analysis”. These biomimetic systems, in opposition to classical approaches, are based on the combination of low selective and/or cross-responsive sensors to obtain rich and complementary analytical information. Next, the coupling with chemometric tools to analyse the data allows to deconvolute complex overlapping electrochemical responses and achieve the simultaneous quantitative determination of several analytes. Thus, such an approach allows to extract meaningful chemical information from these complex data.

In the present work, the capabilities of ET-based systems in forensic applications will be demonstrated by attempting the simultaneous determination of three opiates (heroin, morphine and codeine) in the presence of two common cutting agents (paracetamol and caffeine). The chosen voltammetric sensor array consisted of three screen-printed carbon electrodes (SPCE) modified with graphite, cobalt (II) phthalocyanine and palladium inks, and square wave voltammetry (SWV) was the measuring technique. Firstly, the behavior of the sensors towards each of the compounds was evaluated individually, characterizing its analytical response. Secondly, a partial least square regression (PLS) model for their simultaneous quantification at the μM level was built

from the measured voltammograms.

2. Experimental

2.1. Reagents and samples

Standards of heroin hydrochloride and codeine were purchased from Chiron Chemicals, Australia. Morphine hydrochloride, potassium monophosphate, potassium chloride and potassium hydroxide were purchased from Sigma-Aldrich (St. Louis, MO, USA).

Cobalt(II) phthalocyanine (CoPc) and palladium powder ($< 1 \mu\text{m}$, $\geq 99.9\%$; Pd), which were used as modifiers, as well as mesitylene and polystyrene, which were used for the preparation of the ink composite, were also obtained from Sigma-Aldrich (St. Louis, MO, USA). Graphite powder (particle size $< 50 \mu\text{m}$) was received from BDH (BDH Laboratory Supplies, Poole, UK).

Samples were prepared in 20 mM phosphate buffer (PBS) at pH 7.0 containing 100 mM KCl as supporting electrolyte for the electrochemical measurements. All aqueous solutions were prepared using MilliQ water ($\rho > 18.2 \text{ M}\Omega \text{ cm}$). All reagents were of analytical grade and used without further purification. Fresh stock solutions were prepared daily in order to prevent its degradation.

2.2. Apparatus and voltammetric measurements

SWV measurements were performed using a multi-channel potentiostat/galvanostat/impedance analyzer MultiPalmSens4 (PalmSens, Houten, The Netherlands) controlled by MultiTrace software. Italsens screen-printed carbon electrodes (SPCE) containing a graphite working electrode (3 mm diameter), a carbon counter electrode and a pseudo-silver reference electrode (PalmSens, The Netherlands) were used for the measurements. SWV measurements were performed by placing 50 μL of the sample onto the SPCE. The single scan SWV parameters were as follows: potential range from -0.2 to 1.5 V , step potential of 5 mV , amplitude of 25 mV and frequency of 10 Hz .

2.3. Modification of the electrode surface

SPCE were modified with standard catalysts employed in electroanalysis, as are CoPc and Pd [21,22], incorporated using a self-formulated graphite-polystyrene ink. More in detail, the mixture contained the following mass fractions: 58% of graphite, 32% of powdered polystyrene and 10% of modifier, in this case graphite, cobalt

(II) phthalocyanine or palladium.

The corresponding modifier, graphite and polystyrene were thoroughly mixed with 250 μL of mesitylene for 2 h. After that, the mixture was sonicated for 2 min in order to obtain a medium thick solution. Finally, 1 μL of the ink-like composite was dropped onto the working electrode surface of a SPCE and dried at 40 $^{\circ}\text{C}$ for at least 1 h in order to remove the solvent (Fig. 1). After that, the electrodes were ready to use, not requiring the usage of any activation step.

2.4. Characterization of the electrode by scanning electron microscopy

The morphological characterization of the modified SPCE electrodes was performed by Field Emission Gun-Scanning Electron Microscope (FEG-SEM) of Zeiss, model MERLIN SM0087 and Energy Dispersive X-Ray Analysis (EDX). Imaging was performed based on secondary, back-scattered electrons.

2.5. Samples under study

In the present work, two different scenarios were evaluated with the proposed ET. Firstly, the analysis of ternary mixtures of heroin, codeine and morphine was considered to assess the potential of the ET to achieve their individual quantification. Secondly, the quantification of the same drugs in the presence of two common cutting agents (viz. paracetamol and caffeine) was attempted to assess the potential of the ET in a more realistic scenario.

To this aim, two different sets of samples were prepared (one for each of the above-mentioned scenarios). Each set of samples consisted of a train subset, which is used to build the model, and a test subset, which is used to assess its performance. The concentrations of the compounds mixtures of the train subset were defined by an experimental design, while for the test subset, some extra samples with concentrations for each of the compounds randomly distributed along the experimental domain were also prepared. Besides, in order to keep the number of samples required down to a reasonable level, two different experimental designs were employed as the number of samples required increases exponentially with the number of compounds considered.

In the first case (mixtures of the three drugs), samples for the train

subset were prepared based on a tilted factorial experimental design 3^3 (27 samples) [23]. With this approach it is possible to get a better distribution of the samples that avoids the repetition of concentrations as per the selected levels. The concentrations ranges considered for each of the compounds were in the range 0–750 μM , with 15 extra samples forming the test subset.

In the second case (mixtures of the three drugs plus the two cutting agents), samples for the train subset were prepared based on a central composite face-centered (CCF) experimental design with 3 levels of concentration (27 samples). As already stated, this was preferred as the number of samples required to complete a full factorial design would be just too high ($3^5 = 243$ samples). In this case the concentrations for each of the compounds ranged from 0 to 750 μM , with 17 extra samples forming the test subset.

As an extra precaution to control drifts or periodic trends as the same sensing units were used for the whole series, all this samples were analysed in random order and alternating their measurement with the measurement of a blank solution (PBS), which served as cleaning stage of the electrode surfaces, but also as control.

2.6. Data analysis

Initial analysis of the voltammetric signals was done with MultiTrace software (PalmSens, Houten, The Netherlands), which allowed to calculate the peak heights and areas for the different stock samples. From those, the calibration plots were built using the data of the replicate measurements ($n = 4$) with the aid of Sigmaplot (Systat Software Inc., San Jose, CA, USA), and analytical parameters such as sensitivity, linear range, LOD, etc. were calculated.

Chemometric analysis was done in Matlab R2018b (MathWorks, Natick, MA, USA), making use of its Statistics and Machine Learning Toolbox, by specific routines written by the authors. Briefly, upon measurement of the set of samples described in Section 2.5 with the sensor array, voltammetric responses of the three electrodes were combined into a single vector. Genetic algorithms (GAs) were then used as feature selection tool to reduce the number of inputs to be fed to the chemometric model given the large dimensionality of the voltammetric data [24]. Next, quantitative models to individually quantify each of the analytes were built by partial least squares regression (PLS-1) [25], and their performance was then assessed towards the samples that formed the test subset to obtain more realistic performance indicators.

3. Results and discussion

3.1. Characterization of the sensor array

Modified electrodes can be prepared by several different techniques [23,26]. In the present work, the approach used for the modification of the electrodes is based on the use of a composite material (containing the different modifiers) through the formation of an ink-like paste, which is then casted onto the electrode, generating a new surface highly suitable to carry out electrochemical measurements. Besides, the preparation and modification with these inks is extremely easy and has a very low-cost, making this methodology an interesting approach for the fabrication of chemically-modified transducers.

In our case, after an initial screening of different electrochemical modifiers considered in prior studies involving ETs [27–31], an array of three electrodes was prepared using bare graphite, Pd and CoPc as the modifiers. The selection was based on the suitability of the different electrodes to obtain the discrimination of the different drugs (data not shown) [32]. The inclusion of graphite provided somehow a control point that allowed to actually evaluate the advantages derived from the incorporation of the other modifiers. Pd is well-known for its good (electro)catalytic activity towards a wide range of reactions and compounds, while the usage of nanoparticles has demonstrated to be an attractive alternative to the respective bulk metals given its higher

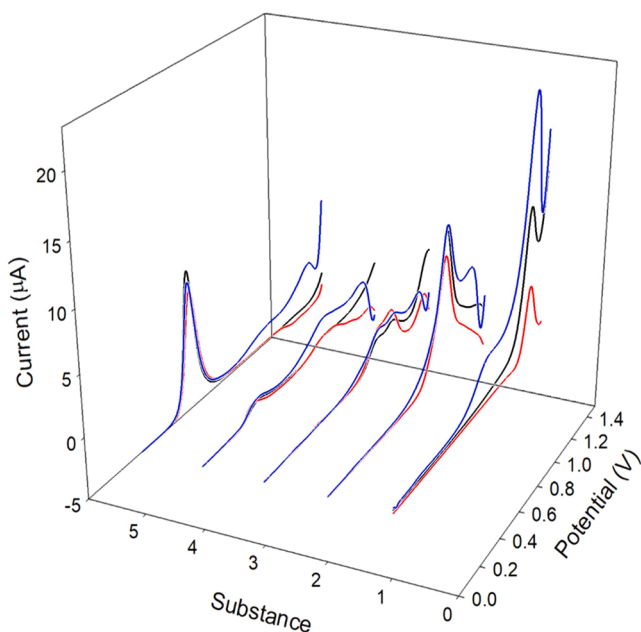


Fig. 2. Electrochemical fingerprint of 300 μM solutions of the five substances under study: 1) caffeine, 2) codeine, 3) heroin, 4) morphine and 5) paracetamol with the proposed array in this work: Carbon (red), CoPc (black) and Pd (blue).

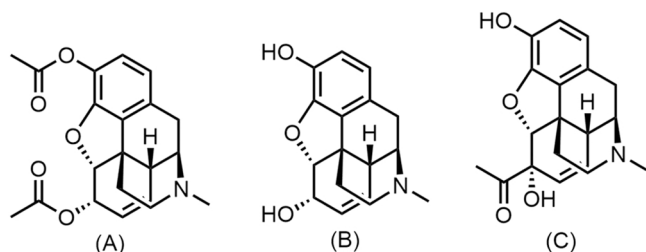


Fig. 3. Chemical structure of (A) heroin, (B) morphine and (C) 6-MAM (a heroin metabolite).

surface/mass ratio and improved electrochemical properties. Lastly, phthalocyanines are reported to be efficient electrocatalysts in the determination of many important inorganic, organic, or biological compounds.

Before tackling the resolution of the mixtures with their corresponding cutting agents, which is the main goal of this work, the modified electrodes were first physically and electrochemically characterized.

Upon modification of the SPCE as described in Section 2.3, those were characterized by SEM imaging. Microscopy studies show that the two modifiers are distributed quasi-homogeneously along the graphite

layers (Fig. S1, supplementary material), and more importantly, confirm the presence of the modifiers inside the ink-like composite.

Next, the evaluation of the voltammetric responses of each of the modified sensors towards each of the compounds individually was carried out to assure that distinguished signals are generated. That is, to ensure that the electrodes respond to the different analytes, and that differentiated responses are also obtained between them. To carry out the measurements, SWV was chosen given its high sensitivity and fast scan rates, which in combination with the compact low-power instrumentation required for electrochemical measurements, offers particular promise for decentralized security screening applications [33,34].

As can be observed in Fig. 2, different overlapping peaks can be remarked. In the case of heroin, an irreversible oxidation split peak is shown around 0.97 V, corresponding to the oxidation of the tertiary amine group (Fig. 3A), resulting in a secondary amine which is then further oxidized (Figs. 3 and S2) [35]. In addition, a smaller extra peak appeared at a lower potential (ca. 0.40 V, which is more evident in Fig. 4), corresponding to the oxidation of the phenol group of 6-monoacetylmorphine (6-MAM, Fig. 3C) present in a 3% w/t in the sample. 6-MAM is an impurity, commonly found in heroin synthesis, that comes both from the incomplete acetylation of morphine as well as from the hydrolysis of heroin (as it is a product of its hydrolysis).

Similarly, morphine also shows the oxidation peak ca. 0.40 V

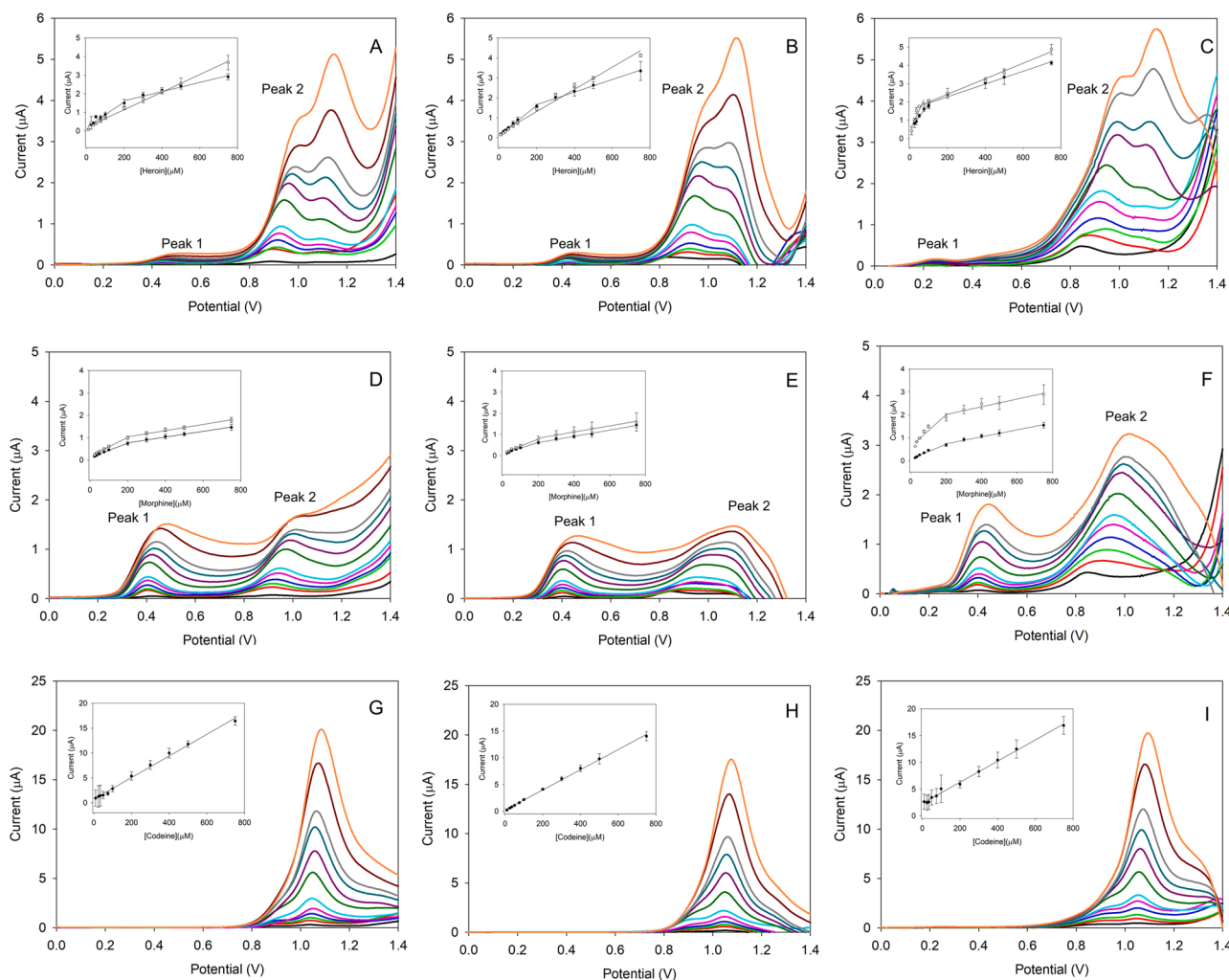


Fig. 4. Square wave voltammograms obtained for (A-C; top row) heroin, (D-F; middle row) morphine and (G-I; bottom row) codeine using (A,D,G; left column) graphite, (B,E,H; middle column) CoPc and (C,F,I; right column) Pd, respectively. Series of plots correspond to increasing concentrations from 10 to 1000 μM. Insets correspond to the linear regressions of peak height (at the observed potential maximum) vs. concentration, excluding the point 1000 μM as saturation of the voltammetric signal was reached for certain compounds.

Table 1

Calibration data (y vs. x) for the separate determination of heroin, morphine, codeine, paracetamol and caffeine employing the proposed sensor array.

Compound	Potential (V)	Sensitivity (nA μM^{-1})	Intercept (μM)	r	LOD (μM)	Linear Range (μM)
Sensor 1: Carbon						
Heroin	0.49	6.1	0.28	0.986	3.33	25–200
		2.5	1.13	0.985		200–750
Morphine	1.16	4.7	0.21	0.997	31.8	25–750
	0.43	3.3	0.10	0.996		25–200
		1.3	0.51	0.997	8.65	200–750
		4.2	0.16	0.995		25–200
Codeine	1.11	1.4	0.76	0.994	1.80	200–750
		21.7	0.72	0.998		25–750
Paracetamol	0.39	22.3	0.12	0.999	0.82	25–750
Caffeine	1.33	15.6	4.02	0.993	44.0	50–750
Sensor 2: CoPc						
Heroin	0.43	7.2	0.15	0.999	3.95	25–200
		3.1	1.03	0.996		200–750
Morphine	1.14	5.5	0.22	0.994	83.3	25–750
	0.40	2.8	0.071	0.994		25–200
		1.5	0.32	0.995	2.88	200–750
		3.4	0.11	0.994		25–200
Codeine	1.09	1.5	0.53	0.991	96.6	200–750
		18.9	0.21	0.999		25–750
Paracetamol	0.40	17.4	-0.16	0.999	0.75	25–750
Caffeine	1.36	10.8	0.0069	0.998	65.0	50–750
Sensor 3: Pd						
Heroin	0.27	14.3	0.41	0.988	5.31	25–200
		3.5	1.59	0.991		200–750
Morphine	1.01	34.8	0.12	0.975	14.8	25–200
	0.46	4.2	1.57	0.966		200–750
		3.2	0.086	0.985	25.9	25–200
		1.5	0.44	0.993		200–750
Codeine	1.01	6.9	0.62	0.954	60.7	25–200
		1.7	1.68	0.961		200–750
Paracetamol	1.11	19.8	2.31	0.997	11.7	25–750
Caffeine	0.38	19.0	-0.11	0.999	3.33	25–750
	1.35	11.6	17.2	0.983	104	200–750

corresponding to the phenol group of 6-MAM [36], but being more prominent in this case. The second peak corresponds to the oxidation of the tertiary amine group (Fig. 3B), which in this case is not further oxidized (Fig. S3). In the case of codeine, only one broad peak can be observed, which again corresponds to the oxidation of the tertiary amine (Fig. S4), but also showing a small shoulder, which is almost superimposed and that is attributed to the oxidation of the 6-hydroxy groups [37]. Finally, in the case of paracetamol, only a well-defined Gaussian peak corresponding to the oxidation of the amide group (Fig. S5) is observed ca. 0.40 V [38,39], while in the case of caffeine, also a single peak (Fig. S6) is obtained, which corresponds to the oxidation of the C-8 to N-9 bond to give the substituted uric acid [39,40]. In this direction, the proposed mechanisms for the electrochemical oxidation of the different evaluated substances are provided in Figs. S7 and Figs. S2 to S6.

It can also be seen that the oxidation of the phenol group is overlapped with the oxidation peak of paracetamol. Similarly, the same situation occurs with the second oxidation peak of heroin and morphine, which also will overlap with the one from codeine. However, this is not an issue given distinguishable voltammetric profiles are obtained; i.e. different peak shapes and sensitivities are still obtained for each of the compounds. Lastly, in the case of caffeine, a single oxidation peak at higher potential is obtained (ca. 1.33 V).

After this first general overview of the voltammetric responses, the calibration curves for the five compounds under study were constructed by measuring solutions of increasing concentration from 25 to 750 μM . This step is relevant for further quantification models as it is important to identify the proper working ranges. All of the electrochemical measurements were performed in PBS at pH 7.0. The selection of this neutral pH is due to the fact that heroin and morphine suffer hydrolysis reactions at basic pH, as is described in the literature [41,42].

In all cases, the peak height which corresponds to the maximum of the oxidation signal was taken. This characterization is essential not

only to evaluate the response of the sensors, but also to determine the concentration ranges which they can operate and that will be used to do the analysis with the electronic tongue approach. As can be observed in Fig. 4s and S7, the responses obtained were linear for the vast majority of cases in the studied ranges ($r > 0.99$), showing one peak or two depending on the compound evaluated.

In the case of heroin, two peaks were shown. C and CoPc modified inks presented two linear ranges for the peak 1 (black), corresponding to the oxidation of the phenol group of 6-MAM. The lower linear range goes from 25 to 200 μM and the high range from 200 to 750 μM . For peak 2 (red), one linear range is presented (from 25 to 750 μM), corresponding to the oxidation of the amine group (Fig. 4AB). Pd modified ink showed a different performance displaying two linear ranges for peak 1 and peak 2 (Fig. 4C).

The next compound analysed was morphine. In this occasion, a similar response was given for the three sensors of the array. Two peaks were observed, with two linear ranges for each of them (Fig. 4D–F). The low range goes from 25 to 200 μM and the high from 200 to 750 μM , similar to heroin as could be expected.

Codeine and paracetamol showed a single peak with good linearity over the whole range (from 25 to 750 μM) with the three modifiers tested (Fig. 4G–I and Fig. S7J–L). Lastly also a single peak is obtained for caffeine, but with different linear range based on the electrode considered. Employing C and CoP, the linear range goes from 50 to 750 μM , whereas with Pd modified ink, the linear range narrows from 200–750 μM (Fig. S7M–O).

Based on the previous results, for the multi-determination of the drugs mixtures, the concentration working ranges were streamlined from 0 to 750 μM for heroin, morphine, codeine, paracetamol and caffeine. The analytical parameters derived from the calibration curves for each sensor are summarized in Table 1.

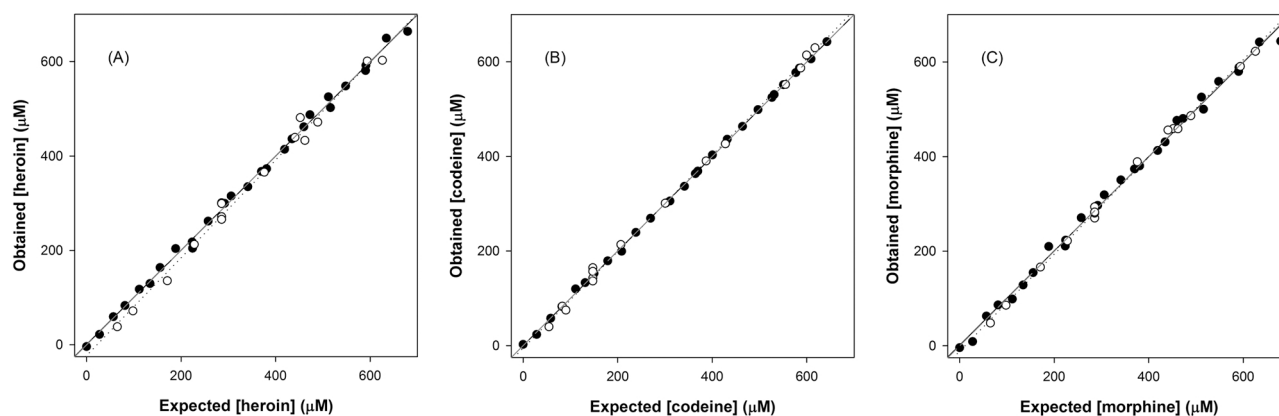


Fig. 5. Modeling ability of the optimized GA-PLS model for the 3 compounds case. Comparison graphs of obtained vs. expected concentrations for (A) heroin, (B) morphine and (C) codeine, for both the train (●, solid line) and test subsets (○, dotted line). The dashed line corresponds to the ideal comparison line ($y = x$).

3.2. Repeatability and reproducibility studies

Upon completing the calibration, a stability study was done in order to demonstrate that the sensors were capable to withstand the large number of measurements necessary when developing ET applications.

To this aim, codeine was selected as the substance to evaluate the variation on its voltammetric response upon successive measurements, assuming a similar behavior for the rest of the drugs. More specifically, a stock solution of codeine of 450 μM was measured for 25 consecutive times employing the same electrodes and measuring also a blank (PBS solution) in between each measurement to evaluate the repeatability of the sensors. Thus, each sensor was used for 50 consecutive measurements; a significant number given the disposable nature of SPEs.

Voltammetric data were collected and analyzed, from which the relative standard deviation (% RSD) was calculated. The values for carbon, CoPc and Pd modified ink-sensors were 1.84%, 2.01% and 2.14%, respectively. Significantly, the three modified sensors presented better stability than the unmodified sensor, which showed a RSD value of 9.87%. Thus, from this study it was concluded that no fouling or drift effects are observed with the proposed sensor array. This, in essence, means that any possible adsorption of the oxidized forms of the studied compounds did not affect appreciably the electrodes' performance or stability, given no differences were observed along consecutive measurements; equivalently, the same could be said for the applied potentials, if there is any doubt on the relatively high values used.

Complementary to the previous study, the reproducibility of construction of the ink-modified SPCE was also assessed. The experiment was done preparing each modified ink by triplicate ($n = 3$) and measuring consecutively with a heroin stock solution. The results for each sensor present a good construction reproducibility with RSD values of 3.97%, 6.95% and 5.67% for carbon, CoPc and Pd inks, respectively.

3.3. Quantitative analysis of drug mixtures using PLS regression

Despite different voltammetric profiles are obtained for each of the compounds when analysed individually (Fig. 4), even with different response for the different considered electrodes, it is clear that there will be an overlap on the voltammetric responses when mixtures of those are to be analysed at pH 7 (Figs. S8 and S9). Thus, in order to achieve the individual quantification of each of the compounds, the use of chemometric methods is required as such quantification cannot be achieved via univariate regression (taking either the peak height or area). In this direction, ET approach relies on the combination of an array of sensors that show complimentary responses towards the compounds of interest, with a multivariate calibration method that allows to build a model that relates the responses of the different sensors with the concentration of each of these compounds [19,43].

In the previous section, the sensitivities of each of the electrodes towards each of the compounds have been shown different (Table 1), a situation highly desirable when developing an ET application. Thus, the next step prior to build the quantitative model that allows to determine the individual substances from the overlapped voltammograms was the selection of the chemometric tool to be used. In this case, given the ultimate goal of this research project is developing a device to detect different illicit drugs, PLS-1 was chosen as the modeling tool given it is one of the simplest (e.g. in comparison to artificial neural networks, ANNs) and widely used multivariate calibration techniques to choose [44].

Lastly, although the use of a pre-processing stage to reduce the number of input variables is not required when PLS is being used, it has demonstrated that even in such cases this data reduction stage improves the model's prediction and generalization ability [43]. Again, as the aim is to develop the simplest model possible, the use of GAs as feature selection tool was chosen given upon identification of the most relevant features, no further computing processing will be required for each new measurement that is being performed. Thus, in this manner, the most relevant features from each of the voltammograms were selected with the aid of GAs and used as input into the PLS model. The outcome of GAs optimization is shown in Fig. S10, where the raw voltammetric responses for 300 μM solutions of each of the considered compounds is plotted with cross marks underneath corresponding to the selected features. On the contrary to the straightforward idea that the algorithm will select essentially the points corresponding to the peaks' maxima, it finally uses regions with less overlap and where the differences between signals are more pronounced. (that is, the points corresponding to the front and back of the peaks).

As already stated in Section 2.5, two different sets of samples were prepared: the first one in which ternary mixtures of the three considered drugs were considered, while in the second one also the presence of two different cutting agents was examined. The aim of the first set was to confirm the potential of the proposed ET to carry out the individual quantification of the opiates, whereas the second one aims to confirm that the ET is able to counterbalance the interferences of the cutting agents and successfully carry out the quantification of the drugs. In both cases, GA-PLS models were built using the data for the train subset, and its performance assessed towards the samples of the test subset, selecting the number of latent variables (LVs) that lead to the lowest root mean square error (RMSE).

3.3.1. Mixtures of the three drugs

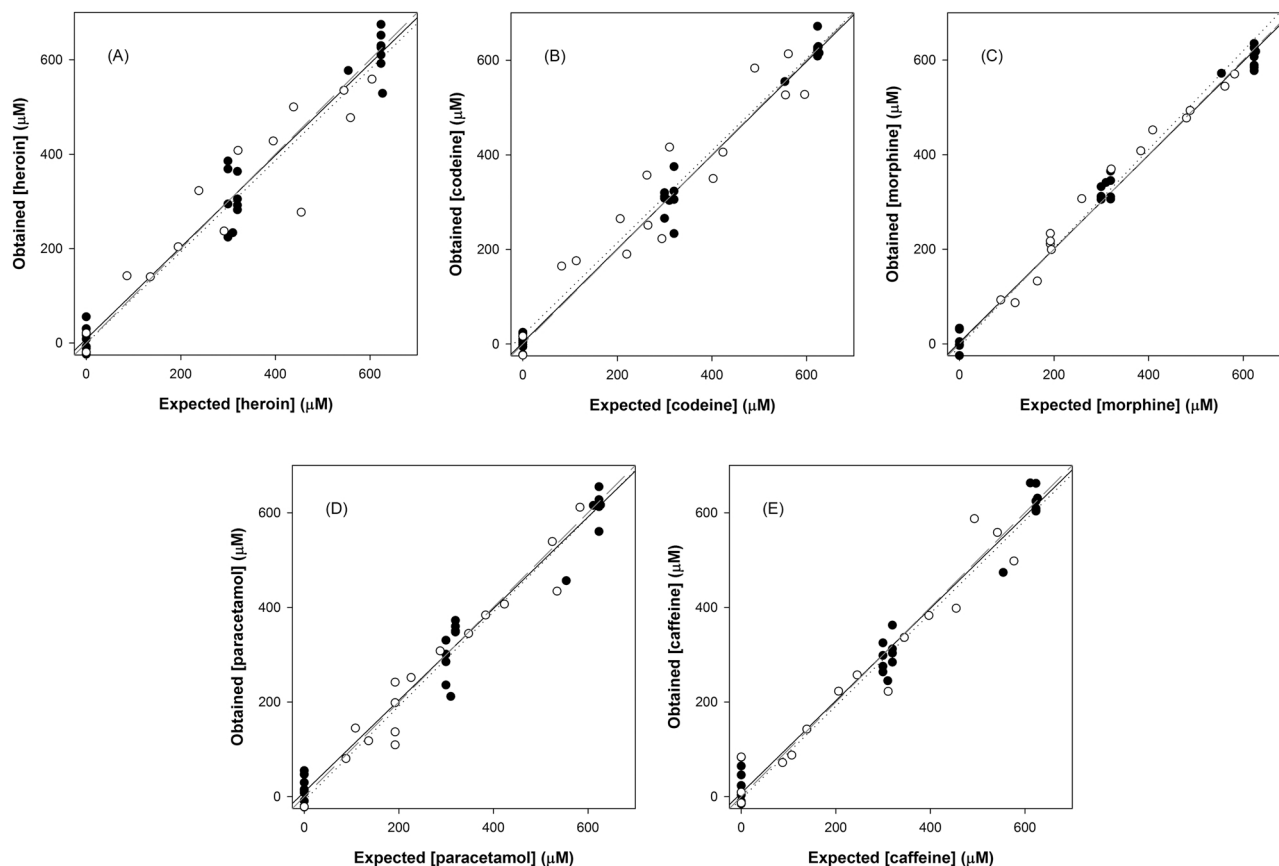
From the raw voltammetric responses of the three electrodes (318 current values \times 3 sensors), a total of 103 features were selected by use of GAs and used to build the PLS-1 models (Fig. S10). The selected number of LVs were 7 for heroin, 15 for codeine and 8 for morphine. Next, the

Table 2

Fitted regression lines for the comparison between obtained vs. expected values for the different sets of samples and the three considered APIs.

Compound	Slope	Intercept (μM)	r	RMSE (μM)	NRMSE	Total NRMSE
train subset (n = 27)						
Heroin	0.998 ± 0.019	0.7 ± 7.5	0.999	9.39	0.014	0.014
Codeine	1.000 ± 0.007	0.1 ± 2.7	1.000	3.35	0.005	
Morphine	0.996 ± 0.026	1.3 ± 10.0	0.998	12.5	0.019	
test subset (n = 15)						
Heroin	1.035 ± 0.064	-22.5 ± 24.3	0.995	20.6	0.030	0.026
Codeine	1.020 ± 0.026	-5.1 ± 9.4	0.999	10.1	0.016	
Morphine	1.026 ± 0.030	-11.3 ± 11.5	0.999	11.1	0.016	

Intervals are calculated at the 95% confidence level. RMSE: root mean square error; NRMSE: normalized root mean square error.

**Fig. 6.** Modeling ability of the optimized GA-PLS model for the 5 Compounds case. Comparison graphs of obtained vs. expected concentrations for (A) heroin, (B) morphine, (C) codeine, (D) paracetamol and (E) caffeine, for both the train (●, solid line) and test subsets (○, dotted line). The dashed line corresponds to the ideal comparison line ($y = x$).**Table 3**

Fitted regression lines for the comparison between obtained vs. expected values for the different sets of samples and the five considered compounds.

Compound	Slope	Intercept (μM)	r	RMSE (μM)	NRMSE	Total NRMSE
train subset (n = 27)						
Heroin	0.972 ± 0.068	8.7 ± 27.3	0.986	43.5	0.061	0.053
Codeine	0.990 ± 0.041	3.1 ± 16.6	0.995	26.2	0.037	
Morphine	0.990 ± 0.040	3.0 ± 16.2	0.995	25.5	0.036	
Paracetamol	0.969 ± 0.071	9.7 ± 28.8	0.984	45.9	0.065	
Caffeine	0.976 ± 0.063	7.5 ± 25.5	0.987	40.6	0.057	
test subset (n = 17)						
Heroin	0.968 ± 0.169	-0.7 ± 69.3	0.953	76.3	0.107	0.077
Codeine	0.974 ± 0.169	19.2 ± 58.0	0.954	63.3	0.089	
Morphine	1.042 ± 0.087	-5.9 ± 28.5	0.989	30.1	0.043	
Paracetamol	0.997 ± 0.124	-8.4 ± 38.8	0.975	41.8	0.059	
Caffeine	0.981 ± 0.130	-4.5 ± 39.7	0.972	50.1	0.070	

Intervals are calculated at the 95% confidence level. RMSE: root mean square error; NRMSE: normalized root mean square error.

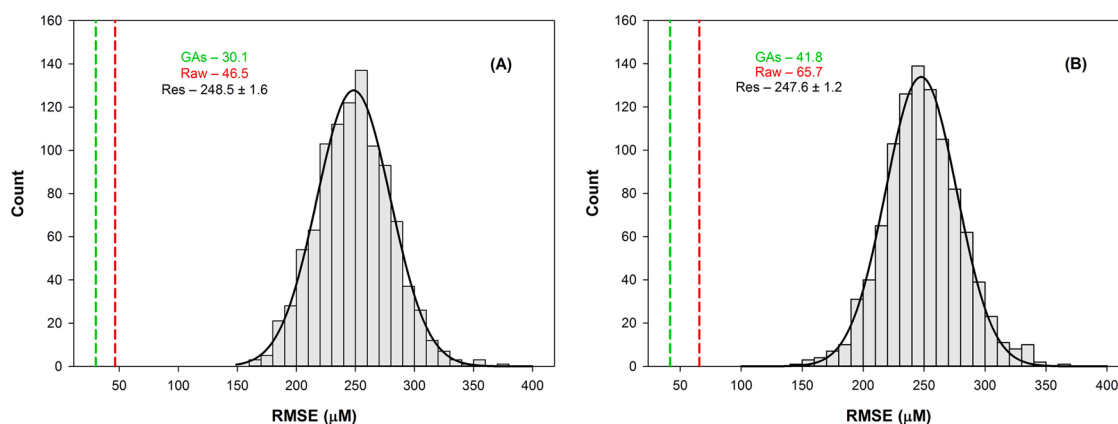


Fig. 7. Histogram comparing the success of PLS models with raw data (red) and GAs-PLS (green) to that of shuffled models (1000 iterations) for (A) codeine and (B) paracetamol, for the set of samples corresponding to mixtures of the 5 compounds. For the shuffled models, the data was fitted to a 3 parameter Gaussian curve and the RMSE values compared to the former. (For interpretation of the references to color in this figure legend, the reader is referred to the web version of this article.)

comparison graphs of predicted vs. expected concentrations were built (Fig. 5) and the linear regressions of the comparison lines fitted (Table 2) for the three drugs. As can be seen from the plot, a satisfactory trend is obtained in all the cases, with regression lines close to the ideal one ($y = x$). Moreover, from the regression parameters in the table we see these are very close to the ideal ones (i.e. 1 slope and correlation coefficient, and 0 intercept), being all of them within the intervals calculated at the 95% confidence level. Fig. S11 displays how obtained values are within the expected joint confidence intervals for all cases.

Despite the satisfactory trend, it has to be reckoned that slightly better performance is obtained for the train subset, but this is due to the fact that the data of the test subset is not used at all during the modeling stage, and thus it provides a more realistic metric of the model performance. However, if comparing the RMSE values obtained for both subsets, it can be seen how the differences are actually not that high, which confirms the goodness of the model and the capability of the proposed ET to achieve the simultaneous quantification of the three drugs. Thus, the next step was to confirm whether using the same approach we are able not to only quantify mixtures of the pure drugs, but also to detect and quantify the cutting agents considered, which would provide a more realistic use of the developed strategy.

3.3.2. Mixtures of the three drugs and the two cutting agents

Under the same conditions as above, but making use of a different experimental design given the larger number of analytes to be considered, a new set of samples was prepared as described in Section 2.5 and measured employing the sensor array. As before, GA-PLS models were built to determine each analyte in the mixture, but in this case selecting a total of 114 features from the raw voltammetric responses (Fig. S10). The selected number of LVs were 13 for heroin, 18 for codeine, 10 for morphine, 6 for paracetamol and 12 for caffeine. Again, the comparison graphs of predicted vs. expected concentrations were built for each of the analytes (Fig. 6), and the linear regression parameters calculated (Table 3). Again, a satisfactory trend is obtained for both subsets, with slightly better behavior for the train subset as already discussed, but with RMSE values of the same order of magnitude.

Although the model performance metrics are slightly worst for the 5 compounds case than for the 3 compounds one (total NRMSE for the three drugs of 0.084 vs. 0.026 for the test subset), it has to be considered the higher complexity of the case. That is, on the one side, the use of a fractional experimental design (as is the CCF) to keep the number of samples required to build the model reasonable. On the other side, and as already reported, the presence of certain cutting agents can influence the voltammetric response, up to the point that the observed peak for the pure compound might not be seen in the presence of the adulterant [16, 17].

In regards to the latter, herein we have demonstrated how making use of a proper set of samples, the model is able to correctly quantify both the drugs and cutting agents. Thus, the same approach can be applied to the identification and quantification of others mixtures. Moreover, if multi-way processing methods are to be used instead of two-way PLS models, the correction of the presence of an interfering species, even if not initially considered in the response model, might be possible thanks to their “second order advantage” [45,46].

Therefore, taking all this into account, it's clear that the use of the herein proposed voltammetric ET shows huge potential to carry the identification and quantification of seized drug samples, either those being pure or already mixed with other drugs and/or cutting agents.

Lastly, despite already taking the precaution of using a separate validation subset of data (the test subset), a permutation test or “target shuffling process” was carried out to demonstrate that neither the high dimensionality of the data nor the use of GAs and PLS-1 is resulting in over-fitted models. Such test allows the identification of incorrectly perceived cause-and-effect relationships in modeling (“chance correlation”) by taking as null hypothesis that samples labels are exchangeable. Briefly, this test involves repeatedly and randomly reordering of the responses variables (Y), followed by the building of a new model upon shuffling of the data labels. In other words, a new model is built upon assignment of an “incorrect” y-value to each sample corresponding to the one from another sample. This process is repeated several times to ensure that the statistics calculated are significant (up to 1000 times in our case). For each of the permutations, the different performance metrics were calculated and compared to the actual model with the proper labels. As an example, a histogram summarizing the RMSE values of the different models for the three drugs plus codeine and paracetamol are shown in Fig. 7, from which the significance of the obtained results is evident.

4. Conclusions

The potential of ETs for the simultaneous determination and quantification of different opiates in the presence of common cutting agents has been demonstrated. More specifically, a voltammetric sensor array consisting in three SPCE modified with graphite, cobalt (II) phthalocyanine and palladium inks were employed to extract the electrochemical fingerprints of heroin, morphine, codeine, caffeine and paracetamol by means of SWV. Despite the advantages that electrochemical methods may offer, the simultaneous determination of the aforementioned compounds can also be challenging given their similar electrochemical response; especially when attempting the discrimination between heroin and morphine, since both molecules present the same functional groups in their skeleton. Thus, a partial least square regression (PLS) model for

the quantification of heroin, morphine, codeine, caffeine and paracetamol mixtures at the μM level was built employing a central composite face-centered (CCF) experimental design. A very satisfactory performance was obtained, demonstrating that the use of the herein proposed voltammetric ET shows huge potential to carry the identification and quantification of seized drug street samples, either those being pure or already mixed with other drugs and/or cutting agents.

Overall, the advantages of ETs to deconvolute complex overlapping electrochemical responses and achieve the simultaneous quantitative determination of several analytes have been shown. Moreover, the use of a properly formulated graphite-polystyrene ink has been demonstrated as a simple approach to obtain an array of modified electrodes with different responses towards the compounds under study.

As for the data processing, GAs allowed to reduce the number of inputs fed to the model through the identification of its most relevant features, what in turn reduced its complexity, and at the same time improved its performance. Lastly, by conducting a permutation test or “target shuffling process”, it was also demonstrated that neither the high dimensionality of the data or the use of GAs and PLS resulted in over-fitted models. In fact, this verification provided a high significance for the obtained RMSE values, higher than 99.99%, both for train and test subsets (P value lower than $3 \cdot 10^{-5}$), as illustrated in Fig. 7.

In conclusion, the results presented herein suggest the potential of these devices to be used as analytical tools for the detection of illicit substances from street samples offering low-cost measurement systems with rapid response, simple usage and high portability; all of them ideal characteristics for point-of-use forensic or law-enforcement applications.

CRediT authorship contribution statement

Dionisia Ortiz-Aguayo: Methodology, Investigation, Writing – original draft. **Ceto Xavier Cetó:** Methodology, Software, Writing – original draft. **Karolien De Wael:** Resources, Writing – review & editing, Funding acquisition. **Manel del Valle:** Conceptualization, Methodology, Writing – review & editing, Funding acquisition.

Declaration of Competing Interest

The authors declare that they have no known competing financial interests or personal relationships that could have appeared to influence the work reported in this paper.

Acknowledgments

This research was funded by the Spanish Ministry of Science and Innovation, MCINN (Madrid) through project PID2019-107102RB-C21. This project has received funding from the European Union's Horizon 2020 research and innovation programme under Grant agreement No. 833787 BorderSens (Border detection of illicit drugs and precursors by highly accurate electrosensors). Karolien De Wael acknowledges the support from the University of Antwerp (IOF)UAntwerp and BELSPO. Dionisia Ortiz-Aguayo was funded by Universitat Autònoma de Barcelona through a PIF fellowship. M. del Valle thanks the support from the program ICREA Academia.

Appendix A. Supplementary material

Supplementary data associated with this article can be found in the online version at doi:10.1016/j.snb.2021.131345.

References

- [1] A. Florea, M. de Jong, K. De Wael, Electrochemical strategies for the detection of forensic drugs, *Curr. Opin. Electrochem.* 11 (2018) 34–40.
- [2] C. Guiney, EU drug markets report 2019, *Drugnet Ireland* (2020) 18–20.

- [3] Bordersens: Border Detection of Illicit Drugs and Precursors by Highly Accurate Electrosensors, 2021. (<https://bordersens.eu/>).
- [4] Drug Enforcement Administration. Drugs of abuse: A DEA resource guide, Drug Enforcement Administration. US Department of Justice, 2017.
- [5] N.E. Hagemeyer, Introduction to the opioid epidemic: the economic burden on the healthcare system and impact on quality of life, *Am. J. Manag. Care* 24 (10) (2018) S200.
- [6] J.K. O'Donnell, R.M. Gladden, P. Seth, Trends in deaths involving heroin and synthetic opioids excluding methadone, and law enforcement drug product reports, by census region — United States, 2006–2015, *MMWR Morb. Mortal. Wkly. Rep.* 66 (34) (2017) 897–903.
- [7] J.M.P.J. Garrido, C. Delerue-Matos, F. Borges, T.R.A. Macedo, A.M. Oliveira-Brett, Electrochemical analysis of opiates – an overview, *Anal. Lett.* 37 (5) (2004) 831–844.
- [8] M.Y. Salem, S.A. Ross, T.P. Murphy, M.A. ElSohly, GC-MS determination of heroin metabolites in meconium: evaluation of four solid-phase extraction cartridges, *J. Anal. Toxicol.* 25 (2) (2001) 93–98.
- [9] C. Meadway, S. George, R. Braithwaite, A rapid GC-MS method for the determination of dihydrocodeine, codeine, norcodeine, morphine, normorphine and 6-MAM in urine, *Forensic Sci. Int.* 127 (1–2) (2002) 136–141.
- [10] Z. Zhang, B. Yan, K. Liu, Y. Liao, H. Liu, CE-MS analysis of heroin and its basic impurities using a charged polymer-protected gold nanoparticle-coated capillary, *Electrophoresis* 30 (2) (2009) 379–387.
- [11] R.B. Taylor, A.S. Low, R.G. Reid, Determination of opiates in urine by capillary electrophoresis, *J. Chromatogr. B Biomed. Appl.* 675 (2) (1996) 213–223.
- [12] Y. Zhuang, X. Cai, J. Yu, H. Ju, Flow injection chemiluminescence analysis for highly sensitive determination of noscapine, *J. Photochem. Photobiol. A Chem.* 162 (2–3) (2004) 457–462.
- [13] Y. Zhuang, D. Zhang, H. Ju, Sensitive determination of heroin based on electrogenerated chemiluminescence of tris(2,2'-bipyridyl)ruthenium(II) immobilized in zeolite Y modified carbon paste electrode, *Analyst* 130 (4) (2005) 534–540.
- [14] J. Moros, N. Galipienso, R. Vilches, S. Garrigues, M. De La Guardia, Nondestructive direct determination of heroin in seized illicit street drugs by diffuse reflectance near-infrared spectroscopy, *Anal. Chem.* 80 (19) (2008) 7257–7265.
- [15] G. Sakai, K. Ogata, T. Uda, N. Miura, N. Yamazoe, A surface plasmon resonance-based immunosensor for highly sensitive detection of morphine, *Sens. Actuators B Chem.* 49 (1–2) (1998) 5.
- [16] A. Florea, J. Schram, M. De Jong, J. Eliaerts, F. Van Durme, B. Kaur, N. Samyn, K. De Wael, Electrochemical strategies for adulterated heroin samples, *Anal. Chem.* 91 (12) (2019) 7920–7928.
- [17] M. de Jong, A. Florea, J. Eliaerts, F. Van Durme, N. Samyn, K. De Wael, Tackling poor specificity of cocaine color tests by electrochemical strategies, *Anal. Chem.* 90 (11) (2018) 6811–6819.
- [18] P. Ciosek, W. Wróblewski, Sensor arrays for liquid sensing – electronic tongue systems, *Analyst* 132 (10) (2007) 963–978.
- [19] M. del Valle, Electronic tongues employing electrochemical sensors, *Electroanalysis* 22 (14) (2010) 1539–1555.
- [20] Y. Vlasov, A. Legin, A. Rudnitskaya, C. Di Natale, A. D'Amico, Nonspecific sensor arrays (“electronic tongue”) for chemical analysis of liquids: (IUPAC technical report), *Pure Appl. Chem.* 77 (11) (2005) 1965–1983.
- [21] F. Arduini, L. Micheli, D. Moscone, G. Palleschi, S. Piermarini, F. Ricci, G. Volpe, Electrochemical biosensors based on nanomodified screen-printed electrodes: recent applications in clinical analysis, *TrAC Trends Anal. Chem.* 79 (2016) 114–126.
- [22] G. Maduraiveeran, M. Sasidharan, V. Ganesan, Electrochemical sensor and biosensor platforms based on advanced nanomaterials for biological and biomedical applications, *Biosens. Bioelectron.* 103 (2018) 113–129.
- [23] X. Cetó, F. Céspedes, M.I. Pividori, J.M. Gutiérrez, M. del Valle, Resolution of phenolic antioxidant mixtures employing a voltammetric bio-electronic tongue, *Analyst* 137 (2) (2012) 349–356.
- [24] E. Richards, C. Bessant, S. Saini, Optimisation of a neural network model for calibration of voltammetric data, *Chemom. Intell. Lab. Syst.* 61 (1–2) (2002) 35–49.
- [25] V. Esposito Vinzi, W.W. Chin, J. Henseler, H. Wang, *Handbook of partial least squares: concepts, methods and applications*, Springer, Berlin, 2010.
- [26] A.J. Bard, Chemical modification of electrodes, *J. Chem. Educ.* 60 (4) (1983) 302.
- [27] D. Ortiz-Aguayo, M. Bonet-San-Emeterio, M. del Valle, Simultaneous voltammetric determination of acetaminophen, ascorbic acid and uric acid by use of integrated array of screen-printed electrodes and chemometric tools, *Sensors* 19 (15) (2019) 3286.
- [28] J.M. Gutiérrez, L. Moreno-Barón, M.I. Pividori, S. Alegret, M. del Valle, A voltammetric electronic tongue made of modified epoxy-graphite electrodes for the qualitative analysis of wine, *Microchim. Acta* 169 (3–4) (2010) 261–268.
- [29] M.L. Rodríguez-Mendez, C. García-Hernández, C. Medina-Plaza, C. García-Cabezón, J.A. de Saja, Multisensor systems based on phthalocyanines for monitoring the quality of grapes, *J. Porphyr. Phthalocyanines* 20 (08n11) (2016) 889–894.
- [30] J.P. Metters, R.O. Kadara, C.E. Banks, New directions in screen printed electroanalytical sensors: an overview of recent developments, *Analyst* 136 (6) (2011) 1067–1076.
- [31] V. Tsakova, R. Seeber, Conducting polymers in electrochemical sensing: factors influencing the electroanalytical signal, *Anal. Bioanal. Chem.* 408 (26) (2016) 7231–7241.
- [32] D. Ortiz-Aguayo, K. De Wael, X. Cetó, M. del Valle, Voltammetric sensing using an array of modified SPCE coupled with machine learning strategies for the

- improved identification of opioids in presence of cutting agents, *Journal of Electroanalytical Chemistry* 902 (2021), 115770.
- [33] M. Galik, A.M. O'Mahony, J. Wang, Cyclic and square-wave voltammetric signatures of nitro-containing explosives, *Electroanalysis* 23 (5) (2011) 1193–1204.
- [34] A.M. O'Mahony, J.R. Windmiller, I.A. Samek, A.J. Bandodkar, J. Wang, "Swipe and scan": integration of sampling and analysis of gunshot metal residues at screen-printed electrodes, *Electrochem. Commun.* 23 (1) (2012) 52–55.
- [35] J.M.P.J. Garrido, C. Delerue-Matos, F. Borges, T.R.A. Macedo, A.M. Oliveira-Brett, Voltammetric oxidation of drugs of abuse III. Heroin and metabolites, *Electroanalysis* 16 (18) (2004) 1497–1502.
- [36] J.M.P.J. Garrido, C. Delerue-Matos, F. Borges, T.R.A. Macedo, A.M. Oliveira-Brett, Voltammetric oxidation of drugs of abuse: I. Morphine and metabolites, *Electroanalysis* 16 (17) (2004) 1419–1426.
- [37] J.M.P.J. Garrido, C. Delerue-Matos, F. Borges, T.R.A. Macedo, A.M. Oliveira-Brett, Voltammetric oxidation of drugs of abuse II. Codeine and metabolites, *Electroanalysis* 16 (17) (2004) 1427–1433.
- [38] D. Nematollahi, H. Shayani-Jam, M. Alimoradi, S. Niroomand, Electrochemical oxidation of acetaminophen in aqueous solutions: kinetic evaluation of hydrolysis, hydroxylation and dimerization processes, *Electrochim. Acta* 54 (28) (2009) 7407–7415.
- [39] M. Khairy, B.G. Mahmoud, C.E. Banks, Simultaneous determination of codeine and its co-formulated drugs acetaminophen and caffeine by utilising cerium oxide nanoparticles modified screen-printed electrodes, *Sens. Actuators B Chem.* 259 (2018) 142–154.
- [40] Y. Tadesse, A. Tadesse, R.C. Saini, R. Pal, Cyclic voltammetric investigation of caffeine at anthraquinone modified carbon paste electrode, *Int. J. Electrochem.* 1 (2013) 2013–2017.
- [41] J. Broséus, N. Gentile, P. Esseiva, The cutting of cocaine and heroin: a critical review, *Forensic Sci. Int.* 262 (2016) 73–83.
- [42] J.R.B. Rodríguez, V.C. Díaz, A.C. García, P.T. Blanco, Voltammetric assay of heroin in illicit dosage forms, *Analyst* 115 (2) (1990) 209–212.
- [43] X. Cetó, F. Céspedes, M. del Valle, Comparison of methods for the processing of voltammetric electronic tongues data, *Microchim. Acta* 180 (5–6) (2013) 319–330.
- [44] E. Richards, C. Bessant, S. Saini, Multivariate data analysis in electroanalytical chemistry, *Electroanalysis* 14 (22) (2002) 1533–1542.
- [45] G.M. Escandar, H.C. Goicoechea, A. Muñoz de la Peña, A.C. Olivieri, Second- and higher-order data generation and calibration: a tutorial, *Anal. Chim. Acta* 806 (2014) 8–26.
- [46] A. Mimendia, J.M. Gutiérrez, L.J. Opalski, P. Ciosek, W. Wróblewski, M. del Valle, SIA system employing the transient response from a potentiometric sensor array—correction of a saline matrix effect, *Talanta* 82 (3) (2010) 931–938.

Dionisia Ortiz-Aguayo received her M.Sc. degree in Chemistry in 2015 from the *Universitat Autònoma de Barcelona*, where she is at the moment completing her Ph.D. in Analytical Chemistry. Her main research topics deal with the development of voltammetric sensors and the application of electronic tongues as a tool in the pharmaceutical and forensic analysis.

Xavier Cetó completed his M.Sc. degree in chemistry in 2009 at the *Universitat Autònoma de Barcelona*, and received his Ph.D. in analytical chemistry in 2013 from the same university. From 2014 to 2017, he worked as Research Associate at the University of South Australia. At present, he is a postdoctoral researcher of the BorderSens project at *Universitat Autònoma de Barcelona*. His main research topics deal with the development of new voltammetric (bio)sensors and the application of electronic tongues and chemometric tools for data analysis, mainly employing voltammetric (bio)sensors, albeit also potentiometric ones.

Karolien De Wael received her Ph.D. in Chemistry from UGent as national science foundation (FWO) fellow. After a prestigious FWO postdoctoral fellowship at the same university, she started as tenure track research professor at University of Antwerp in 2011. In 2018, she was appointed as full professor. Currently, she is spokesperson of the AXES Research Group performing fundamental, methodological and application-oriented research involving a wide range of analytical techniques. Her strategic vision aims at a portfolio of sensor technologies (fulfilling relevant criteria) that can be applied in different markets/sectors embracing the idea of responsible research and innovation. The AXES research group is part of the Nanolab Center of Excellence and the IOF Enviromics consortium in the University of Antwerp.

Manel del Valle received his Ph.D. in Chemistry in 1992 from the *Universitat Autònoma de Barcelona*, where he is full professor in Analytical Chemistry since 2018. He is a member of the Sensors & Biosensors Group where he is a specialist for instrumentation and electrochemical sensors. He has initiated there the research lines of sensor arrays and electronic tongues. Other interests of his work are the use of impedance measurements for sensor development, biosensors and the design of automated flow systems.

Resolution of opiate illicit drugs signals in the presence of some cutting agents with use of a voltammetric sensor array and machine learning strategies

Dionisia Ortiz-Aguayo^a, Xavier Cetó^a, Karolien De Wael^b and Manel del Valle^{a,1*}

^a *Sensors and Biosensors Group, Department of Chemistry, Universitat Autònoma de Barcelona, Edifici Cn, 08193 Bellaterra, Spain*

^b *AXES Research Group, Department of Bioscience Engineering, University of Antwerp, Groenenborgerlaan 171, 2020 Antwerp, Belgium*

Supplementary Material

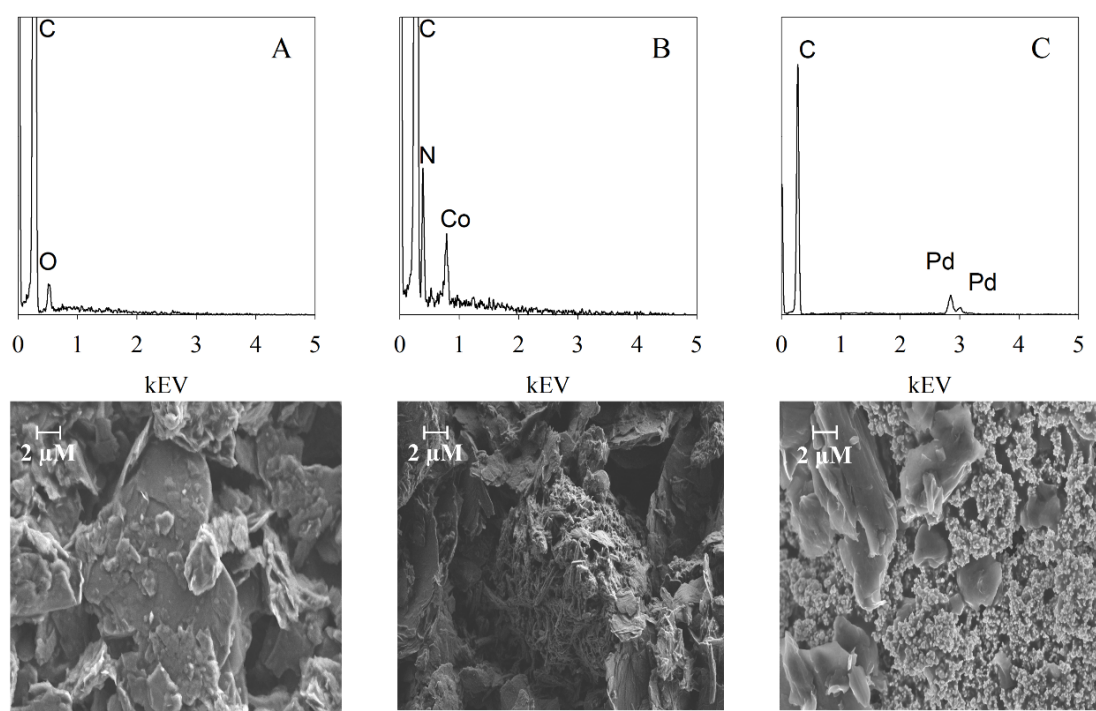


Figure S1. EDX (top) and SEM (bottom) characterization of (A) Graphite/SPCE-Ink, (B) Cobalt (II) phthalocyanine/SPCE-Ink, (C) Palladium/SPCE-Ink.

* E-mail: manel.delvalle@uab.cat; tel: +34 93 5813235; fax: +34 93 5812477

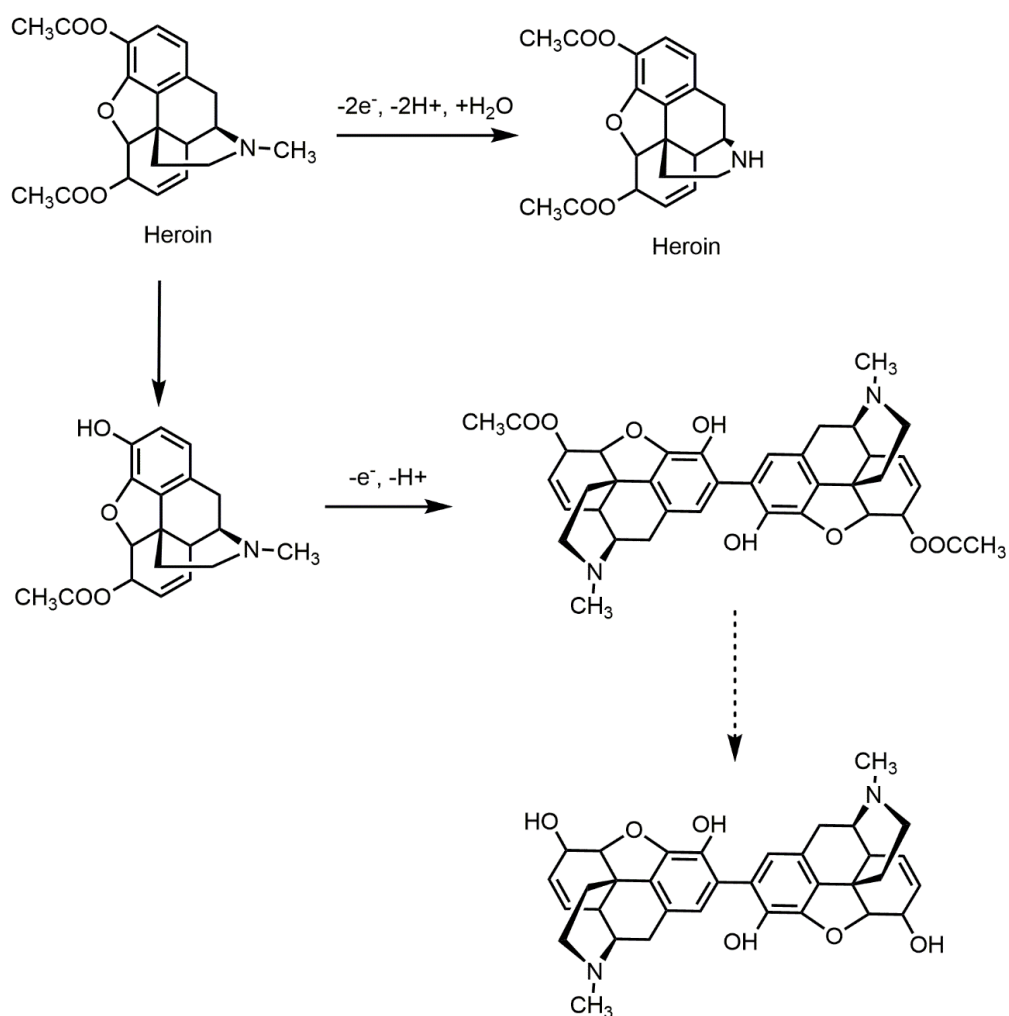


Figure S2. Electrochemical oxidation mechanism of heroin proposed by Garrido et al [1].

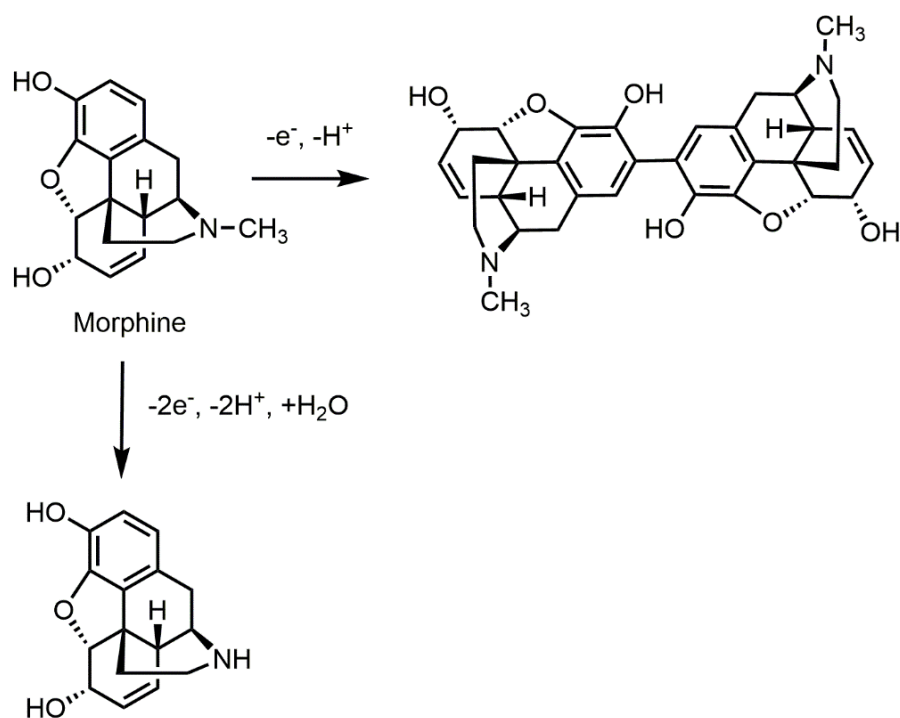


Figure S3. Electrochemical oxidation mechanism of morphine proposed by Garrido et al [2].

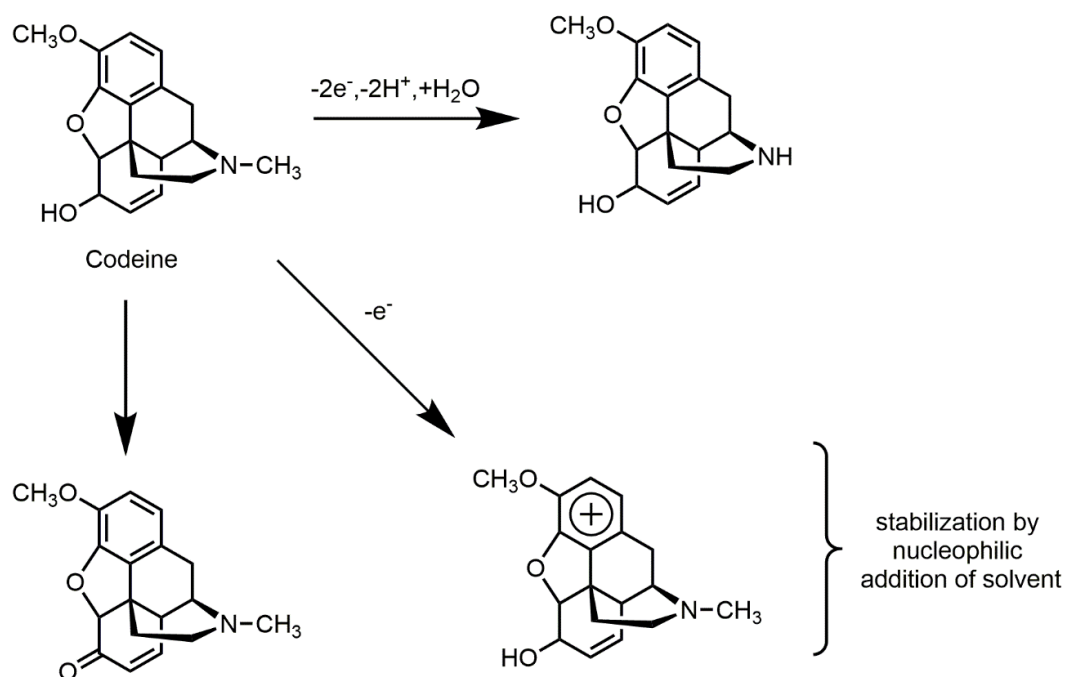


Figure S4. Electrochemical oxidation mechanism of codeine proposed by Garrido *et al.* [3].

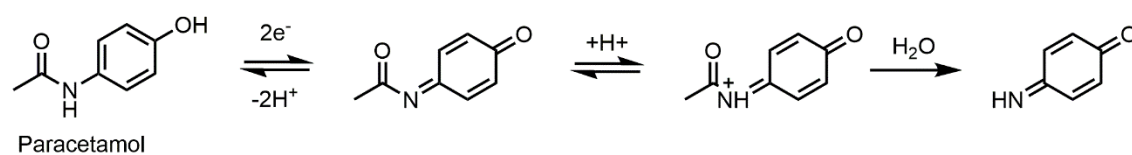


Figure S5. Electrochemical oxidation mechanism of paracetamol proposed by Khairy *et al* [4].

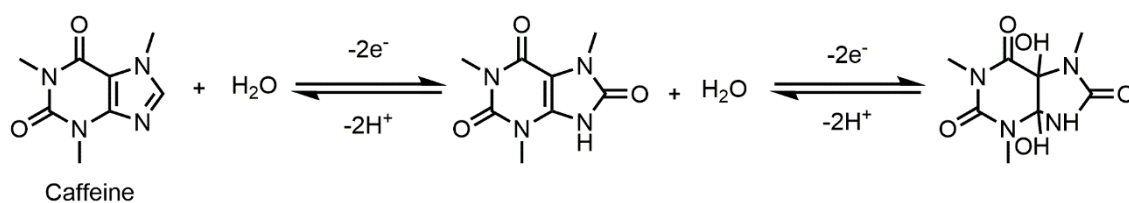


Figure S6. Electrochemical oxidation mechanism of caffeine proposed by Tadesse *et al.* [5].

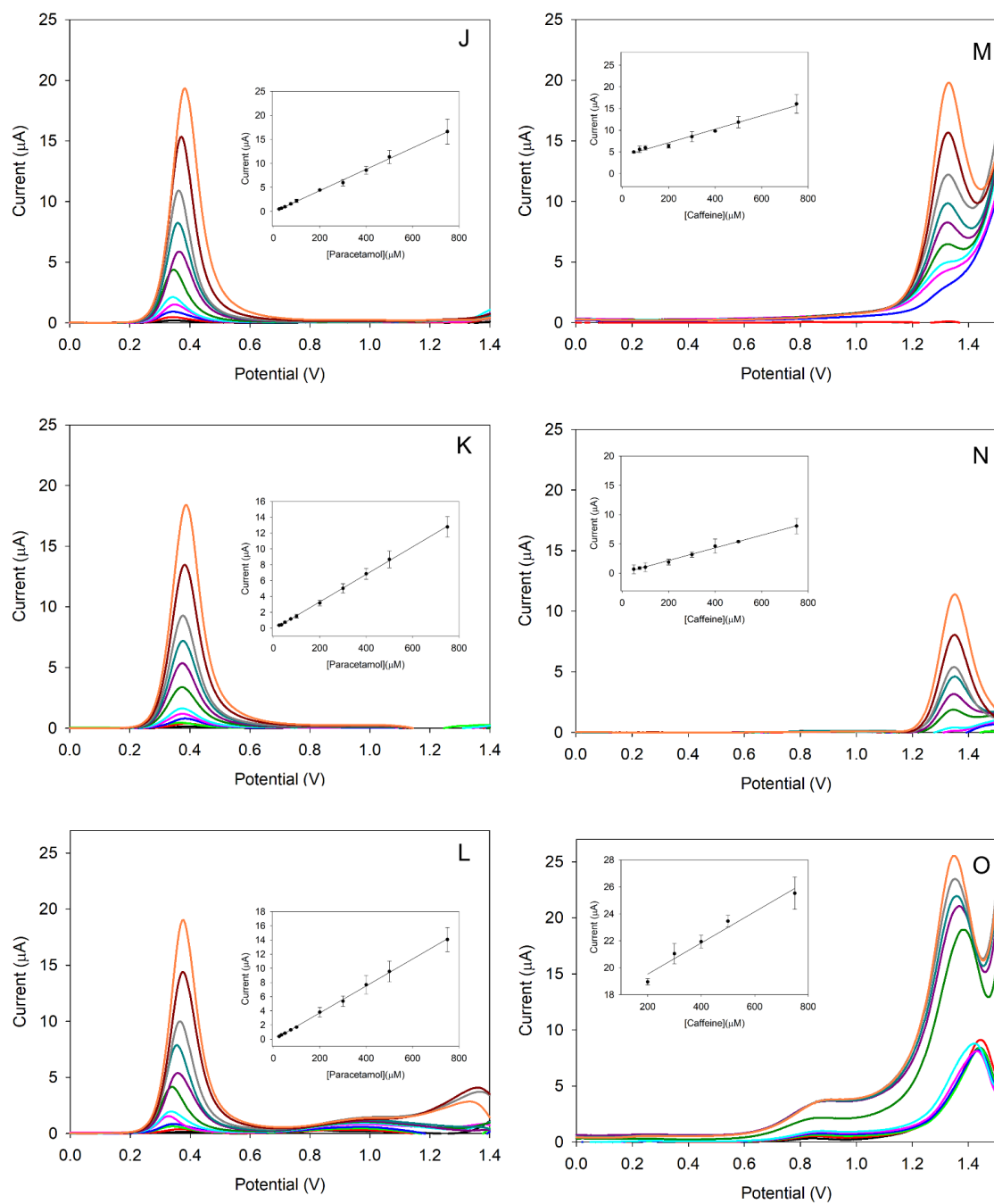


Figure S7. Square wave voltammograms obtained for (J-L; left column) paracetamol and (M-O; right column) caffeine using (J,M; top row) graphite, (K,N; middle row) CoPc and (L,O; bottom row) Pd modified sensors, respectively. Series of plots correspond to increasing concentrations from 10 to 1000 μM . Insets correspond to the linear regressions of peak height vs. concentration, excluding the point 1000 μM as saturation of the voltammetric signal was reached for certain compounds.

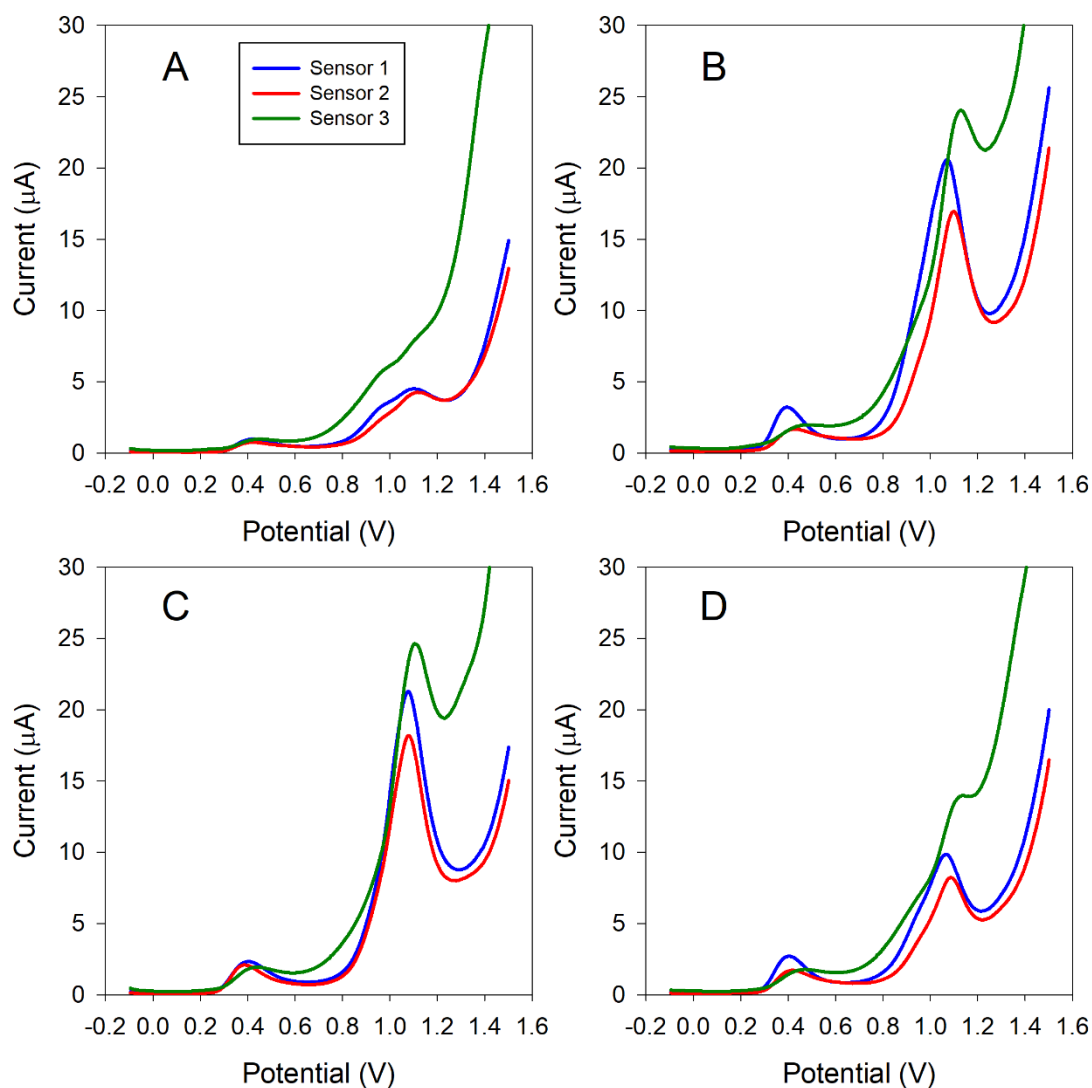


Figure S8. Example of the voltammograms obtained for certain arbitrary mixtures of heroin, morphine and codeine with concentrations for the three compounds of (A) 560 μM , 239 μM , 28 μM , (B) 627 μM , 577 μM , 435 μM , (C) 180 μM , 617 μM , 626 μM and (D) 156 μM , 531 μM , 156 μM . The samples were prepared in PBS pH 7. The three colours represent the sensor array: Graphite/SPCE-Ink (blue), Cobalt (II) phthalocyanine/SPCE-Ink (red) and Palladium/SPCE-Ink (green).

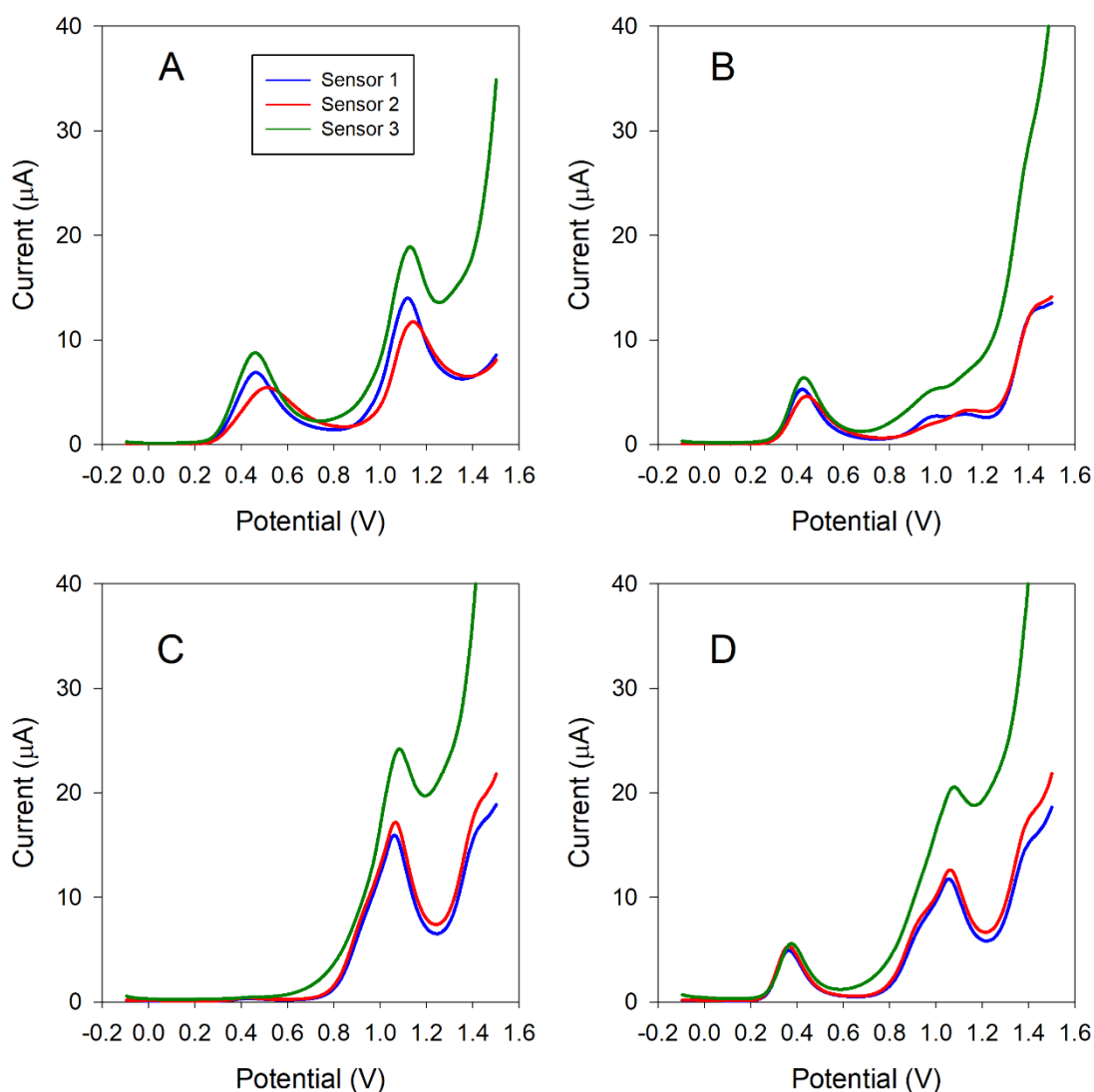


Figure S9. Example of the voltammograms obtained for certain arbitrary mixtures of heroin, morphine, codeine, paracetamol and caffeine with concentrations for the five compounds of. (A) 0 μM , 623 μM , 623 μM , 623 μM , 0 μM (B) 623 μM , 0 μM , 0 μM , 623 μM , 623 μM , (C) 623 μM , 0 μM , 623 μM , 0 μM , 623 μM and (D) 438 μM , 82 μM , 384 μM , 384 μM , 493 μM . The samples were prepared in PBS pH 7. The three colours represent the sensor array: Graphite/SPCE-Ink (blue), Cobalt (II) phthalocyanine/SPCE-Ink (red) and Palladium/SPCE-Ink (green).

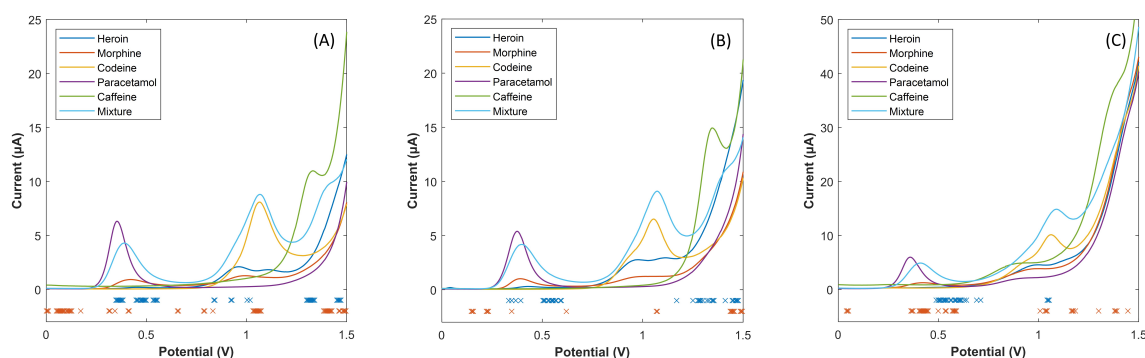


Figure S10. Outcome of the feature selection step using GAs. Square wave voltammograms obtained using (A) graphite, (B) CoPc and (C) Pd sensor for pure solutions of the different compounds under study at 300 μM as well as for an arbitrary mixture of those are plotted, and underneath the features selected for the mixtures of the (x) 3 compounds and (x) 5 compounds.

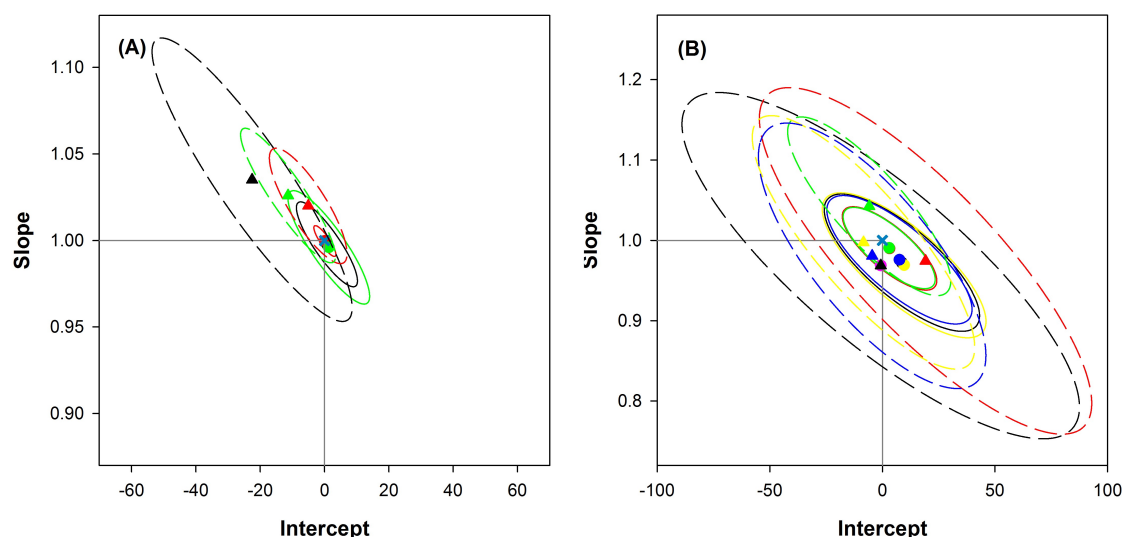


Figure S11. Joint confidence intervals for (A) the three drugs, and (B) the three drugs and the two cutting agents: (black) heroin, (red) codeine, (green) morphine, (yellow) paracetamol and (blue) caffeine, both for the training (●, solid line) and testing (▲, dashed line) subsets. Also, the ideal point (1,0) is plotted (x); intervals are calculated at the 95% confidence level.

References

- [1] Garrido, J.M.P.J., Delerue-Matos, C., Borges, F., Macedo, T.R.A., and Oliveira-Brett, A.M., Voltammetric Oxidation of Drugs of Abuse III. Heroin and Metabolites, *Electroanalysis*, 16, 18, 1497, 2004.
- [2] Garrido, J.M.P.J., Delerue-Matos, C., Borges, F., Macedo, T.R.A., and Oliveira-Brett, A.M., Voltammetric oxidation of drugs of abuse: I. Morphine and metabolites, *Electroanalysis*, 16, 17, 1419, 2004.
- [3] Garrido, J.M.P.J., Delerue-Matos, C., Borges, F., Macedo, T.R.A., and Oliveira-Brett, A.M., Voltammetric Oxidation of Drugs of Abuse II. Codeine and Metabolites, *Electroanalysis*, 16, 17, 1427, 2004.
- [4] Khairy, M., Mahmoud, B.G., and Banks, C.E., Simultaneous determination of codeine and its co-formulated drugs acetaminophen and caffeine by utilising cerium oxide nanoparticles modified screen-printed electrodes, *Sensors Actuators B Chem.*, 259, 142, 2018.
- [5] Tadesse, Y., Tadesse, A., Saini, R.C., and Pal, R., Cyclic Voltammetric Investigation of Caffeine at Anthraquinone Modified Carbon Paste Electrode, *Int. J. Electrochem.*, 2013, 1, 2013.

